THE CHARACTERISATION OF ALGINATE SYSTEMS

FOR BIOMEDICAL APPLICATIONS

A thesis submitted for the degree of Doctor of Philosophy

by

Céline Sartori

Department of Materials Engineering, Brunel University

May 1997

Designed by Folium Corporate Design

ABSTRACT

This research project focused on a range of polysaccharides, including sodium alginates (with varying mannuronic (M)/guluronic (G) acid ratio), pectin and sodium carboxymethylcellulose (CMC), for wound dressing applications. The samples were prepared as mixed salts such as sodium/calcium salts as Ca^{2+} ions are known to promote faster healing.

The aims of this research were:

1- to provide a greater insight into the nature of binding between various ions (Na^{+}, Ca^{2+} as well as Zn^{2+} and Ag^{+}) and the polysaccharide molecules. Interactions between alginate/pectin and alginate/CMC molecules were also studied. This was achieved using a range of analytical techniques such as Fourier transform infrared spectroscopy, Raman spectroscopy and neutron spectroscopy, thermogravimetric analysis, microprobe analysis, X-ray diffraction and atomic absorption spectroscopy.

It was found that sodium ions were bound to the carboxyl groups of the alginate molecules, whilst calcium ions attached themselves onto COO^{-} as well as onto the alginate backbone, leading to crosslinked structures. Appearance of OH...$^{-}$OOC to the detriment of OH...OH bonding was also observed. Addition of zinc ions involved greater constraint in the alginate network and the silver ions were believed to produce insoluble alginate salts, due to their larger ionic radius; furthermore hydroxyl-hydroxyl interactions in the silver alginate were rather between the polymer molecules than with the water.

The addition of pectin to alginate led to partial binding between the two polysaccharides via hydrogen bonds. By contrast, carboxymethylcellulose molecules were found to act as independent entities in contact with alginate, and therefore suggested incompatibility.

2- to determine the performance of sodium/calcium alginate systems as well as Na/Ca alginate/pectin and Na/Ca alginate/CMC systems, in order to improve properties such as absorbency, gel strength and calcium release (to assess the haemocompatibility) in a simulated serum solution. A greater calcium and guluronic acid content was found to improve the gel strength of alginate samples, but decrease the swelling ability. Calcium release was favoured with a low G and a high calcium content. Addition of a second polysaccharide enhanced these gel properties. For example, the gel strength could be significantly increased with a 25 % pectin addition, while addition of CMC up to 50 % increased both the swelling and the calcium release.

3- to develop a new model of the ion release process for a polysaccharide system brought into contact with a simulated serum solution. It was based on a "hopping-trapping" mechanism for the calcium ions, whereby different release rates are due to different affinities with the polysaccharide blocks.

THE CHARACTERISATION OF NOVEL ALGINATES FOR BIOMEDICAL APPLICATIONS

ACKNOWLEDGMENTS

At the end of this research project, I would like to thank Dr. Dudley S. Finch and Prof. Brian Ralph for their valuable time and their helpful comments all through these last three years.

I am particularly grateful to Innovative Technologies Ltd for their sponsorship, and more particularly to Dr. Keith Gilding for his guiding and advice.

Special thanks go to Drs. Stewart F. Parker (ISIS, Rutherford and Appleton Laboratory) and David James (Nicolet Instruments Ltd) for giving me the opportunity to use the Neutron and Raman spectroscopic facilities, respectively. I would like to thank Dr. Robert Bulpett, Dr. Alan J. Reynolds and Ms. Jenny Moses, from the Experimental Techniques Centre (Brunel University), for their guidance with regards to the SEM analysis. I would also like to thank Dr. Lan Qin, from Innovative Technologies Ltd, for her help on the atomic absorption spectrometer, and Dr. Gaer Yu, from Manchester University, regarding the gel permeation chromatography measurements. I am grateful to Mr. John Felgate, Mr. Prakash Dodia and Dr. Sue Woodisse for their technical support.

Finally, I wish to thank my partner, Mr. Martin Beth, for his help in the calculations, and for his continual encouragement.

ABBREVIATIONS

AAS: atomic absorption spectroscopy.

CMC: carboxymethylcellulose.

D.M.: degree of methoxylation (for pectin).

D.S.: degree of substitution (for carboxymethylcellulose).

FTIR: Fourier transform infrared.

G: guluronic acid (for alginate).

H.M.: high methoxyl (pectin).

INS: inelastic neutron scattering.

L.M.: low methoxyl (pectin).

M: mannuronic acid (for alginate).

MRI: magnetic resonance imaging.

NMR: nuclear magnetic resonance.

SEM: scanning electron microscopy.

WDX: wavelength dispersive spectroscopy.

XRD: X-ray diffraction.

ZAF: atomic number Z, absorption A and fluorescence F.

INTRODUCTION

With the constant search for new materials, always more efficient, more reliable and of greater performance, one would not naturally consider seaweeds as a potential class. However, not only do they play a vital role in the ecological system (algae are the basis of all food chains in the sea providing up to half of the earth's oxygen), but some have also been used for centuries as food, as manure or as a source of chemicals. Alginates, a kind of brown seaweed, have been collected in Scotland since the XVIIIth century for the treatment of blisters and lacerations. From the 1960's, seaweeds have been farmed and today, alginates find widespread applications in both the food and the pharmaceutical industries.

The benefit gained from using these natural polymers comes mainly from their ability to form a hydrogel with most divalent cations, such as Ca^{2+} ions. Furthermore, their high absorbency and intrinsic haemocompatibility make them of particular interest in the making of wound dressings. Thirty years ago, it was discovered that wounds heal better in a moist environment Additionally, on contact with blood, calcium alginate rapidly releases the calcium ions in exchange for sodium ions, stimulating both platelet activation and whole blood coagulation (Jarvis *et al.*, 1987).

This research project was primarily intended to gain a greater insight into ion exchange and ion binding within alginates. The second point of interest was how to improve properties such as strength and swelling of these biomaterials. This was carried out following the route of polymer blends such as alginate/pectin (a polysaccharide particularly abundant in fruits) and alginate/carboxymethylcellulose (principal constituent of the cell wall of plants).

Three polysaccharide systems were considered in this work: pure alginates, alginate/pectin blends and alginate/carboxymethylcellulose blends. The study of each system was performed following the same pattern. Firstly, the samples received as powders were dissolved in distilled deionised water and the pH as well as viscosity were determined. These solutions were subsequently immersed in a calcium chloride bath where sodium-calcium ion exchange took place. The films so-produced were analysed in

the dry state for their ion content (using atomic absorption and wavelength dispersive spectroscopy), their way of ion binding (using infrared, Raman and neutron spectroscopy), their crystallinity (using X-ray diffraction), their tensile properties, etc... The samples were then tested in contact with a simulated serum solution. The tests included calcium release, swelling and gel strength measurements. Finally, some models were derived from the experimental results.

CHAPTER I: PRESENTATION OF ALGINATES AND OTHER POLYSACCHARIDES FOR MEDICAL APPLICATIONS

Before presenting the different materials used in this research project, it is worthwhile describing briefly polysaccharides as alginates, pectins and celluloses belong to this family of natural polymers. Polysaccharides are carbohydrate polymers based on monosaccharide units (i.e. simple sugar units) linked with glycosidic bonds. They include a large variety of polymers, varying in monomeric composition, anomeric configuration, sequence, position of linkages, charge density and molecular size, and exhibit a wide range of physical properties (Skjåk-Bræk *et al.*, 1986b).

Typically, the monosaccharides have six-membered structures, known as pyranoses (i.e. they contain five carbon atoms and one oxygen atom). The representation of these structures follow a number of conventions (Rees, 1977):

-many of the carbon and hydrogen atoms are omitted for convenience and clarity;

-the conformations are designated C for chair, B for boat, S for twist-boat and H for half-chair;

-it is common to insert enantiomeric (one of an isomeric pair whose molecules are non-superimposable mirror image) prefixes (D or L) and anomeric (one of an isomeric pair resulting from creation of a new point of symmetry when a rearrangement of the atoms occurs at the aldehyde or ketone position) prefixes (α or β);

-to refer to particular carbon atoms, the pyranoid ring is numbered as follow (clockwise from above):

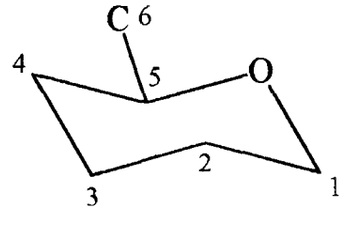

Figure 1. Carbon numbering in a pyranoid ring.

The most widely used polysaccharides are derived from terrestrial plant material such as cellulose and starch, or from marine algae such as agar, alginate and carrageenan. Some of their functions are:

-to provide the essential structural elements in plants or to serve as energy reserves in many organisms;

-to lubricate bone-joints (in animals);

-to protect the bark of trees after damage;...

Polysaccharides find applications in food industry, paper making, manufacture of adhesives, biomedicines...

Like all natural polymers, the molecules of alginate, pectin or cellulose are not all identical, so their average characteristics will be considered in the following presentation.

SECTION A: WHAT ARE ALGINATES ?

I.A.1. Introduction to alginates

I.A.1.1. Alginates :

Alginates are hydrophilic polysaccharides found in brown seaweed, comprising of up to 40 wt% of dry matter (the seaweed contains other ionic polymers such as fucoidan). They occur in the intercellular matrix as a mixed sodium-magnesium-calcium-strontium gel, the relative proportions of these ions being determined by an ion-exchange equilibrium reaction with sea-water (Smidsrød, 1974). Their main function is skeletal, giving both strength and flexibility to the algal tissue (Skjåk-Bræk, 1992). These polymers have found great industrial use due to their ability to form a gel with divalent cations such as Ca^{2+} and Sr^{2+}.

A process for the extraction of alginates was patented originally by Stanford in 1881. However the first products from the Stanford process were very crude (they contained high levels of nitrogen; Clare, 1993). Kelco Company (San Diego) appeared to be the first to produce and to commercialise pure sodium alginates, in the 1920's. Nowadays, approximately 15 000 tonnes dry weight of alginates are processed annually from 400 000 tonnes of seaweed (Gacesa, 1988). Most of the alginates are extracted from just three of the 265 reported species of the marine brown algae. *Macrocystis* is the most common one and is harvested off the west coast of the USA. In addition *Laminaria* and *Ascophyllum* are

obtained from Northern Europe. The decision on which seaweed to process commercially is based upon the price of the raw material and its alginate content. Another important criterion is the type of alginate contained in the seaweed, since the structure of the alginate determines its performance (see I.A.2).

While seaweed is the main source of alginates, several microbial sources have also been discovered, like *Azotobacter vinelandii* and *Pseudomonas aeruginosa*. Unlike seaweed alginates, bacterial alginates are acetylated. Even though they are not at present widely used, bacterial alginates might become a viable alternative as marine pollution has produced instability in the long-term seaweed alginate supply (Ott & Day, 1995).

I.A.1.2. Manufacturing process:

Alginates from seaweeds need to undergo a series of treatments before they can be used in a suitable form, and for applications where they are required to be highly purified. The general pattern for alginate extraction is presented in figure I.A.1.2.:

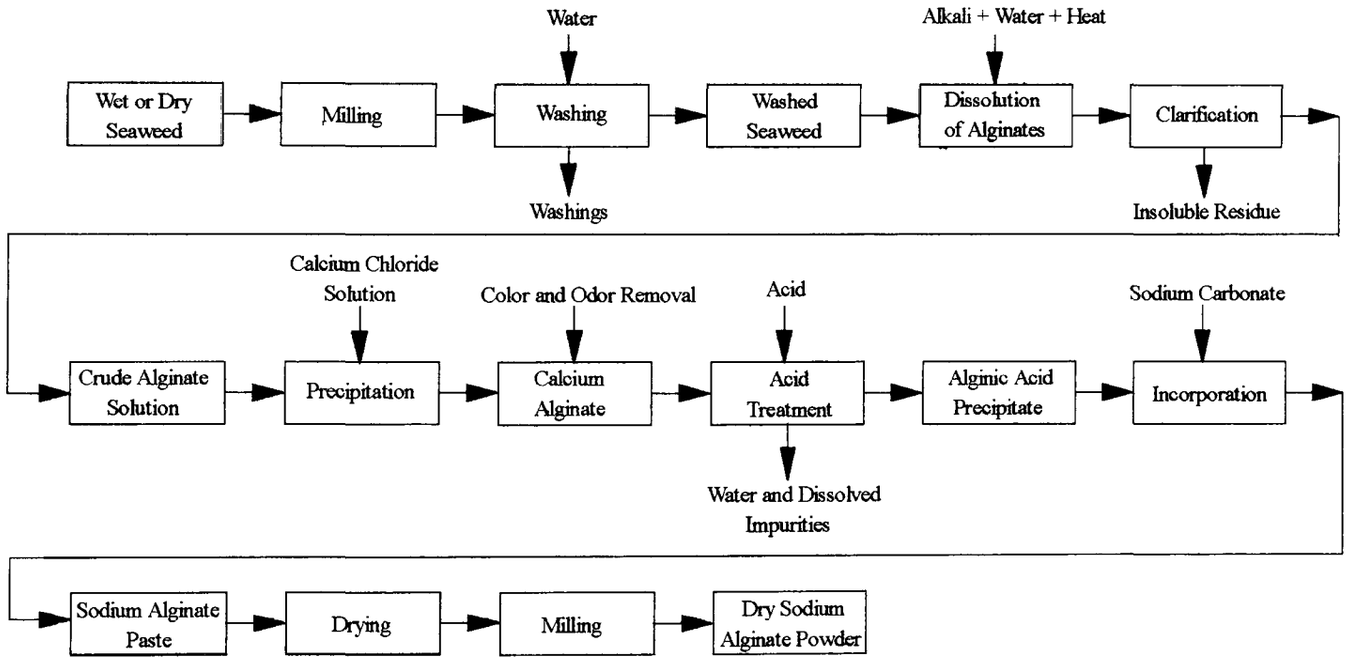

Figure I.A.1.2. Sodium alginate manufacturing process (Clare, 1993).

Since alginate salts found in seaweeds are insoluble, it is necessary to transform them into sodium alginate, which is soluble. They are then easier to process.

I.A.1.3. Major applications of alginates:

There are a number of articles dealing with various applications of alginates, thus underlying the great potential offered by this polymer. One important area of application is in the food and drinks industry, where alginates have been officially approved. They may be used as (Gacesa, 1988):

-a stabiliser against phase-separation in ice-cream or for beer (in the form of a foam);

-a viscosifier for suspension of fruit pulp, or as a thickener in sauces, milk shakes;...

-a gelling agent for the reconstitution of foods (stoneless fruit, onion rings...); gelation may be encouraged, retarded or made to be temperature dependent, by adjusting the relative proportions of additives;

-an entrapment matrix for enzymes, such as ß-galactosidase, which catalyses the hydrolysis of lactose to glucose and galactose (these two products are more digestible than lactose) (Decleire *et al.*, 1985);

-a film for the coating of fish.

Another major area of alginate application is the pharmaceutical industry. Some examples are listed below (Gacesa, 1988) :

-stabiliser for emulsions in cosmetic preparations or as a binder in tablets and lozenges;

-gelling agent for moulds for dental impressions;

-therapeutic agents in anti-acid and anti-ulcer compounds; alginate is insoluble in the presence of acid and therefore forms a protective film in the stomach lining;

-film/fibres for gastroenteric coatings for tablets or for haemostatic bandages (Ryan, 1993; Thomas, 1992); alginate in its calcium or sodium salt form has been used as a haemostat for many years. It was harvested from brown seaweeds in Scotland since the XVIIIth century for treatment of blisters and lacerations.

Kaltostat® is an example of an absorbent, haemostatic wound dressing; it absorbs blood up to 20 times its own volume. It is composed of non-woven sodium calcium alginate fibres into a flat sheet. Its low cost makes it very attractive. It was originally developed to cover exposed wounds of the skin, but other applications have been examined. Alginate has been used successfully as a dressing for skin grafts (Varma *et al.*, 1991; Porter, 1991) or for deep hand burns (Kneafsey *et al.*, 1996). The advantages of the Kaltostat® sheet are that it is porous

enough to allow the saline solution to drain through and suitable to be used over the raw wounds. Kaltostat® has also been tested in tooth extraction sockets (Matthew *et al.*, 1993), showing satisfactory healing. However, the same material inserted into mandibular third molar sockets in patients and left *in situ* (Speculand *et al.*, 1990) has presented postoperative problems. Steriseal Sorbsan®, another wound dressing made from calcium alginate fibres (Barnett & Varley, 1987), has been found to reduce blood loss successfully from skin graft donor sites (Groves & Lawrence, 1986).

The release of a macromolecule (blue dextran) from alginate gel beads has been studied by Kim & Lee (1992). They have shown that alginate beads with reproducible release behaviour can be prepared. Therefore, the alginate gel beads may be used as a potential oral controlled release system of such macromolecules as vaccines and polypeptide drugs.

Alginates have found successful applications as immobilisation agents for the entrapment of cells (Scott, 1987; Smidsrød & Skjåk-Bræk, 1990). This immobilisation procedure is carried out under very mild conditions and is compatible with most living cells. Some uses are :
-immobilisation of living or dead cells in bioreactors;
-artificial seeds for plant propagation (Fujii *et al.*, 1987) (alginate has been chosen for ease of capsule formation as well as for its low toxicity to the embryo);
-entrapment of animal cells for implantation of artificial organs;
-immobilisation of hybridoma cells for production of monoclonal antibodies;...

Finally, it has been reported that various alkali-metal alginates are extremely effective as a water/ethanol separation membrane (Kawarada *et al.*, 1990).

I.A.1.4. Wound dressings- their requirements:

This project deals with alginates in medical applications and, more precisely, as wound dressings. It is, therefore, important to consider the specification involved in such an end-use. In the early 60's, it was recognised that faster healing, with higher rate of epithelialisation (growth of cells "barrier"), was promoted by keeping the wound in a moist state. This finding was based on the fact that natural skin contains 85 % water and, thus, a dressing should try to simulate this environment. The discovery led to a new generation of wound dressings, such

as hydrocolloids. Some of their main requirements are presented below (Ryan, 1993; Horncastle, 1995):

-the dressings must quench blood or excessive exudate;

-they must be protective from further injury and infection;

-although they should remain firmly in place (by adhering to the surrounding skin), the dressings should adhere as little as possible to the surface of the wound;

-they should provide an environment for healing and prevent dehydration. According to Ryan, they should aid natural healing without being a substitute for it. By contrast, Horncastle reckons that wound dressings should not just be passive agents for natural healing processes, but a treatment in themselves (bioactive dressings);

-Horncastle underlines the necessity for a dressing to allow for gaseous interchange. However, Ryan points out that the degree of permeability of a dressing is bound to decrease dramatically in the presence of exudate. This may not enable sufficient oxygen to pass through, and thus may not have a reasonable effect on the behaviour of the wound. He also questions the extent to which oxygen is needed for wound healing.

Alginates, although known for a very long time to have special properties (gelling, haemostatic,...), regained interest in the past decades as "moist" dressings. They can be made into convenient dressings at relatively low cost. They are generally easy to use, and no prior preparation is required (such as drying of the surrounding skin). Calcium alginates interact with the wound exudate to form a moist and non-adherent gel. Absence of wound leakage has been observed, compared with hydrocolloid dressings (Porter, 1991). Complete removal of alginate dressings is possible using saline solution or weak alkali (Clare, 1993), and causes minimal pain (Dawson *et al.*, 1992). The haemostatic properties of alginates will be described further in section I.A.2.8.

I.A.2. Structure and properties of alginates

I.A.2.1. Molecular structure:

Alginates are the salt forms of alginic acid, the most common of these salts being sodium alginate and calcium alginate. Alginates are a family of unbranched binary copolymers, β-D-

mannuronic acid (M) and α-L-guluronic acid (G), linked together by -β 1,4 and -α 1,4 glycosidic bonds respectively. The M and G blocks are illustrated in figure I.A.2.1.a.

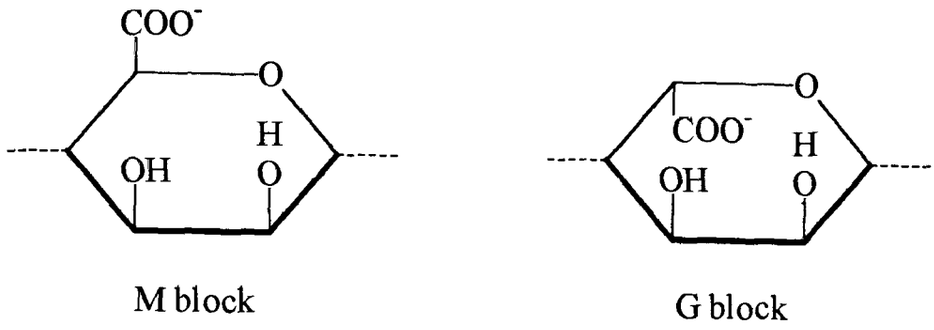

Figure I.A.2.1.a. The M and G blocks (Aspinall, 1982).

A more usual representation is shown in figure I.A.2.1.b., for a fragment of an alginate chain.

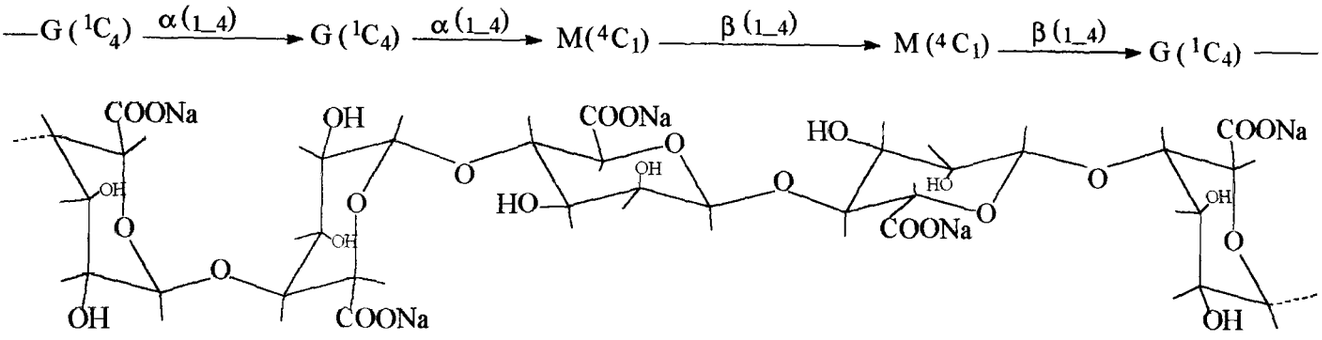

Figure I.A.2.1.b. Molecular structure of sodium alginate (Smidsrød & Skjåk-Bræk, 1990).

The $^4C_1$ and $^1C_4$ conformations refer to the chair form. The two numerals represent the carbon atoms which are above and below the plane of the ring (containing the atoms O, C(2), C(3) and C(5)), respectively, when the ring is viewed so that the numbering appears clockwise from above.

The two monomers are arranged in homopolymeric blocks (M-blocks and G-blocks) as well as in alternating MG-blocks (Haug *et al.*, 1967b). Alginates do not have any regular repeating unit. They are of widely varying composition and sequence, depending on the organism and tissue they are isolated from (Smidsrød & Skjåk-Bræk, 1990). A progressive increase has been observed in the G content through the series frond, stipe, unattached haptera and attached haptera in the alginate *Laminaria digitata* (shores of Britain). Seasonal variations are also observed, with a higher M content at times of rapid growth (Stockton *et al.*, 1980b).

Differences in the block contents have been observed from one type of algae to another one : *Ascophyllum nodosum* and *Macrocystis pyrifera* have relatively low G content (35 to 42%) while some parts in *Laminaria hyperborea* have a G content between 65 and 75% (as given by Pronova Biopolymers a.s).

The two uronic acids (M and G) adopt different conformations, independently of their nearest neighbouring unit (Atkins *et al.*, 1970; Skjåk-Bræk, 1992), with the carboxylic group COO in a favoured equatorial position. It has been found by conformational analysis that the rotation around the glycosidic linkages is severely restricted; this may explain the highly extended molecule and the high degree of mechanical inflexibility in the polymer chain observed (Smidsrød, 1974). Regions where ß-D-mannuronic acid predominates form an extended ribbon structure, whereas those rich in α-L-guluronic acid form a buckled chain (Gacesa, 1988).

I.A.2.2. Biosynthesis:

As shown below in figure I.A.2.2., the basic pathway for synthesis is now well established:

Fructose 6-phosphate
⇓ Phosphomannose isomerase
Mannose 6-phosphate
⇓ Phosphomannomutase
Mannose 1-phosphate
⇓ GDP mannose pyrophosphorylase
GDP mannose
⇓ GDP mannose dehydrogenase
GDP mannuronate
⇓ Alginate polymerase
poly-D-mannuronate
⇓ Mannuronan C-5-epimerase
Alginate

Figure I.A.2.2. Biosynthesis of alginate (Gacesa, 1988; Skjåk-Bræk, 1992).

But there is still some controversy concerning both the connection of intermediates into the pathway and the final stages of modification (Larsen *et al.*, 1969). The C-5 epimerase is known to be capable of converting D-mannuronic acid into L-guluronic acid residues. But the precise step at which epimerisation occurs in the seaweeds is still unclear. While in bacteria, there is little doubt: the initial polymeric product is poly D-mannuronic acid, and it is subsequently modified to produce the final alginate containing both M and G blocks. Little is known about this reaction mechanism except that the epimerase leads to an exchange of the C-5 proton on the uronic acid with the solvent (Larsen & Grasdalen, 1981; Skjåk-Bræk *et al.*, 1986a).

Alginates modified with the C-5 epimerase (from *Azotobacter Vinelandii*) have been used (Skjåk-Bræk *et al.*, 1986b) to produce polymers with a high content of guluronic acid, and therefore to improve the gel forming ability (see Section I.2.4). The enzyme requires calcium ions both for its activity and for the stability of the gel.

I.A.2.3. Gelation:

i. Gel formation- The "egg-box" model:

In most of the applications listed in section I.A.1.3., alginates are used because of their ability to form a gel. Therefore, it is of primary importance to study this gelation phenomenon. By definition, a gel is a three dimensional network of molecules which is held together by junction zones entraining the soluble and aqueous media to resemble a solid. Gelation in alginates occurs in the presence of most divalent metal cations (except Mg^{2+}). From light scattering and viscosity measurements, Clare (1993) proposed that the magnesium ions were involved preferably in intramolecular crosslinks within the alginate molecules, rather than intermolecular ones, thus leading to solubility. The gelation model now presented is for calcium alginate gels, which are the most extensively studied, as they are used in both food and medical systems.

NMR and circular dichroism studies (Grant *et al.*, 1973, Rees, 1972; Wang *et al.*, 1993) suggested that firstly, the Ca^{2+} ions were bound to the G blocks until the available binding sites were saturated. Then binding by the M blocks proceeded (at least at the microscopic level, and especially when their neighbouring units were G residues) until chain-association

was constrained by the network. These observations can be explained as follows. The M and G blocks differ in their ability to form junction zones with Ca^{2+} ions. They are both polyanionic and will form intermolecular ionic bonds with divalent cations. However, G blocks are also able to chelate Ca^{2+} because of the spatial arrangement (forming a binding site between two adjacent G blocks), thus creating a stronger type of interaction (Gacesa, 1988). Dimeric junctions are formed rather than aggregates. This is known as the "egg-box" model (Grant *et al.*, 1973; Bryce *et al.*, 1974), a commonly accepted model, where the Ca^{2+} ions are the "eggs" within the "egg-box" formed by the guluronic acids. By contrast, the M blocks lead to a much flatter structure with more shallow "nests" for the cations to occupy.

The "egg-box" model is illustrated in figure I.A.2.3.

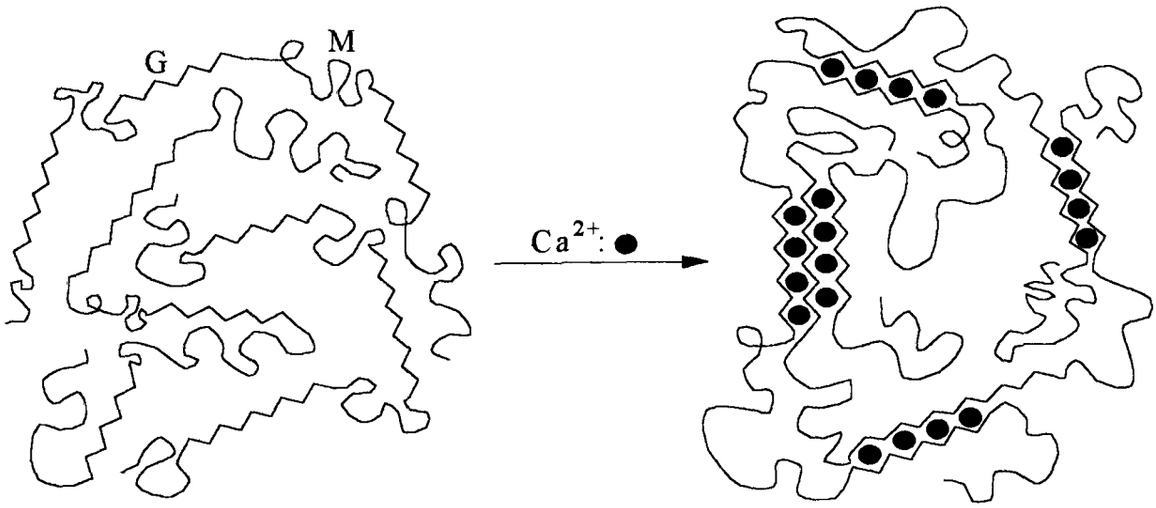

Figure I.A.2.3. The "egg-box" model.

This type of association is co-operative because binding of the first cation between any pair of chains causes alignment which facilitates binding of the next, and so on along the sequence. Therefore the gel forming properties are mainly related to the content and the length of the G blocks in the alginates. There is a minimum length of G blocks needed for the formation of a junction, and the average length of these junction zones is of the order of 20 monomer units (Stokke *et al.*, 1991 & 1993). Ca^{2+} binding increases rapidly between 18 and 26 L-guluronic acid units, although L-guluronic acid alone does not bind Ca^{2+} ions (Clare, 1993).

Commonly defined parameters to describe the gel forming ability are the ratio of the two uronic acids, M/G, and the percentages of G diads (GG) and triads (GGG) (determined by NMR spectroscopy).

A different type of interaction has been observed with metal ions such as Cu^{2+}, Co^{2+} and Mn^{2+}, during gel formation (Wang *et al.*, 1993). Here a sol-gel transition is characterised by a complex formation in which only the carboxyl groups (in both mannuronic and guluronic acids) are co-ordinated to the metal ions.

ii. Gel preparation:

There exists several methods to prepare an alginate gel. The main ones are based on calcium ions:

-the dialysis/diffusion method is the most common because it is the simplest method. An aqueous alginate solution is gelled by diffusion of calcium ions from an outer reservoir (usually $CaCl_2$). This forms a spatially inhomogeneous gel, with a higher concentration of alginate in the region which first comes in contact with the Ca^{2+} ions. Inhomogeneity seems to be favoured by factors such as a low concentration of Ca^{2+}, low molecular weight, high concentration of alginate and high L-guluronic acid content (Skjåk-Bræk *et al.*, 1989). The main drawback of this method is that it is limited to relatively thin strips of gelled products due to slow diffusion rates (Clare, 1993).

-the *in situ* gelation (Draget *et al.*, 1991), used to produce larger shapes. By this method, a defined supply of Ca^{2+} (calcium salt with limited solubility or complexed Ca^{2+} ions in $CaCO_3$) is mixed with an alginate solution into which the calcium ions are released, usually by addition of a slowly acting acid such as D-glucono-d-lactone (GDL). This method helps to get a homogeneous, non-syneretic gel (i.e. the gel does not undergo contraction, and exudation of water from the gel is not observed).

-the setting by cooling (Clare, 1993); this third gelation technique is based on the fact that calcium ions in solution cannot bind alginate chains at elevated temperatures. Therefore Ca^{2+} ions/alginate molecules association occurs only when the solution is cooled. The gels thus

formed are thermoreversible. This method, as well as the *in situ* gelation, leads to gel stability. Since calcium ions are available to all the alginate chains, the most energetically favoured systems are formed.

Divalent ions other than Ca^{2+}, and such as Cu^{2+}, Co^{2+} or Mn^{2+}, have been also used to prepare alginate gels (Wang *et al.*, 1993). Regarding Fe^{2+} ions, the amount of divalent cations required to produce an alginate gel may be larger than anticipated. This was thought to be due to free radical catalysed depolymerisation, leading to the production of lower molecular weight alginate that is more difficult to precipitate (Clare, 1993).

Finally, sodium alginate gel can be produced by crosslinking of calcium alginate with epichlorohydrin (ECH) and subsequently removing the Ca^{2+} ions by treatment with a sequestering agent such as ethylenediamine tetraacetic acid (EDTA) (Moe *et al.*, 1991, 1993a & 1993b). ECH crosslinks alginate by a nucleophilic attack from the hydroxyl groups giving rise to a stable gel. The long, inflexible, junction zones in the ionically crosslinked alginate gel (obtained with the two first gelation methods) are substituted by discrete, small, covalent crosslinks throughout the gel. This alginate gel is known as a superswelling material. Gel beads prepared with ECH may swell by 50 to 200 times their dry volume, without losing their integrity and spherical form

iii. Mathematical modelling of gelation:

Skjåk-Bræk *et al.* (1989) prepared gel cylinders by the dialysis/diffusion method, and derived the alginate concentration by physical sectioning of the gel, followed by weight measurements. Finally, they compared their experimental results with a theoretical model (based on the theory developed by Sherwood & Pigford, 1952). This model describes the time course of an extremely fast second-order chemical reaction between two freely diffusing species (the Ca^{2+} ions and the alginate molecules) in solution. It implies that gelling is an irreversible and stoichiometric process, with diffusion as the rate determining step. Initially, the concentration in the alginate is considered uniform. When it is exposed to a calcium solution, Ca^{2+} ions will enter by diffusion, bind to unoccupied binding sites on the alginate and form a gel state. When diffusing through an already formed gel, there is no opportunity for

Ca^{2+} to bind until it reaches available binding sites at the gel/sol interface. The gelling zone will be nearly planar, parallel to and moving away from the $CaCl_2$/alginate interface. The polymer diffusing towards the gelling zone from the opposite direction will be immobilised immediately by calcium ions in the gelling zone, and the gel will be extended. Excellent agreement between measured and calculated concentrations of alginate in the first segment of an "infinitely" long tube has been found. A similar theory with data is not available for a tube of finite length (as the gel is then inhomogeneous).

Other mathematical studies have been carried out from magnetic resonance imaging (MRI). The spin-spin relaxation times of the water protons within the gel is dependent on the alginate concentration, and this leads to a variation in the image intensity across the gel. This technique enabled Potter *et al.* (1993a & b) to visualise an inhomogeneous calcium alginate gel and to map the alginate concentration as a function of the distance along the axis of the gel, during the gelation process. One advantage of this technique is that it is non-destructive (compared with the physical sectioning method mentioned earlier). From a mathematical model (also based on Sherwood & Pigford's theory, 1952), Potter *et al.* (1994) were able to extract a diffusion coefficient for calcium ions through an alginate gel. It was found dependent on the initial concentration of calcium, the ionic strength of the alginate solution, and the size of pores in the gel which is formed. The range of values for this diffusion coefficient was between 2 and 7 10^{-4} $mm^2.s^{-1}$ (compared with 7.9 10^{-4} for self diffusion of calcium ions at infinite dilution).

iv. Selectivity coefficients:

It can be useful to evaluate the affinity of various divalent metal ions towards sodium alginate to produce gels. For this purpose, selectivity coefficients, k, have been introduced (Haug, 1959). They relate the concentrations of the sodium ion and the metal ion in question, in both solution and gel phases:

$k = [\text{metal ion in gel}][\text{sodium ion in solution}]^2/[\text{sodium ion in gel}]^2[\text{metal ion in solution}]$.

Clare (1993) has measured this parameter for various ions in two different alginates. The results are presented in table I.A.2.3.

	L. Digitata (M/G = 1.6)	*L. Hyperborea* (M/G = 0.5)
Cu^{2+}	230	340
Ba^{2+}	21	52
Ca^{2+}	7.5	20
Co^{2+}	3.5	4

Table I.A.2.3. Examples some values of the selectivity coefficient (Clare,1993).

The affinity series of alginate for various divalent cations is in the following order :
$Pb^{2+} > Cu^{2+} > Cd^{2+} > Ba^{2+} > Sr^{2+} > Ca^{2+} > Co^{2+}=Ni^{2+}=Zn^{2+} > Mn^{2+}$ (Haug & Smidsrød, 1965).

I.A.2.4. Chemical properties:

Low chemical stability is a major problem encountered in alginate use. Because alginate gels are most of the time crosslinked with calcium ions, substances with a high affinity for calcium (such as phosphate or citrate) will sequester the Ca^{2+} ions, thus destabilising the gel. The gel will also be destabilised by concentrations of non-gelling cations, such as Na^{+} and Mg^{2+} (due to an ion exchange reaction) (Smidsrød & Skjåk-Bræk, 1990). Increasing the G content will help to enhance the stability.

I.A.2.5 Physical properties:

The gel forming property is related to the content of guluronic acid in alginate. This essential physical property has already been extensively reviewed (section I.A.2.3), and will not be discussed further.

When Ca^{2+} ions are added to a sodium alginate solution, the viscosity of the mixture increases, due to the formation of a loose gel. Further addition of calcium leads to a decrease of viscosity and gel volume, followed by precipitation (Smidsrød & Haug, 1965). The critical behaviour of alginate solutions viscosity near the gelation point (using Ca^{2+}, Cu^{2+}, Mn^{2+} or Co^{2+} ions) has been studied by Wang *et al.* (1991) and found to be in good agreement with the percolation theory.

Light scattering and viscosity studies of alginate solutions and solids containing different amounts of the three types of blocks have indicated that their relative, unperturbed dimension increases in the order: MG-blocks < MM-blocks < GG-blocks (Smidsrød *et al.*, 1972b, 1973; Smidsrød, 1974). Iso *et al.*(1988) have shown, using viscosity measurements, that the G-rich sample exhibits a greater chain entanglement in solution than the M-rich sample. However, although the intrinsic flexibility of the alginate molecules in solution is dependent on the blocks, the viscosity is mainly a function of the molecular size.

After the gel formation and the viscosity analysis, the swelling of alginate gels is another important physical property to consider. Moe *et al.* (1993a & b) have studied the swelling of covalently crosslinked sodium alginate gels. The ionic contribution seems to be the main determining factor for the solution uptake of these gels. They used maximum gel volume measurements to evaluate the crosslink density of the alginate gels. The swelling of gels is supposed to increase with decreasing crosslink density.

While high-G alginates exhibit high porosity and low shrinkage during gel formation, high-M alginates shrink and their porosity is reduced. Another fact concerns the gel transparency. Highly transparent gels are achieved using an alginate with a guluronic content greater than 60 % (Smidsrød & Skjåk-Bræk, 1990); by contrast, samples containing predominantly M blocks present a high turbidity. Finally, calcium alginate gels are, in contrast to other algal gels (like carrageenan and agarose), thermostable in the temperature range 273-373 K (Gacesa, 1988).

I.A.2.6. Mechanical properties- Gel strength:

An important feature to consider, when working on alginate gels, is the gel strength. Most of the work reported on this property concerns calcium/sodium salts, prepared by the dialysis/diffusion gelation method. Several parameters have been found to influence the gel strength. One of them includes the composition and sequence of the monomers. As a general trend, it has been observed that the high-G alginate gels are strong, brittle and have excellent heat stability. By contrast, high-M alginates produce gels with medium-to-low strength, which are softer and more flexible. Samples rich in alternating blocks are characterised by low modulus and high volume (Smidsrød, 1974). The function of the MG blocks seems therefore

to be more to bind water than to form junctions; this may be due to their high flexibility.

If the M/G ratio is an important parameter to examine, so is the calcium content. Clare (1993) has summarised the effect of both on gel strength in a graph, reproduced below:

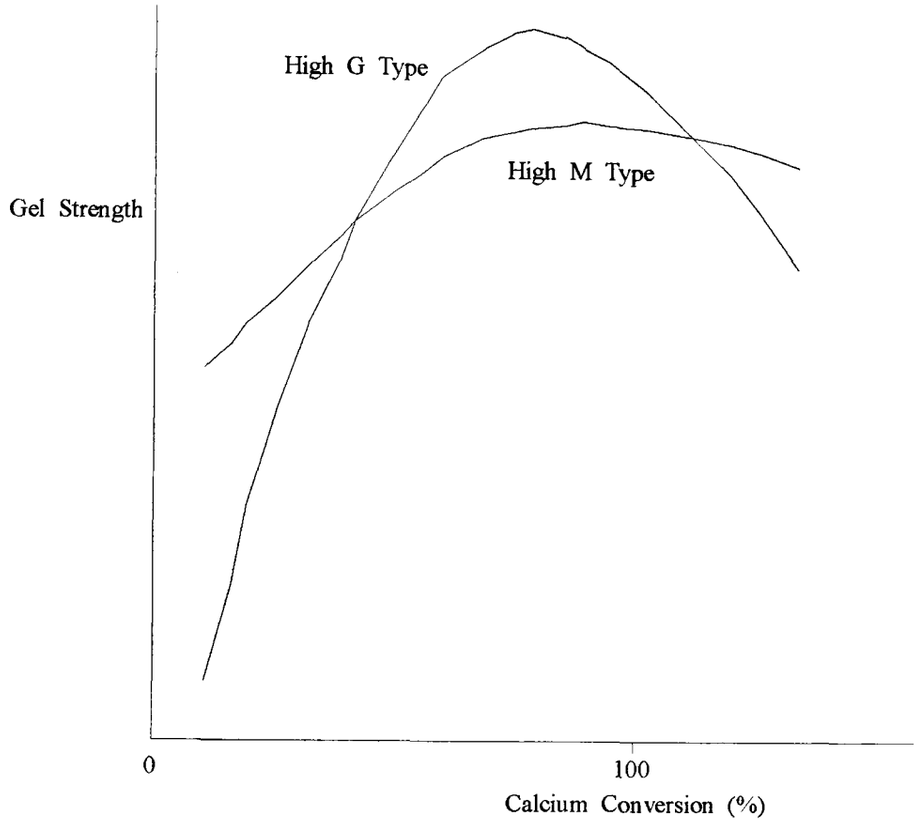

Figure I.A.2.6. Gel strength as a function of calcium conversion and alginate type (Clare, 1993).

The calcium conversion refers to the ratio of calcium ions to sodium alginate; for example, a molar ratio of 0.5 (when the sodium salt is fully converted into a calcium salt) gives a calcium conversion of 100 %. At low calcium content, the co-operation between Ca^{2+} ions and the alginate molecules is more pronounced for the high-M sample, leading to higher strength. At higher calcium levels, all the G blocks are already filled with calcium in the high-M sample, and little change is observed in the gel strength. By contrast, the high-G alginate displays a maximum strength close to 80 % conversion.

Gel strength has also been found to depend on the molecular weight of alginates. For high-G samples, Martinsen *et al.* (1989) observed an increase of the gel strength with increasing

molecular weight of the alginate (as determined from the intrinsic viscosity), until this latter reached the value of 2.4×10^5. Above this value, the gel strength became independent of the molecular weight. Other influential parameters with respect to the gel strength include the alginate concentration and the temperature. Martinsen *et al.* (1989) noticed an increase in gel strength with increasing alginate concentration. Discrepancies arise in the literature, regarding the effect of the temperature. Segeren *et al.* (1974) prepared gels using D-glucono-δ-lactone and dicalcium orthophosphate; they found that the storage modulus was proportional to the temperature in the range 295-322 K. By contrast, Andresen & Smidsrød (1977) found that the elastic moduli (determined by compression) of gels (prepared by dialysis/diffusion) decreased with increasing temperature. From these conflicting observations (which may be due to the different gel preparations), it seems that the application of the rubber elasticity theory to alginate gels is questionable.

Other observations are outlined below:
-the parts of the alginate molecules between the junctions are very restricted in their movement so that the energy applied for compressing the gels is partly used to rupture junctions (Smidsrød, 1974);
-Andresen & Smidsrød (1977) have observed that the modulus of elasticity of calcium alginate gels and lead alginate gels increases with time after preparation. Therefore it is suggested that the crosslinking reaction continues after the gels are set, confirming that alginates are non-equilibrium gels. The rate of ageing is markedly temperature dependent. Andresen & Smidsrød (1977) have also suggested that the junctions are "weak points" in the gels, and that even small deformations can cause partial rupture;
-above a certain threshold concentration, the gel strength increases in proportion to the square of the alginate concentration (Smidsrød, 1974, Smidsrød *et al.*, 1972a), and this indicates a bimolecular mechanism for junction formation (Martinsen *et al.*, 1989);

However, most of these studies were carried out on alginate beads or small cylinders. Moe *et al.* (1994) have analysed wet calcium alginate fibres under stretching, and observed some differences in the gel strength behaviour. Firstly, the modulus they measured on the fibres increased with increasing alginate molecular weight. This was apparent over a larger molecular weight range than for alginate gel cylinders and beads. Secondly, the modulus for

the low-G alginate fibres was considerably higher than for the high-G alginate (of the same intrinsic viscosity). The opposite trend is observed for gel beads. The weaker chain-chain interactions present in the high-M alginate are believed to allow for a better alignment of the polymer molecules, which in turn gives rise to a higher strength in the fibre axis.

There have been a wide range of experiments designed to measure the gel strength of alginates. These include:

-compression of alginate beads (Smidsrød *et al.*, 1972a; Martinsen *et al.*, 1989);

-measurement of the amount of water (converted to force per unit area) necessary to turn a blade 30 degrees within the alginate gel (Draget *et al.*, 1993);

-low deformation stretching for alginate fibres (Moe *et al.*, 1994).

-dynamic measurements leading to the storage modulus (use of a rheometer) (Draget *et al.*, 1993).

I.A.2.7. Degradation of alginates:

Haug *et al.*(1963) have suggested that above pH=10, the increased rate of degradation is due to an increase in the rate of a ß-elimination, while at pH values less than 5, a proton-catalysed hydrolysis is responsible for the rapid degradation.

Alginate lyases have been isolated from a wide range of organisms, including bacteria, marine fungi, molluscs and brown seaweeds. According to Gacesa (1988), these alginate enzymes are invariably specific for either the ß-D-mannuronic acid or the α-L-guluronic acid linkage. By contrast, Larsen *et al.* (1993) suggested that the enzymes prepared from *Bacillus circulans* degraded both block types, although with different efficiency. They are typically endo in their mode of action (Gacesa, 1988). So far, most of the alginate lyases that have been reported are ß-eliminases. Lyases are able to degrade the polymer to produce oligosaccharides containing the unsaturated product 4-deoxy-L-*erythro*-hex-4-ene pyranosyluronate. The proposed mechanism of the lyases action is based on a three-step reaction, comprising :

(i) the removal of the negative charge on the carboxylate anion (COO^-),

(ii) a general base-catalysed abstraction of the proton on C(5) and finally,

(iii) a ß-elimination of the 4-*O*-glycosidic bond (Gacesa, 1987).

I.A.2.8. Biocompatibility:

The main concern when considering alginate as a dressing material is its contact with wounds, and therefore its blood compatibility. Alginates are highly absorbent gel-forming materials with haemostatic properties. In contact with blood, calcium alginate releases Ca^{2+} ions in exchange for sodium ions. This stimulates platelet activation and clotting factors (VII, IX and X; Kneafsey *et al.*, 1996), and shortens the blood coagulation time (compared with surgical gauze) (Jarvis *et al.*, 1987). The sodium alginate salt is then known to break down to simple monosaccharide residues and to be totally absorbed by dissolution. Any residual fibres remaining within the wound are therefore biodegradable; this eliminates the need for complete removal (Barnett & Varley, 1987). Mayer *et al.* (1987) analysed the biological activity of sodium alginate on tumor-bearing mice. The sodium salt presented no effect on tumors, no significant *in vitro* cytotoxycity, and it was relatively non-toxic.

Attempts have been made to use alginate sheets in dental surgery. A concern about any absorbable dressing in a tooth socket or bony cavity in the jaw is the long-term behaviour of the material during bone healing and the tissue reaction. Although alginates are known to be efficient haemostatic agents generally well tolerated, when they are used in cavities, the ratio of alginate to wound fluid becomes critical, particularly in the latter stages of healing (Barnett & Varley, 1987).

Rosdy & Clauss (1990) have studied different dressings, checking that they permit reepidermization of superficial wounds (i.e. that they do not interfere with the proliferation and migration of epidermal cells). To this end, they have performed cytotoxicity (toxicity towards cells) tests. Some of these tests showed that Kaltostat® (sodium/calcium alginate non-woven fibres) was cytotoxic *in vitro* to fibroplasts and epidermal cells by either direct contact or via the extraction medium. Steriseal Sorbsan® (made of calcium alginate fibres) induced cytotoxicity by direct contact (exclusively because of an excessive acidity), but its extraction media was not found cytotoxic. Matthew *et al.* (1994) have complemented Rosdy & Clauss *in vitro* studies by performing experiments in a clinically analogous situation (on dogs). This work suggested that the haemostatis in shallow oral mucosal wounds was more effective with Kaltostat® gauze than with standard surgical gauze. However, there was no significant difference in the rate of epithelial repair between the test and the control sites, nor

in the area of the resultant scar. Therefore Kaltostat® did not accelerate mucosal wound healing.

Antitumor activity has been found to be related to the content of uronic acids (using NMR; Fujihara & Nagumo, 1992), concluding that alginates have a higher antitumor activity as the MM block content increases.

The prolonged contact of alginate with body fluids requires a statement on its toxicity. A daily consumption of 25 mg/kg body weight can produce speckling of teeth. In practice, this dose is unlikely to be attained unless very large wounds are treated (Groves & Lawrence, 1986).

SECTION B: INTRODUCTION TO OTHER POLYSACCHARIDES

I.B.1. Pectins

Pectins are, like alginates, natural polysaccharides. They are found in the peel of many fruits and vegetables, where they act as cellular binders. Here the pectins are insoluble because of their high molecular weight. They are traditionally used as gelling agents in the jam industry. The following paragraphs present in more detail pectins and their uses.

I.B.1.1. Manufacture:

Pectins are mostly extracted from citrus peel, which contains about 25 % of the polysaccharides. The manufacture of high methoxyl pectins has been extensively described (El-Nawawi & Heikal, 1995; Keller, 1984a). The most common method employs alcohol precipitation. First, pectins are extracted from lemon peel at 323-373 K with an acid solution. The extract is separated from the insoluble plant material by filtration; precipitation with alcohol follows. It is then washed in more alcohol solution to remove inorganic acid and sugars from the raw materials. The pure pectins are finally dried, milled and may be standardised with sucrose or dextrose to lead to defined firmness of the resultant gel.

Low methoxyl pectins are obtained from high methoxyl pectins via de-esterification. This can be achieved by either chemical (leading to random esterification pattern) or enzymatic methods (leading to regular sequences of esterified and non-esterified residues) (Thom *et al.*, 1982).

I.B.1.2. Molecular structure:

Pectins usually exist as branched polymers. Their backbone is based on linear partially methoxylated sequences of $\alpha(1\rightarrow4)$ linked D-galacturonic acid residues, and will typically account for 65-80 % of the material. The molecular structure of these groups is sketched in figure I.B.1.2. They are interrupted by L-rhamnose residues (which contain branches). The side chains are composed principally of neutral sugars, such as rhamnose, arabinose or galactose (Keller, 1984a; Morris *et al.*, 1980).

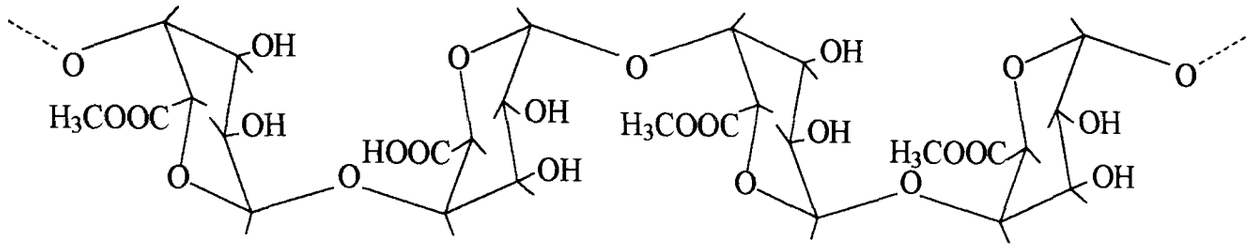

Figure I.B.1.2. Molecular structure of pectin (degree of methoxylation = 75 %) (Keller, 1984a).

Comparison of the galacturonic acid groups of pectin and the guluronic acid groups of alginate reveals that they are almost complete mirror images, with the exception of the configuration at C(3) (Thom *et al.*, 1982).

An important parameter in the description of pectins is the degree of methoxylation, DM (also called degree of esterification, DE). It represents the number of esterified carboxyl groups calculated as the percentage of the total number of galacturonic acid units. Pectins with more than 50 % of the carboxylic groups (on the galacturan units) esterified with methyl alcohol are termed high methoxyl (H.M.) or high ester pectins. By contrast, low methoxyl (L.M.) pectins contain less than 50 % of methoxylated units. The highest DM for citrus pectin is around 75 % (Keller, 1984a).The remaining free acids are usually in the Na^+ or K^+ salt form.

Filippov (1984) has developed a method to determine the fractions of free, metal-ion bound and methylated carboxyl groups in pectin samples, derived from infrared spectroscopy. This is based on the ratio of the absorbances of the bands at 1610 (COO^- stretching) and 1740 cm^{-1} (C=O stretching). For this purpose, the original pectin sample, as well as the pectin treated in $CaCl_2$, need to be scanned. In the latter, all the hydrogens in the non-ionised carboxyls are assumed to be replaced by calcium ions.

Walkinshaw & Arnott (1981) have performed X-ray diffraction on uniaxially oriented fibres of pectinic acid and calcium pectate. The diffraction patterns revealed only local ordering. They modelled pectinic acid chains as 3_1 helices containing the O(2)...O(6A) hydrogen bond. A parallel arrangement of pectinic acid chains seemed to provide the best way of packing. It

was suggested that this structure was stabilised by hydrophobic binding from columns of methyl groups as well as by specific intermolecular hydrogen bonds. For the calcium pectate, the main interactions between chains seemed to be bridges formed by Ca^{2+} ions, including also oxygen atoms.

I.B.1.3. Gelation process:

Two distinct gelation phenomena are observed, whether we are dealing with H.M. or L.M. pectins.

For the high methoxyl pectins, gelation is achieved with a low pH (< 3.5) and a high soluble solids content (at least 55 % sucrose). The low pH induces hydrogen bonding (and minimises intermolecular electrostatic repulsion); an optimum is obtained at pH = 2.8 (Keller, 1984a). This hydrogen bonding prevents high methoxyl pectin gels from thermal or mechanical reversion. As for sugars (i.e. soluble solids), they suppress the solubility of pectins (i.e. leading to low water activity), and promote chain-chain (or hydrophobic) rather than chain-solvent interactions, thus favouring gel formation (Keller, 1984a; Thom *et al.*, 1982). The methoxyl groups (low charge density) are the ones contributing predominantly to chain interaction. Finally, the junction zones have been suggested (Morris *et al.*, 1980) to contain large aggregates of esterified chain regions.

In the low methoxyl pectins, the carboxylic acid groups provide negative charge and strong affinity for metal ions. Therefore, gelation is mainly controlled by the reaction of divalent cations (generally Ca^{2+}) with the free acid groups. Thom *et al.* (1982) have shown, by circular dichroism, that calcium pectate gels present a two-fold structure. Therefore the main type of binding between calcium ions and the pectin molecules is the same as for alginate molecules, i.e. the "egg-box model". However, X-ray diffraction studies on the solid state have exhibited a three-fold conformation (this change responds to packing constraints and to more favourable hydrogen bonding possibilities in the condensed phase). The non-esterified galacturonate blocks are the important sequences for calcium binding, and a very limited number of chains are involved in the junction zones. The gels obtained are reversible, and of ionic type. Binding with calcium ions is dependent on the temperature, the percentage of soluble solids and the calcium content.

When high methoxyl pectins contain blocks with consecutive non-esterified carboxylic acid groups, it is possible to induce gelation of H.M. pectin with Ca^{2+} ions. It is also possible to prepare low methoxyl pectin gels without divalent cations, providing the pH is low enough.

I.B.1.4. Other properties:

Degradation can occur as a function of pH. At a pH lower than 2.5, hydrolysis or de-esterification may take place (depending on the temperature). At a higher pH, a process of β-elimination may occur, reducing the molecular weight. Above pH = 6, this process occurs at room temperature.

Gel strength for H.M. pectins increases with ester content up to a level close to 70 % (Morris *et al.*, 1980). Surprisingly, a sharp reduction is observed for degrees of esterification greater than 80 %. For L.M. pectins, the gel strength increases up to an optimum with increasing level of calcium.

I.B.1.5. Applications:

Pectins are almost exclusively used in the food industry. They are important emulsifying, gelling, stabilising and thickening agents. About 75 % of the pectins produced are used in making fruit jams, jellies, marmalades, and similar products. Additional uses include the preparation of mayonnaise, salad dressings, ice cream, and the stabilisation of acidified milk drinks. In many food products, the use of pectins as stabilisers is preferred, since they blend better into the flavour complex than do many gums or starches. Pectins also have a limited number of non-food uses, including pharmaceuticals and cosmetics.

I.B.2. Carboxymethylcelluloses (CMC's)

Cellulose is the principal constituent of the cell wall of plants. CMC's are derived from cellulose, and their properties and uses are now described.

I.B.2.1. Manufacture:

The raw materials used to prepare CMC's may be derived from cotton linters or wood pulp.

CMC's are then manufactured from celluloses via a two-step process (Keller, 1984b). In the first step, celluloses are steeped in strong alkali to open the tightly bound cellulose chains (held together by hydrogen bonding), allowing water to enter. The swollen celluloses are then reacted with sodium monochloroacetate to give sodium carboxymethylcelluloses. The reactions are detailed in figure I.B.2.1.

$$R\text{-}OH + NaOH \rightarrow R\text{-}ONa + H_2O,$$

$$R\text{-}ONa + Cl\text{-}CH_2\text{-}COONa \rightarrow R\text{-}O\text{-}CH_2\text{-}COONa + NaCl$$

Figure I.B.2.1. Manufacture of CMC (R: anhydroglucose unit (see I.B.2.2.)).

I.B.2.2. Molecular structure:

Cellulose is a linear carbohydrate, composed of anhydroglucose units, and each monomer contains three hydroxyl groups. Carboxymethylcelluloses (CMC's) are obtained from cellulose, with some of the OH groups serving as reaction sites for the introduction of carboxymethyl groups, as seen in the previous section. The molecular structure of sodium CMC is depicted in figure I.B.2.2.

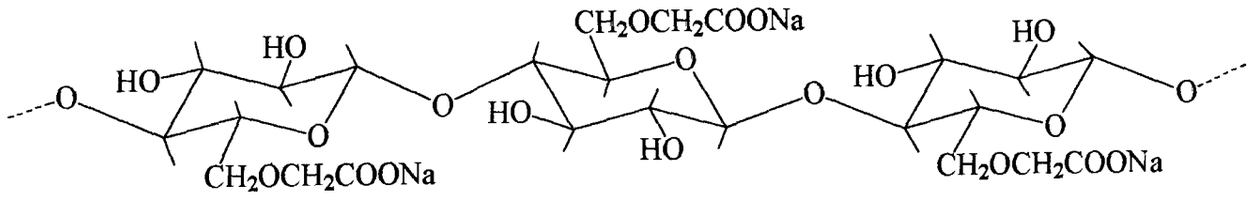

Figure I.B.2.2. Molecular structure of carboxymethylcellulose (degree of substitution = 1) (Baar *et al.*, 1994).

The degree of substitution, DS, is an important parameter for CMC characterisation. The DS of the sodium CMC shown in figure I.B.2.2. is 1; if each monomer had another hydroxyl substituted, then the DS would be equal to 2. The minimum DS required to get CMC in solution is 0.4, and the maximum DS which can be obtained is 2.0.

I.B.2.3. Main properties:

Most CMC properties are dictated by the degree of substitution and its uniformity along the

polymer chain. If the DS is increased, or if the uniformity of substitution is enhanced, the CMC's become more soluble, and their compatibility with other ingredients is higher. The uniform charge distribution along the polymers results in mutual repulsion of the chains at all points for better solubility (this is called Coulombic repulsion), and it keeps the chains in an extended form.

pH is another important factor to be considered. With acidic pH (< 3), sodium CMC, the salt form, reverts to carboxymethyl cellulose, the free acid form, which is insoluble (due to increased intermolecular interactions). At pH > 10, cellulose gum undergoes viscosity loss (Keller, 1984b)

Proper care must be taken when dissolving CMC's as the particles tend to aggregate when entering the water. This is made easier by using a low CMC percentage, and by agitating the system vigorously. As a general rule, lower DS types are more difficult to dissolve than higher DS types (Keller, 1984b). CMC solutions are pseudo-plastic (the viscosity decreases as the rate of shear increases). However, if the shear stress is removed, the solution will revert to its original non-flowing viscosity.

CMC's are compatible with a range of food ingredients including protein, sugar, starches and other hydrocolloids; they are also compatible with most monovalent salts. They precipitate and become hazy with divalent and trivalent cations; the polyvalent ions function as crosslinking agents. Several metal chelates have been studied, including Cr^{3+} (El-Saied *et al.*, 1994), Cu^{2+} and Ni^{2+} (Hosny *et al.*, 1995) and Co^{2+}-CMC (Abdel-Hadi *et al.*, 1994). Binding between the metallic cations and the cellulose usually involves the carboxymethyl groups as well as the hydroxyl groups. The degree of substitution is found to influence the chelation process.

As far as stability is concerned, CMC's are susceptible to breakdown from cellulases (enzymes that hydrolyse cellulose) originating from microbiological or other sources (Keller, 1984b).

I.B.2.4. Applications:

CMC's have found substantial application in the food industry such as in doughnut and cake mixes, frostings and icings, pie fillings, dairy products, pet foods, etc... CMC's must be 99.5% pure for food grade, and the most common DS value is 0.7. One of the most important reasons for using CMC's in many foods is their ability to serve as a water binder for prevention of syneresis. CMC's are also used in paints, pharmaceuticals, cosmetics, toothpaste, petroleum, paper, cements, adhesives and textiles (Keller, 1984b).

Sahin & Saglam (1994) have shown that sodium CMC is able to reduce the formation of post-operative adhesions in rat uterine horn. Improved results are obtained when the sodium CMC is used in conjunction with low molecular weight heparin.

I.B.3. Mixed polysaccharides systems

Investigations on alginate/pectin blends have revealed that these systems may be induced to gel at low pH (less than 4), under conditions where neither alginate nor pectin alone would gel. The formation of these gels is relatively independent of the sugar level (Toft, 1982). However, the presence of calcium ions has been found to be deleterious to the gelling of the mixture (Thom *et al.*, 1982; Clare, 1993). Calcium sequestrants can be used to offset this problem in most circumstances.

The common way to prepare these gels is to mix the components at high temperature, to acidify the blend and to allow gelation to occur on cooling. Morris & Chilvers (1984) have also derived a cold-setting technique, using a slow acidifier (Glucono-delta-lactone). The strongest gels are formed with high-G alginate and H.M. pectin, the optimum ratio being 1:1 (Toft, 1982). These are heat resistant and thermoreversible (Clare, 1993). Soft spreadable gels are produced with L.M. pectin and a small addition of alginate. It has been proposed, on the basis of circular dichroism studies, that gelation involves intermolecular binding between methyl esterified polygalacturonic acid blocks and polyguluronic acid blocks (Thom *et al.*, 1982). Molecular model building suggested that these blocks are packed together in a parallel, two-fold symmetry structure, with no cavities between the polymer chains (unlike the

homotypic functions). Each methyl group of pectin can be opposed to the hydrogen atoms attached to C(1) and C(2) of guluronic acid residues in such a structure, minimising their interactions with water.

By contrast, no work on alginate/CMC blends has been found in the literature to date.

Another polymer commonly found in polysaccharide systems is chitosan. It is readily derived by deacetylation of chitin which is naturally abundant (in crustacean shells). Chitosan has been found to form strong polyelectrolyte complexes with alginate (Polk *et al.*, 1994; Matsumoto *et al.*, 1993) as well as with CMC (Argûelles-Monal *et al.*, 1993), due to the combination of anionic (alginate and CMC)/ cationic (chitosan) character. The most common uses of these complexes are as controlled drug delivery systems and as encapsulation.

Pectin and CMC have been used in wound dressings such as Granuflex®. This dressing consists of a hydrocolloid layer of pectin, gelation and sodium CMC with a backing of polyurethane foam covered with a polyurethane film. It has been used with success on acute and chronic wounds (Forshaw, 1993).

SECTION C: CHARACTERISATION OF POLYSACCHARIDES

I.C.1. Spectroscopic studies

In order to get information about molecular structure and strength of bonds between atoms for a given material, a range of spectroscopic techniques is available. The knowledge of the molecular structure enables in turn to understand some properties on a macroscopic level.

I.C.1.1. Fourier transform infrared spectroscopy (FTIR):

Fourier transform infrared (FTIR) spectroscopy is the most common method for molecular structure analysis. It involves the twisting, bending, rotating and vibrational motions of atoms in a molecule. Upon interaction with infrared radiation, portions of the incident radiation are absorbed at specific wavelengths by the sample. The multiplicity of vibrations occurring simultaneously produces a highly complex absorption spectrum which is unique for each material (Willard *et al.*, 1988). It is important to realise that vibrations in a molecular system are not isolated from each other. This is even more evident for complex molecules such as polysaccharides which contain many C-C and C-O bonds that have similar force constants and masses (Aspinall, 1982).

IR frequencies commonly encountered in polysaccharides are shown in table I.C.1.1.:

Group	Wavenumber (cm^{-1})	Vibrational mode
O-H (free; monomeric)	3650 - 3600	O-H stretching
(H-bonded)	3600 - 3200	O-H stretching
	1100 - 1050	O-H related deformation
C-H	2900 - 2800	C-H stretching
	1470 - 1380	C-H deformation
COOH (Monomer)	1760	C=O stretching
(Dimer)	1710	C=O stretching
COO^-	1600 - 1550	C=O asymmetric stretching
	1450 - 1400	C=O symmetric stretching
CONH (Acetamido)	3300 - 3250	N-H stretching
	3100 - 3070	N-H stretching
	1650	Amide I, C=O related stretching
	1550	Amide II, N-H related deformation
COOR	1735	C=O stretching
	1250	C-O-C stretching
S=O (Sulfates)	1240	S=O asymmetric stretching
(Sulfonates)	1200 - 1150	S=O symmetric stretching
NO_2 (Nitrates)	1640 - 1620	N=O asymmetric stretching
	1285 - 1270	N=O symmetric stretching

Table I.C.1.1. IR frequencies of polysaccharides (Aspinall, 1982).

I.C.1.2. Raman spectroscopy:

Raman spectroscopy, like FTIR, is a vibrational spectroscopy. The principal difference between these two techniques is that infrared spectroscopy detects vibrations during which the electrical dipole moment changes, while Raman spectroscopy is based on the detection of vibrations during which the electrical polarisability changes. This results in a change in the electron density distribution of the molecule; hence a different response to an electrical field is observed (Pistorius, 1995).

Gòral & Zichy (1990) performed Raman spectroscopy on materials and compounds of biological importance, and more particularly on polysaccharides such as cellulose, agarose and starch. They concluded that almost all solid specimens give spectra easily, rapidly and non-destructively. However, they did not provide any interpretation of the various spectra.

I.C.1.3. Inelastic neutron scattering spectroscopy (INS):

A third technique to analyse molecular vibrations is inelastic neutron scattering spectroscopy (INS). For this purpose, the time focused crystal analyser (TFXA) can be used. This is an inverted geometry instrument designed to minimise multiple scattering effects by using a low analysing energy (Parker, 1994).

Whether a mode is infrared or Raman active (or is inactive in both) is determined by the symmetry of the molecule. By contrast there are no selection rules for INS spectroscopy and all modes are allowed. However, modes that involve significant hydrogen displacement dominate the spectra, due to the high scattering cross-section of hydrogen. The intensity of the INS bands is proportional to the inelastic neutron scattering cross-section (σ) of all atoms involved in the mode considered. The scattering cross-sections are a characteristic of each element and do not depend on the chemical environment. σ for hydrogen is around 80 barns while that for virtually all other elements is less than 5 barns.

I.C.2. Determination of M/G, DM and DS

I.C.2.1. Determination of the mannuronic/guluronic acid ratio of alginates:

As seen previously, there exists a close correlation between properties, such as gelation, and composition of alginates. Furthermore, seaweeds show a very wide range of uronic acid percentages, depending where and when they have been harvested. Therefore, it has become necessary to have convenient methods for the determination of the proportion of the mannuronic and guluronic acids, expressed as the M/G ratio, and a knowledge of the block structure. The contribution of individual blocks to the overall structure of alginates may be quantitated by chemical or physical methods.

i. By the chemical method:

The chemical method used to determine the M/G ratio has been originally described by Haug & Larsen in 1962. It is based on hydrolysis of the alginate with sulphuric acid at 293 K, followed by treatment with 2N acid at 373 K, and subsequent separation of the uronic acid in the hydrolysate by chromatography on an anion exchange column. The amount of each uronic acid can be determined by colorimetric methods. Attempts have been made to correct the results for the different rates of breakdown of the two uronic acids (because relatively harsh conditions are required for hydrolysis, and consequently some decarboxylation occurs, particularly of the L-guluronic acid). The authors have suggested to multiply the proportion between M and G acids by 0.66.

The main advantage of this method is that it is straightforward and does not require sophisticated equipment. However, restrictions have been encountered. First, it is very time-consuming and not suitable for routine characterisation of a large number of samples. Some colorimetric reactions, like the carbazole method, consistently overestimate guluronic acid content (Penman & Sanderson, 1972). Other researchers (Grasdalen *et al.*, 1979) have suggested that the relative amounts of the two uronic acids degraded during complete hydrolysis may depend on the sequence distribution, and substantial errors may arise when corrections are attempted.

ii. By nuclear magnetic resonance spectroscopy (NMR):

In nuclear magnetic resonance (NMR) spectroscopy, certain nuclei absorb energy when they undergo transitions from one alignment in an applied field to another alignment. This enables the identification of atomic configurations in molecules (Willard *et al.*, 1988). NMR spectrometers have proved to be an efficient tool for the determination of the M/G ratio.

Yet the first attempts were rather disappointing as broad signals were obtained. The use of concentrated alginate solution to improve the signal was impossible due to the high viscosity and the chain stiffness of the polymer. However, a significant enhancement in sensitivity (giving sharper signals) can be obtained by simply raising the operating temperature (to around 373 K) (Aspinall, 1982). The key to successful NMR spectroscopy proves to be an initial, limited depolymerisation of the alginates in order to decrease the viscosity to a level

suitable for spectroscopy (because only a slight hydrolysis is used, the correction for end groups is usually negligible).

Nowadays, ^{1}H-NMR and ^{13}C-NMR have been developed into routine analytical techniques (Grasdalen *et al.*, 1979; Kawarada *et al.*, 1990; Penman & Sanderson, 1972; Wang *et al.*, 1993). The solvent commonly used is deuterium oxide (D_2O). These techniques provide information on nearest neighbour frequency (diad frequency) : F_{MG}, F_{GM}, F_{MM} and F_{GG}.

The advantage of ^{13}C-NMR over ^{1}H-NMR is that it increases the resolving power of the technique (giving rise to a wide range of shifts) although the method is less sensitive than ^{1}H-NMR (which is a problem for quantitative work). The use of ^{13}C-NMR enables the triad frequencies (frequencies of the nearest nearest neighbour) to be determined (Grasdalen *et al.*, 1977 & 1981). However, ^{13}C-NMR is less suited to routine use because it requires an extended accumulation time to obtain spectra with good resolution (Gacesa, 1988).

Grasdalen *et al.*(1981) have measured the whole range of triads by increasing the frequency from 25 to 50 MHz (which led to resolution of the diads into triads). The consistency of the values can be checked by the relation between diad and triad frequencies, which for M units are given by : $F_{MM} = F_{MMM} + F_{MGM}$ and $F_{MG} = F_{MMG} + F_{GMG}$. Later, Grasdalen (1983) has managed to get triad frequencies with ^{1}H-NMR using 400 MHz. The determination of diad and triad frequencies gives the sequential arrangements of the two uronic acids. The NMR methods may be considered superior to the chemical method because only a very moderate depolymerisation is needed. Practically, the samples may be considered as intact.

iii. By circular dichroism:

It has been shown that the circular dichroism spectrum of alginates is dependent on the M/G ratio and on the arrangement of block structures within the molecule (Gacesa, 1988; Stockton *et al.*, 1980a). One of the principal advantages of the circular dichroism approach is the very low sample requirement (around 10 mg) which may be particularly attractive in biological studies.

iv. By FTIR spectroscopy:

Mackie (1971) has attempted semi-quantitative analysis of the composition of alginate films. The areas of the bands at 808 and 787 cm^{-1}, measured directly from the infrared traces, give values which are generally in good agreement with the M/G ratios determined by the chemical method. The figures obtained from the infrared spectra are reproducible within 10 %, and apparently independent of the sample preparation. Filippov & Kohn (1974) have used KBr techniques. The composition determination is based upon the ratio of absorbances of bands at 1320 and 1290 cm^{-1}, and the ratio at 1125 and 1030 cm^{-1}. The first ratio gives a mean quadratic error of ± 3 % while for the second ratio, the error of the analysis is increased to ± 8 % .

I.C.2.2. Determination of the degree of methoxylation of pectin:

Filippov & Vaskan (1987) have developed a method enabling the determination of the content of amide, methylated and free carboxylic groups in pectin substances. This method is based on infrared spectroscopy, by measuring absorbances of peaks at 1675 ($-CONH_2$) and 1740 cm^{-1} (overlapped C=O of carboxylic and ester groups), for the same pectin film in the acid and the potassium salt form. The contents are given within 5 % error.

I.C.2.3. Determination of the degree of substitution of sodium carboxymethylcellulose:

The procedure followed by the manufacturer Aqualon to determine the degree of substitution of CMC consists of:

-purification of the sodium CMC by washing, neutralising, drying and burning;

-titration of the resulting sodium carbonate with a standard solution of sulphuric acid;

-calculation of the DS from the titration volume required.

Baar *et al.* (1994) also reported on the use of ^{13}C NMR for the determination of DS in sodium CMC samples.

I.C.3. Ion content determination

It is of prime importance to determine the ion content (usually Na^+ and Ca^{2+} for medical

applications) in polysaccharide salts as these are found to influence dramatically most of the material properties.

A first method commonly used for this purpose is atomic absorption spectroscopy (AAS). There, a combustion flame provides a means of converting analytes in solution to atoms in the vapour phase, freed of their chemical surroundings. These free atoms are then transformed into excited electronic states by absorption of radiant energy from an external source. The absorbance is measured and the concentration of the analyte is finally related to the signal (Willard *et al.*, 1988).

AAS has been widely used in alginate studies (Morris *et al.*, 1978; Skjåk-Bræk *et al.*, 1989; Smidsrød, 1974; Smidsrød & Haug, 1968). Typically the samples in the gel state are dialysed against large volumes of water to remove the excess of metal ions from the alginate. Atomic absorption spectroscopy is then used to analyse the content of ions (such as calcium) in the dialysates (Andresen & Smidsrød, 1977). Selectivity coefficients may be derived (see section I.A.2.3.iv).

Another way to determine ion content is by SEM/electron probe microanalysis. An advantage of this technique over AAS is that it enables one to obtain ion profiles. In the electron probe analyser, an energetic beam of electrons is focused by an evacuated electron optical column, onto the surface of the specimen. The electrons interact with the specimen, giving rise to the emission of primary backscattered electrons, secondary electrons, light and X-rays. The X-ray spectrum consists of a band of continuous radiation with a number of discrete lines superimposed. These lines are characteristic of the elements contained in the surface irradiated.

Wróblewski *et al.* (1987) have used X-ray microanalysis to study biological samples. They have reviewed relevant cryopreparation techniques for biological tissue. The objective of the preparation should be to preserve the distribution of the elements of interest as close to the *in vivo* state as possible.

When attempting quantitative analysis, it is necessary to apply ZAF corrections because of matrix effects (for the atomic number effect, absorption effect and fluorescence effect). The application of the ZAF corrections encounters problems in biological microanalysis. Commercially available ZAF corrections programs have been developed for metal and mineral specimens. These contain assumptions and approximations that are invalid for biological samples, because biological materials are largely composed of light elements. Furthermore, the composition of the light element matrix (H, C, N and O), which constitutes more than 90% of the freeze-dried sample, cannot be determined with conventional energy-dispersive detectors. Finally, biological bulk specimens cannot be polished and, therefore, have a rough surface which makes absorption corrections difficult.

An analysis of irregularly shaped particles (Wróblewski *et al.*, 1987) has shown that the use of the ratio of the characteristic intensity with the continuum intensity (in the same energy region) is much less sensitive to surface variations than the intensity alone. This "Peak/Background method" provides a correction for absorption effects which, in quantitative analysis of biological tissue, is the most important one. This technique is useful when studying ion distribution.

I.C.4. Surface studies

The interaction of a biomaterial with its environment occurs primarily at the material/biological fluid interface. The surface of a material is inevitably different from the bulk; surfaces will try to minimise their interfacial energy, leading to different atomic structure and chemistry. Therefore defining the nature of biomaterial surfaces is crucial for understanding interactions with biological systems and for monitoring surface reproducibility and contamination. The surface region of hydrated hydrogel polymers is generally characterised by high chain mobility, gradients in composition, heterogeneous chain lengths and unique water structuring. All of these properties also contribute to the difficulty in precisely analysing and characterising hydrogel surfaces (Ratner *et al.*, 1987).

Dynamic contact angle measurement is one of the earliest methods used to investigate surface structure, and it still yields much useful information. It is used routinely to describe wettability

or to estimate surface energy in biomaterials.

The angle taken by a drop on a solid surface results from a balance between the cohesive forces in the liquid and the adhesive forces between solid and liquid. This is generally described by Young's equation : $s_{sv} - s_{sl} = s_{lv}.\cos\Theta$ where :

-s_{sv} is the surface tension of the solid in equilibrium with the saturated vapour of the liquid,

-s_{sl} is the interfacial tension between the solid and the liquid,

-s_{lv} is the surface tension of the liquid in equilibrium with its saturated vapour and

-Θ is the equilibrium contact angle.

Theoretically, the wetting liquid must be a neutral probe, so that neither physical nor chemical interactions occur with the solid. However, it is found that for a given liquid-solid system, a number of stable angles can be measured. Two of them are relatively reproducible: the advancing angle Θ_a (the largest) and the receding one Θ_r (the smallest angle) (Matijević, 1969). This is due to hysteresis (Morra *et al.*, 1990). In general, contact angle hysteresis is caused by surface roughness, surface heterogeneity, penetration or swelling of a wetting liquid during contact angle measurements (commonly used liquids do not behave as neutral probes) (Morra *et al.*, 1990; Tagawa *et al.*, 1992). The effect of roughness is to magnify the wetting properties of the solid. Contact angle studies are generally difficult to interpret if the surface roughness is 1 μm or greater (Ratner *et al.*, 1987).

The method commonly used is based on the Wilhelmy plate, by continuously measuring the force on a plate and immersing it in a liquid. When the edge of the plate just touches the liquid, a meniscus is formed and the force on the plate increases by an amount equal to the weight of liquid in the meniscus. As the plate is immersed, the force decreases because of buoyancy. Contact angles, Θ, can be derived from the Wilhelmy relation :

$F = Pt\cos\Theta$, where F is the wetting force,

t is the surface free energy of the liquid,

P is the perimeter of the solid.

The contact angle is sensitive to the top 0.1 nm of the material. This technique offers the advantage of studying sample surfaces in different environments (while most of other surface techniques analyse the polymer-vacuum interface).

Tagawa *et al.* (1992) have performed wetting force measurements on fibrous solids, using different solvents. Deviation in contact angles has been related to surface heterogeneity. Morra *et al.* (1990) have reported a study on different polymeric films on glass. It was found that the thinnest film (15 nm) presents time dependent-contact angle behaviour while thicker ones show stable hysteresis (probably related to the confinement of the water penetration to the outermost region of the film). The effect of water interaction with a non-hydrated hydrogel was also reported. The swelling of the gel is accompanied with change of mass, dimensions and wettability as a function of time. A large hysteresis has been observed, certainly due to a rapid re-orientation of the hydrophilic groups towards the surface, when the gel is brought into contact with the water (in order to lower the solid-liquid interfacial tension).

CHAPTER II: MATERIALS AND METHODS

II.1. Description of the raw materials

II.1.1. Alginates:

The sodium alginates were prepared from strips of *Laminaria Hyperborea*, and provided as powder by Pronova Biopolymer a.s. (Drammen, Norway). They were used in this study without further purification. These polymers are highly refined products which conform to all the quality requirements of the European Pharmacopoeia.

The most extensively examined alginate was labelled: PROTANAL LF 10/60; it was characterised by an average molecular weight of 60,000-70,000 (from viscosity), and a M/G ratio of 31/69. Another alginate was investigated in order to assess the effect of the M/G ratio: PROTANAL LF 10/60 LS (M_v = 60,000-70,000; M/G = 60/40). The average sodium content was 9.3 wt% for the dry matter, as given by the manufacturer.

II.1.2. Pectin:

The pectin powder was supplied by Bulmer Pectin, Citrus Colloids Ltd (Hereford, U.K.), with the trade name Citrus Pectin USP. It is a purified high methoxyl pectin derived from citrus peel and it does not contain any diluents nor other additives. It complies with the United States Pharmacopoeia and with EEC Directives. It contained no less than 6.7 wt% of methoxy groups (dry weight), and the galacturonic acid content was at least 74 %, leading to a degree of esterification close to 55 %. The molecular weight was typically 500,000 as determined by GPC (based on literature provided by the manufacturer).

II.1.3. Carboxymethylcellulose (CMC):

The CMC was provided by Aqualon (Alizay, France) which is a division of Hercules Incorporated (New York, USA), and it was labelled Blanose 7MF. It was purified to meet the European Pharmaceutical and Food Regulations. The sodium content lay between 7.0 and 8.9 wt%, and the degree of substitution was 0.8. The molecular weight was typically 155,000 (manufacturer data).

II.1.4. Calcium chloride, zinc chloride, sodium chloride and silver nitrate:

All these inorganic salts were supplied by BDH-Merck Ltd (Dorset, U.K.) as coarse powders. They were all soluble in water.

II.1.5. Distilled deionised water:

All the water used was purified in order to eliminate as much as possible the influence of impurities (such as inorganic salts and organic compounds) on sample preparation and experimental tests. This was carried out in two stages; the water was first distilled via a high capacity, all-glass water still assembly (from BDH) to remove heavy particles. It was then passed through a deioniser, Permutit CD 100 (also from BDH), which removes cations and anions in exchange for hydrogen and hydroxyl ions. The conductivity of the water obtained was typically less than 1 $\mu S.cm^{-1}$ at 298 K.

II.2. Procedure for the sample preparation

Although mainly fibres are used for the production of wound dressings, films were preferred in this study because they are easier to characterise and to make experimental tests upon. In order to correlate as closely as possible experimental results with wound dressings, the film preparation tried to simulate the fibre making process.

II.2.1. Preparation of sodium/calcium alginate thick films:

The thickness of the so-called thick films was around 120 μm. They were used in all the experimental measurements, except for FTIR spectroscopy. Attempts to produce thicker films resulted in samples exhibiting a distorted surface due primarily to the increased water content giving rise to higher shrinkage.

The sample preparation was divided into several steps, as detailed below:

i. Alginate solution:

8 wt% of sodium alginate powder was dissolved in distilled deionised water, with vigorous stirring. Typically, 6-7 wt% of solid content is used for alginate fibre making. The solution was left overnight to allow for bubbles removal. 30 cm^3 of the alginate still

in solution was subsequently poured into a rectangular poly(methyl methacrylate) dish (surface: 80 mm × 170 mm = 13,600 mm^2).

ii. Gelation in $CaCl_2$ solution:

The dish containing the polymer in solution was then immersed in a 0.8 wt% $CaCl_2$ (0.07M calcium) bath for different lengths of time, with occasional stirring. During fibre processing, fibres with a radius of 35 μm have a residence time of around ten seconds in $CaCl_2$. Assuming a linear relationship between $CaCl_2$ immersion time and sample thickness, the residence time of a film of 2 mm thick polysaccharide solution would be close to ten minutes. Thus immersion times in $CaCl_2$ solution were chosen to be 30 seconds, 3, 30, 100, 300 and 3,000 minutes.

In the commercial production of alginate fibres (at Innovative Technologies Ltd, Cheshire, U.K.), a weight percentage of $CaCl_2$ of 0.8 is chosen. Alginate fibres are produced by extruding alginate solution through a spinneret into a calcium chloride bath, and then stretched. If the metal ion concentration is too high, the diffusion of metal ions into the spinneret orifice can cause spinneret blockage. On the other hand, if the $CaCl_2$ solution is too dilute, the fibres are not properly coagulated and filament breakage may occur. 0.8 wt% $CaCl_2$ has been found to be a good compromise.

Experiments such as swelling or mechanical tests were performed mostly on samples immersed for 30 minutes in $CaCl_2$ solution. A lower immersion time would not have led to a sufficient ion conversion, and a higher time would have produced very brittle films.

iii. Final stage of preparation:

The sample was then washed twice for three minutes in distilled deionised water, with frequent stirring, to remove excess calcium. The film was dried in an oven at 323 K over four or five hours, with the door slightly opened to allow water vapour to be removed.

II.2.2. Preparation of other salts of alginate:

Other salts of alginates were prepared, such as sodium/zinc and sodium/silver alginates. The sample preparation was similar to the one described above; the gelation baths were prepared from $ZnCl_2$ and $AgNO_3$ for the different samples respectively. Furthermore, as

silver nitrate is light sensitive, all experiments in which $AgNO_3$ was involved were performed in the dark.

II.2.3. Preparation of deuterated samples:

Deuterated samples were prepared for spectroscopic studies. This preparation was carried out in a glove box under dry nitrogen. The alginate powder was dissolved in deuterium oxide, and subsequently immersed in $CaCl_2$ dissolved in D_2O. A hot plate was then placed underneath the glove box, with nitrogen flowing through it to enable the removal of the water vapour.

II.2.4. Preparation of polysaccharide blends:

For the blend studies, lower percentages of polymers were used than for the pure alginate samples. Pectin was difficult to dissolve at high percentages (maybe due to the great content of methoxyl groups leading to increased hydrophobicity) and CMC has a higher viscosity than alginate. Therefore 3 wt% of (alginate + pectin) powder and 6 wt% of (alginate + CMC) powder were dissolved in water. 100 cm^3 of alginate/pectin and 45 cm^3 of alginate/CMC solution were then poured into the sample dish. The rest of the sample preparation was identical to that of the pure alginates.

II.2.5. Preparation of thin films:

Due to the high absorption of alginates in the infrared region, it was necessary to produce films of the order of 10 μm for transmission spectroscopy. To achieve this, 1 wt% of polymer powder was dissolved in water, and 3 cm^3 of the solution obtained were poured into a poly(styrene) petri dish (diameter = 85mm). The ion exchange process was achieved following the same procedure as described above, for 300 minutes. The film was then rinsed once in distilled deionised water and dried for two hours at 323 K.

II.3. Characterisation of the polysaccharides in solution

II.3.1. Viscosity:

For each study (alginates, alginate/pectin or alginate/cellulose), the percentage of dry matter was kept constant (8, 3 or 6 wt% respectively). However, the viscosities of the

various solutions were very different (for example, LF 10/60 LS has a lower viscosity than LF 10/60, while CMC has a higher viscosity). The knowledge of the viscosity was important to the determination of its influence on the ion mobility within the polymeric network during gelation.

Viscosity measurements were performed at Innovative Technologies Ltd on a Brookfield model DV-II+ viscometer. The samples were left in a thermoregulated bath at 293 K (a common temperature used for these measurements) for a couple of hours prior to the tests. Spindle 21 (diameter: 16.760 mm; side length: 31.240 mm) was used for the 1% solutions, and spindle 34 (diameter: 9.390 mm; side length: 24.230 mm) was used for all the other solutions (3, 6 and 8 wt%). The speed was set to 5.0 or 10.0 rpm according to the sample.

II.3.2. pH measurements:

pH measurements were performed on all the polysaccharide solutions using a JENWAY 3020 pH meter, at room temperature (≈ 293 K). Beforehand, the pH meter was calibrated for pH = 4 and pH = 7.

II.3.3. Molecular weight determination:

Molecular weight of the raw materials was determined by gel permeation chromatography (GPC). The columns used were TSKgel PW×L 4000 + 3000; the temperature was set at 413 K. The polysaccharides were calibrated using poly(ethylene glycol). The solvent used was water + o.o2 wt% NaN3 (it acts as a salt and antioxidant).

II.4. Characterisation of the polysaccharide films in the dry state

II.4.1. Thermogravimetric analysis:

In order to determine the water content of the films, the weight measurements as a function of temperature were obtained using a Perkin Elmer TGS-2. Weight loss was recorded between 303 and 523 K at a heating rate of 2.5 or 5 K.minute^{-1} with the sample held under a nitrogen atmosphere (flow rate of 25 cm^3.minute^{-1}). The average initial sample weight was 5 mg for the thick films and 1 mg for the thin films. Isotherms were

also carried out.

II.4.2. X-ray diffraction:

The degree of ordering in the polymeric films was analysed using a Philips 1050 X-ray diffractometer, equipped with a nickel-filtered copper $CuK\alpha_{1,2}$ source operating at 36 kV and 26 mA. The angle 2Θ was varied from 5 to 60°, with a step size of 0.02° and a scan speed of $0.02°.s^{-1}$.

II.4.3. Scanning electron microscopy (SEM):

A JEOL 840 scanning electron microscope enabled us to analyse the morphology of the polysaccharide samples. In order to study the internal surface of the materials, the films were fractured after immersion in liquid nitrogen. Observation was performed at 10 kV (to prevent any beam damage) with a current of 3×10^{-10} A. The samples were gold-palladium coated for three minutes prior to examination to ensure good conductivity. The coating thickness was of the order of 35 nm. Typical magnifications used were 500×, 2 k× and 5 k×.

II.4.4. Atomic absorption spectroscopy (AAS):

To determine the sodium content and the calcium content in the polysaccharide films, chemical analysis was performed. This was carried out first at Rooney Laboratories (Basingstoke, UK) on a Shandon Southern A4400 spectrophotometer, and subsequently at Innovative Technologies Ltd (Winsford, UK), on a Spectronic spectrophotometer. Prior to analysis, the samples were digested overnight in sulphuric and nitric acid, and diluted with distilled water. An air-acetylene flame was used for the detection of both sodium and calcium, and the results were obtained in weight percentages.

II.4.5. Microprobe analysis:

Microprobe analysis was performed in order to study the ion distribution (Na^+, Ca^{2+} and Cl^-) in the films. Prior to analysis, samples were cut by microtomy with a glass knife to give a flat cross-section. They were then carbon-coated using an Edwards 306 coater. The thickness was then scanned to get the sodium, calcium and chlorine contents. The X-ray analysis was carried out on a JEOL 840 probe microanalyser (SEM), using a wavelength dispersive crystal analyser (WDX). The setting conditions were chosen to

optimise the appropriate signals and were:

-Accelerating voltage: 6 kV for sodium ion detection,
9 kV for chlorine ion detection,
12 kV for calcium ion detection.

The voltage was chosen to correspond approximately to 3 times the excitation energy of each element, keeping in mind that a voltage lower than 6 kV is not advisable (otherwise the detector is not sufficiently ionised).

-Current: 2.10^{-8} A.

-Aperture: diameter = 170 μm.

-Magnification: 300×.

On the X-ray wavelength dispersive spectrometer, the crystals used were:

-Thallium acid phtalate for the sodium determination, and

-Pentaery thritol for the calcium and chlorine determination.

These crystals were set at the following Bragg angles:

-128.9 degrees for sodium (background taken at 126.0 and at 130.0 degrees),

-107.6 degrees for calcium (background taken at 106.0 and 108.5 degrees) and

-151.4 degrees for chlorine (background taken at 151.1 and 151.9 degrees).

The total X-ray counts were recorded for ten seconds.

X-ray counts for sodium, calcium and chlorine were recorded every 10-15 μm across the cross-section. For each immersion time, two scans were carried out on two samples. Therefore, each count used for the determination of ion content is an average of four different values. A peak minus background (taken on both sides of the peak of interest) correction was made for each element. The background counts were found to lie between 0.3 and 3.0 % of the peak counts. Standards were used for the different elements, and studied by SEM/WDX to convert the Na^+, Ca^{2+} and Cl^- counts into weight percentages (wt%).

For sodium ions and calcium ions, the standards were prepared from the alginate samples themselves. Indeed other standards (such as $NaAlSi_3O_8$ for sodium and $CaCO_3$ for calcium) would not have proved to be a judicious choice as these are stable compounds, whereas alginates are matrices of light elements and therefore the ion mobilities (i.e. Na^+ and Ca^{2+}) are expected to be greater within the alginates. These alginate standards were

analysed chemically by atomic absorption spectroscopy. The chlorine ion content could not be detected by this method (atomic spectroscopic methods are in general insensitive to non-metallic elements). Another standard was used, KCl (from Micro-analysis Consultants Ltd, Cambridgeshire, UK).

II.4.6. Mechanical tensile tests:.

Samples used for tensile tests were dumbbell specimens, cut into standard shapes and sizes (strips of 4 mm width and 28 mm length). Because alginate samples are very brittle, a few drops of deionised distilled water were poured on the films to soften them prior to cutting. The test samples were then dried at room temperature for 24 hours between two perspex plates to keep them flat. The test type was BS 903 part A2/1995 - ISO 37/1994. Tensile tests were performed using an INSTRON 4206 in a controlled environmental room. The maximum load was 5 N, the initial distance between grids was set to 20 mm, and the speed of the top grid was 1 mm.minute^{-1} for all samples (the speed value was relatively slow as most samples are of the brittle type). The temperature was between 294 and 296 K, and the humidity was 35 ± 3 %.

II.5. Spectroscopy studies

To get a greater understanding of the binding between a polysaccharide and various ions, or between two polysaccharides, a range of spectroscopic techniques were used.

II.5.1. Fourier transform infrared spectroscopy (FTIR):

Infrared experiments were performed on 10-20 μm thin films in transmission mode, using a Nicolet 710 FTIR spectrometer. The spectra were averaged over 128 scans at a resolution of 4 cm^{-1}. This value was chosen to minimise the noise. The spectral range covered frequencies from 4000 to 400 cm^{-1}. Each reported wavenumber value is a mean result taken from four different samples.

II.5.2. Raman spectroscopy:

Raman spectroscopy was carried out on thick films at Nicolet Instruments Ltd

(Warwick, UK) using a FT-Raman 750 series II spectrometer. A gain of 64 was used at a resolution of 8 cm^{-1}, and the average number of scans was 760.

II.5.3. Neutron spectroscopy:

Neutron spectra were obtained using the ISIS facility at Rutherford Appleton Laboratory (Chilton, Didcot, UK), with a pulsed spallation neutron source. The spectrometer used was a time-focused crystal analyser (TFXA). Each sample was run for approximately 12 hours. The energy ranges from 2 to 1500 meV, and the average sample temperature was kept around 5 K using liquid helium.

II.6. Interaction of the polysaccharide films with a simulated wound exudate

Once the samples were prepared (as sodium/calcium salts) and fully characterised, they were brought into contact with a simulated serum solution (containing 0.277 $g.dm^{-3}$ $CaCl_2$ and 8.298 $g.dm^{-3}$ NaCl, as mentioned by Thomas & Loveless, 1992). Subsequent experiments included the determination of the calcium release, the swelling and the gel strength provided by the specimens.

II.6.1. Calcium release measurements:

Visible spectroscopy was used to determine the calcium ion release of sodium/calcium polysaccharide films into a sodium/calcium solution (simulated serum). For this purpose, tetramethylmurexide (from Sigma Aldrich Ltd, Dorset, U.K.), a metal indicator which changes colour from purple to orange upon interaction with Ca^{2+} ions, was introduced into the solution. Visible spectroscopy on the liquids was performed on a Perkin Elmer UV/VIS/NIR spectrometer Lambda 19. The range of wavelength scanned was 650-380 nm, at 240 $nm.minute^{-1}$, with a resolution of 0.8 nm.

II.6.2. Study of the swelling behaviour:

i. Wicking rate experiments:

Dynamic contact angle analysers are commonly used to study the interface between a solid and a liquid. For samples that readily absorb liquids, a wicking rate analysis can be more meaningful than a contact angle measurement. Wicking rate tests were performed

on a Cahn Instruments DCA-322. This contact angle analyser is based on the Wilhelmy plate technique. The rapid solution uptake occurring as soon as the film enters in contact with the liquid was recorded, and the maximum wicking rate was derived (in $mg.s^{-1}$). The stage speed was set at 100 $\mu m.s^{-1}$, and a force measurement was made every second. These conditions were found suitable to obtain enough data points over the short uptake process.

ii. Volume ratio measurements:

While the previous method described for swelling characterisation was very much surface sensitive, the following method is more a measurement of the bulk swelling property. A simple device was designed in order to record the changes in film dimensions (thickness, width and length) as a function of immersion in a simulated serum solution (referred to as Na/Ca solution), as sketched in figure II.6.2.

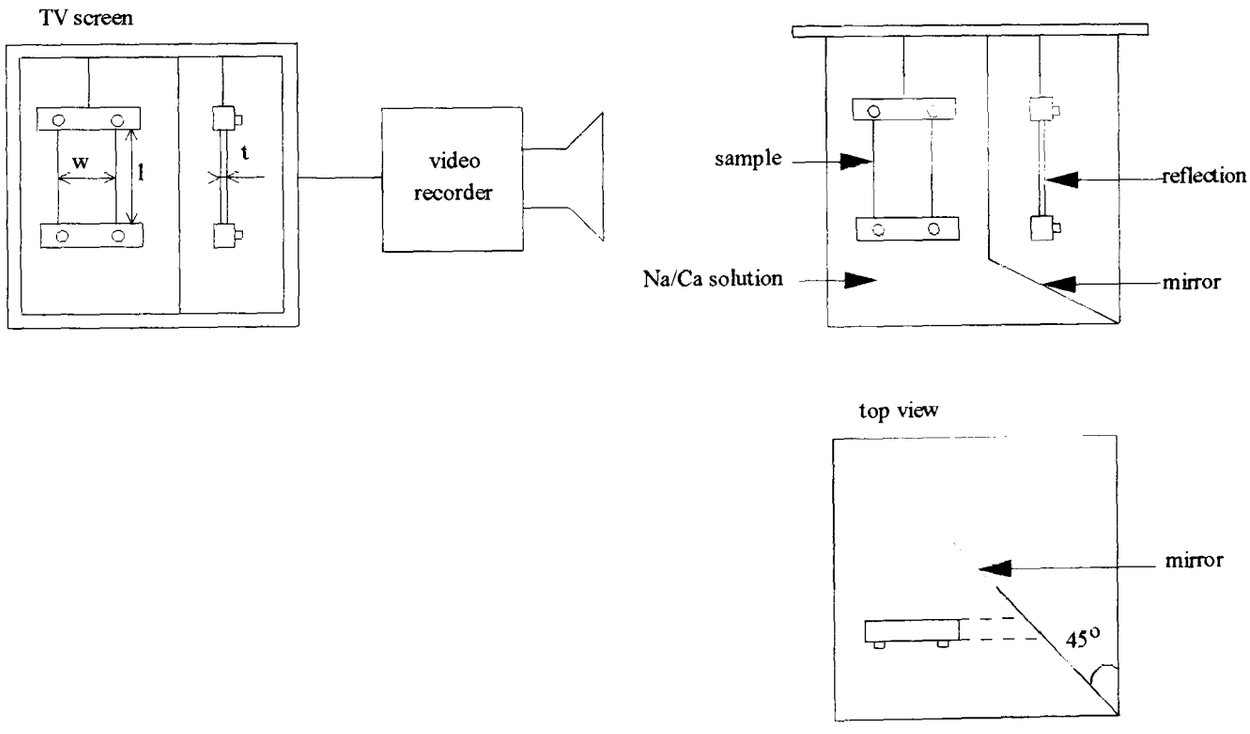

Figure II.6.2. Design for volume ratio measurements.

The sample, held vertically between two grips (with a mass of 8 g) to keep it straight, was fully immersed in the simulated serum solution. The different dimensions were taken for the hydrated sample at various immersion times (from 1 to 30 minutes) by recording the image on a TV screen (via a mirror in the bath set at 45 degrees from the TV camera,

all three dimensions, magnified, could be visualised at once). The average dimensions of the dry films were 100 μm × 20 mm ×30 mm. These were measured using a micrometer (for the thickness) and a vernier. After only five minutes of immersion, the thickness was already of the order of one millimetre (appearing as 2-3 mm on the TV screen, and measured using a vernier). After 30 minutes, the sample was removed from the solution and the real dimensions were measured. From both measurements at 30 minutes (from the TV screen and in reality), a ratio was worked out to convert the other dimensions taken from the screen. The precision was estimated to be of the order of 10 %.

II.6.3. Strength measurements on gels:

Further measurements were performed following the same principle as creep/recovery tests, with masses of 10, 50 and 100 g applied, over a short period of time (1.5 + 0.5 hours). Not only dimensional stability but also handling properties and gel strength were of interest. Sample strips (20 mm × 30 mm) were clamped between two grips, with a mass applied on the bottom grip, and they were immersed in the simulated serum solution (Na/Ca solution). The change of length was recorded as a function of time, using a travelling microscope. Some tests were carried out at 303 and 313 K by using a hot plate to adjust the simulated serum solution to the right temperature. This was achieved within ± 1.5 K over the two hours of the experiment. Figure II.6.3. illustrates this test.

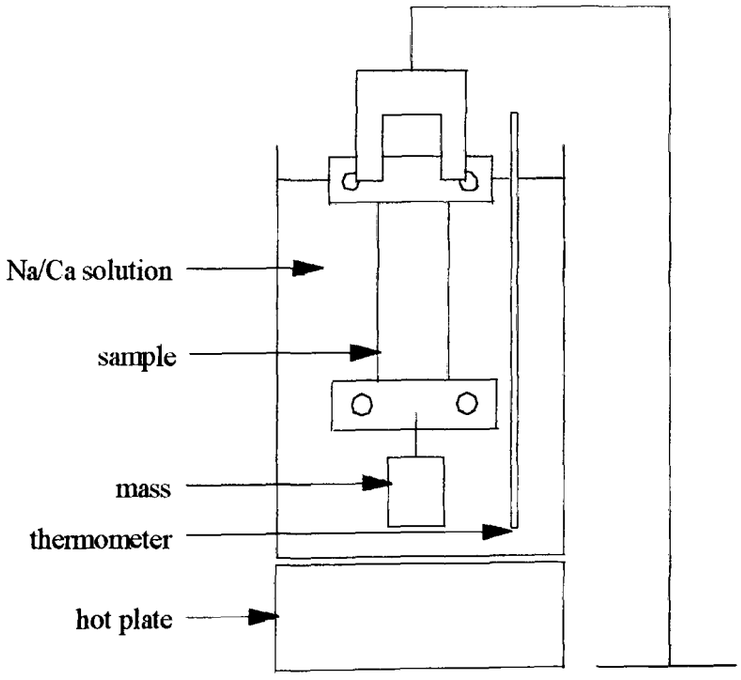

Figure II.6.3. Design for gel strength measurements.

CHAPTER III: SODIUM ALGINATES AND THEIR CONVERSION TO INSOLUBLE SALTS

III.1. Characteristics of sodium alginates

The raw materials used in this study were sodium alginates. It was necessary to characterise them since there exists a wide range of such natural polymers whose characteristics depend on the place and the time they have been harvested, the part of the seaweed they come from, etc.

III.1.1. An intrinsic property: the M/G ratio:

Two different alginates have been compared, namely LF 10/60 and LF 10/60 LS; they have similar molecular weights but different M/G ratios. Indeed this ratio has been proved to be a dominant factor for most alginate properties (see Chapter I).

The M/G ratio was obtained, for the particular batch used, by determining the ratio of the bands at 1320 and 1290 cm^{-1}, from the infrared spectrum. This method is based on Filippov & Kohn's work (1974) and is illustrated in figure III.1.1.:

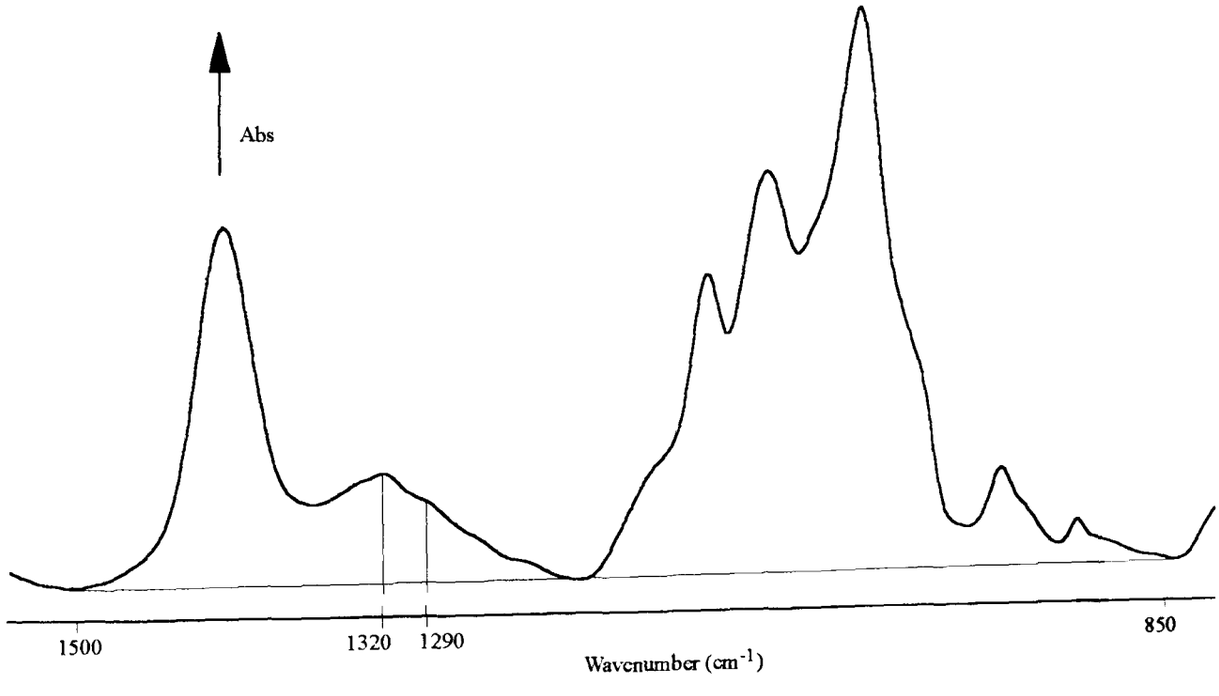

Figure III.1.1. Determination of the M/G ratio of alginate.

Calculation gave a M/G ratio equal to 25/75 for LF 10/60, and to 52/48 for LF 10/60 LS. The main error is estimated to be ± 3% (according to Filippov & Kohn, 1974), compared to the chemical method. Following these values, PROTANAL LF 10/60 was termed the high-G alginate, whereas PROTANAL LF 10/60 LS was referred to as the medium-G alginate.

III.1.2. Characterisation of sodium alginates in solution:

After dissolution in distilled deionised water, the sodium alginates were tested for their pH and their viscosity (table III.1.2.). These parameters are expected to influence the ion exchange process, which is the following step in the sample preparation. 1 wt% solutions were prepared for FTIR spectroscopy, whereas the 8 wt% solutions were used for all the other studies. The speed of the spindle was set at 10 rpm.

Sample	Viscosity (mPa.s)	Shear rate (s^{-1})	pH
1% LF 10/60	25	9.3	6.0
1% LF 10/60 LS	20	9.3	6.2
8% LF 10/60	13,400	2.8	6.3
8% LF 10/60 LS	3,800	2.8	6.1

Table III.1.2. Viscosity and pH of alginate solutions.

The precision in the viscosity values is estimated to be of the order of ± 5 %. The resolution of the pH meter was 0.01pH.

Alginate LF 10/60 gives a higher viscosity than alginate LF 10/60 LS, mostly due to its higher content of G blocks. M and G blocks adopt different chain conformations in solution (Grasdalen *et al.*, 1977) and, due to different orientations of the glycosidic bonds between the blocks, guluronic acids form more buckled chains than mannuronic acids. Therefore, the presence of more G blocks is expected to lead to higher viscosities. A 1 wt% dilution can be considered low enough not to produce any significant change in the alginate solution viscosity and, therefore, should not be an influential factor for the ion conversion. However, an increase in powder content to 8 wt% shows a significant

difference between the two alginates. The influence of the viscosity on the ion exchange process during sample preparation will be assessed in section III.2.1.

pH is another important parameter in the characterisation of an alginate solution, as different activities in the O-H groups are bound to influence the ion binding. For the particular samples studied, however, there is no noticeable change in the pH values, and all are found to be close to 6. It must be stressed that for pharmaceutical purposes, the pH of the wound dressing material is required to be contained between 6 and 8 (from the Drug Tariff Technical Specification N°41- July 1994).

III.1.3. Characterisation of sodium alginates as films:

From the 8 wt% sodium alginate solutions, films were obtained by water evaporation. They were then tested for their physical and mechanical properties, to enable subsequent comparison with the converted salts.

i. Water content:

The water content of the polysaccharide films was determined by thermogravimetric analysis. A typical TGA curve is shown below for the high-G sodium alginate, heated under nitrogen from 303 to 823 K:

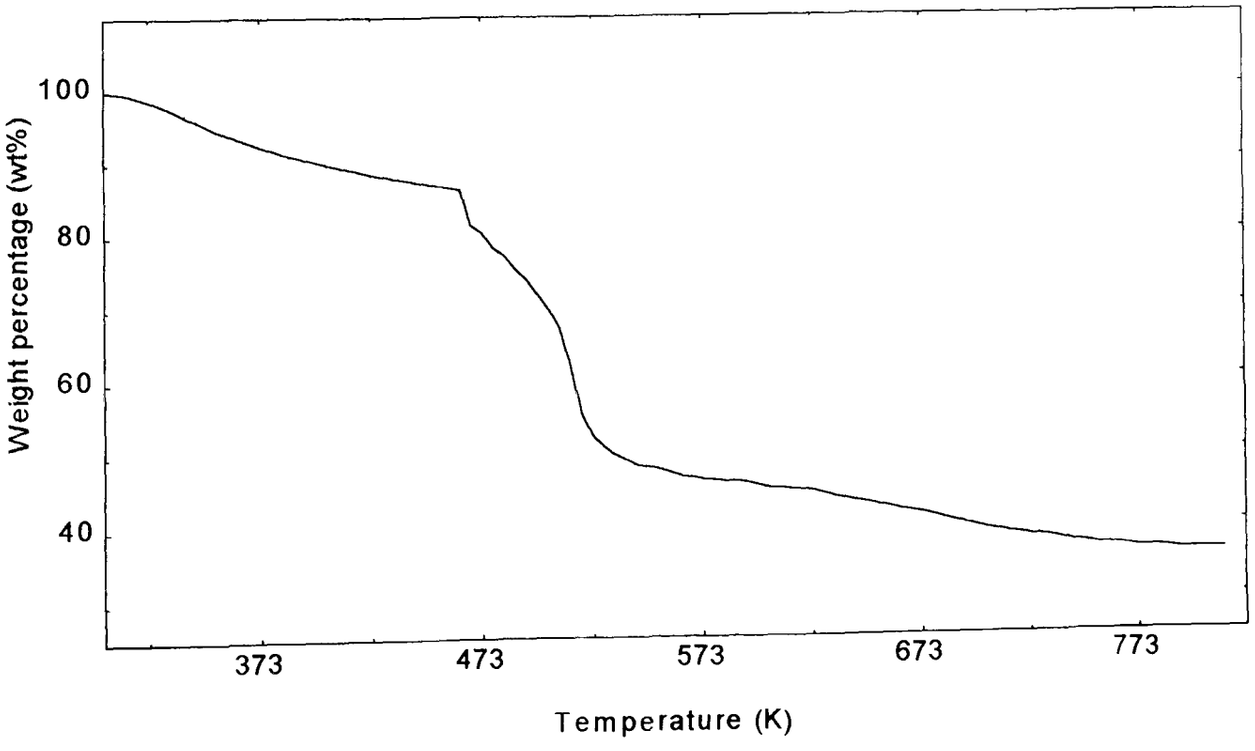

Figure III.1.3.a. TGA curve for high-G sodium alginate.

The initial weight loss in the TGA curve corresponds to water evaporation, from both free water and bound water. This starts as soon as the sample is heated (303 K). At the first point of inflection, between 453 and 463 K, a more pronounced slope is obtained. There, dramatic decomposition must occur, followed by a loss of mass integrity of the sodium alginate. Decomposition occurs at temperatures lower than the melting point, and it is possible that decomposition is occurring prior to all water removal. This may influence the calculations of water wt%. However, it was assumed that this effect was negligible.

Figure III.1.3.b. represents isotherms at 393, 413, 433 and 453 K, performed in order to determine more precisely the amount of water contained in the samples.

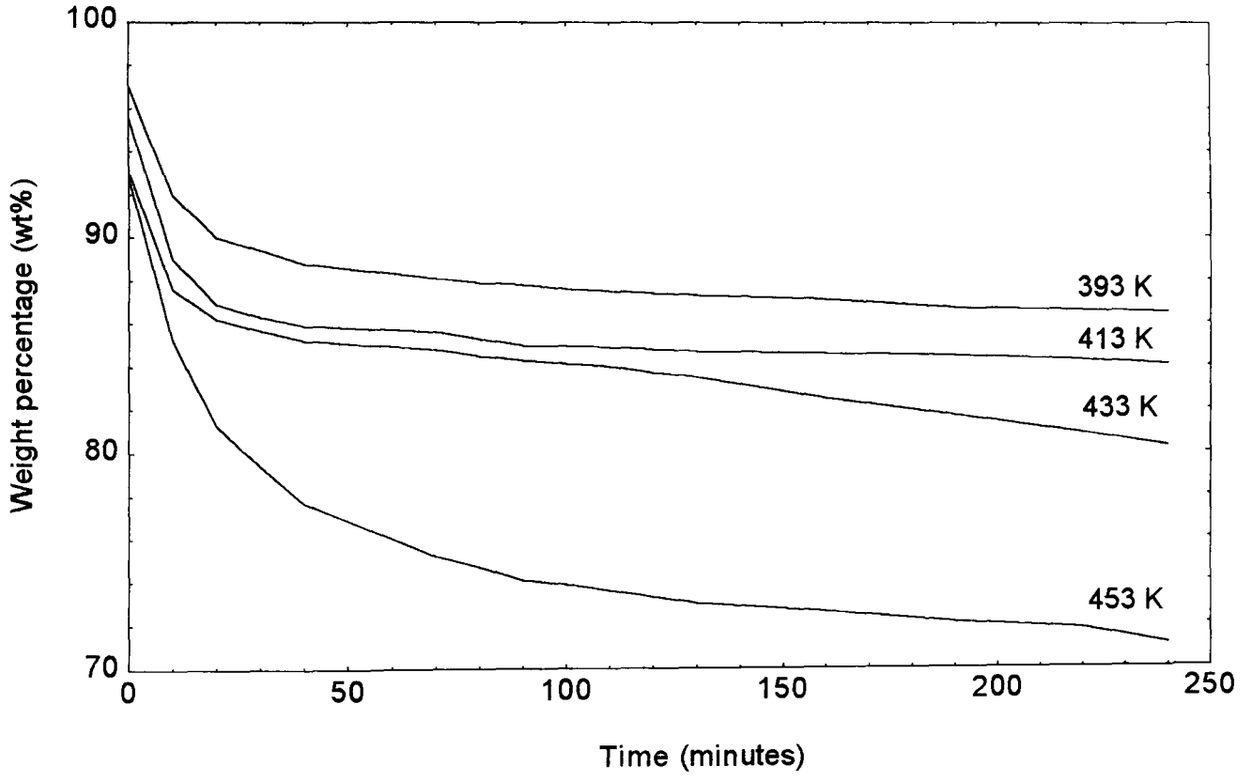

Figure III.1.3.b. Isotherms of high-G sodium alginate, including weight loss occurring during heating from ambient to measurement temperature, at 80 K.minute^{-1}.

The isotherm curves at 393 and 413 K present a plateau after two hours of heating, corresponding to 13.5 and 16.0 wt% loss respectively. By contrast, the isotherm at 433 K displays a change in slope after two hours, leading to further increased weight loss. As for the last curve, there is a continuous and large weight loss as a function of time. It is believed that from 433 K onwards, dehydration is followed or superimposed by sample

degradation. Therefore the amount of water contained in the alginate films corresponds to the plateau value found after heating for a few hours around 413-423 K, and is equal to 15-16 wt% of the total weight (averaged on three TGA curves). Similar results were obtained for the medium-G sodium alginate. This water percentage gives an average close to two water molecules per M and G block. Water can be bound to the hydroxyl groups (two per M and G group), to the oxygen atoms (in the backbone or in the glycosidic bond), or can be present as free water.

ii. Crystallinity:

The X-ray diffraction spectrum obtained for the sodium alginate film is shown below:

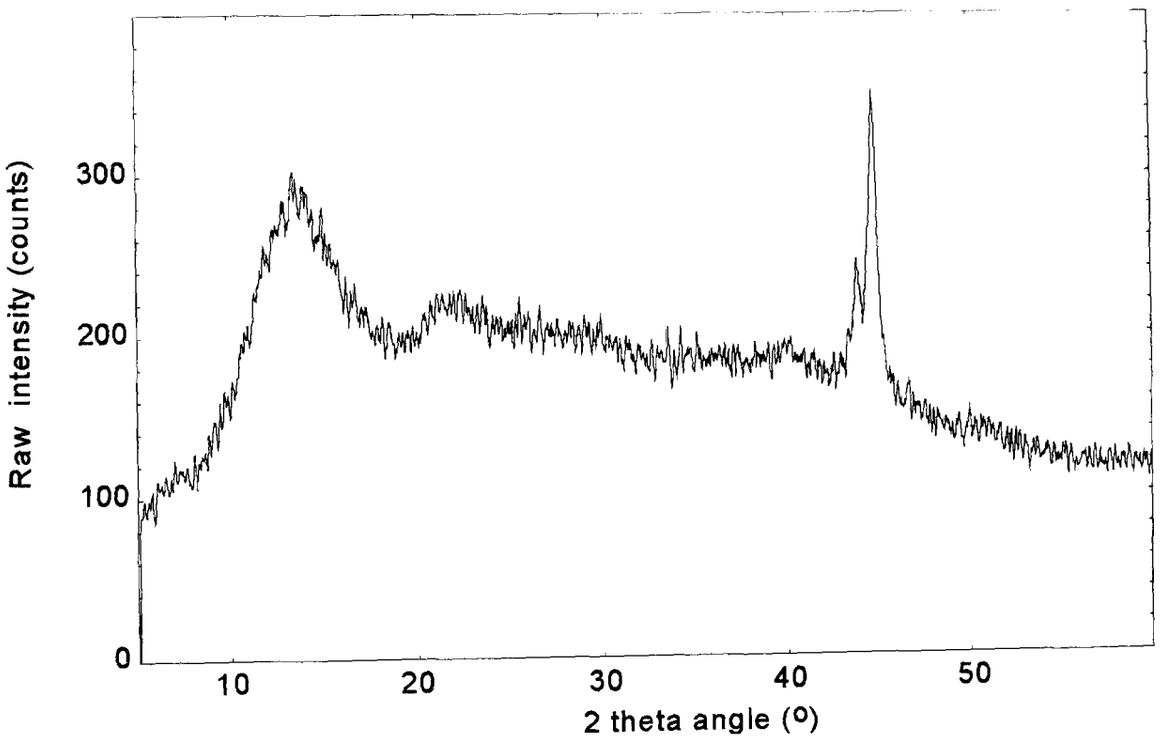

Figure III.1.3.c. X-ray diffraction pattern for high-G sodium alginate.

The shoulder at 17° and the doublet between 43 and 45° are characteristic of the adhesive tape and the steel stub, respectively. These were necessary to hold the sample in place during acquisition of the data. This spectrum is characteristic of an amorphous sample. Previous work using X-ray diffraction on high-G and high-M samples (Atkins *et al.*, 1970, 1973) revealed evidence of crystallinity. However, it was performed on oriented specimens, as alginic acid fibres (therefore some crystallinity was induced from the stretching process; Clare, 1993).

iii. Tensile tests:

A typical strain-stress curve is presented below, for sodium high-G alginate films, in the dry state. The strain rate was 0.05 mm.minute^{-1}.

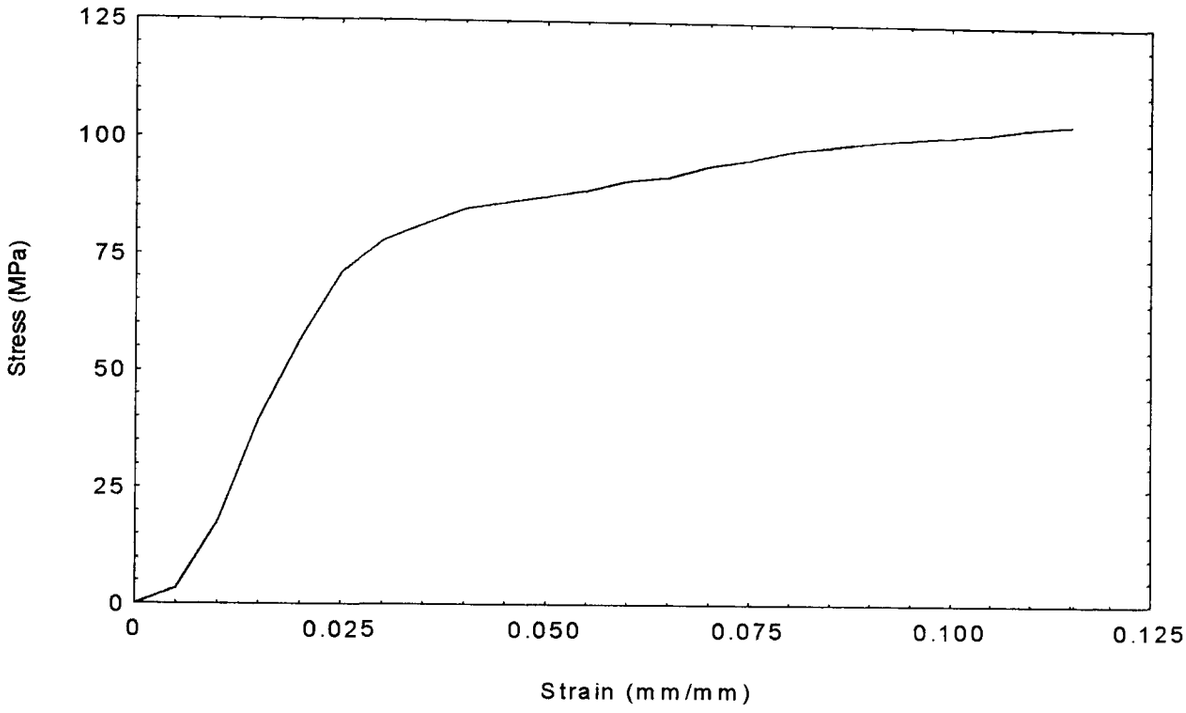

Figure III.1.3.d. Typical stress-strain curve for high-G sodium alginate.

The values of modulus, fracture stress and fracture strain are summarised below (averaged on five tests), for the two different types of alginate, prepared from the 8 wt% solutions:

Sample	Young's modulus (GPa)	Fracture stress (MPa)	Fracture strain (%)
High-G alginate	4.6 ± 0.4	117 ± 22	12.4 ± 2.8
Medium-G alginate	5.0 ± 0.2	109 ± 24	8.2 ± 2.5

Table III.1.3. Mechanical properties of sodium alginates.

Sodium alginates have high moduli (of the order of GPa) at ambient temperatures, and they break before the yield point is reached. They belong to the category of hard-brittle materials.

The values obtained for the high-G and the medium-G samples are similar, within experimental error. Therefore it seems that in the dry state, the M and G blocks behave in a comparable way, in terms of their mechanical properties. The low strain values obtained are due to the dominant effect of the glycosidic bonds between the blocks which are stiff and do not allow much alignment of the alginate molecules under tension.

III.2. Conversion of sodium alginate into other salts

From the sodium alginate solutions, different alginate salts were obtained by ion exchange. Mixed sodium/calcium alginate samples were extensively analysed as they are the salts commonly used in wound dressing production. Other salts, such as zinc and silver alginates, were also prepared in order to compare the way ions are bound within the polymeric network (see following chapter). Upon $CaCl_2$ immersion (or $ZnCl_2$/$AgNO_3$), many parameters are expected to influence the ion exchange in alginates, such as the M/G ratio (already extensively studied, for more than 25 years; e.g. Grant *et al.*, 1973; Smidsrød & Haug, 1968), but also other factors such as viscosity and volume of solution used, for a given alginate.

III.2.1. Influence of viscosity and film thickness:

This study was carried out on PROTANAL LF 10/60. For all samples, the sodium alginate solution was immersed for a fixed time of 30 minutes in $CaCl_2$ solution. The sodium and calcium weight percentages of the mixed sodium/calcium salts were obtained by AAS.

The viscosity can be varied via the percentage of alginate powder dissolved in water; three different percentages were prepared: 3, 6 and 8 wt%. To determine the influence of the viscosity, the volume of water required to prepare the alginate solution was varied (which lead to different path lengths in the solution state for the ions to go through), but not the amount of powder. Therefore, the number of alginate molecules in all samples was similar, so as to give similar thickness upon film drying, and to provide the same number of sites for the calcium ions. This was carried out for two different thicknesses: $\approx$100 and $\approx$150 μm. Table III.2.1. summarises the results obtained. The ionic weight

percentages were performed on a dry basis. From these values, atomic percentages were worked out (the detailed calculation is given in appendix 1).

Sample	Thickness (μm)	Viscosity (mPa.s)	Na wt%	Ca wt%	Na at%	Ca at%
3% solution	120	670	5.5	4.4	2.4	1.1
	150		6.5	3.2	2.8	0.8
6% solution	100	5,300	4.8	4.6	2.1	1.1
	155		7.0	2.9	3.0	0.7
8% solution	90	13,400	4.2	5.8	1.8	1.4
	160		7.2	2.5	3.1	0.6

Table III.2.1. Influence of viscosity and film thickness on ion contents.

The standard error in measured ion content is typically ± 2-3 %, while the film thickness is given within ± 4-5 % (measured with a micrometer).

An increase of viscosity gives rise to an increase of the polymeric entanglement in the solution, therefore Ca^{2+} ions are expected to be hindered in their diffusion process. As their mobility is lowered, the probability of ion exchange is also reduced. However, an increase in alginate molecule concentration gives rise to more sodium ions for a given volume, and therefore a higher density of sites for calcium ions, for a given path. These two phenomena are expected to compete with one another.

For a similar thickness, when the viscosity is dramatically altered (an increase of up to 2,000 % from the 3 to the 8 wt% solution), comparatively, the ion percentages do not greatly vary (deviating around 20 % for the sodium % and around 30 % for the calcium wt%) and a very viscous alginate can still lead to a very good ion conversion. It may be concluded that if viscosity does have some influence on the ion exchange, it is not a dominant factor. Furthermore, the changes observed in Na^+ and Ca^{2+} % may also be due to the different initial volumes of solution rather than to the viscosity itself. By contrast, an increase in thickness by 50 % leads to variations from 20 to 70 % in the sodium

content, and from 40 to 130 % in the calcium. The greatest differences are observed for samples prepared from the higher viscosity solutions.

It is interesting to note that for a film thickness close to 100 μm, the sodium content is observed to decrease while the amount of calcium increases with increasing viscosity. By contrast, for a film thickness close to 150 μm, the sodium percentage is seen to increase while the calcium content decreases with higher viscosity. This may be due to the thicknesses being only approximate.

Figure III.2.1. represents the ion contents as a function of film thickness, irrespective of the viscosity. It includes all the data points from table III.2.1, plus AAS results for 1 % films which are around 15 μm thick.

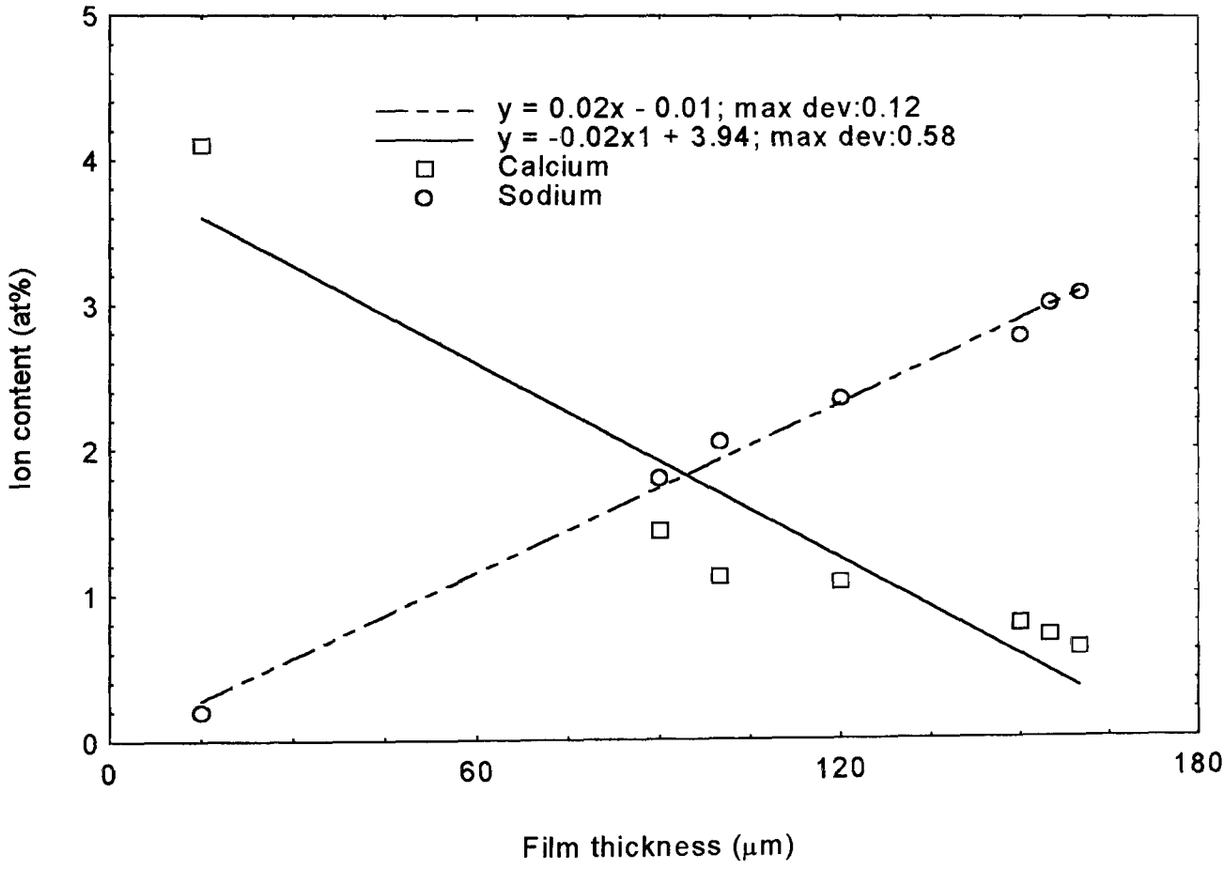

Figure III.2.1. Film thickness as a function of ion content, after 30 minutes exposure to $CaCl_2$.

This graph shows a quasi-linear relationship between Na^+, Ca^{2+} at% and film thickness. The measurement of the sample thickness in the dry state appears thus to give a quick

and very simple quantitative determination of the ion content, providing the sample has been prepared by immersion for just 30 minutes in the calcium chloride bath.

In conclusion, it can be seen that many factors influence the ion exchange process, and it is impossible to isolate just one of them as they are all interdependent. However, the amount of sites available for calcium ions (related to a certain volume of solution and leading to a given film thickness in the dry state) emerges as a predominant factor for the ion binding, within the range of viscosities and film thicknesses studied. Each subsequent study was, thus, carried out with approximately constant film thickness.

Potter *et al.* (1994) studied the diffusion of calcium ions from an outer reservoir into an alginate solution. They found that the concentration of the alginate did not have much effect on the value of the calcium diffusion, which confirms the observations of the present studies. Potter *et al.* (1994) also found that the concentration of the calcium reservoir was a very influential parameter. This was kept constant in the present work.

III.2.2. Influence of the M/G ratio and the $CaCl_2$ time of exposure:

As extensively shown in the literature (Grant *et al.*, 1973; Rees, 1972; Wang *et al.*, 1993), calcium ions are predominantly bound to the G blocks. This different behaviour between the alginate G and M blocks has been more closely studied for our two particular samples. The importance of the immersion time in calcium chloride solution has also been assessed. Results presenting Na^+ and Ca^{2+} atomic percentages as well as the charge equivalence (Na^+ at% + 2×Ca^{2+} at%) are summarised in table III.2.2. The charge equivalence gave an indication of the amount of ions bound or free in the alginate. It could also be used as a check on the overall neutrality of the sample.

Immersion	High-G alginate			Medium-G alginate		
time (min)	Na at%	Ca at%	Charge eq.	Na at%	Ca at%	Charge eq.
0	4.9	0.01	5.1			
0.5	4.4	0.14	4.7			
3	4.0	0.4	4.8	4.2	0.3	4.8
30	2.9	1.0	4.9	2.8	0.9	4.6
100	2.2	1.8	5.8	2.2	1.6	5.4
300	0.8	2.6	6.0			
3,000	0.04	2.9	5.8			
30,000	0.04	2.9	5.8			

Table III.2.2. Na and Ca at% as a function of M/G ratio and exposure to $CaCl_2$.

The number of calcium ions available for exchange in $CaCl_2$ solution was, at all time, in excess (this was checked by AAS). For a given exposure time to $CaCl_2$ solution, the Ca^{2+} wt% is slightly lower for the medium-G alginate.

The following figure shows the above values plotted for alginate LF 10/60.

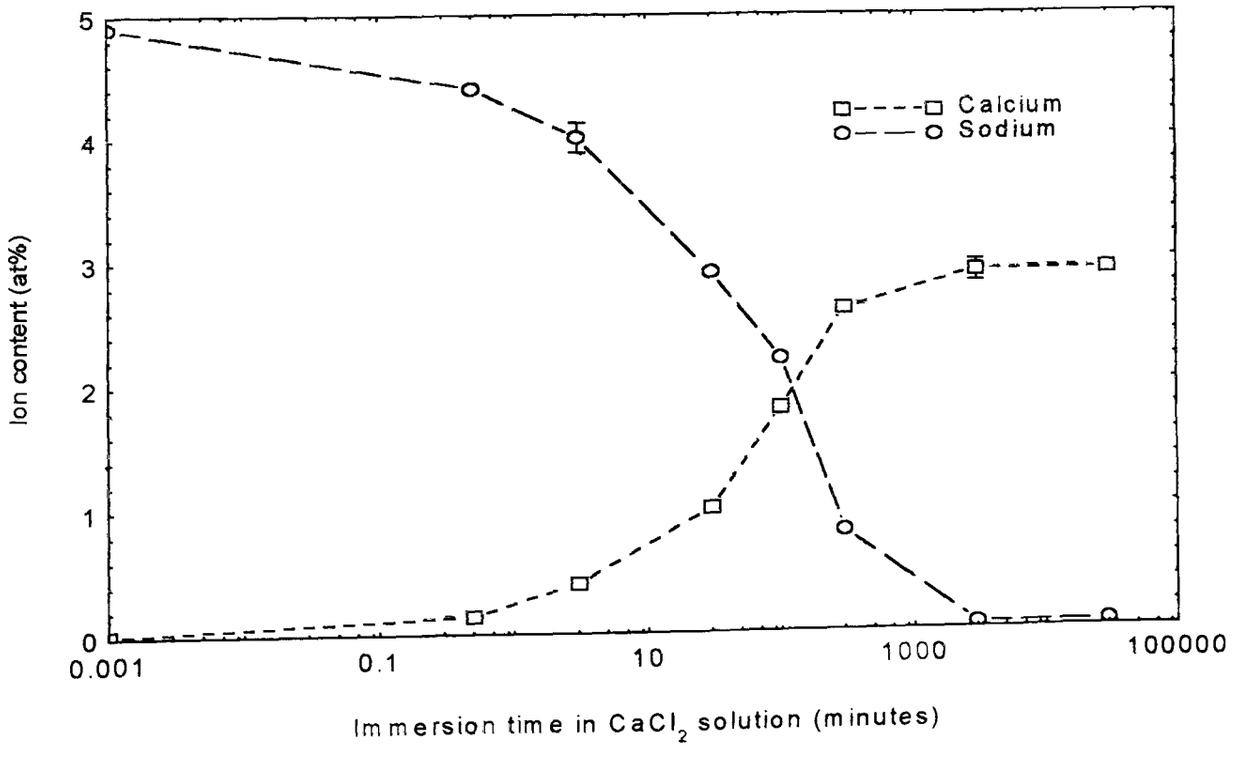

Figure III.2.2. Ion content of high-G alginate as a function of immersion time in $CaCl_2$.

During ion exchange, when a sodium alginate is immersed in a $CaCl_2$ solution, the sodium ion, bound to the carboxyl groups, escapes from the alginate and is replaced by the calcium ion, which sits in a "box", preferentially in the G blocks (according to the "egg-box model"; Grant *et al.*, 1973). The maximum sodium atomic percentage is 4.9 for the pure alginate (no immersion). This corresponds to an alginate with slightly more than all its COO^- sites bound with Na^+ ions (all sites filled would lead to approximately 4.4 at%). After a long immersion time in $CaCl_2$ (more than 30,000 minutes), all the sodium ions have left the alginate matrix, and 2.9 at% of calcium is obtained. This correlates with an exchange of more than one calcium ion per two sodium ions, which is the rate of exchange expected to keep the charge balanced (all sites filled in both M and G blocks would lead to 2.3 at%). According to Kohn (1975), while Ca^{2+} ions are found to be predominantly bound to G blocks, an excess of $CaCl_2$ is likely to cause precipitation in the M blocks. However, in contrast to the irreversible coagulation which occurs between calcium and guluronic blocks, precipitates of calcium mannuronate are easily dissolved in distilled water.

By looking closer at the charge equivalence values, it can be seen that there is an initial drop in positive charge, from 5.1 to 4.7, essentially due to a massive depletion of the Na^+ ions from the polysaccharide. This must leave an overall electronegative alginate, and therefore leads to a jump of the Ca^{2+} % after 3 minutes of immersion. After 100 minutes in $CaCl_2$, the charge equivalence increases to the average value of 5.8, and remains practically unchanged until complete ion conversion. Compared with the starting material (pure sodium alginate), the charge equivalence for the converted calcium sample is slightly higher, indicating an excess of positive charges. This is discussed further in the following section.

III.2.3. Ion distribution across the film cross-section:

These measurements were performed with a view to studying the homogeneity of the sodium ion and the calcium ion distribution across the film thickness, as a function of immersion time in $CaCl_2$. The introduction of chlorine ions from the $CaCl_2$ solution into the alginate was also assessed.

i. Standards:

For each alginate sample immersed for a specific time in calcium chloride solution, approximately 40 sodium and calcium counts were measured and averaged by wavelength dispersive spectroscopy over the cross-section. These counts were then plotted as a function of weight percentages, as determined for the same samples by atomic absorption spectroscopy, to produce standard curves (see figures III.2.3.a and III.2.3.b). The curvature of these plots could not be explained physically, and therefore it was assumed that it represented some error in experimental results.

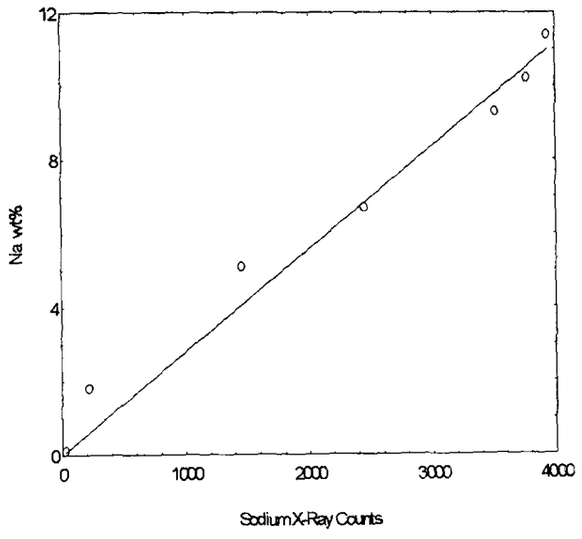

Figure III.2.3.a. Sodium standard curve.

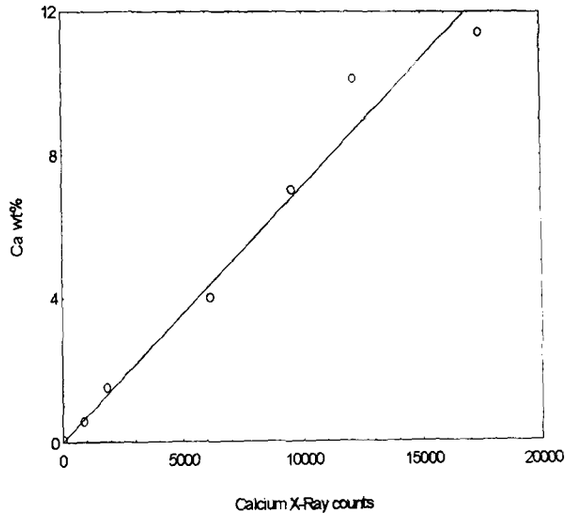

Figure III.2.3.b. calcium standard curve.

Straight lines were extrapolated from these experimental points with the following equations:

$y = 2.8\ 10^{-3}\ x$ for sodium (maximum deviation = 1.2) and

$y = 7.1\ 10^{-4}\ x$ for calcium (maximum deviation = 1.5).

These lines were used to convert counts (x) into weight percentage (y).

Previous measurements were performed on the alginate samples, relating their X-ray counts to those of $NaAlSi_3O_8$ and $CaCO_3$ standards (from Micro-Analysis Consultants Ltd, Cambridgeshire, UK), for the sodium and calcium determination, respectively. These measurements led to a Na^+ wt% of 14 for the sodium sample, and an average calcium content as high as 26 wt% for the sample immersed for 30,000 minutes in $CaCl_2$. These percentages, and specially the calcium one, were clearly overestimated by

comparison with the AAS results of the corresponding samples (of the order of 9-10 wt% of Na^+ and Ca^{2+}), and with values found in the literature (Skjåk-Bræk *et al.*, 1989). The high values may be explained by the different penetration depth of the electron beam in the standards and in the alginate. The penetration is expected to be deeper in the polysaccharide as it contains light elements (the accelerating voltage was between 6 and 12 kV, according to the element studied). Therefore these standards were not suitable for this work, and the alginates themselves were then used as standards.

For the chlorine ions, a simple equation was used to obtain the weight percentages:
Cl wt% = (Cl counts x 47.55) / 11,770
where 47.55 corresponds to the weight percentage of Cl in the standard KCl, and 11,770 is the Cl X-ray counts for this same standard, recorded for 10 seconds.

From these weight percentages, atomic percentages were calculated (the calculation is detailed in appendix 1).

ii. Ion profiles across the cross-section:

Figures III.2.3.c, d and e represent Na^+, Ca^{2+} and Cl^- atomic percentages, respectively, as a function of the position on the alginate cross-section for different immersion times in $CaCl_2$ solution. The samples immersed for 30 seconds and for 3 minutes in calcium chloride solution were partially dried by spraying some acetone on their surface. Acetone is commonly used in fibre making (for the production of wound dressings) to accelerate the drying process. Samples dried without the use of acetone were also prepared for these two $CaCl_2$ immersion times, but their curves are not shown here, for clarity. The side in contact with the calcium chloride solution corresponds to a thickness equal to zero, and the side in contact with the perspex dish is at a thickness of approximately 110 µm. In practice, because the electron beam was fairly large (close to 10 µm), the first measurement was taken at 15 µm (to ensure that it was entirely contained in the sample), while the last measurement was made at 95 µm. The standard error in the atomic percentages was typically ± 10-15 %.

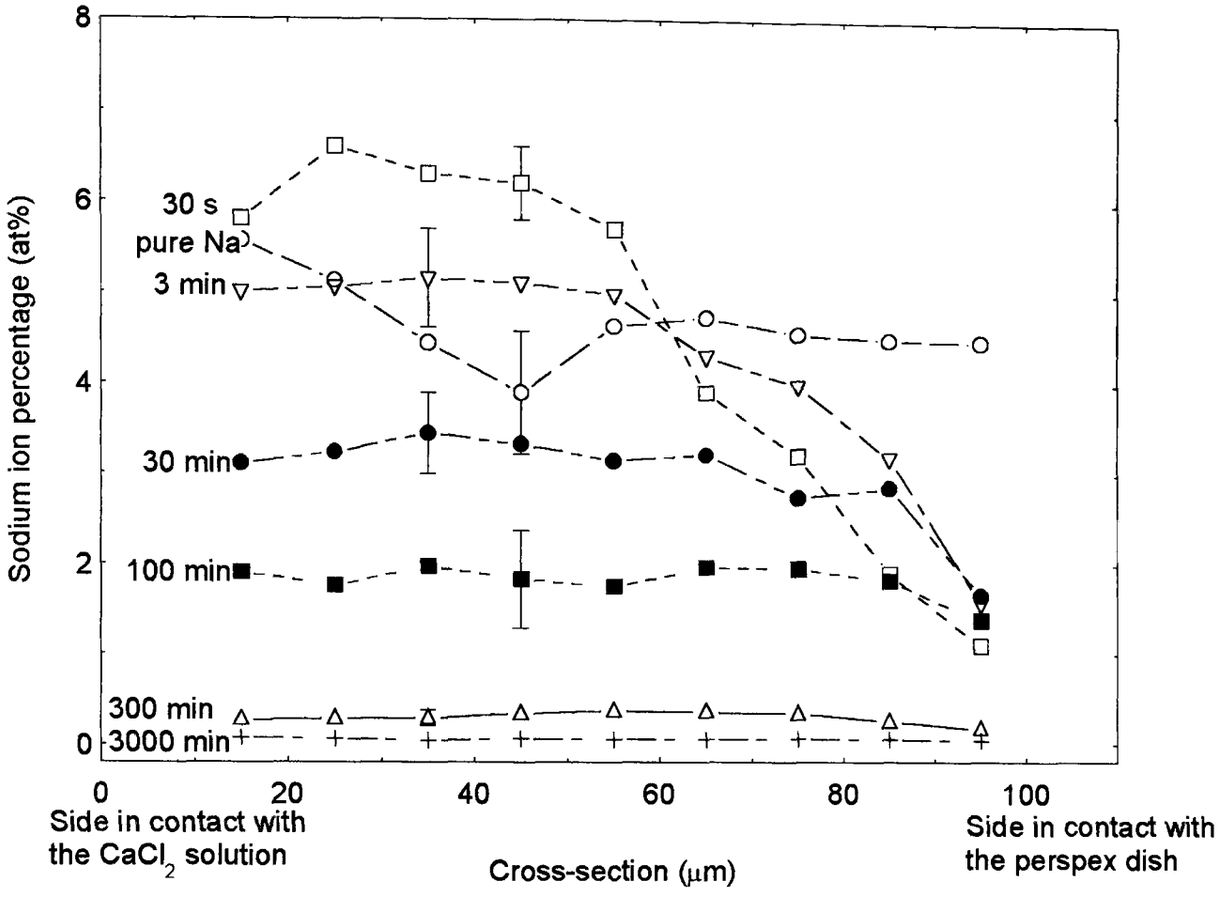

Figure III.2.3.c. Sodium ion content across the cross-section of alginate films.

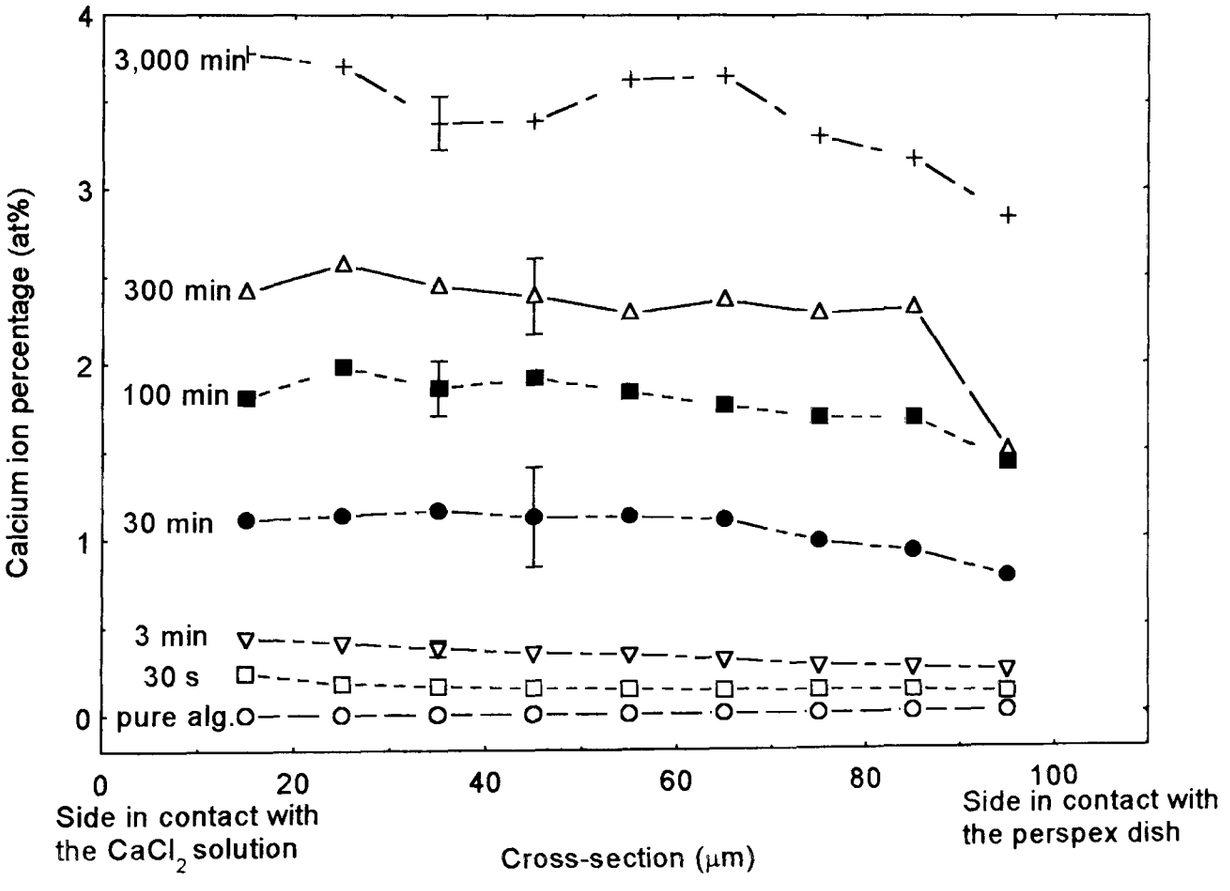

Figure III.2.3.d. Calcium ion content across the cross-section of alginate films.

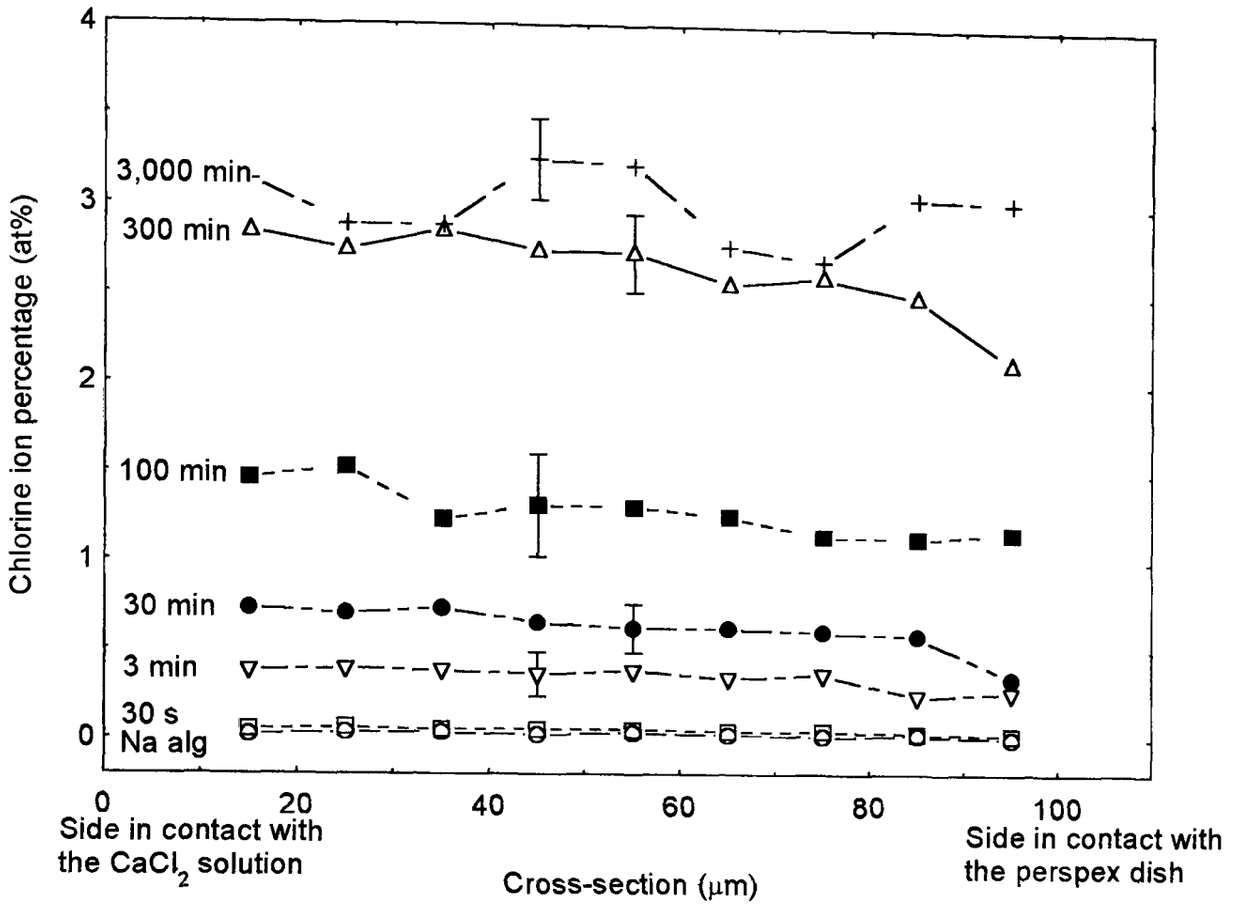

Figure III.2.3.e. Chlorine ion content across the cross-section of alginate films.

The trend between the samples is a decrease of sodium ions and an increase of both calcium and chlorine ions with greater immersion time in $CaCl_2$, as expected for ion conversion. For most of the samples, the profiles are quite even across the cross-section. However, the sodium profiles of the alginates immersed for 30 seconds and for 3 minutes present different patterns, according to whether they have been dried using acetone or not. The samples dried only in the oven have a uniform composition (not shown here), similar to the profiles obtained for longer immersion times. By contrast, a clear decrease in sodium content is obtained for the samples dried with acetone (and subsequently in the oven), as the perspex dish interface is reached. The "rush" of the Na^+ ions towards the $CaCl_2$ solution, as soon as the alginate is immersed, is thought to arise from an important driving force that is due to attraction to the Cl^- ions in the bath. The acetone seems to act as a "freezer" for the ion redistribution. When drying the films in the oven, the ions have enough mobility and time to reorganise themselves to give a homogeneous distribution across the cross-section afterwards. Alginate fibres, due to their small diameter, are not expected to present a marked inhomogeneous ion profile, even after acetone drying.

To counterbalance the excess of positive charges occurring after long $CaCl_2$ exposure (observed in the previous section), it is apparent that Cl^- ions are introduced. However, the large amount of Cl^- ions found after 300 minutes of immersion in $CaCl_2$ leads to a dramatic drop of the charge equivalence ($Na^+ + 2\times Ca^{2+} - Cl^-$) of 2.4, compared with sodium alginate. Again, it must be recalled that the chlorine content may have been overestimated due to the choice of standard for SEM/WDX. In this study, it was not possible to distinguish between Cl^- ions introduced into the alginate matrix in the form of $CaCl_2$ or as free ions.

Skjåk-Bræk *et al.* (1989) have reported a calcium concentration gradient across alginate gel cylinders. The inhomogeneity in the calcium content was favoured by factors such as low concentrations of calcium ions in the $CaCl_2$ bath, low molecular weight, high concentration of alginate and high G content. The calcium gradient observed by Skjåk-Bræk *et al.* were observed over a much longer distance (19 mm) than for our samples. Furthermore, their measurements were carried out in the gel state. Reorganisation in the ion profile is supposed to occur during drying.

III.2.4. Other characteristics of the alginate salts:

i. Water content:

Calcium alginate gives similar weight losses (15-16 %) and decomposition temperatures (≈458 K) as the sodium samples. The zinc salt has a lower average content of water, 10 wt%, and the first TGA inflection point occurs between 443 and 448 K. The silver salt contains 4 to 5 wt% of water, and its inflection point is found around 428 K.

While there is an average of two H_2O molecules per M or G blocks in the sodium and calcium salts, this value is lower for the other samples. Just over one molecule of water per alginate block is found in the zinc salt and only half an H_2O molecule in the silver alginate. These different water contents may be explained by the different packing density arrangements in the alginate network. These different packing arrangements undoubtedly influence the water affinity when the samples are immersed in liquids.

The temperatures at the inflection point may be indicative of the degree of interaction between water and the alginate; i.e. a low temperature is most likely associated with

loosely bound water molecules, while a higher temperature would be more characteristic of tightly bound water within the alginate molecules.

ii. Crystallinity:

X-ray diffraction carried on the calcium, zinc and silver alginate salts did not reveal any more signs of crystallinity than what was found for the sodium sample. Therefore there does not seem to be any greater ordering induced by the addition of Ca^{2+}, Zn^{2+} or Ag^{+} ions.

iii. Mechanical tensile tests measurements:

Tensile tests were performed to mimic handling properties during storage, prior to exposure to a wound. Mixed sodium/calcium salts were tested, after various $CaCl_2$ immersion times. The mechanical properties of these alginates are summarised in table III.2.4. Each value represents the average of five tests.

Sample	Young's Modulus (GPa)	Fracture stress (MPa)	Fracture strain (%)
High-G + 3 min in $CaCl_2$	6.4 ± 1.8	144 ± 9	6.0 ± 1.4
+ 30 min in $CaCl_2$	5.8 ± 0.2	104 ± 10	5.4 ± 1.8
Medium-G + 3 min in $CaCl_2$	5.8 ± 1.4	128 ± 3	6.8 ± 1.5
+ 30 min in $CaCl_2$	6.3 ± 1.5	112 ± 21	5.7 ± 1.7

Table III.2.4. Mechanical properties of sodium/calcium alginate salts.

Although these results are associated with fairly large experimental errors, some trends can be observed, compared with pure sodium samples (table III.1.3). Upon calcium addition, the modulus is seen overall to increase while the strain values decrease. Therefore the alginates are rendered less ductile and tougher. Ca^{2+} ions either bring the alginate molecules closer to one another, giving rise to a better packing, or they introduce more inter/intramolecular bonding thus stiffening the polymeric molecules. For the two types of alginates studied, no clear differences appear in their mechanical properties. The same observation was made for the sodium salts.

CHAPTER IV: SPECTROSCOPIC ANALYSIS OF DIFFERENT ALGINATE SALTS

The aim of this section of the investigation was to gain a greater insight of alginate salts at a molecular level, by means of three complementary spectroscopic techniques. FTIR has been the most extensively reported method (Aspinall, 1982; Dupuy *et al.*, 1994; Filippov & Kohn, 1974; Mackie, 1971; Sartori *et al.*, 1997). Raman spectroscopy gives rise to molecular vibrations, either weak or absent in the infrared spectra. Finally, inelastic neutron spectroscopy (INS) has been used in the past to study the interaction of water with materials, as well as to analyse the hydrogen vibrations, but no work to date has been reported on alginates.

IV.1. FTIR study of sodium alginate

IV.1.1. FTIR assignment of sodium alginate:

The infrared spectrum of high-G sodium alginate is presented below, from 4000 down to 400 cm^{-1}:

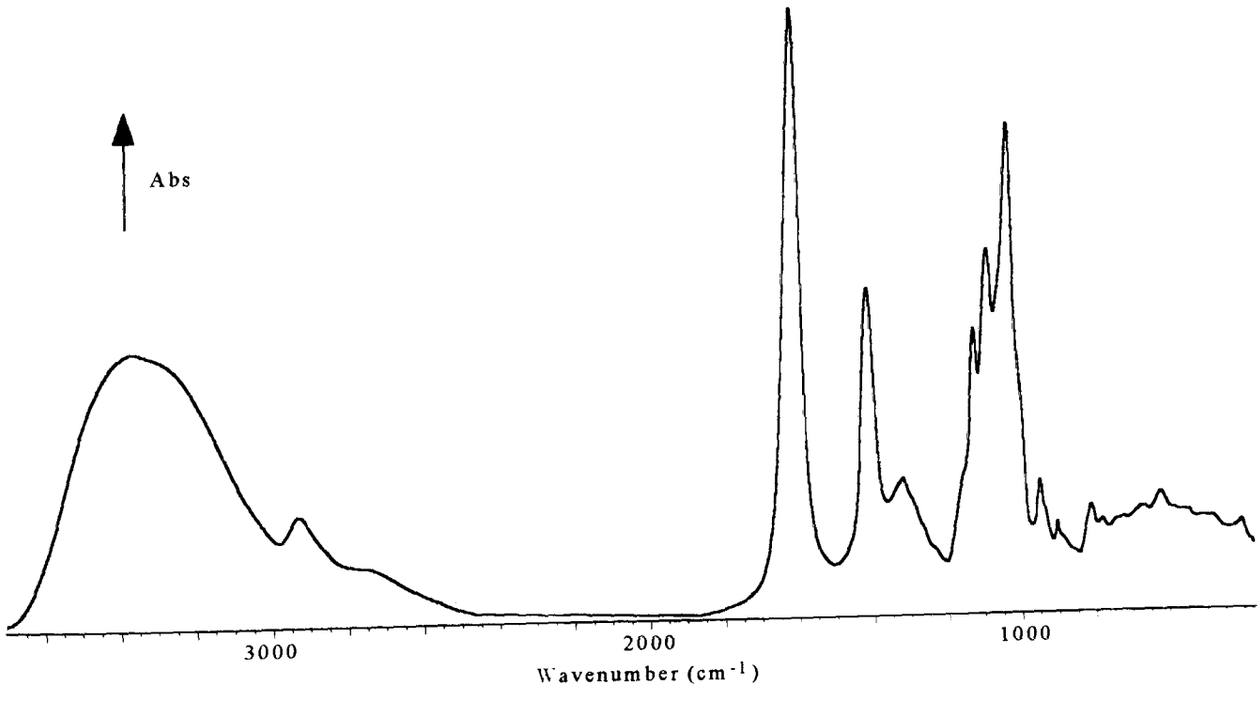

Figure IV.1.1.a. FTIR spectrum of high-G sodium alginate.

Assignment of this spectrum was carried out mostly from previous studies on polysaccharides (Aspinall, 1982; Rodd, 1965), and more particularly on alginates (Dupuy *et al.*, 1994). Furthermore, simplification of the IR pattern by deuterium exchange of relatively loosely bound hydrogens enables the location of most O-H vibrations. These bands are present in the protonated but missing in the deuterated sample (due to a large change in mass between O-H and O-D groups), as shown in figure IV.1.1.b for sodium alginate, at 1060 and 903 cm^{-1}. Similar observations were obtained when comparing mixed sodium/calcium salts. There are additional changes between the protonated and the deuterated samples, as the vibration of most groups of atoms are expected to be influenced by the introduction of different ions in the network.

Both samples, prepared as thick films (as they were also used for INS studies), were scanned with an attenuated total reflectance (ATR) unit; therefore only a couple of μm on the surface were analysed.

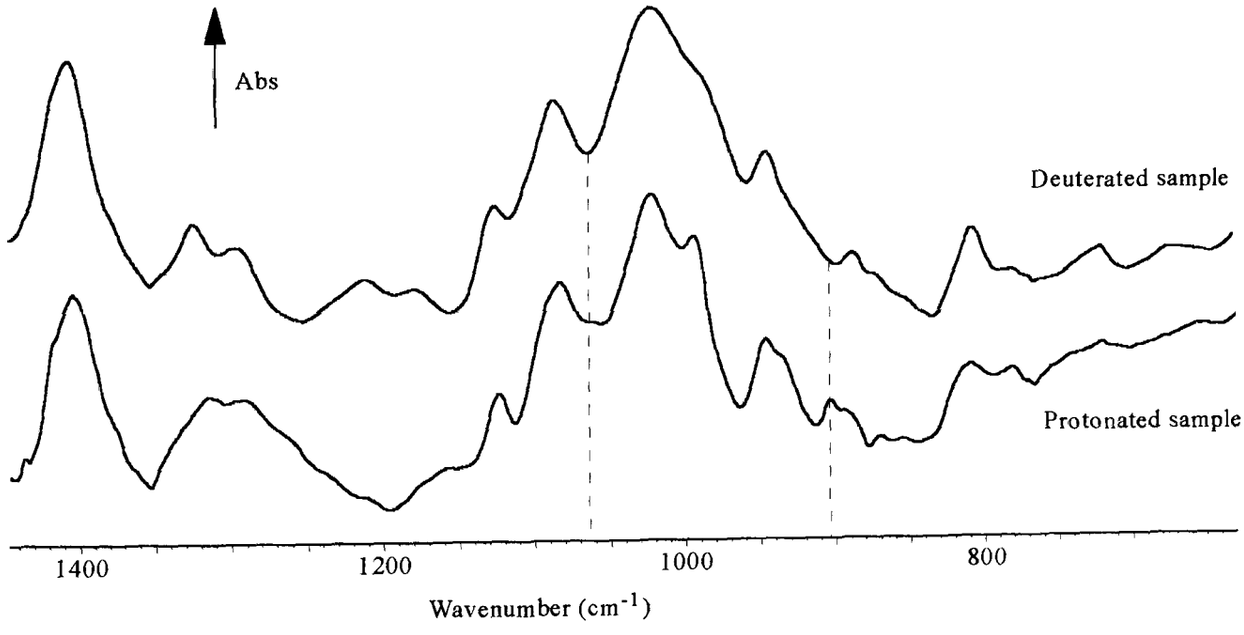

Figure IV.1.1.b. Comparison of protonated and deuterated sodium alginates.

Other assignments, such as the C-H vibrations, were made easier from the Raman and INS spectra, as they appear strongly. However, the convoluted profile of the alginate spectrum (specially the fingerprint below 1400 cm^{-1}) does not permit a complete and definitive interpretation.

From the previous points, table IV.1.1. was drawn up so as to give detailed band assignments for sodium alginate.

Wavenumber (cm^{-1})	Intensity - Shape	Assignment
3370	very strong - broad	O-H stretching, H-bonded
3250	strong - shoulder	O-H stretching, H-bonded
2930	weak - broad	C-H stretching asym.
2750	weak - shoulder	C-H stretching sym.
1610	very strong - sharp	COO^- stretching asym.
1414	medium - sharp	COO^- stretching sym.
1335	weak - shoulder	?
1320	weak - broad	C-H in-plane deformation
1295	weak - shoulder	C-H in-plane deformation
1165	weak - shoulder	?
1125	medium - sharp	C-O & C-C stretching
1088	medium - sharp	C-O, COC & C-C stretching
1060	medium - shoulder	O-H in-plane deformation
1030 - 1035	very strong - sharp	C-O, COC & C-C stretching
997	medium - shoulder	COC stretching
948	weak - sharp	CCH deformation
935	weak - shoulder	?
903	weak - sharp	O-H out-of-plane deformation
892	weak - shoulder	C-H out-of-plane deformation
815	weak - sharp	C-C stretching
780	weak - broad	C-C stretching
670	weak - broad	C-H out-of-plane deformation
625	weak - sharp	?
500	weak - broad	C-O deformation

Table IV.1.1. Band assignments of sodium alginate.

IV.1.2. Influence of the M/G ratio:

Figure IV.1.2. shows the fingerprint and difference infrared spectrum taking O-H

stretching peak (3370 cm^{-1}) as a reference, of PROTANAL LF 10/60 (high-G) and LF 10/60 LS (medium-G) alginate samples to analyse the influence of the M/G ratio.

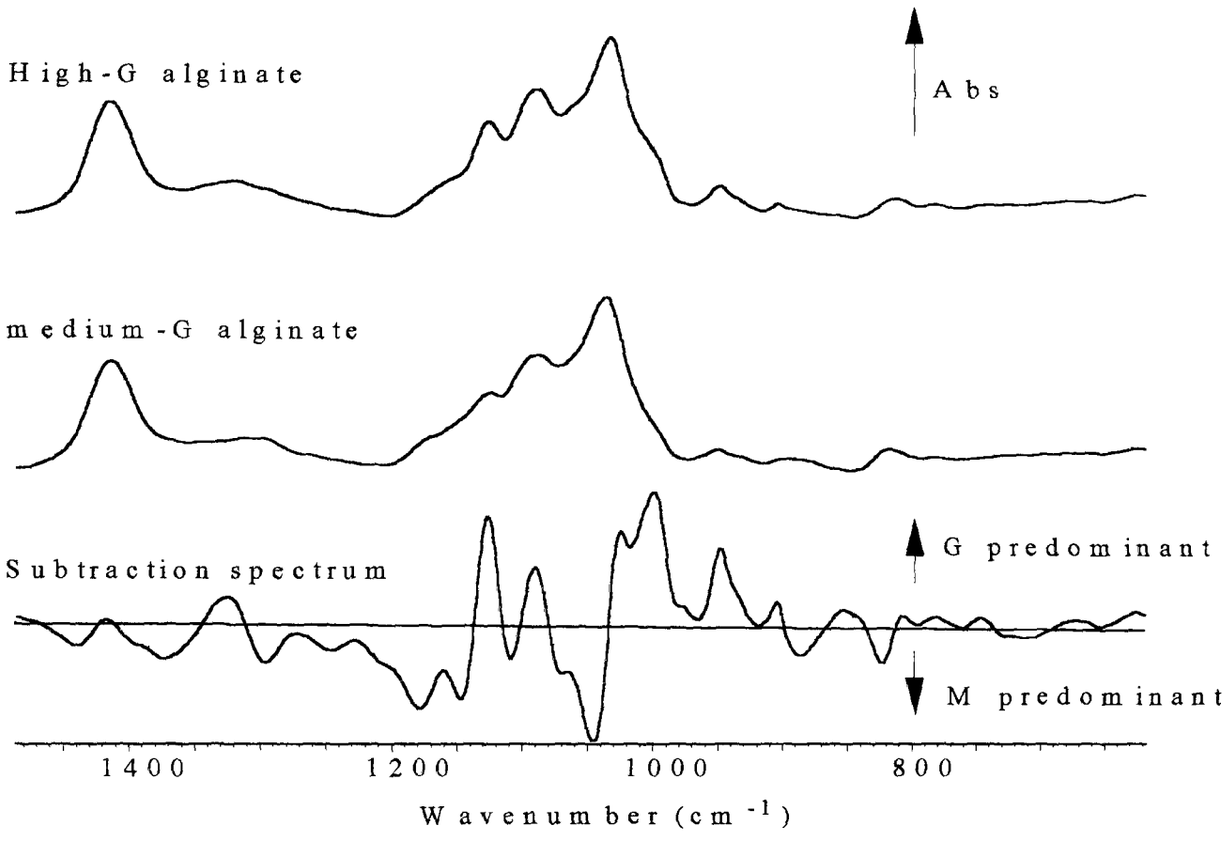

Figure IV.1.2. Fingerprint region of sodium alginates.

The infrared spectra of alginates containing different M/G ratios show some variations in relative band intensities. For the high-G alginate (LF 10/60), the bands or shoulders around 1320, 1130, 1090, 1020, 1000 and 950 cm^{-1} are of greater intensity than for the medium-G alginate (LF 10/60 LS). By contrast, the bands or shoulders at 1370, 1295, 1250, 1180, 1150, 1050, 890 and 820 cm^{-1} are more pronounced for the medium-G sample. Therefore the first set of wavenumbers is characteristic of guluronate (G) while the second is typical of mannuronate (M) blocks.

Other authors (Mackie, 1971; Filippov & Kohn, 1974) obtained infrared spectra of pure G- and pure M-alginates (obtained via fermentation) by infrared, and they observed similar differences. One further peak, located at 780 cm^{-1} (very weak in our difference spectra) was also attributed to the G blocks.

IV.2. FTIR spectroscopy of calcium salts with different M/G ratio

The FTIR spectra of calcium high-G and medium-G alginates are presented in figure IV.2., together with a difference spectrum (taking O-H stretching as the reference peak).

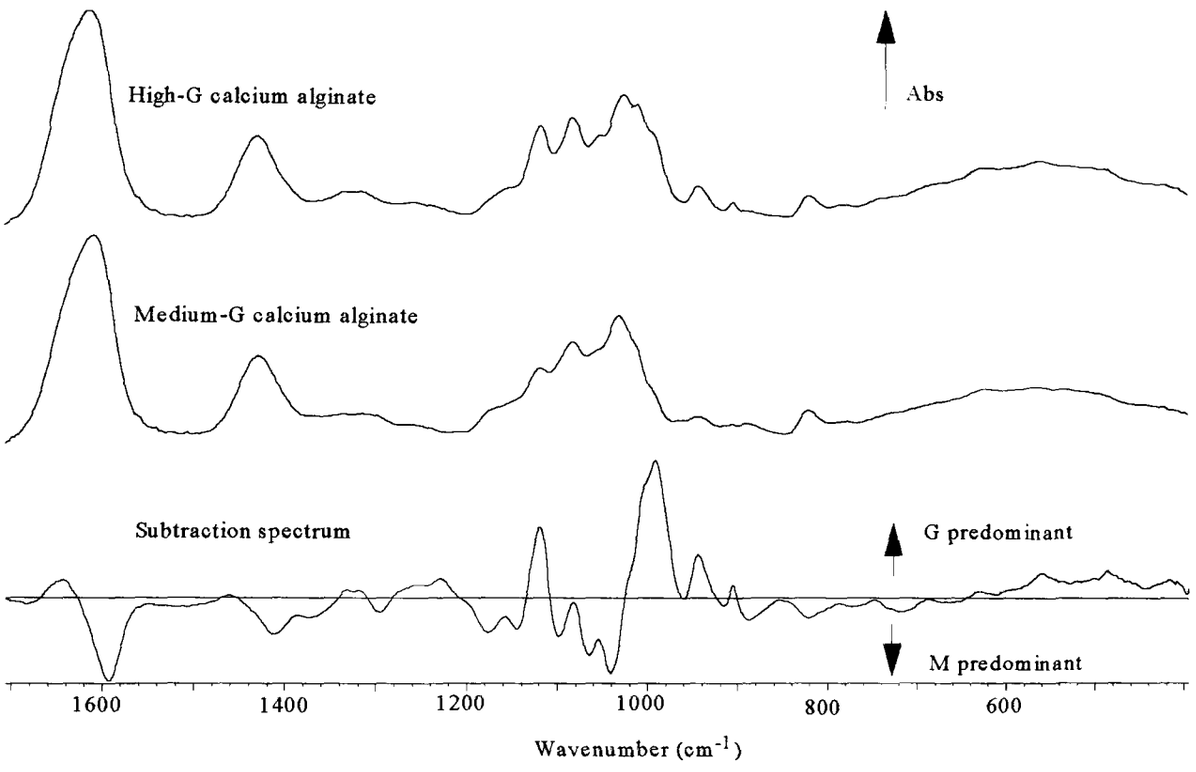

Figure IV.2. Fingerprint region of calcium alginates with their subtraction.

The subtraction spectrum presents overall similar features to the one between sodium alginates (figure IV.1.2.). However, some differences emerge, the main ones being:

-the lowest wavenumber contribution of the COO^- stretching peaks (*ca.* 1610 and 1425 cm-1) is stronger for the medium-G sample; this implies that $COO^-...Ca^{2+}$ bonding is more important in the medium-G than in the high-G alginate (as opposed to COO^-...H-O bonding; justification of these assignments is given in the following section);

-the shoulders at ≈ 1060 and 1010 cm^{-1} become peaks in the high-G alginate; the first peak would suggests stronger O-H deformation vibration in the high-G sample. The second peak could be related to metal-oxygen-metal bonds (Perry *et al.*, 1991), leading to more favoured bonding between the oxygen atoms and the calcium ions in the high-G alginate.

IV.3. FTIR spectroscopy of different high-G alginate salts

Whilst calcium ions are believed to be chelated preferentially to the G blocks (due to their unique spatial arrangement), other ions such as Cu^{2+}, Co^{2+} and Mn^{2+}, have been shown to be bound to the carboxyl groups in both M and G blocks (see section I.A.2.3). In order to get a better understanding of the ions binding to the alginate molecules, several alginate salts were prepared and analysed.

IV.3.1. FTIR spectra of high-G alginate salts:

Four different salts were prepared from alginate PROTANAL LF 10/60: sodium (which is the starting material), calcium (for its haemocompatibility properties and to look into the "egg-box" model), zinc (due to its haemocompatibility properties as well; Liyanage *et al.*, 1995) and silver alginates (Ag^+, although a monovalent ion, has been shown to induce gelation in alginates- Yonezawa *et al.*, 1992). It is known that the wider the separation between two elements in the periodic table, the more ionic the bond is between them, and the closer the two elements, the greater the degree of covalence (Callister, 1994). Therefore silver and zinc are expected to present mainly a covalent character with the alginate molecules (C and O atoms) while sodium and calcium will have a more ionic type of bonding.

The sodium alginate solution was immersed for 300 minutes in $CaCl_2$, $ZnCl_2$ or $AgNO_3$, respectively. Because the films obtained were relatively thin (less than 10 μm), the sodium/calcium (or sodium/zinc or sodium/silver) conversion proceeded more quickly than for the thick films (120 μm on average). Therefore an immersion of 300 minutes is expected to produce calcium (or zinc or silver) alginates rather than mixed salts (such as sodium/calcium).

Various changes in both the shape and position of peaks were observed between the different alginate salts. This would be expected as the various ions studied have different radii, as given in table IV.3.1. Therefore their surrounding is bound to be perturbed, leading to peak variations.

Ion	Radius (nm)
Ag^{+}	0.13
Ca^{2+}	0.10
Na^{+}	0.10
Zn^{2+}	0.07

Table IV.3.1. Ionic radius (Brandrup & Immergut, 1975).

FTIR subtraction was rendered difficult as there was no obvious reference peak, constant with all samples. Comparison was thus carried out by simple observation rather than by spectral subtraction. This was performed in relation to the sodium alginate, which was taken as the reference spectrum. Figure IV.3.1.a. presents the FTIR of the four alginate salts, from 4000 to 400 cm^{-1}, while figure IV.3.1.b. shows the fingerprint region, for the same samples:

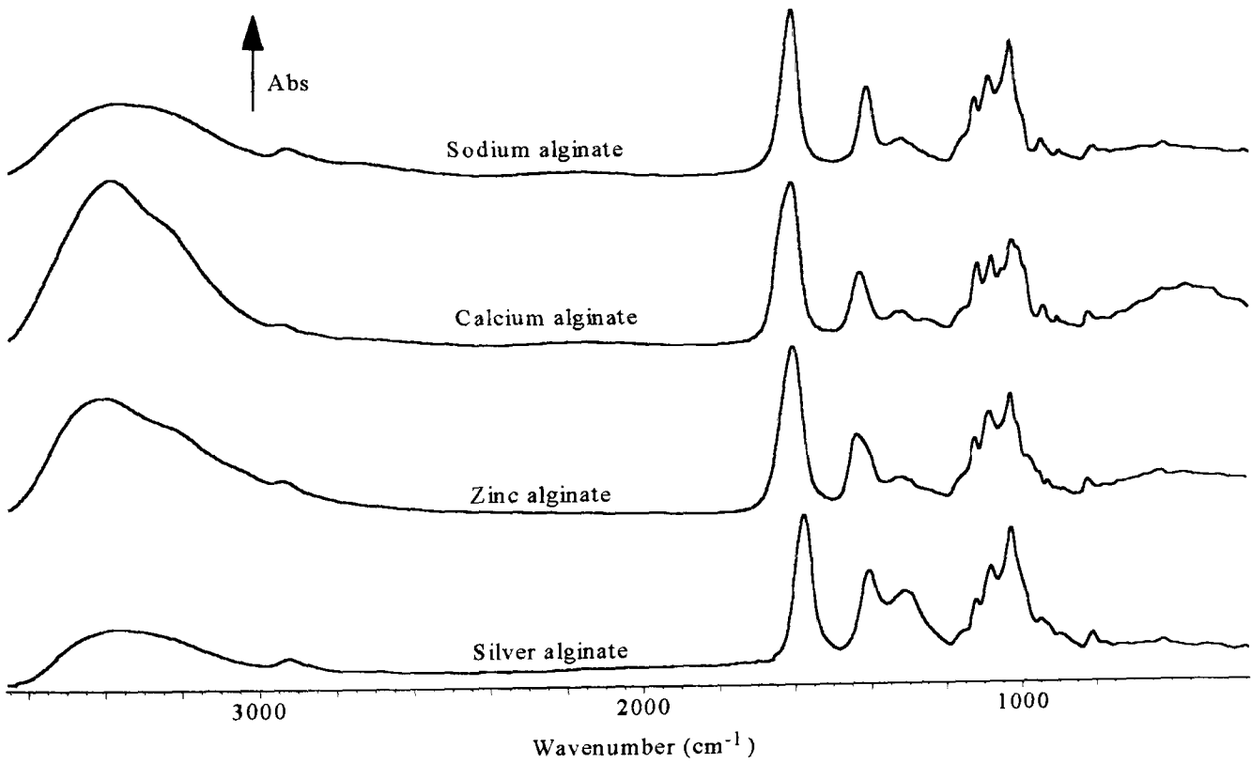

Figure IV.3.1.a. FTIR spectra of different high-G alginate salts.

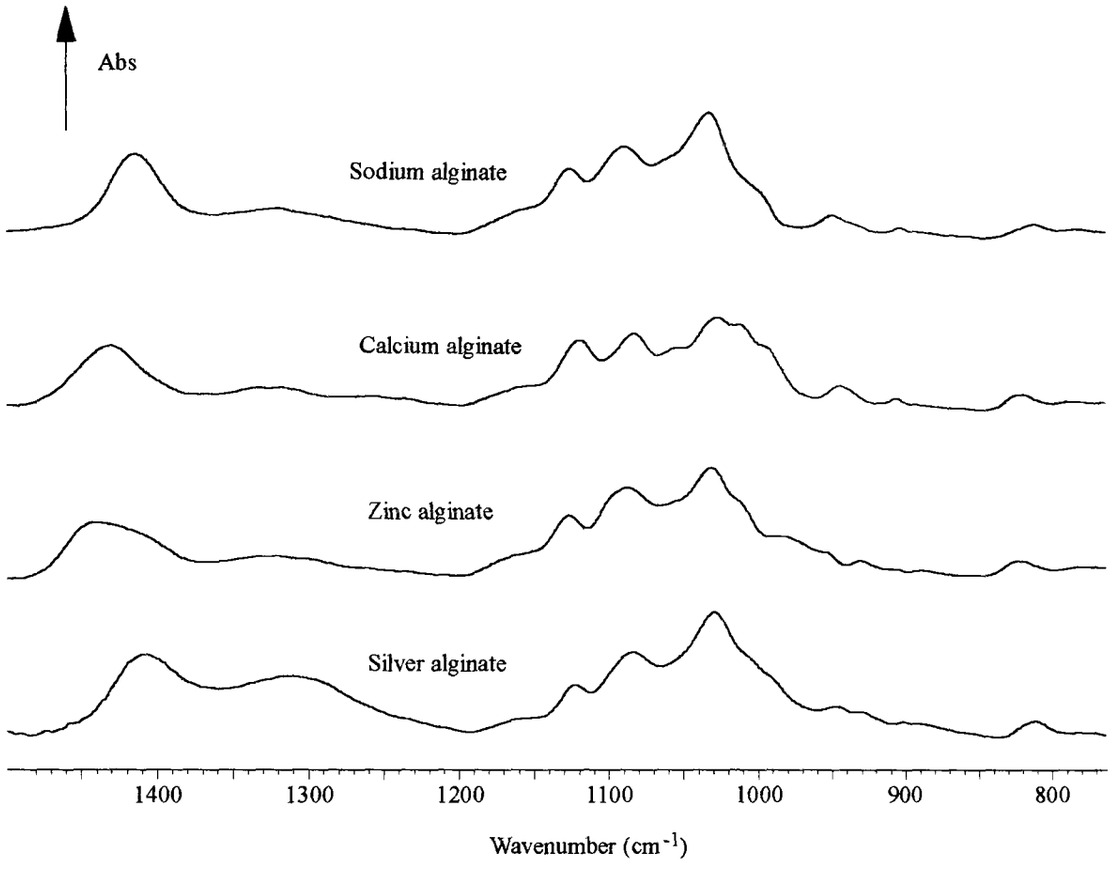

Figure IV.3.1.b. FTIR fingerprint region of different high-G alginate salts.

FTIR alginate spectra can give direct information on the type of bonding involved, and on the ion exchange process. The major peak variations are described below.

IV.3.2. Hydroxyl vibrations:

The O-H stretching vibration appears as a broad peak between 3400 and 3370 cm^{-1}, with a shoulder at slightly lower wavenumbers, around 3250 cm^{-1}. Deconvolution was performed in order to determine the relative proportion of each contribution.

i. Deconvolution:

The procedure to deconvolute the O-H stretching peaks was as follow:

-a baseline correction was performed between 3800 to 2800 cm^{-1} (using the Omnic software);

-the second derivative of the region of the spectrum selected was visualised. This enabled us to locate the exact peak or shoulder position;

-a multiple Gaussian deconvolution was performed, using the Microcal Origin software.

The curves obtained for the different alginate salts are displayed in figure IV.3.2.

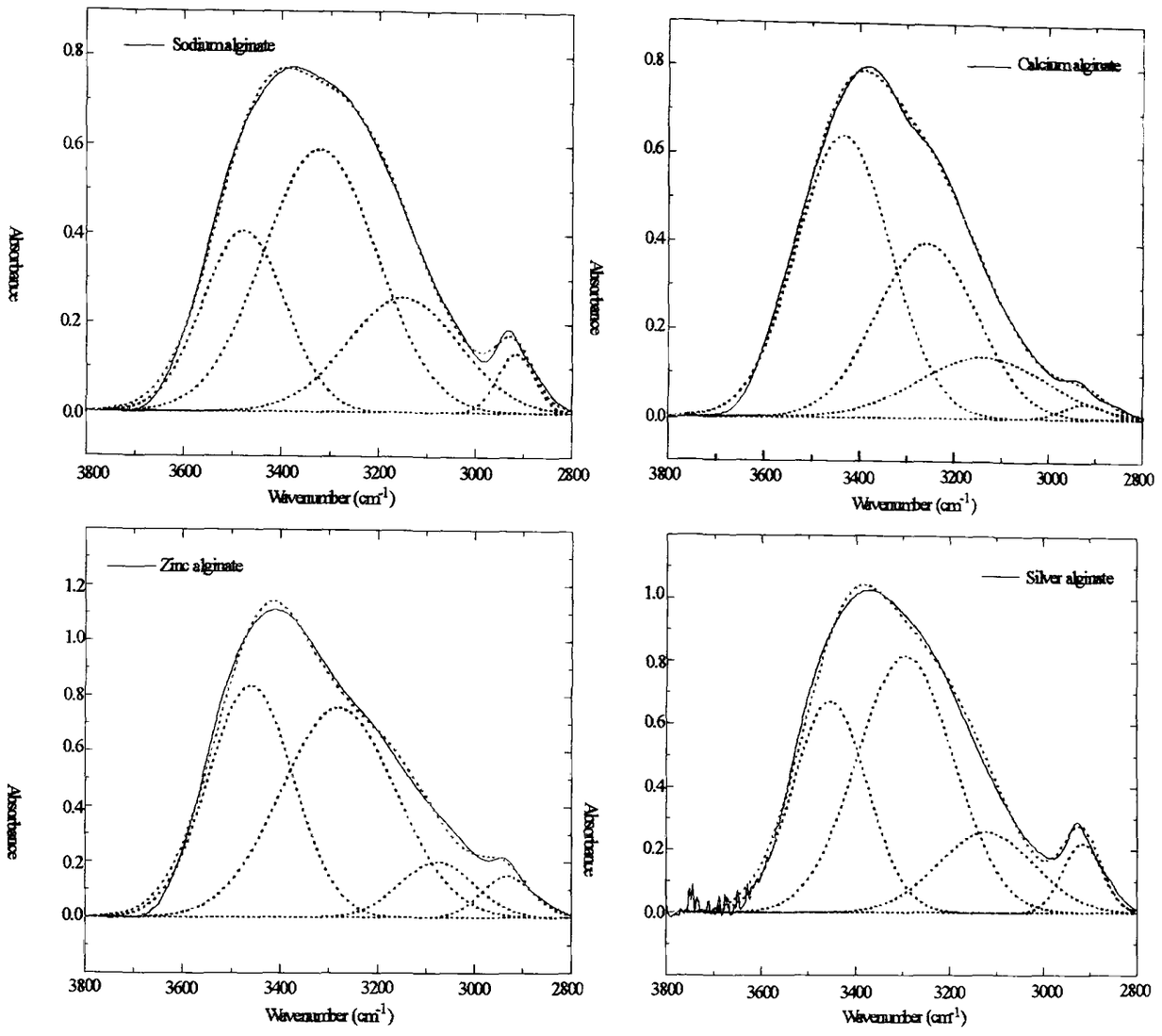

Figure IV.3.2. Deconvolution of the O-H stretching peak for different alginate salts.

The black lines correspond to the infrared spectra; the blue dotted curves are the deconvolution, and the red dotted lines are the summation of these blue lines. If one considers only the two main contributions to the O-H peak (i.e. *ca.* 3450 and 3300 cm^{-1}), then it is apparent that the lower wavenumber peak is stronger for the monovalent ions. By contrast, the high wavenumber peak is more pronounced for the divalent cations.

ii. Interpretation:

From the relatively low frequency values of both O-H stretching peaks, it is evident that free O-H groups are not present in these samples (otherwise, a peak or shoulder at 3600 cm^{-1} would be apparent), and therefore all the hydroxyl groups (from both water and alginate molecules) are involved in hydrogen bonding. The lower the stretching frequency, the greater the strength of the hydrogen bonding (Rodd, 1965). These bonds

are of prime importance in stabilising the conformations of carbohydrate molecules (Zhbankov, 1992).

Two possibilities arise for a more detailed assignment of the two hydroxyl peaks. The first one distinguishes between intramolecular and intermolecular bonding (Dupuy *et al.*, 1994; Aspinall, 1982). An alternative is to consider that, due to the weakness of intramolecular compared with intermolecular bonding in the solid state, the first bond cannot be discernible. Indeed Zhbankov (1992) found, from calculations, that within one monosaccharide cycle, only relatively weak intramolecular hydrogen bonds could be detected. Therefore both peaks are expected to be due to intermolecular bonding (Michell, 1990) between alginate molecules and between alginate and water.

In our spectra, the main O-H stretching peak (at *ca.* 3360 cm^{-1}) becomes narrower and of greater intensity for calcium and zinc alginates; this is paralleled by a broadening of the COO^- stretching peaks. Thus the strongest peak can be assigned to O-H...$^-$OOC (only the hydrogen atom is involved in bonding), while the second peak corresponds to O-H...O-H bonding (as both atoms O and H are involved in bonding in this latter case, the wavenumber of the resultant peak is expected to be lower than in O-H...$^-$OOC). Similar combinations were observed by Coleman & Painter (1984) for poly(ε-caprolactone)-poly(vinyl phenol) blends.

The dominance of the main O-H stretching peak (as opposed to the shoulder) for the divalent cations (figure IV.3.2.) reveals an overall higher intermolecular bonding between hydroxyl and carboxyl groups. An alternative, for the zinc alginate, is that its relatively small size leads to more freedom of movement in the alginate molecules, thus presenting higher frequencies (3410 cm^{-1}) compared with sodium alginate (3375 cm^{-1}). Regarding the calcium ion, its radius is similar to that of sodium; therefore many changes observed in peak shifts must be due to the different electronic structure and the chemical interaction. For the silver salt, a decrease in band shift of 15 cm^{-1} (i.e. 3360 cm^{-1}) compared with sodium alginate can be characteristic of more OH...OH bonds, or can be due to constraint in block movement from the increased size of the silver ion.

From the comparison between protonated and deuterated alginates, the O-H in-plane deformation has been localized at *ca.* 1060 cm^{-1}. It appears as a peak for calcium alginate, as a shoulder for zinc alginate, and is even weaker for the sodium and the silver salts. This peak is certainly indicative of O-H...$^{-}$OOC bonding.

Finally, the O-H out-of-plane deformation peak was observed at approximately 900 cm^{-1}, as a small peak (particularly low in intensity for the zinc alginate). However, due to its weakness, it seems hazardous to try to interpret the peak in more detail.

Hydroxyl-hydroxyl and hydroxyl-carboxyl interactions not only involve bonding between alginate molecules but also alginate-water interaction. Alginate-water interaction is thought to prevail in the sodium alginate, compared to the silver alginate, as sodium alginate dissolves in contact with water while silver alginate forms a strong gel. This statement is corroborated by the thermogravimetric measurements (see section III.2.4.i.), where the weight percentage was estimated to be 4 %, compared with 15 % in the sodium salt. Therefore much more water is expected to be bound to the sodium alginate than to the silver alginate molecules. Unfortunately, the two types of binding (O-H...O-H between alginate/alginate and alginate/water) cannot be differentiated via FTIR spectroscopy. A second hypothesis is that intermolecular bondings are created via Ag^{+} ion-alginate backbone interactions (due to its bigger size, compared with the other ions) rather than via hydroxyl interactions. Aggregation of silver particules may also occur (Yonezawa *et al.*; 1992).

IV.3.3. C-H vibrations:

In a detailed analysis of FTIR on polymer blends, Coleman & Painter (1984) noted that for most atomic groups, the observed frequency shifts are not only associated with changes in the force field, but also with changes in geometrical conformation. Fortunately, some group frequency modes such as C-H and C=O stretching do not couple significantly to backbone vibrations.

In our materials, C-H stretching is found as a weak peak around 2930 cm^{-1}. Relatively small shifts are observed for zinc alginate (2939 cm^{-1}) and silver alginate (2923 cm^{-1}) from the sodium alginate wavenumber (2930 cm^{-1}). By contrast, the calcium sample shifts to much higher frequencies (2952 cm^{-1}); but this value is affected by the end tail of the O-H stretching peak, being added to the C-H peak, thus "emphasizing" the shift. It can be concluded, nevertheless, that calcium alginate exhibits a higher degree of freedom of its C-H groups, compared with the other salts; to a lesser extent, a similar observation can be made for zinc alginate.

The weak peak at *ca.* 1320 cm^{-1} and the shoulder at *ca.* 1300 cm^{-1} in the sodium alginate spectrum have been assigned to C-H in-plane deformation, in G and in M blocks, respectively (determined from sodium LF 10/60 and LF 10/60 LS subtraction). The peak appears at a lower wavenumber for the silver salt (1312 cm^{-1}), whilst the shoulder does not change position. The intensity in absorbance is much higher for the silver sample. Indeed this difference is the more striking one between the monovalent cations. The rest of their spectra are very similar. Therefore, the introduction of Ag^{+} ions into the alginate either gives rise to a greater degree of deformation vibration of the C-H groups, or creates a specific type of bonding with C-H. The shoulder close to 1300 cm^{-1} practically disappears for calcium alginate. The bending movement of the C-H groups in the M blocks may be hindered by the introduction of divalent cations. Surprisingly, the C-H vibration of the G blocks does not seem affected, but it may be influenced by the many other vibrations that absorb in this region.

The shoulder present in sodium and silver alginate, and measured at 1335 cm^{-1}, becomes more dominant with zinc ion and calcium ion additions. This may be due to a new form of binding, but this has not been assigned so far. Likewise a new peak appears around 1250 cm^{-1} (this wavenumber is specific to G blocks) for calcium alginate, and may arise from new bonding between Ca^{2+} ions and the guluronates.

C-C-H deformation occurs around 950 cm^{-1} (also G predominant). It is well pronounced for the calcium sample, showing the dominance of this vibration with calcium over other salts. This peak is particularly weak for zinc and silver salts; and may

be due to the existence of some covalent bonding (due to the nature of the ion) with the carbon atom. The 892 cm^{-1} peak (weak intensity) has been assigned to C-H deformation, and is more specific of M blocks. It is more pronounced for zinc alginate.

Overall, it appears that some C-H vibrations are hindered, others not, depending on the ion introduced in the alginate network. However, most of these peaks are weak in FTIR, and therefore analysis is made difficult. Greater freedom of movement for these groups is found in the calcium and the silver samples. It must be pointed out that there are five C-H groups per M or G block. Each one is expected to present different degrees and types of freedom, according to its neighbouring atoms, and thus to give rise to different vibrational peaks. However, it is not possible from these FTIR spectra to distinguish between them all. Therefore a general, broad picture of these groups is obtained, rather than a detailed analysis of the individual vibrations.

IV.3.4. Carboxyl vibrations:

COO^- stretching is split into asymmetrical and symmetrical C=O vibrations. The first one is found at *ca.* 1610 cm^{-1}, and the second one between 1440 and 1410 cm^{-1}. The former is more characteristic of the carboxyl groups, as it is generally more constant in frequency, whilst many other skeletal vibrations occur in the range 1400-1300 cm^{-1} (Aspinall, 1982). These two peaks are represented below, for the different alginate salts:

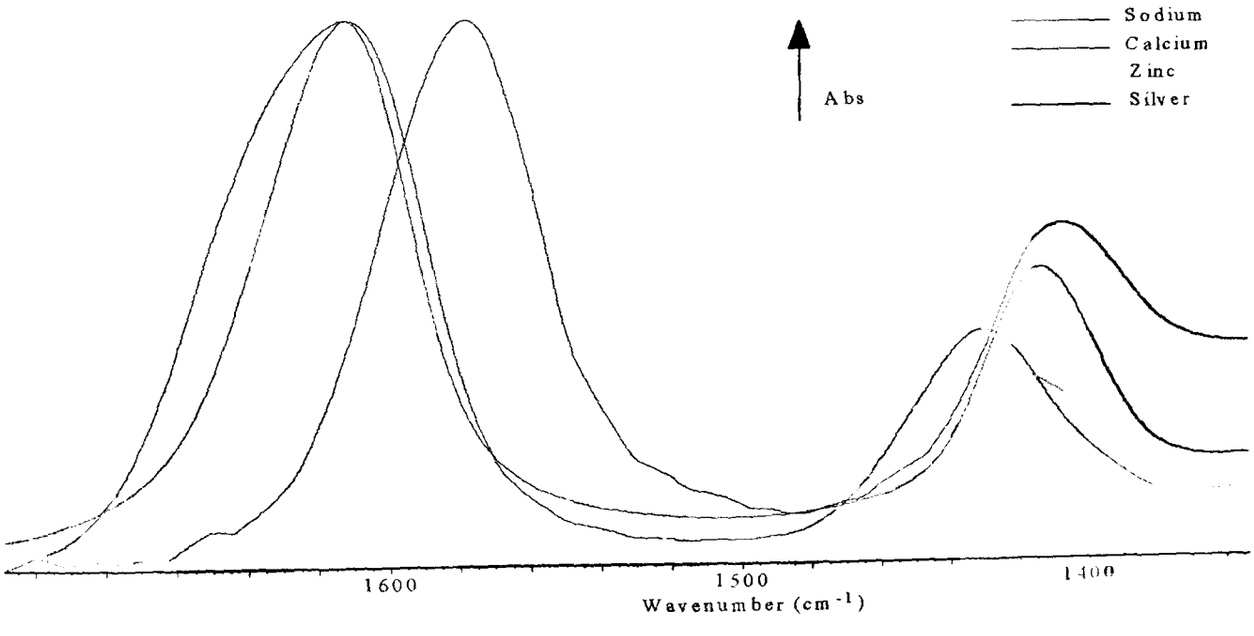

Figure IV.3.4.a. COO^- stretching peaks of different alginate salts.

The sharpest COO^- stretching peaks are found for the sodium alginate. This is indicative of a more specific type of bonding (i.e. mainly $COO^-...Na^+$) compared to the other salts. To a lesser extent, this seems also true for the silver alginate. For both zinc and calcium alginates, if O-H is assumed to have hydrogen bonding with the carboxyl groups, and if the divalent cations are also believed to be bound to COO^-, then two peaks are expected for both COO^- stretching vibrations. Indeed, both asymmetrical and symmetrical COO^- stretching peaks are observed to broaden upon calcium and zinc immersion (a similar observation was made by Coleman & Painter (1984), on the interaction between PVDF and PMMA). These statements have been verified by performing deconvolution on the COO^- asymmetric peak for the various salts:

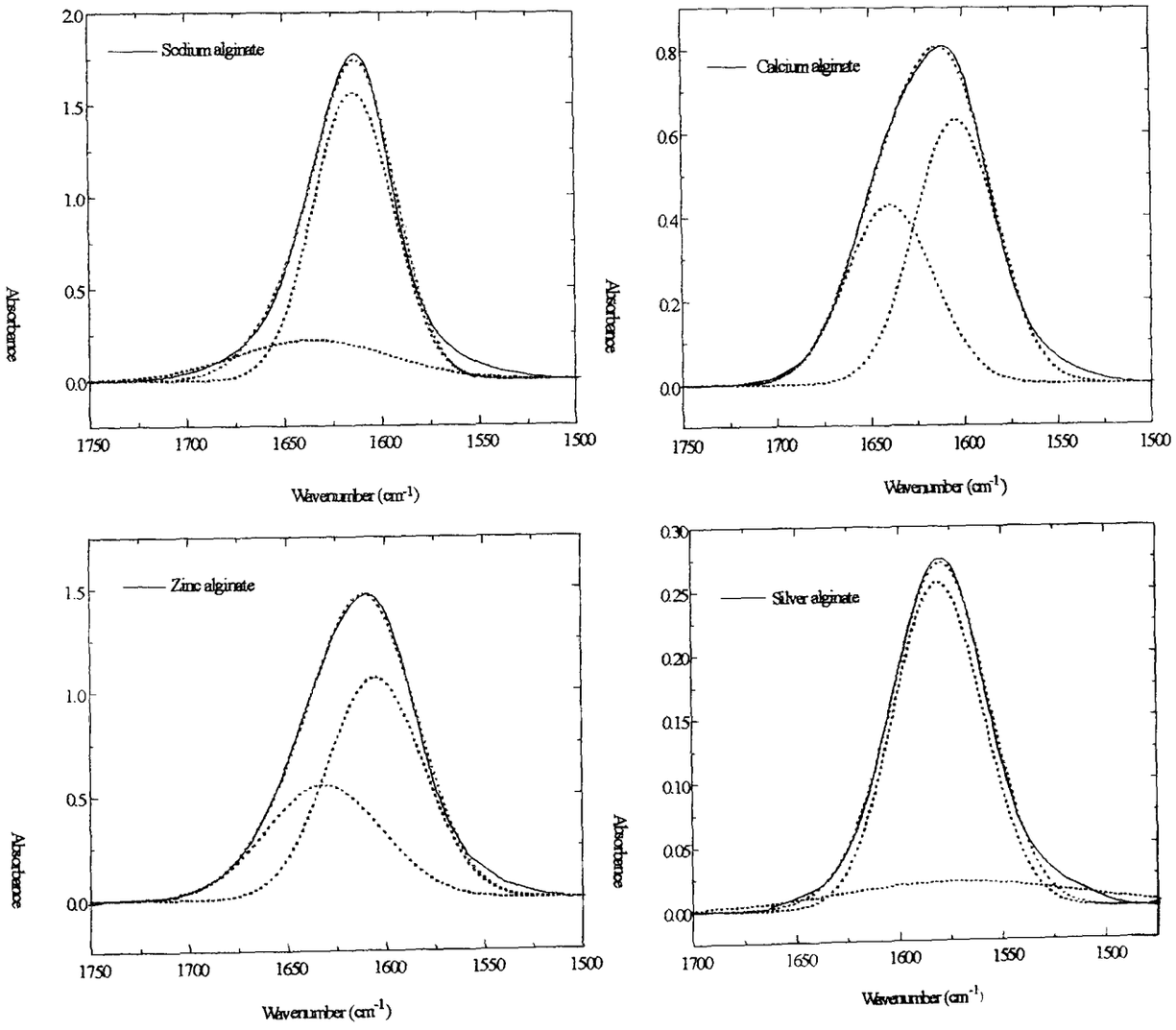

Figure IV.3.4.b. Deconvolution of the COO- asymmetric stretching peak for different alginate salts.

COO^-...OH is a hydrogen type of bonding (with a typical energy around 50 $kJ.mol^{-1}$- Callister; 1994) while the interaction between the COO^- groups and the metal ion is either primarily an ionic bond, with Ca^{2+} (600-1500 $kJ.mol^{-1}$), or a covalent bond, with Zn^{2+} (50-800 $kJ.mol^{-1}$). Therefore, when the COO^- peaks can be decomposed into two sub-peaks, the higher frequency peak will be attributed to COO^-... HO binding, and the second peak will arise predominantly from carboxyl-metal bonding. Surprisingly, wavenumbers for the COO^- asymmetric peak are almost identical for sodium (1610 cm^{-1}), calcium (1612 cm^{-1}) and zinc (1608 cm^{-1}) alginates. But it must be pointed out that HOH bending vibration is strong in this region, and may be the cause for the frequency narrowing. By contrast, the vibration for the silver alginate is found at *ca.* 1577 cm^{-1}, most certainly due to the larger radius. Regarding the COO^- symmetric stretching peak, important shifts are observed, towards higher frequencies for the divalent cations (1430 cm^{-1} for calcium, 1437 cm^{-1} for zinc and only 1414 cm^{-1} for sodium alginate). These peak shifts, accompanied by broadening, are mainly due to COO^- groups involved in different types of binding, as described previously (specially COO^-...HO which seems practically non-existent for sodium alginate).

Whereas the two divalent cations follow a similar behaviour, with regard to the O-H and the COO^- groups, silver alginate presents a different, more complex type of binding than the other monovalent ion, sodium. Its COO^- asymmetric stretching suggests one type of bonding only (presumably COO^-...Ag^+), similarly to the sodium salt, and it vibrates as low as 1580 cm^{-1}. The important shift is certainly due to a constriction of the COO^- groups by the large size of the silver ion. However, the COO^- symmetric stretching is not observed to shift to such an extent (1408 cm^{-1}; opposite to what was obtained for the divalent ions), and it broadens, compared with sodium alginate. Therefore a specific type of bonding assumed previously is no longer valid for these silver systems. There exists either different types of bonding or different levels of bonding between COO^- and the silver ions (depending on whether the silver ions are on their own or as aggregates for example).

From Socrates (1994), rocking-in-plane and out-of-plane deformation vibrations of the carboxylic ion are assigned to medium-to-strong bands in the region 760-400 cm^{-1}. This

part of the infrared spectrum is more marked for the calcium sample and, to a lesser extent, for the zinc alginate. This prevalence may ensue from COO^- groups being involved in hydrogen bonding.

IV.3.5. C-O and C-C vibrations:

Several groups containing C-O are found in the alginate molecules: the alcohol groups (COH), the glycosidic bonds (COC) and the skeletal groups, in each M and G block (COC). However, no distinction between these was possible.

In the fingerprint region of the FTIR spectra, numerous peaks due to C-O and C-C vibrations overlap. Therefore analysis is rendered very difficult, since no peak is due to "pure" vibrations, but rather to mixed modes. Significant changes are observed regarding peak shapes.

The peak of medium intensity at 1125 cm^{-1} is higher for calcium alginate, while quite similar for the three other salts. It has been assigned to C-C stretching and to C-O stretching in COH groups (from the INS spectra; see IV.5.4.), and is characteristic of the G blocks. This may reflect a higher degree of freedom for COH in contact with calcium (where O-H is preferentially bound to COO^- than to the other OH groups, thus leading to more mobility for the C-O groups).

The next peak, around 1085 cm^{-1}, is related to C-O, C-C and to COC stretching vibrations, and is again, more specific to G blocks. This band weakens upon calcium ion immersion. Thus, movement of these groups is made more difficult in the presence of Ca^{2+} ions, certainly due to a stronger bonding between the calcium ions and the G blocks (this would support the "egg-box" model). The broadening with zinc ions implies a new type of bonding. One possibility is of partial covalent binding between Zn^{2+} and the skeletal groups.

The strong and sharp peak at *ca.* 1030 cm^{-1} is also assigned to C-C and to COC vibrations. As the wavenumber is lower than for the previous peak, these COC groups are expected to be more flexible, and thus must belong to the glycosidic bonds. This

band decreases in intensity for the divalent cations, indicating some constraint in these groups, maybe due to a greater packing of the alginate molecules.

This set of three strong peaks is observed to shift towards lower wavenumbers for calcium (1119/ 1083/ 1026 cm^{-1}), silver (1121/ 1083/ 1028 cm^{-1}), and partially for zinc (1126/ 1087/ 1030 cm^{-1}), compared with the sodium sample (1125/ 1089/ 1032 cm^{-1}). These shifts are influenced by bond sharing, but also by the cation characteristics (radius, charge, mass) as already mentioned. However, a greater packing of the alginate molecules is, once more, anticipated in contact with the divalent ions.

A peak appears for calcium alginate (and as a shoulder for zinc alginate) at 1010 cm^{-1}; a new type of bonding must occur between the divalent ions and some skeletal groups.

The shoulder around 996 cm^{-1}, for sodium and calcium alginates, characteristic of COC stretching vibration, is lowered to 992 cm^{-1} for the silver sample and to 985 cm^{-1} for the zinc sample. This implies some preferential binding between COC and Zn^{2+} , rather than with the other cations.

Many other peaks are present below 1000 cm^{-1}, all of fairly weak intensity. Amongst them, the two small peaks at 820 and 780 cm^{-1} have been assigned to C-C stretching, in M and G blocks respectively. Overall, no great change is observed for these. However, the first peak appears asymmetric, towards the higher wavenumbers for Ca^{2+} and Zn^{2+}, and towards lower wavenumbers for Na^{+} and Ag^{+}. Again different types of bonding are involved with the skeletal vibrations.

The outcome of this section is a higher level of constraint in the skeletal alginate groups upon the introduction of calcium and zinc, and the appearance of new types of bonding, compared with the sodium alginate. However, no dramatic changes are observed upon silver addition.

IV.4. Raman spectroscopy of the different alginate salts

FTIR provides valuable information on the molecular structure, but it is related only to the presence of polar groups. However, polar groups give rise to weak peaks in Raman spectra, thus enabling one to get more information about the backbone structure of the molecule (Aspinall, 1982). Whilst thin films were necessary for the infrared experiments, thick samples were scanned by Raman spectroscopy, to improve the signal. The thick films were either pure sodium or mixed salts (sodium/calcium or sodium/zinc), as the pure salts of divalent cations were too brittle to handle; likewise the mixed sodium/silver salts were too brittle to handle. Only high-G samples were prepared.

IV.4.1. Raman spectra:

Here, sodium, sodium/calcium and sodium/zinc alginates were analysed. The different spectra are presented in the following figure IV.4.1.a.:

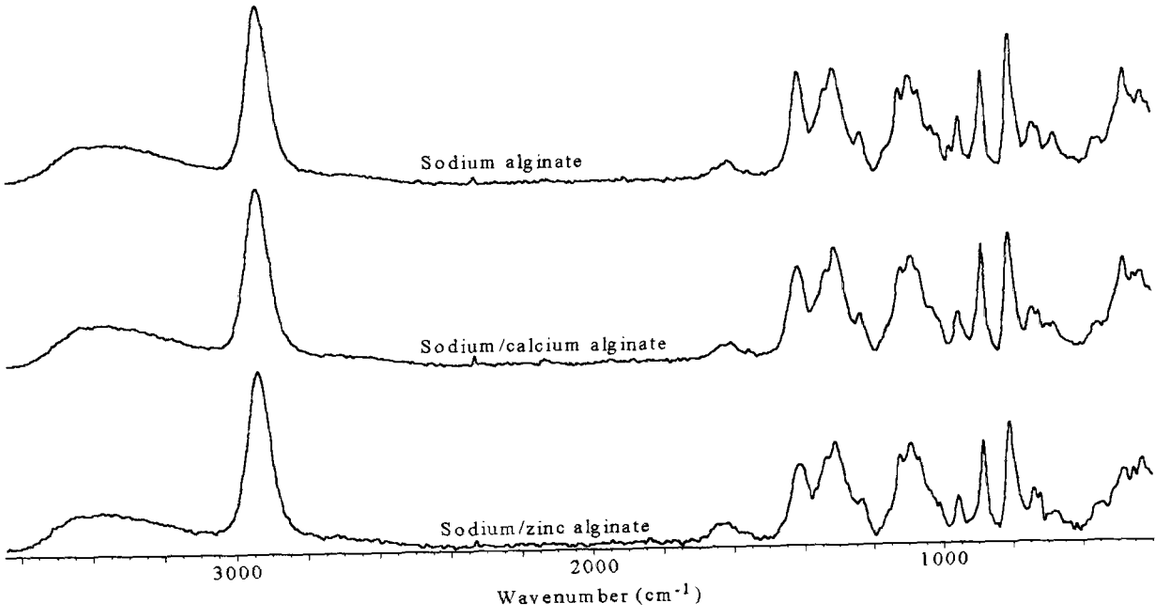

Figure IV.4.1.a. Raman spectra of different high-G alginate salts.

The fingerprint of the above spectra is now presented in figure IV.4.1.b.:

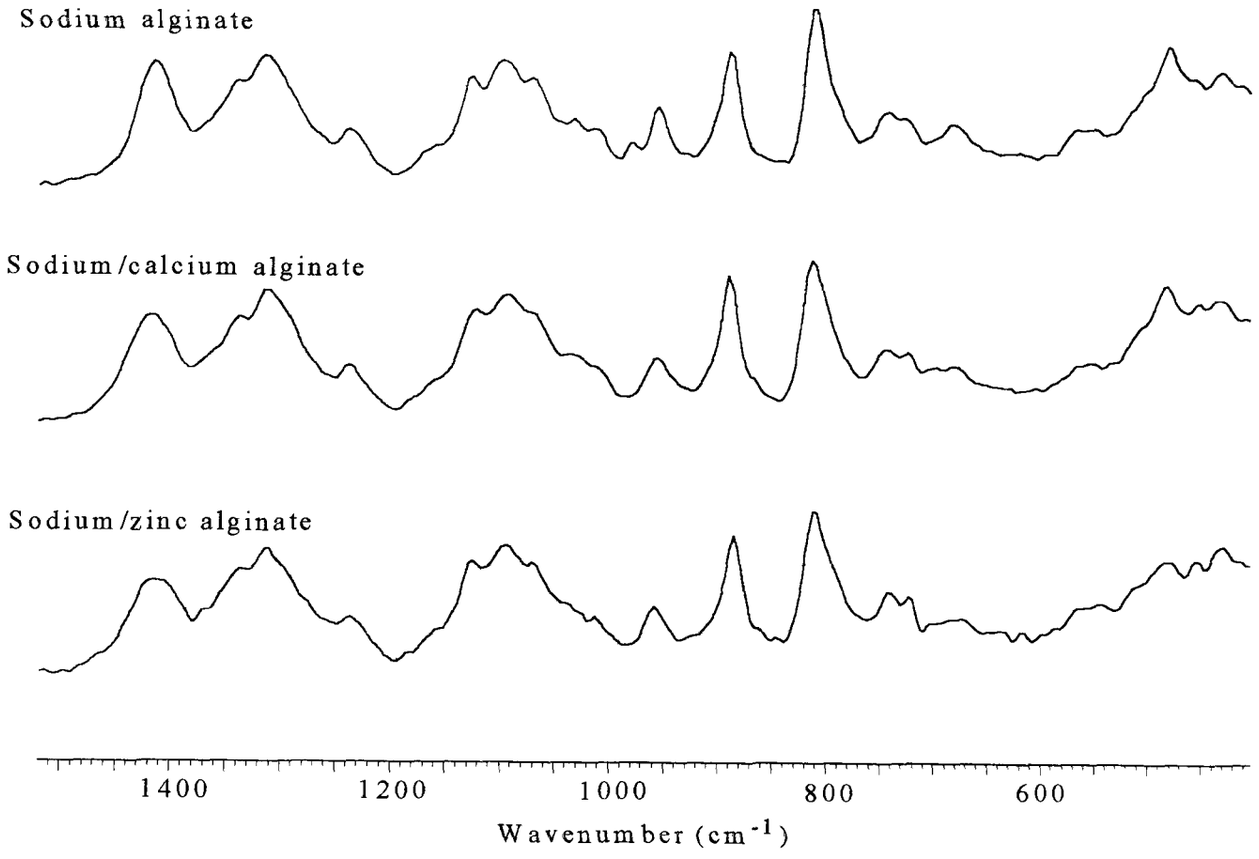

Figure IV.4.1.b. Raman fingerprint region of different high-G alginate salts.

The main peaks of the Raman and the FTIR spectra occur at similar positions, and therefore have been assigned to the same vibrations.

O-H vibrations are usually weak in Raman spectra, and will not be studied here as both FTIR and INS spectra give clearer information on this aspect.

Subtraction spectra are helpful to determine changes in the spectra between the different cations. The difference spectra between sodium/calcium and sodium, and between sodium/zinc and sodium, are shown below (figure IV.4.1.c.). O-H and COO^- asymmetric stretching peaks were taken as reference peaks, as they appear very similar for the different alginate salts.

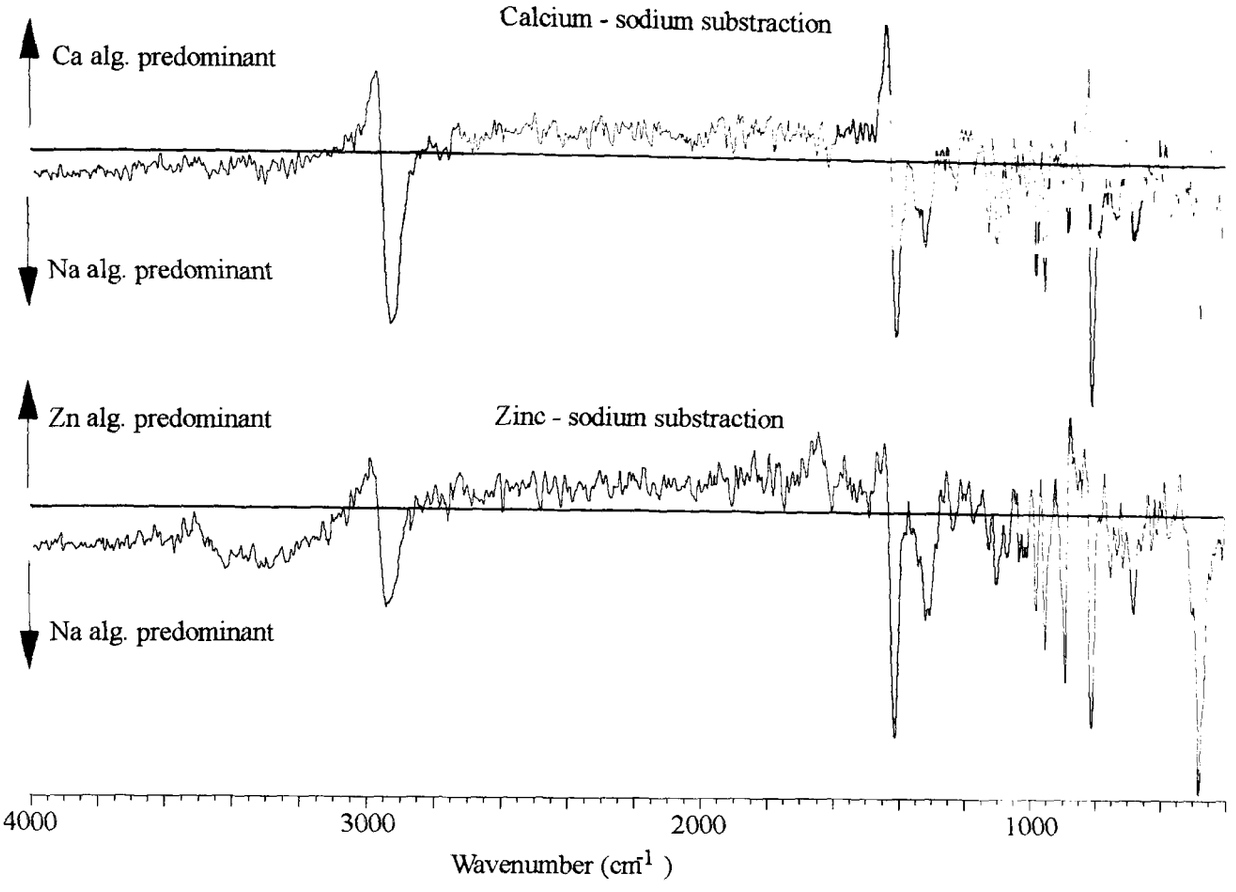

Figure IV.4.1.c. Raman subtraction spectra between alginate salts.

IV.4.2. C-H vibrations:

C-H vibrations are well resolved, and appear as strong peaks in Raman spectra. Firstly, C-H stretching is a strong, sharp peak, located at *ca.* 2940 cm^{-1}. Higher wavenumbers slightly prevail for the calcium salt, revealing a higher degree of freedom in the C-H groups for this sample, compared with the sodium alginate.

C-H in-plane deformation is found as a marked peak around 1310 cm^{-1}. Subtraction spectra display a predominance of this peak for the sodium salt, which leads to more freedom, mainly in the G blocks. The shoulder at 1290 cm^{-1} (typical of M blocks) is merged in the main peak for sodium alginate, while apparent for the two other samples.

CCH deformation, at 950 cm^{-1}, is again sharper and of higher intensity for sodium alginate. The C-H out-of-plane deformation peak, just below 900 cm^{-1}, weakens upon zinc addition, indicative of constraint in these groups. This does not correlate with what we had previously found in the FTIR analysis. However, this peak is much more

pronounced in the Raman spectra, and thus is more easily and unambiguously studied. The band close to 725 cm^{-1} has been also assigned to C-H deformation (from the INS spectra). It appears slightly more marked for the zinc salt. Finally, the peak around 680 cm^{-1} is stronger for the sodium alginate.

From these observations, it seems that most C-H vibrations are inhibited in the zinc alginate, while they are relatively free in the sodium alginate network (except for the stretching vibration). Calcium alginate presents an intermediate state, with some free vibrations, while others are constrained.

IV.4.3. Carboxyl vibrations:

The asymmetric C=O stretching is almost non-existent while the symmetric stretching peak follows the same trend as what was observed in the FTIR spectra (i.e. a decrease in intensity and broadness with Ca^{2+} and Zn^{2+} ions).

IV.4.4. C-O and C-C vibrations:

Two peaks around 1125 and 1090 cm^{-1}, related to C-C, C-O and COC stretching and characteristic of G blocks, are slightly more preponderant for the sodium salt (especially when compared with the calcium alginate).

A peak present at 985 cm^{-1} in sodium alginate, certainly due to COC stretching, is completely absent for the divalent cations. Therefore the excess charge is most likely neutralised by interaction with C and O atoms from the alginate backbone, reducing their mobility and eliminating some vibrations.

C-C groups from the alginate skeleton have their stretching vibration close to 810 cm^{-1} with a shoulder at 780 cm^{-1}. The subtraction spectra reveal a prevalence of the main peak for the sodium salt, compared with the other salts.

The peak around 480 cm^{-1}, attributed to C-O deformation, is again stronger for sodium alginate; it is particularly weak with zinc ions.

Many other peaks are present in the Raman spectra, between 1300 and 400 cm^{-1}, but they have not been assigned, due to the complexity of the spectra. However, it can be seen from this partial analysis that skeletal vibrations are stronger in the sodium alginate, while more restrained with the inclusion of divalent cations.

IV.5. Inelastic neutron spectroscopy (INS) of different alginate salts (Sartori *et al.*, 1996)

Many of the links found in carbohydrate molecules are via hydrogen bonding (Zhbankov, 1992), therefore their study is of prime importance in the understanding of alginate gelation. The best way to analyse such types of binding is by neutron scattering spectroscopy.

IV.5.1. INS spectra of protonated and deuterated sodium alginates:

INS spectra of protonated and deuterated sodium alginates are shown in figure IV.5.1.:

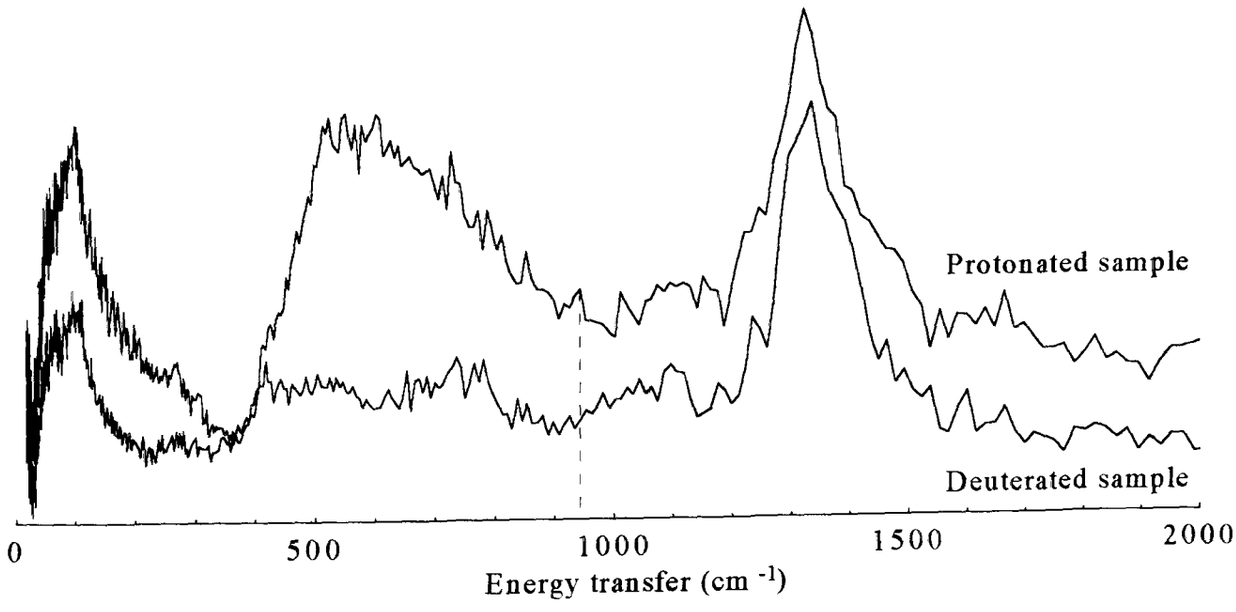

Figure IV.5.1. INS spectra of sodium alginate in the protonated and in the deuterated forms.

Comparison between the protonated and the deuterated samples uncovers essentially the vibrations of light water as aggregates, i.e. the translational mode (< 200 cm^{-1}), the

librational mode (500-800 cm^{-1}) and the scissor vibration (1650 cm^{-1}). Further O-H assignments were made difficult because of the high level of noise. Only the small peak at *ca.* 940 cm^{-1} was ascribed to O-H deformation in the alginate molecules (which would correspond to the small peak at *ca.* 900 cm^{-1} in the FTIR spectrum).

IV.5.2. INS spectra of the various alginate salts:

The spectra obtained for the different salts of alginate PROTANAL LF 10/60 are shown in figure IV.5.2., from 0 to 2000 cm^{-1}:

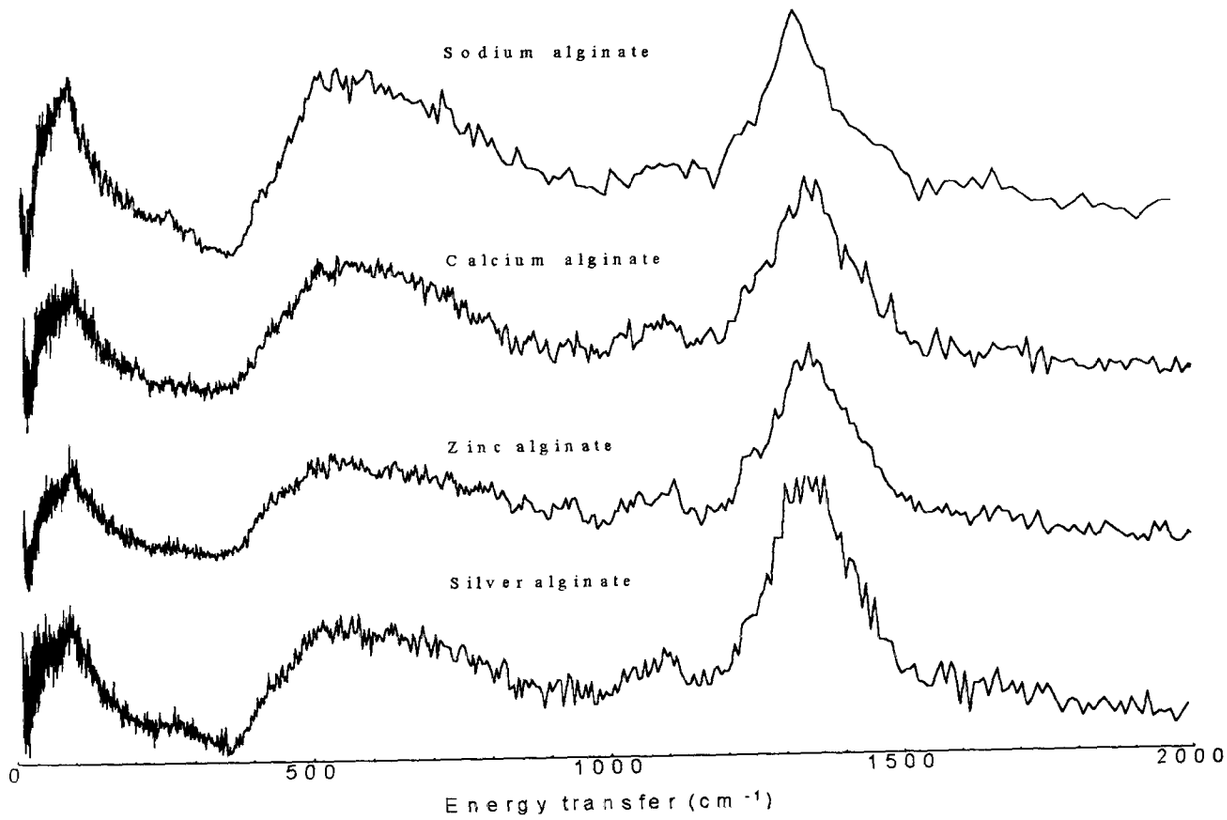

Figure IV.5.2. INS spectra of different high-G alginate salts.

Some of the major peaks of the INS spectra have been assigned by comparing protonated and deuterated samples, and by comparing vibrational modes (such as C-H and C-O) with literature values (from previous experiments carried out on the TFXA, or from infrared and Raman spectroscopies). This scheme is given in the following table:

Wavenumber (cm^{-1})	Intensity	Assignment
280	weak	ring torsion
450	weak	skeletal deformation
680	medium	C-H deformation
725	medium	C-H deformation
940	weak	O-H deformation
1025	medium	C-O stretching
1100	medium	C-O stretching
1350	very strong	C-H deformation

Table IV.5.2. INS assignment of alginate.

All the INS spectra show, at first sight, similar fingerprints. Furthermore, the rather poor signal-to-noise ratio makes comparison difficult. However, there are observable changes, described in the following paragraphs.

IV.5.3. Water vibrations:

The different alginate spectra are dominated by the broad peak at *ca.* 600 cm^{-1} (librational mode of vibration of water). Not all the vibrational peaks are present though, compared with the spectrum from ice (Tomkinson, 1992). This is due to hindering of the water molecules motion within the polymeric network. Furthermore, the wavenumber of the main peak is shifted to lower values, when compared with ice; this reveals that the bond between the molecules of water, in the alginate, is not as strong as when they are in their pure state. By calculating the ratio of the 600 cm^{-1} peak against the highest peak at 1350 cm^{-1}, it appears less dominant for silver and zinc than for the two other salts. This correlates with the thermogravimetric results (presented in section III.2.1.), where the water content of sodium and calcium alginates was found to be higher than for zinc and silver alginates. Furthermore the different shapes observed for this peak implies that there are different types of binding present between water and the alginate salts.

IV.5.4. Other vibrations:

-Lattice modes (at 280 and 450 cm^{-1}) are apparent for sodium and silver alginates, but

they are not distinct for the divalent cations. Therefore the introduction of Ca^{2+} and Zn^{2+} ions induce hindrance in the movement of the polymeric chains.

-There is no dramatic change in the C-H deformation vibrations between the different alginate salts. The peak at 725 cm^{-1} is noticeable for sodium alginate, whilst burried in the noise for the other samples.

-The peaks at 1025 and 1100 cm^{-1} are characteristic of C-O involved in hydrogen bonding, presumably from the COH groups. They are strongly marked for the silver alginate, and to a lesser extent, for the zinc alginate, followed by calcium alginate. It seems that in these salts, C-O is involved with strong hydrogen bonding. The bands appear weakest for the sodium sample.

IV.6. Summary

IV.6.1. Sodium alginate:

Mainly hydroxyl-hydroxyl binding occurs, firstly between alginate molecules (two O-H groups are present per G or M block), and also, presumably, between alginate and water (this could explain why sodium alginate dissolves in water). The sodium ions are bound predominantly to the carboxyl groups (certainly in an ionic way, due to sodium and oxygen positions in the periodic table). Most other vibrations (C-H, C-C, C-O) are fairly free, compared with the other samples. As Na^+ ions are replaced by Ca^{2+}, Zn^{2+} or Ag^+ ions during the gelation process, the charge density, the radius and/or the atomic mass of the cation are changed, creating a new environment around the alginate molecules. Thus differences in bonding within the polymeric network are expected.

IV.6.2. Calcium alginate:

When Na^+ are exchanged for Ca^{2+} ions, the intermolecular hydrogen bonding is altered from strong O-H...O-H to mixed O-H...O-H and O-H...$^-$OOC bindings. Some C-H vibrations are hindered (thus involved in partial bonding), while others vibrate more freely. Calcium ions, in contrast with sodium ions, are bound only partially to the

carboxyl groups. It is possible that one calcium ion is bound to several COO^- groups at once, thus creating strong bridges between the alginate molecules. It seems that there is some affinity for the G blocks. This may strengthen the intermolecular interactions. Compared with the sodium salt, more atomic groups are involved in bonding; this bonding is, in general, non-specific.

IV.6.3. Zinc alginate:

Similar observations are made, regarding the O-H and the COO^- groups, for zinc and for calcium samples. Introduction of new types of bonding is revealed by the appearance of new peaks, and overall, more vibrations of the C-H, C-C and C-O groups are hindered by the introduction of the zinc cations. Therefore more bondings are involved between Zn^{2+} ions and the alginate molecules. These bondings are supposed to be primarily of a covalent type.

IV.6.4. Silver alginate:

A similar proportion of O-H...O-H binding is found in silver and sodium samples. However, TGA curves show that most of the water evaporates at ≈ 428 K for silver alginate, and ≈ 473 K for sodium alginate. This leads to the conclusion that sodium alginate molecules are more tightly bound to water than silver ones. Therefore the hydroxyl-hydroxyl interactions occurring in the silver alginate are rather between the polymer molecules than with the solvent. This might be one of the reasons why silver alginate does not dissolve in contact with water, but forms a gel. Another reason certainly involves the large size of the Ag^+ ion, which may create more interaction than Na^+ with the alginate molecules. However, partial bonding, in this salt, is encountered to a far lesser extent than with the divalent ions. Finally, the silver ions may exist as aggregates in the alginate network.

CHAPTER V: SIMULATED WOUND EXUDATE / ALGINATE INTERACTION

Once sodium/calcium alginate samples had been prepared and characterised, they were tested for their performance as potential wound dressings. Properties such as ion exchange, swelling and strength were assessed when the films were exposed to a solution containing similar concentrations of sodium ions and calcium ions to those found in wound exudate (i.e. 142 millimoles of Na^+ and 2.5 millimoles of Ca^{2+} (from Thomas & Loveless, 1992)). This solution is also referred to as Na/Ca solution.

V.1. Ion exchange

Mixed sodium/calcium alginates are intrinsically haemostatic. The release of free calcium ions from the alginates provides one of the essential factors in the clotting cascade (Jarvis *et al.*, 1987). Therefore, it is of prime importance to characterise the ion exchange properties "in-vitro" (which should be followed by "in-vivo" studies). However, hardly any literature has been found regarding this property. For this purpose, an experimental method was developed. Alginate films were immersed in a Na/Ca solution containing an indicator (tetramethyl murexide). With release of calcium ions from the sample into the simulated wound exudate, the solution turned from purple to orange. This change in colour was paralleled by a peak shift when the solution was scanned by visible spectroscopy. Tetramethyl murexide was used previously by Skjåk-Bræk *et al.* (1989) to visualise the migration of the gelling zone in calcium alginate gel.

V.1.1. Standard curves:

Standards were prepared by dissolving between 0.9 and 9.0 $mmol.dm^{-3}$ of Ca^{2+} (from $CaCl_2$), 142 $mmol.dm^{-3}$ of Na^+ (from NaCl) and 0.02 $g.dm^{-3}$ of tetramethyl murexide in deionised distilled water. Their spectra were then recorded by visible spectroscopy. A typical curve is shown in figure V.1.1.a. Figure V.1.1.b. gives the difference in calcium concentration ($mmol.dm^{-3}$) between the standard and the simulated serum solution (2.5 Ca^{2+} $mmol.dm^{-3}$ + 142 Na^+ $mmol.l^{-1}$) as a function of wavelength (taken at the peak maximum) in nm:

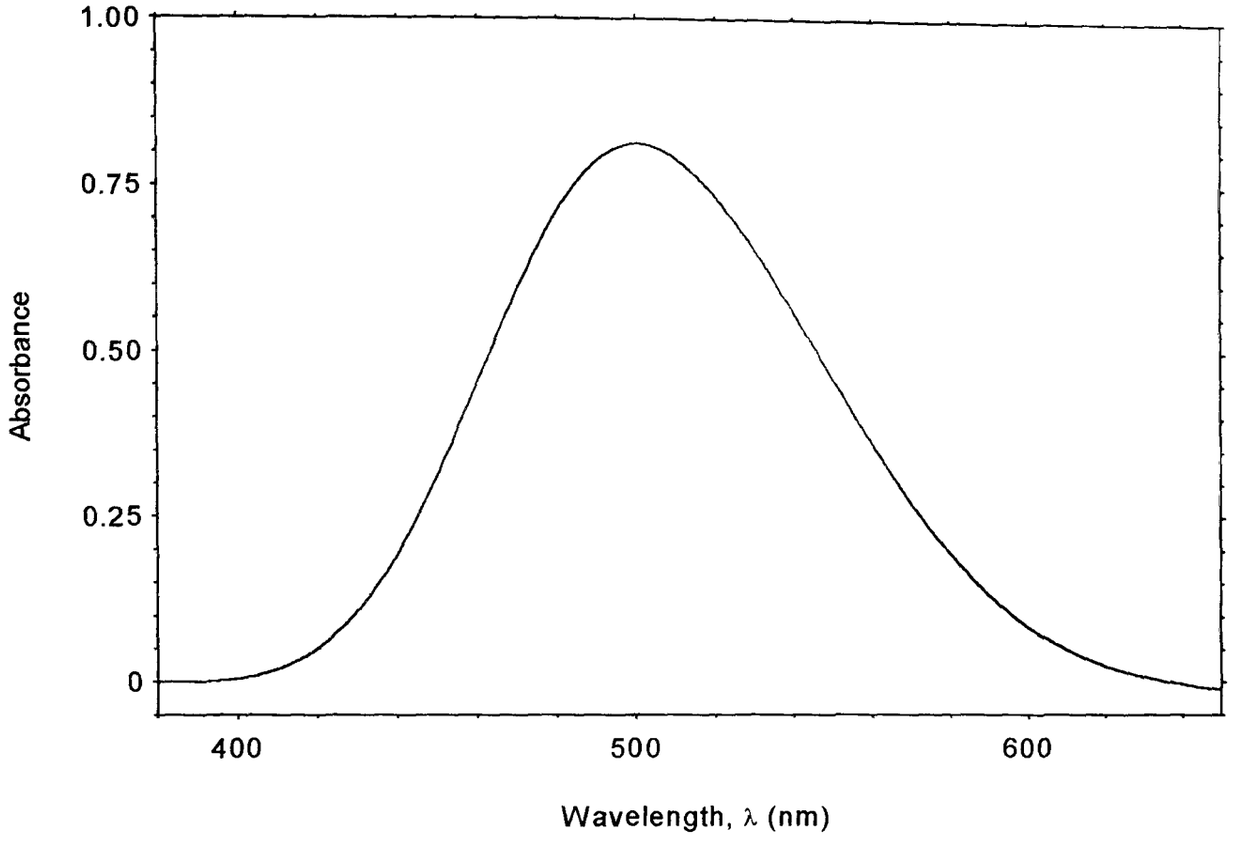

Figure V.1.1.a. Typical visible spectroscopy curve.

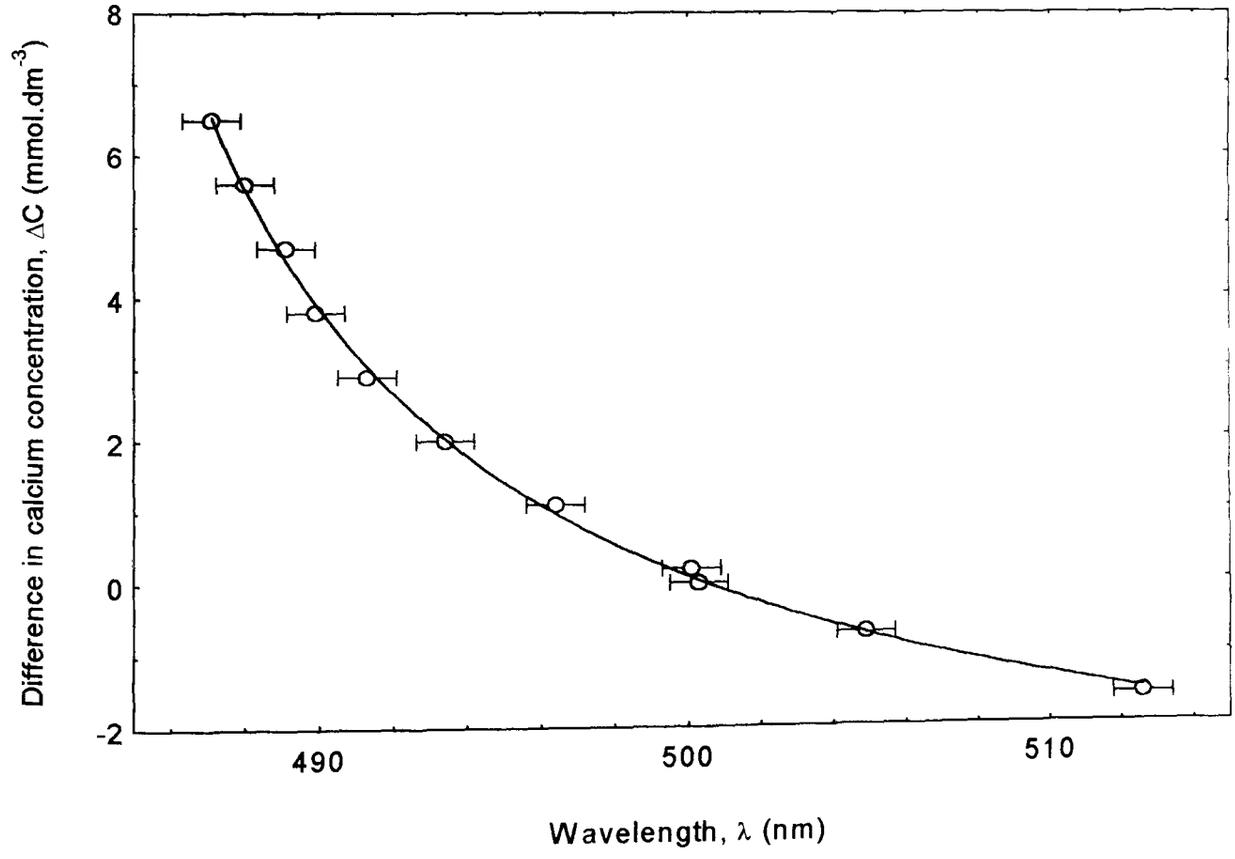

Figure V.1.1.b. Calibration curve for visible spectroscopy.

The resolution in wavelength was 0.8 nm, which leads to a standard error of less than 0.2 %. The error bars on ΔC are not drawn on the above graph as they appear smaller than the data markers. They are equal to ± 2 % on average.

The experimental points (averaged over three measurements) can be extrapolated to a curve, whose equation (1) is:

$$\Delta C = (1 / (a\lambda + b)) + c \qquad (1)$$

where a = 0.0103, b = -4.92 and c = -4.35.

This equation is used in the following two subsections, in the determination of the proportion of calcium released by the alginate samples. All the calculations are detailed in appendix 2.

V.1.2. Release of Ca^{2+} ions from high-G alginate films:

i. Influence of the initial calcium content in the samples:

Sodium high-G alginates immersed for 3, 30, 100 and 300 minutes in $CaCl_2$ were prepared. Their calcium content was known from AAS (see III.2.2. These values do not take into account the chlorine content as it is assumed to be low, and is also difficult to measure quantitatively). The films were then immersed in a simulated serum solution for 1 minute, 30 minutes, 1, 24 and 100 hours (alginate dressings are rarely kept in contact with a wound for longer times). The proportion of calcium ions released from the samples into the simulated serum solution, as a function of time, is recorded in figure V.1.2.a:

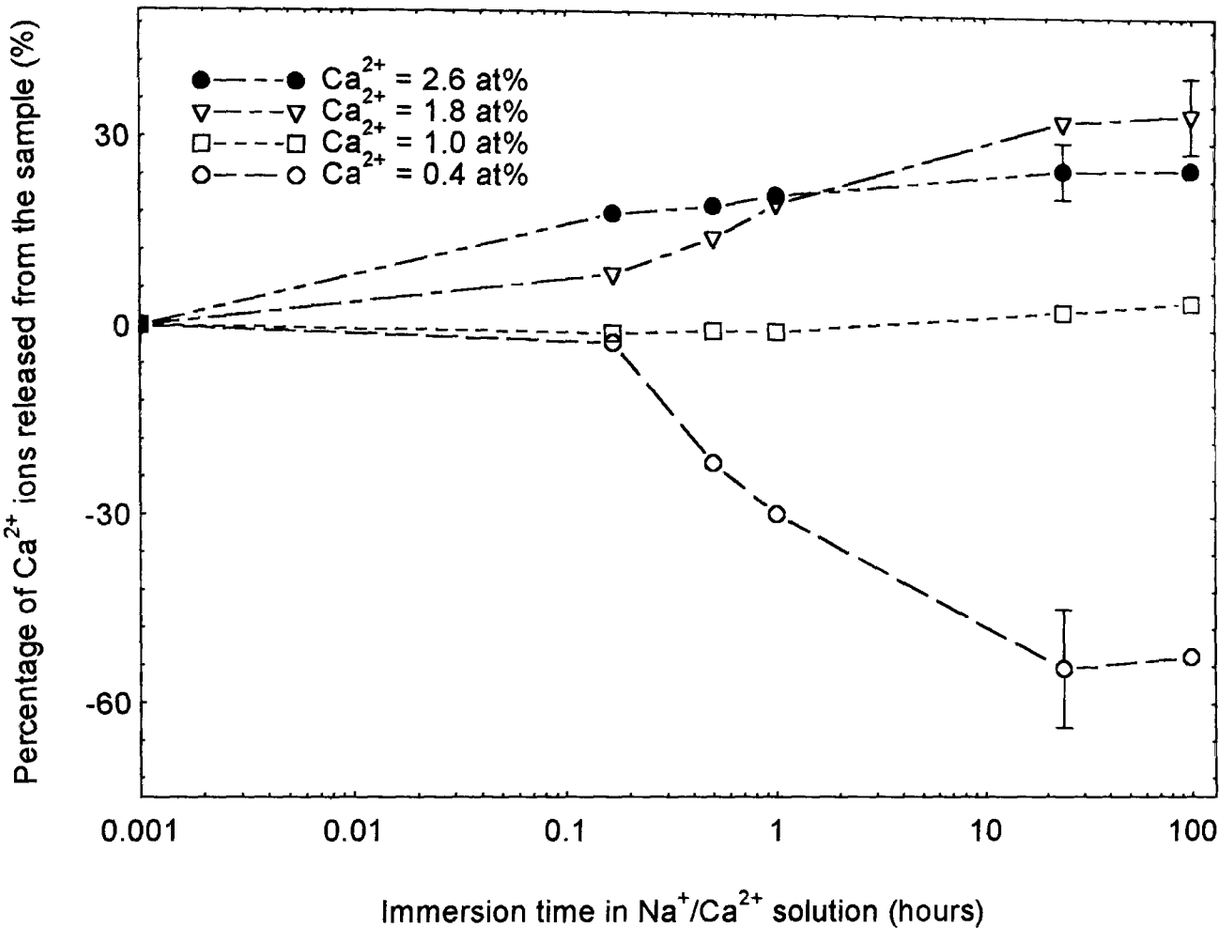

Figure V.1.2.a. Percentage of calcium ions released from high-G alginate samples.

The sample containing only 0.4 at% Ca^{2+} does not seem to release any calcium into the Na/Ca solution, but rather absorbs the cations (as a negative percentage is obtained), as if prolonging the gelation process. The sample containing 1.0 at% Ca^{2+} is close to equilibrium with the simulated serum solution, as far as calcium ions are concerned, and its curve deviates little from the horizontal line. By contrast, the two other alginate samples (having higher calcium contents) released noticeably their divalent ions.

Following the "egg-box model" whereby Ca^{2+} ions are bound preferentially to the G blocks, let us consider the stage where all the G blocks have been filled with Ca^{2+} ions, while the M blocks remain filled with Na^{+} ions. For 100 blocks (25 M and 75 G for the high-G alginate), there are (19*200*100) / 175 = 2171 atoms of C, O and H (see appendix 1), 25 Na^{+} ions and (75 / 2) Ca^{2+} ions (due to the divalence). The calcium atomic percentage is given by: at% Ca^{2+} = (37.5*100) / (2171+37.5+25) = 1.7 %. The case where all the alginate is converted into a calcium salt leads to at% Ca^{2+} = (50*100) /

(2171 + 50) = 2.3 % (0.6 % attached to the M blocks and 1.7 % to the G blocks). Therefore two of the samples (0.4 and 1.0 at%) have their G blocks only partially filled with the calcium ions. The 1.8 at% Ca^{2+} alginate is expected to have virtually all its G blocks plus some of the M blocks bound with Ca^{2+} ions. Finally, in the 2.6 at% Ca^{2+} sample, all the M and G blocks are filled by calcium, and there is an average of more than one Ca^{2+} ion per site.

After 10 minutes immersion, the 1.8 at% Ca^{2+} alginate has released slightly more than 8 % of its initial calcium (leading to 0.1 % gone into the solution and 1.7 % left in the sample, from the initial 1.8 at% Ca^{2+}). The 0.1 % Ca^{2+} possibly corresponds to the quantity of Ca^{2+} ions bound mainly to the M blocks. Indeed, according to Kohn (1975), calcium ions bound to the M blocks are expected to be released immediately after immersion in the solution, as they are loosely attached. The 2.6 at% Ca^{2+} sample liberates 18 % of its calcium ions (i.e. 0.5 at% Ca^{2+} out of 2.6 at%). The greater proportion of loosely bound cations, compared with the previous alginate, justifies the higher activity observed initially. However, if the Ca^{2+} ions in the alginate film are supposed to be divided solely between the M and the G blocks, then all the loose cations (bound to M, and accounting for 25 % of the total) have not left the sample. Kohn's statement (1975) is thus contradicted in the case of fully converted calcium alginates, under our experimental conditions.

At 100 hours in the Na/Ca solution, most samples have reached a release plateau. At this point, the 0.4 at% Ca^{2+} sample has absorbed around a third of the calcium initially contained in the simulated serum solution. The 1.0 at% Ca^{2+} sample has released only 4 % of its calcium content. The 1.8 at% Ca^{2+} sample has released 34 % of its calcium content (which corresponds to 0.6 at% Ca^{2+}, while 1.2 at% Ca^{2+} remain in the sample). Therefore both M and G blocks have been depleted in calcium ions. For the 2.6 at% Ca^{2+} alginate, 26 % of the initial calcium concentration has been released after 100 hours immersion, i.e. 0.7 at% Ca^{2+}, which is slightly higher than in the previous sample (15 % more released). The 0.7 at% Ca^{2+} may correspond to the calcium ions bound predominantly to the mannuronic acid blocks. It follows that the G blocks have hardly been depleted in calcium. Most of the remaining cations are thought to act as crosslinks in the alginate network, and to hinder dissolution (similarly to what occurs between

seaweed and salt water).

Calcium ions may be released from an alginate sample until an ionic equilibrium at the sample and the solution interface has been reached. Cl^- ions (from NaCl in the solution) are expected to be an influential factor to reach the charge balance.

Thomas & Loveless (1992) performed fluid handling measurements on Kaltostat® and Sorbsan® in a similar simulated serum solution. They suggested that complete dissolution of the dressings was prevented, and an equilibrium was achieved. No further interpretation was attempted.

Jarvis *et al.* (1987) have carried out a similar study on Kaltostat®. This fibre dressing is made from high-G alginate, and contains 20 % sodium and 80 % calcium ions (Thomas & Loveless, 1992) (our alginate film immersed for 300 minutes in $CaCl_2$ solution contains 15 wt% Na^+ and 85 wt% Ca^{2+}). Jarvis *et al.* (1987) measured calcium release from 15 mg samples (our samples weigh 20 mg on average) in 20 cm^3 of 0.9 % saline solution (this solution is made from NaCl; therefore no calcium ions were present initially in the solution). The method used for this determination was not specified. They observed a release of 26 % of calcium ions within the first minute, with only slight further release after ten minutes. A similar behaviour is observed with our sample, but over a longer time scale; our alginate film has released 18 % of its initial calcium ion content after ten minutes in the Na/Ca solution, and a 26 % release is reached after 24 hours only. This difference in behaviour can be explained most certainly by the fact that Kaltostat® is made from fibres, and these offer a much higher surface area than our films (however their diameter was not specified). Therefore Ca^{2+} ion release is significantly favoured. The different solutions used may also influence the migration of calcium. The saline solution contains 9.1 NaCl $g.dm^{-3}$ while the Na/Ca solution is comprised of 8.3 NaCl $g.dm^{-3}$ + 0.3 $CaCl_2$ $g.dm^{-3}$. The difference in quantity and constituents leads to different ionic mobilities. Finally, the different volumes of solution between the two experiments certainly generate different ionic equilibria within the samples.

Liyanage *et al.* (1995) treated some Kaltostat® tows to produce newly metal-impregnated alginates, containing sodium, calcium, zinc and copper ions. After

immersion of the samples in a blood serum, they measured the ion transfer by atomic absorption spectroscopy on the gels. They concluded that the alginate tows were capable of releasing extensively Zn^{2+} and Cu^{2+} ions (70-90 %), and to a lower extent Ca^{2+} ions (about 40 %) to blood serum, and, in exchange, absorbing sodium ions from the serum, although not in a strict 1:1 ratio.

ii. Influence of the M/G ratio:

Two alginate samples, differing in M/G ratio, were prepared as sodium/calcium salts (immersion for 30 minutes in calcium chloride solution) and tested for their Ca^{2+} release ability in the simulated serum solution (Na/Ca solution) (figure V.1.2.b.).

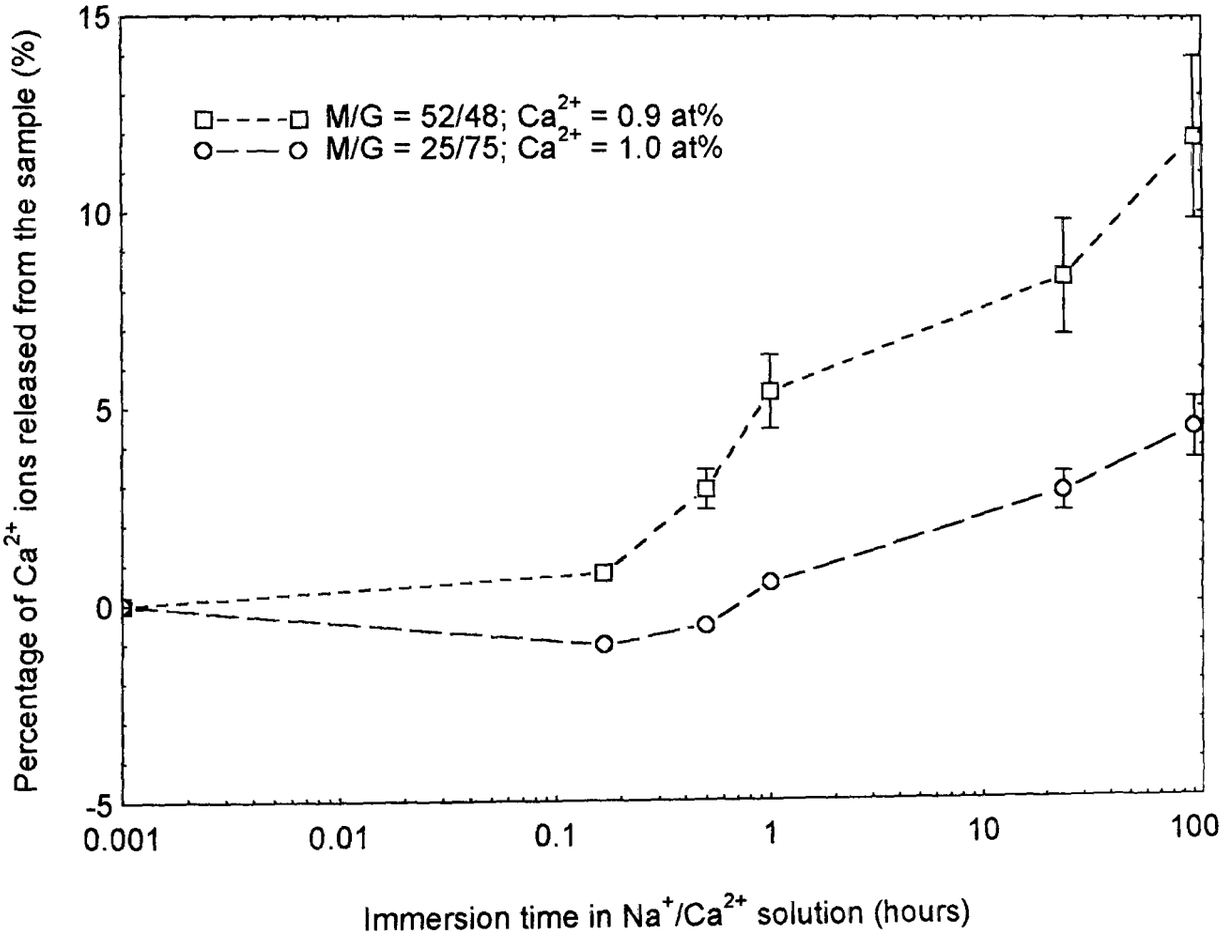

Figure V.1.2.b. Percentage of calcium release from different types of alginate.

Both alginate samples possess a similar initial calcium content (within 10 %); therefore the M/G ratio is their principal difference. From their initial % Ca^{2+}, it is suspected that the G blocks are only partially filled with the calcium ions, while the M blocks are hardly

filled at all (otherwise, the at% Ca^{2+} would be at least equal to 1.1 and to 1.7 for the medium-G and the high-G samples respectively). This would explain why hardly any changes are observed during the first ten minutes of immersion (since few or no loosely bound cations are present). Afterwards, the medium-G alginate offers a higher calcium release, with 12 % reached after 100 hours in the Na/Ca solution, compared with only 4 % for the high-G alginate. The released Ca^{2+} ions are assumed to come from the guluronic blocks. Overall, the divalent cations must be less tightly bound to the G blocks in the medium-G alginate than in the high-G alginate, in the gel state. This may be due to their different environment, and to the different block conformation (the M blocks form an extended ribbon structure while the G blocks form buckled chains; Gacesa, 1988).

V.2. Wicking rate

Wicking rate experiments in the simulated serum solution were performed on alginates with various sodium and calcium initial contents. These tests try to simulate the serum uptake as soon as the dressing is brought into contact with the wound (during the first seconds). The results are presented in table V.2.:

Alginate sample	Max. wicking rate ($mg.s^{-1}$)
High-G; Na^+=4.5/ Ca^{2+}=0.14 at%	46 ± 16
High-G; Na^+=4.0/ Ca^{2+}=0.4 at%	66 ± 18
High-G; Na^+=2.9/ Ca^{2+}=1.0 at%	98 ± 9
Medium-G; Na^+=2.8/ Ca^{2+}=0.9 at%	87 ± 12

Table V.2. Maximum wicking rate values of alginate films.

As the calcium content is increased, the initial absorption increases in parallel. When the percentage of M blocks is raised, the wicking rate is only slightly decreased. From the tendency observed, the ion exchange between Na^+ in the solution and Ca^{2+} in the sample must be the dominant driving force for the wicking rate. However, the variability in the experimental results is high: ± 20 % on average. This suggests that the wicking rate test

is not highly suitable for the analysis of alginate films. This technique is very sensitive to surface inhomogeneities. Due to the large size samples prepared (70 mm × 120 mm), a surface roughness may be generated during the drying process, and encrustations from the air may also cause a problem. Ratner *et al.* (1987) suggested that a surface roughness greater than 1 μm renders contact angle measurements difficult to interpret. From these observations, it follows that the wicking results will not be used as one of the key parameters in the understanding of the behaviour of alginate films.

V.3. Swelling behaviour

As alginate films were held vertically in a Na/Ca solution, the change in volume was recorded as a function of time. The aim was to simulate the swelling over long exposure to the simulated serum (compared with the wicking rate experiments).

V.3.1. Effect of the calcium content:

The swelling behaviour of high-G alginates containing different amounts of sodium and calcium ions is presented in Figure V.3.1.:

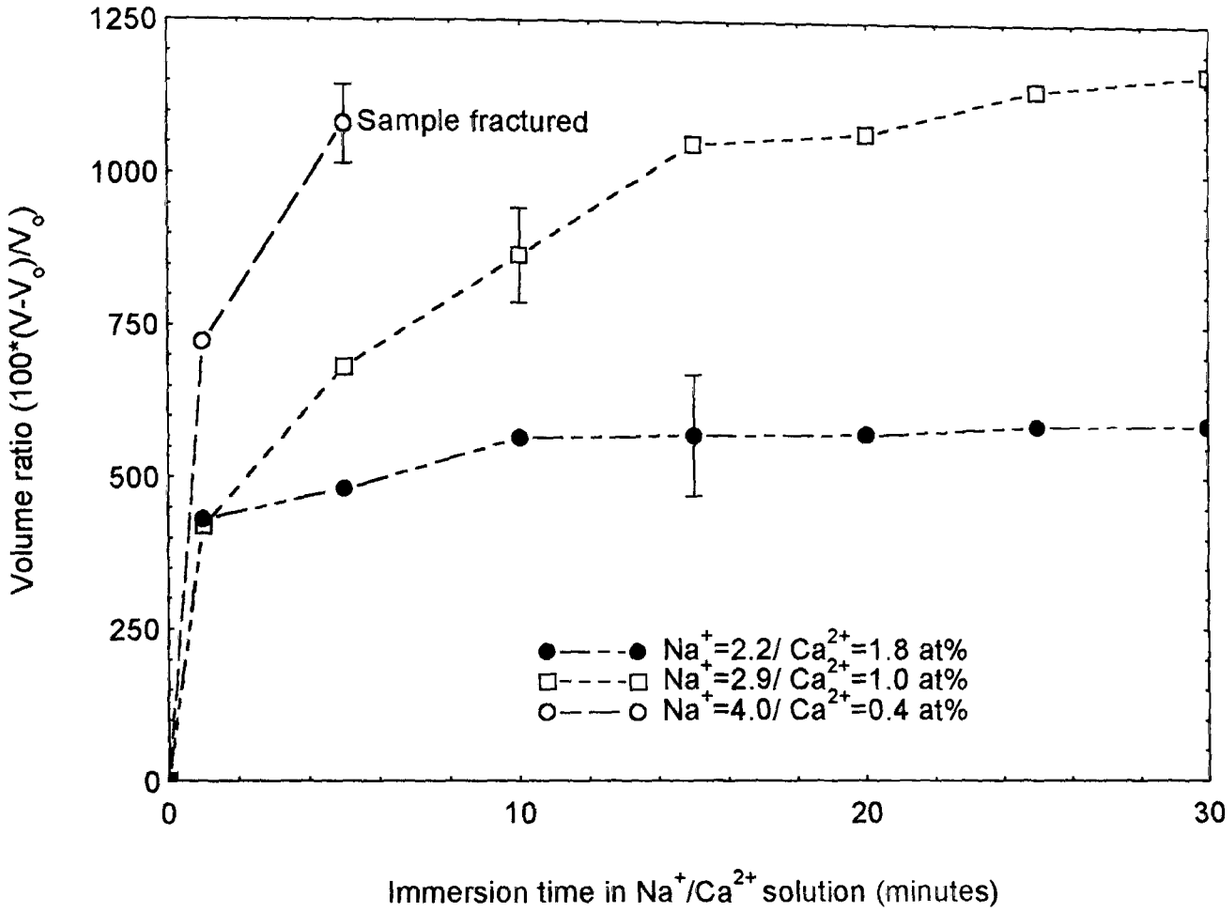

Figure V.3.1. Swelling behaviour of alginates with different sodium and calcium contents.

Experimental errors in the volume ratio were found to be around ± 10 %. During immersion, increases were observed in the three dimensions. The maximum increase was found to occur in the thickness. For the 1.0 at% Ca^{2+} sample, the increase in the thickness was equal to + 1000 %; the change in the length was + 7 %, and the width was swollen by + 4 % on average.

Swelling occurs as soon as the samples are immersed in the simulated serum solution. After five minutes, the 1.0 and 1.8 at% Ca^{2+} alginates have reached 60 and 80 % of the maximum volume ratio value, respectively. The alginate film containing only 0.4 at% Ca^{2+} breaks soon after being immersed. On the other hand, for a calcium content greater than 1.0 at%, no breakage occurs, even after 30 minutes of immersion. The sample containing just 1.0 at% Ca^{2+} reaches a plateau after 25 minutes of immersion, while the 1.8 at% Ca^{2+} sample does not swell much after 10 minutes.

From these curves, it appears that there is a minimum calcium content required to prevent film breakage. Below this % Ca^{2+} value, only a small degree of crosslinking exists. It follows that during immersion, a large amount of solvent molecules are able to diffuse into the alginate network, causing the chains to expand (a greater swelling is thus obtained). The more the water content, the heavier the film (the effect of gravity is important as these samples are held vertically; however, buoyancy may also play a role). Some bonds in the alginate molecules may be broken under the applied stress, allowing more water to enter the polymeric network. As this cascade of events proceeds, breakage finally occurs.

With increasing calcium content, and thus crosslinking, the alginate chains are restricted in their movement. Less water molecules are able to penetrate the sample, and hence the swelling is reduced. The time required to reach a constant volume (as shown in figure V.3.1.) appears to be reduced with increasing Ca^{2+} content. Stable high-G alginate gels with lower swelling seem therefore to be obtained at higher calcium contents. From previous observations (see section VII.1.2.), there is still some calcium to be released after 30 minutes of immersion; this is especially true for the 1.8 at% Ca^{2+} sample. Therefore the swelling curve has not truly reached its equilibrium state over the timescale of these measurements and an additional volume change response may be observed.

V.3.2. Effect of the M/G ratio:

The swelling curves of the high-G and medium-G alginates are compared in figure V.3.2.:

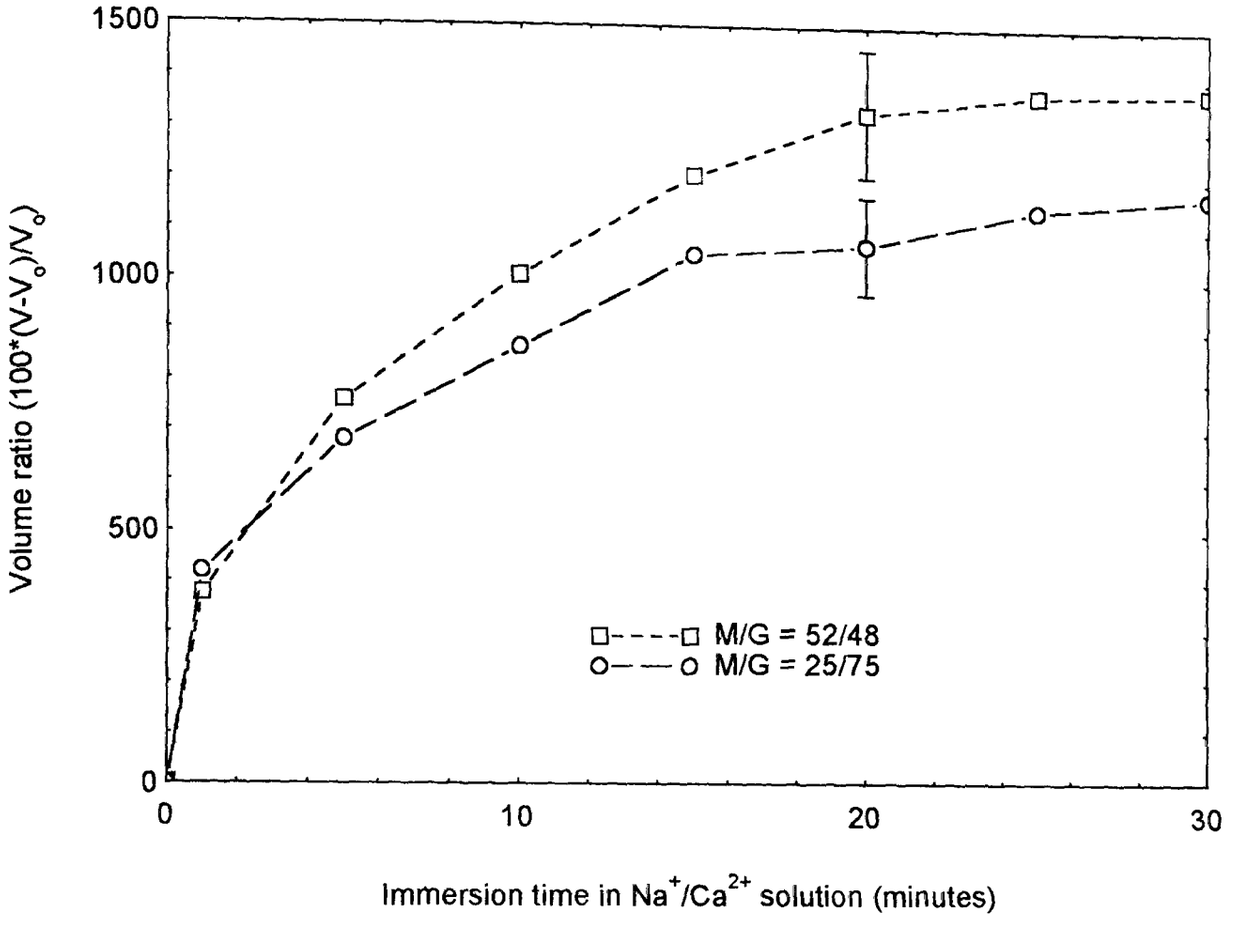

Figure V.3.2. Swelling behaviour of alginates with different M/G ratio.

The medium-G alginate exhibits a greater degree of swelling than the high-G alginate (almost 20 % more). This different behaviour is thought to be due to the different conformation between the M and G blocks. Water molecules will diffuse more freely in an extended structure (characteristic of the M blocks) than in a buckled one (found with the G blocks). The fact that the medium-G sample, in contact with the simulated serum solution, releases more Ca^{2+} ions than the high-G alginate (V.1.2.ii) also influences the swelling behaviour. During immersion, the lower calcium content of the medium-G film allows more water to penetrate the network which increases the volume change.

V.4. Gel strength

These measurements were performed in order to ensure that the wound dressings, when used on a lesion, remain in one piece, and do not disintegrate. The dimensional stability of the alginate gel was also of interest. The basic test was the recording at room

temperature of the increase in length of a high-G alginate film, containing 2.9 at% Na^+ and 1.0 at% Ca^{2+} (corresponding to an immersion in $CaCl_2$ of 30 minutes) with a 50 g mass for 90 minutes. The stress was then removed and the length was still being measured for a further 30 minutes. This led to creep/recovery type of curves. From this experiment, several parameters were modified in turn, to assess the influence of the ion content in the sample, the type of alginate used, the stress applied and the temperature of the test. Each test was repeated three times, and the curves presented below were obtained from the average values.

It must be pointed out that the 50 g mass, when immersed, has an apparent decreased weight compared with that in air (due to the Archimedes' principle) which is equivalent to 43 g. Furthermore, due to swelling, the cross-section of the samples varied as a function of time, and so did the applied stress. Therefore for all tests, the strain/time curves are accompanied by stress/time curves. However, these could only be approximated as the cross-section values were calculated from the swelling measurements (i.e. without stress applied); the stress/time curves were plotted only for the first 30 minutes of testing. Some samples did reach equilibrium after this time while others were still expanding.

V.4.1. Influence of the calcium content:

Gel strength curves are shown in figure V.4.1.a., for high-G alginate films containing different ion content. The stress/time curves are presented in figure V.4.1.b., using a 50 g weight.

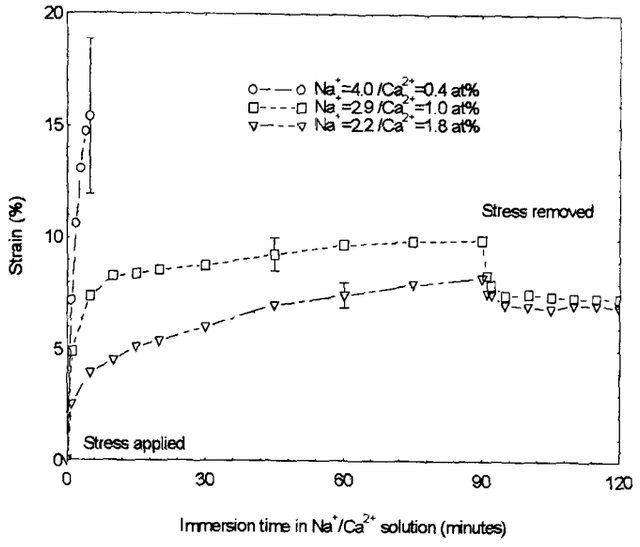

Figure V.4.1.a. Gel strength as a function of ion contents in alginate films.

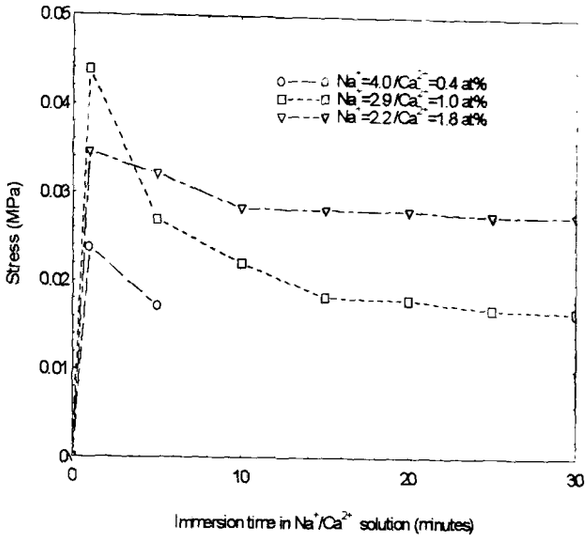

Figure V.4.1.b. Stress as a function of ion contents in alginate films.

The average experimental error in strain is found to be around ± 7 %, apart from the sample immersed for a short time in $CaCl_2$ (4.0 at% Na^+ + 0.4 at% Ca^{2+}; ± 23 % error on average). Deformation was occurring very rapidly for this sample therefore making measurements was more difficult.

The higher the sodium content (or the lower the calcium content), the higher the strain and the lower the stress applied (as the swelling effect is important) for immersion times greater than five minutes, i.e. the weaker the gel. For the film containing the lower % Ca^{2+}, the rapid deformation leads to catastrophic failure soon after bringing the sample into contact with the simulated serum. This sample contains predominantly sodium ions. In contact with the solution, dissolution is bound to occur, weakening considerably the gel. Furthermore, this sample exhibits high absorption, and the swelling itself is enough to break the gel (see figure V.3.1.). The other gels are strong enough to sustain their weight with water, as well as the stress applied.

The recovery process gives rise to a plateau value of 7.4 % strain for the 1.0 at% Ca^{2+} sample, which corresponds to the maximum swelling contribution (after 30 minutes immersion, derived from V.3.1.). Therefore the stress applied does not seem to give rise to any permanent deformation. The 1.8 at% Ca^{2+} alginate displays a similar value of 7.0 % for the strain at the recovery stage. This permanent deformation is due to both the

swelling (3 %) and the stress. It must be recalled that the applied stress was the highest for this sample. Furthermore, as the alginate film is immersed, calcium ions are released. The 1.0 at% Ca^{2+} sample releases only 4 % of its initial calcium content after 90 minutes immersion, while the higher calcium content sample releases as much as 35 % (from section V.1.). The reduction in calcium ions and hence the number of intermolecular crosslinks results in permanent deformation of the alginate film.

V.4.2. Influence of the M/G ratio:

Strain/time and stress/time curves (for a 50 g mass) for two different alginates are presented below:

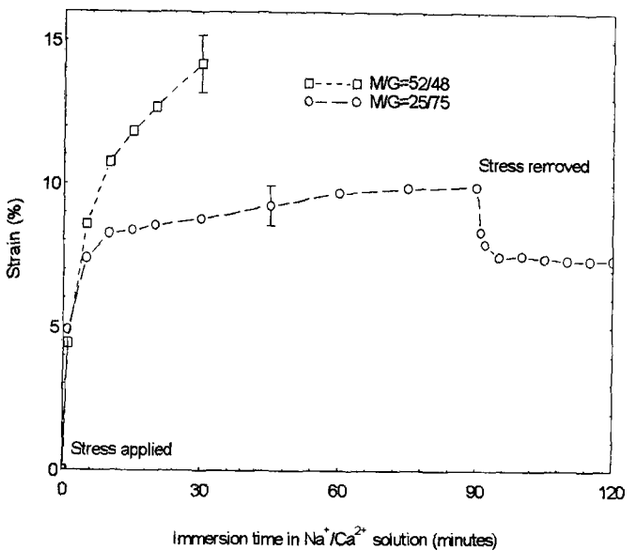

Figure V.4.2.a. Gel strength curves as a function of the M/G ratio.

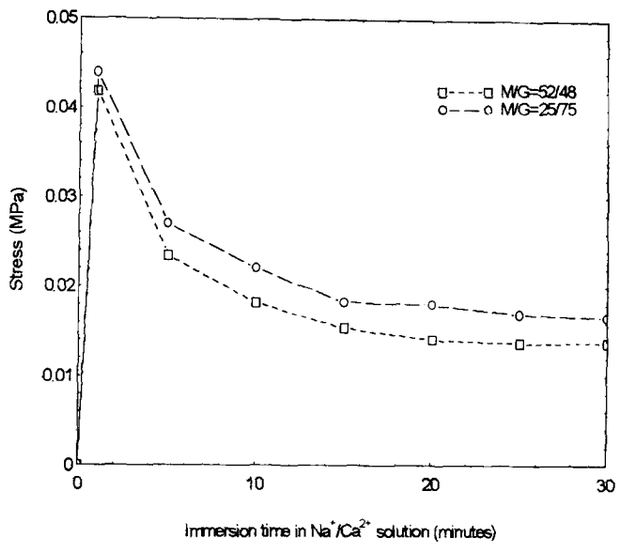

Figure V.4.2.b. Stress as a function of the M/G ratio.

The average spread of the strain results is ± 7 %. The medium-G alginate appears much weaker than the high-G alginate, as it breaks before completion of the test, even though the stress applied is smaller. Several reasons may be involved in this poor gel strength. Higher calcium release into solution has previously been observed for the medium-G alginate; the depletion in Ca^{2+} ions results in an increase in deformation. The higher water content in this sample also contributes to reduce the gel strength. Finally, under strain, the M blocks are expected to extend more rapidly and to a greater extent than the G blocks (due to their conformation, as already mentioned).

V.4.3. Influence of the imposed stress:

The influence of the imposed stress on high-G alginate films can be assessed from the gel strength curves displayed in figure V.4.3.a. (the stress/time curves are displayed in figure V.4.3.b.). This enables one to simulate different levels of applied stress in sample handling in the gel state.

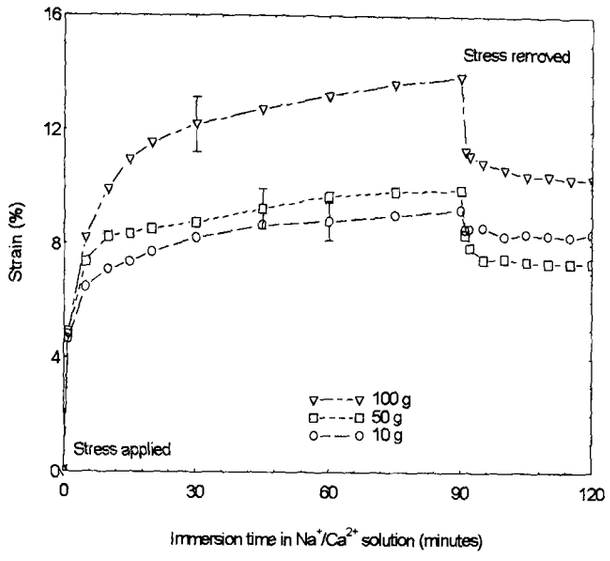

Figure V.4.3.a. Gel strength of high-G alginate films with different stresses.

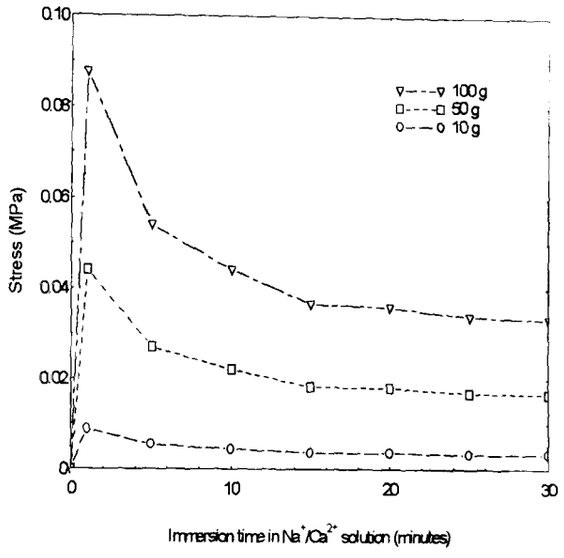

Figure V.4.3.b. Corresponding stresses for various weights.

There is ± 8 % spread on average in the experimental strain results. With a 10 g mass, hardly any change is observed compared with the 50 g mass, within experimental error. In these two cases, the permanent deformation is due exclusively to the swelling (V.4.1.). By contrast, the sample loaded with the 100 g mass gives rise to a large strain, leading to increasing permanent deformation. With this greater stress, some bonds between the alginate molecules are expected to be broken, but the gel still remains strong as it does not break.

V.4.4. Influence of the temperature:

Finally, the effect of the temperature was assessed. The part of the alginate gel in contact with the wound is typically at 303-307 K, while the exterior part is at room temperature (typically 293-298 K). Therefore it is very important to evaluate the gel performances at temperatures between 293 and 313 K to ensure the sample is suitable to be used as

wound dressing. Gel strength curves at 293, 303 and 313 K are presented in figure V.4.4.a., for a similar variation of stress with time.

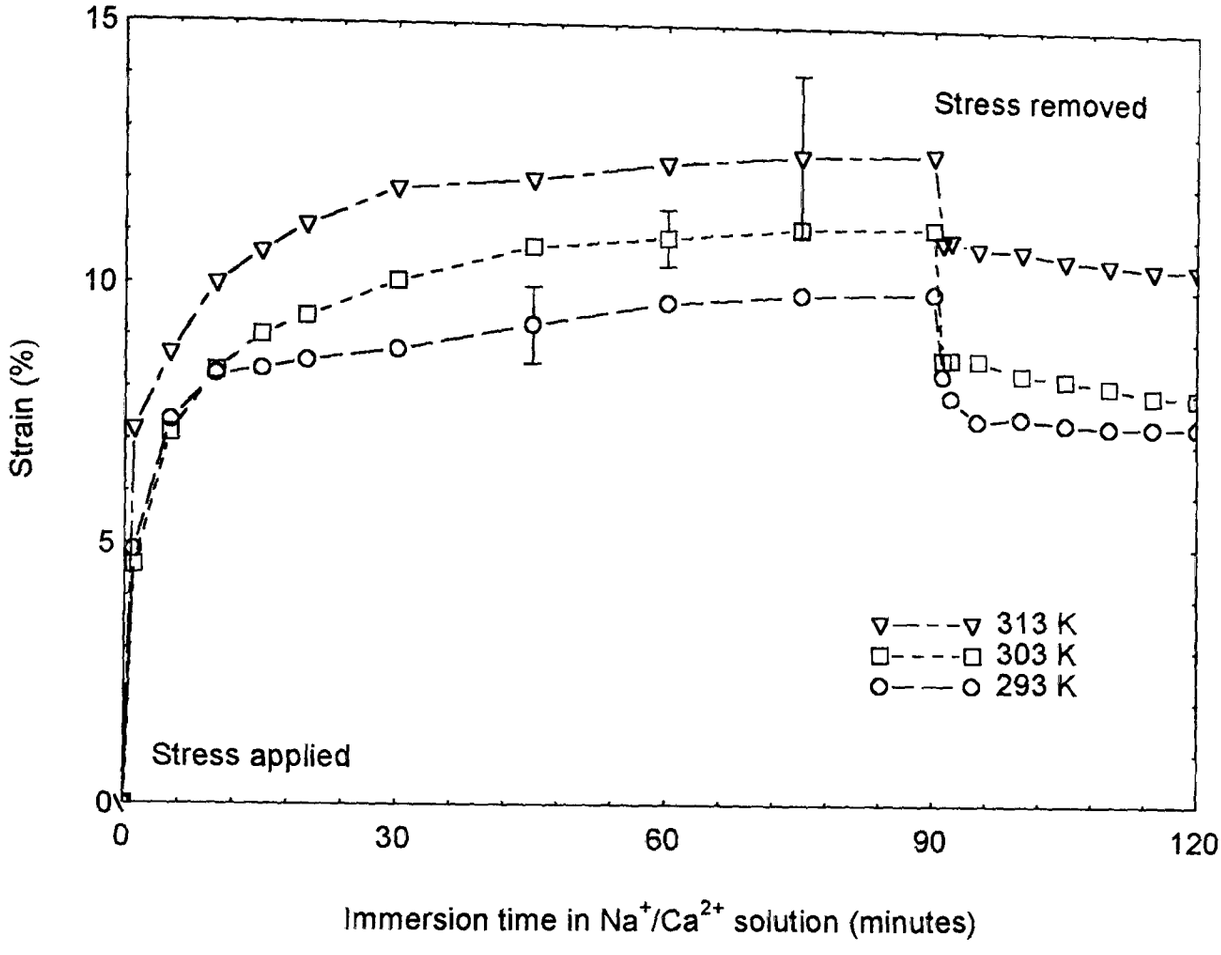

Figure V.4.4.a. Gel strength of high-G alginate films as a function of temperature.

The experimental error is ± 7 % at 293 K, ± 4 % at 303 K and reaches ± 13 % at 313 K. As the temperature of the simulated serum is increased, the gel strength of the high-G alginate films is lowered. Raising the temperature induces greater molecular motion and thus favours deformation. However, the change in strain observed between the different temperatures is not so important. Indeed high-G alginate gels are commonly referred to as strong gels (Clare, 1993), retaining their strength at high temperature (Gacesa, 1988). Andresen & Smidsrød (1977) also found that the elastic moduli of alginate gels decreased with increasing temperature. This decrease was interpreted as a breaking and rearrangement of junction zones in the dense network of stiff chains. The calcium junction zones were regarded as the weak points in the alginate gel.

Figure V.4.4.b. shows the Arrhenius plots for the strain values after 15, 10, 45, 60 and 90 minutes immersion in the Na^+/Ca^{2+} solution:

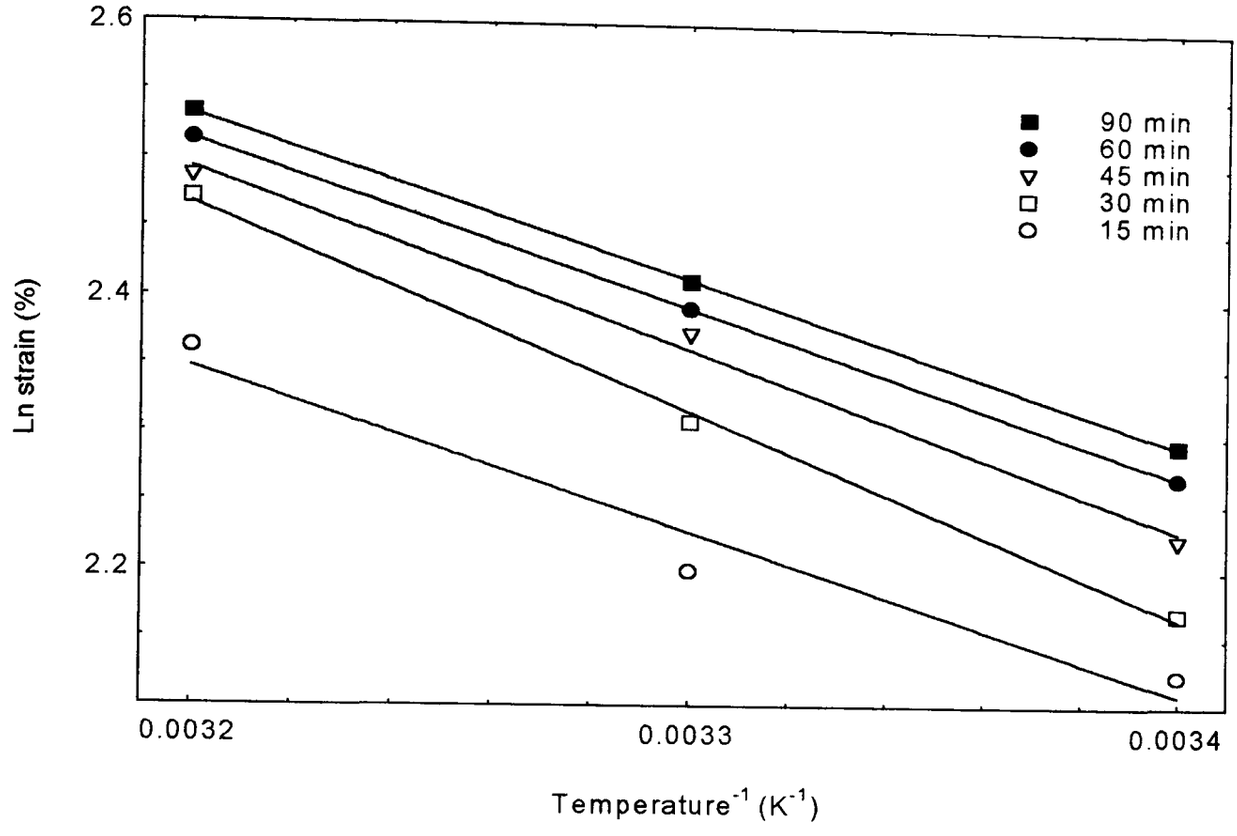

Figure V.4.4.b. Arrhenius plots.

The equation of each straight line can be given by: $\ln \epsilon = -E_a/RT + \text{constant}$, where ϵ is the strain, E_a the activation energy of the process, R the gas constant and T the temperature in Kelvin.. Therefore the apparent activation energy for chain slippage can be obtained from the slope of each line. However, since only three data points are available for each curve, the E_a values can only be approximated. They are presented in table V.4.4.

Time (minutes)	Activation energy E_a for chain slippage(kJ.mol^{-1})
15	9.9
30	12.6
45	10.9
60	10.2
90	9.9

Table V.4.4. Activation energies for the gel strength process.

Most activation energies are similar (10-11 $kJ.mol^{-1}$), suggesting that the mechanism of deformation under stress (i.e. chain extension and slippage) remains the same as time elapses. The higher E_a value found at 30 minutes is thought to be due to experimental error rather than to a different mechanism at this particular time.

V.5. Summary

From the different tests performed on alginate films in a simulated serum solution, some trends emerge.

A minimum initial calcium content in the sample is found necessary to initiate the blood coagulation process (i.e. release of the Ca^{2+} ions in the Na/Ca solution). It also ensures sufficient gel strength. On the other hand, a lower calcium percentage promotes swelling. The M/G ratio is another important factor when considering alginate properties. While the M blocks release the Ca^{2+} ions more quickly than the G blocks (thus speeding the clotting process up) and enhance the swelling behaviour, they dramatically reduce the wet strength, making the gel handling very difficult (as it falls apart).

Depending on the type of wound, different dressings can be prepared with more or less swelling, strength and blood coagulation ability. However, from the results obtained, the sample offering the best compromise appears to be the high-G alginate with 1.8 at% Ca^{2+} and 2.2 at% Na^{+} (or a proportion of 58 wt% Ca^{2+} and 42 wt% Na^{+}). These experiments would need to be repeated in contact with blood to get a more precise picture of the material in use.

In practice, commercial alginate wound dressings such as Sorbsan® and Kaltostat® contain more calcium (95 wt% and 80 wt% Ca^{2+} respectively). The first is made from high-M alginate while the second is derived from high-G alginate fibres.

CHAPTER VI: ALGINATE/PECTIN BLENDS

The mannuronic/guluronic ratio has been proved to be one of the major parameters influencing alginate properties (Haug *et al.*, 1967a; Iso *et al.*, 1988; Martinsen *et al.*, 1989). Pectin, another natural polymer, is primarily formed of partially methylated polygalacturonic acids. The remainder of pectin consists of sugar units. An important parameter in the description of this polymer is the degree of methoxylation. Whilst low methoxyl (L.M.) pectins form gels in the presence of divalent ions (in a similar way to calcium alginate gels), gelation at low pH (3.0- 3.5) and high sugar content (> 55 %) is favoured for high methoxyl (H.M.) pectins (Toft, 1982). Yet under specific conditions, combinations of alginate and pectin have been shown to gel at low pH (< 4) and low solids (20 % sucrose or less) (Clare, 1993; Thom *et al.*, 1982). Optimum gel strength for these blends is obtained with high-G alginate and H.M. pectin (Morris & Chilvers, 1984; Toft, 1982). However, most of the work carried out on these blends is concerned with their use in food products. By contrast, our interest is in wound dressing applications, and our sample preparation tried to simulate the dressing manufacture. The alginate used in this study was PROTANAL LF 10/60, with M/G = 25/75. The pectin was citrus pectin USP, with a degree of esterification close to 55 wt%, which contained around 25 % of sugars (as given by the manufacturer Bulmer Pectin- Citrus Colloids Ltd). Both materials were highly purified. H.M. pectin was preferred to L.M. pectin because stronger gels are observed with the former. Although H.M. pectin does not gel in the presence of Ca^{2+} ions, it was postulated that small additions of this polysaccharide could still improve the gel strength properties of the sodium/calcium alginate/pectin blends (i.e. the wound dressing).

VI.1. Characteristics of the sodium alginate/pectin blends

From the GPC technique, the number average molecular weight of both sodium alginate and pectin was approximately 2.1×10^5 (standard: poly(ethylene glycol)). The polydispersity of the alginate was 2.0, and that of pectin was 2.3.

All the alginate/pectin solutions were prepared using a similar powder content of 3 wt%. This percentage gave a good dispersion of the polysaccharides and a reasonable

viscosity. The pH and viscosity were measured before drying these solutions to produce sodium films. More tests were performed on the samples as films, to determine their crystallinity and morphology.

VI.1.1. Characteristics of the sodium alginate/pectin blends as solutions:

i. pH measurements:

Measurements of pH were performed on sodium alginate/pectin solutions, with varying proportions of each polymer. The resolution of the instrument was 0.01pH. The results are summarised in table VI.1.1.a.

Sample	pH
100% sodium alginate LF 10/60	6.3
97.5% alginate + 2.5% pectin	5.7
95% alginate + 5% pectin	5.4
75% alginate + 25% pectin	4.6
50% alginate + 50% pectin	4.1
25% alginate + 75% pectin	3.6
100% pectin	2.9

Table VI.1.1.a. pH values of sodium alginate/pectin solutions.

pH is an important factor in controlling the gelling behaviour of high methoxyl pectin. As already mentioned, gelation of high methoxyl pectin and high-G alginate blends is not observed above pH 4. From our values, only the 25 % alginate/75 % pectin blend meets this requirement. Cold gelation can be controlled by release of hydrogen ions from D-gluco 1,5-lactone (Clare, 1993). However, in this study, no attempts were made to reduce the pH and to optimise the gelation phenomenon. The first reason is that, after making sodium alginate and pectin solutions, the next step in sample preparation requires sodium/calcium ion exchange (calcium ions are necessary as they have been found to stimulate blood coagulation). For this purpose, it might be more suitable to deal with a polysaccharide solution rather than with a gel, to ensure high calcium ion mobility and binding. The second reason comes from the drug tariff technical specification for calcium alginate dressing (1994), which requires a pH between 5.5 and 8.0. Although we are dealing with sodium samples and not calcium samples at this stage, a significant addition of pectin does not seem appropriate for medical applications.

The pH values of sodium alginate/pectin solutions have been plotted below as a function of the pectin content:

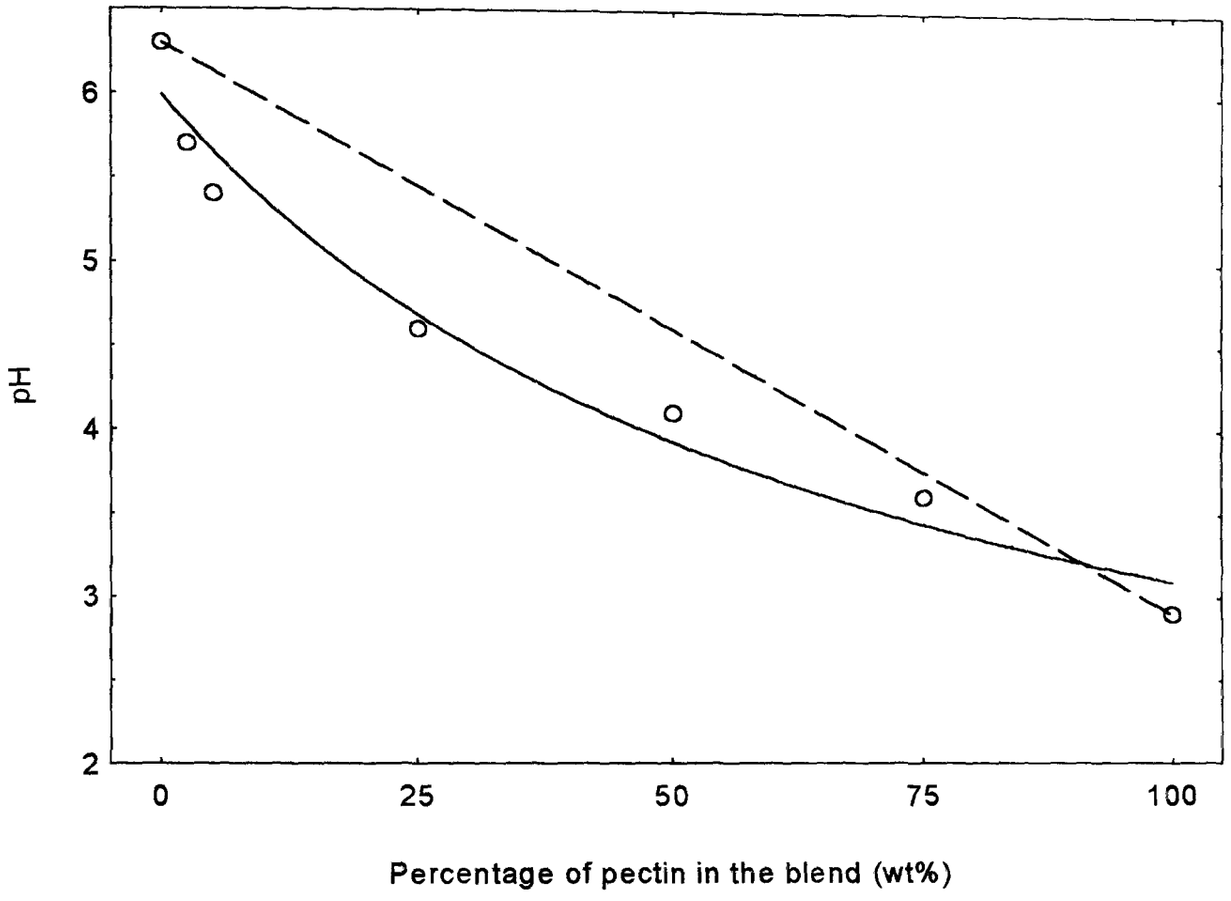

Figure VI.1.1. pH as a function of pectin content.

The blends show an initial rapid drop in pH suggesting minimisation of electrostatic repulsion, and possibly interaction between the polysaccharide chains in solution (Thom *et al.*, 1982).

ii. Viscosity:

The blends in solution have also been tested for their viscosity. The results, measured at 10 rpm (shear rate = 2.8 s^{-1}), follow.

Sample	Viscosity (mPa.s)
100% alginate LF 10/60	670
97.5% alginate + 2.5% pectin	430
95% alginate + 5% pectin	500
75% alginate + 25% pectin	510
50% alginate + 50% pectin	620
25% alginate + 75% pectin	3,400
100% pectin	700

Table VI.1.1.b. Viscosity values of sodium alginate/pectin solutions.

The precision in the viscosity values is ± 5 %. Most viscosity values are similar (except for the 25/75 blend). This would be expected as the number average molecular weight and the polydispersity of the two polysaccharides are of the same order. Therefore the degree of entanglement of these polymers in solution is comparable. There is a surprising increase in viscosity for the 25% alginate/75% pectin blend. This observation may be correlated with the fact that this blend offers the best conditions for gelation as far as pH is concerned. For these proportions, a high level of binding between the two polymers, leading to high entanglement, and thus to greater viscosity, is expected.

VI.1.2. Characteristics of the sodium alginate/pectin as films:

i. Crystallinity:

The X-ray diffraction spectra of the various sodium alginate/pectin blends are presented in figure VI.1.2.a.

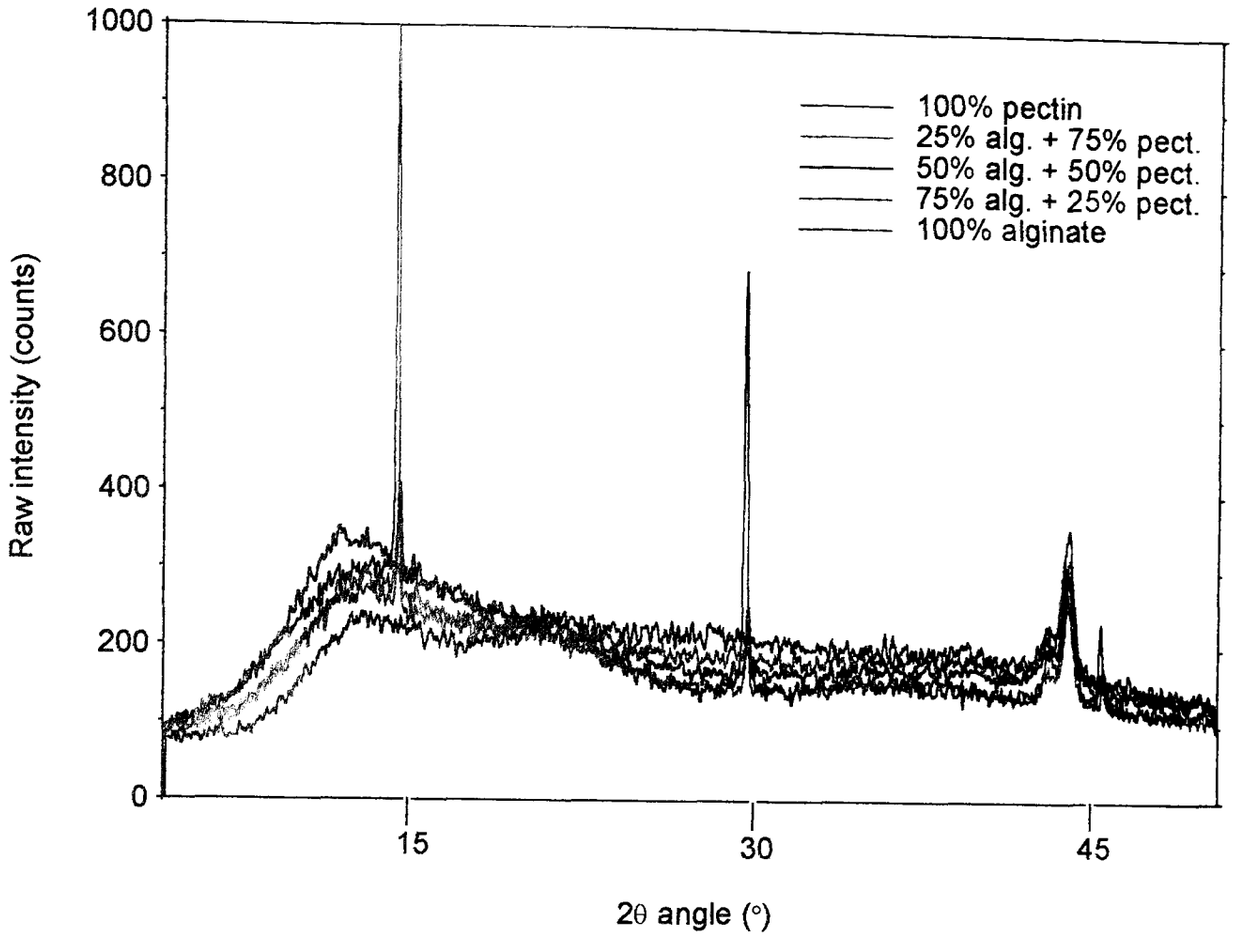

Figure VI.1.2.a. X-ray diffraction spectra of sodium alginate/pectin blends.

The peak doublet present at 43-45° is due to the steel stub onto which the samples were secured during the scan. While the sodium alginate film displays two broad peaks (at 13.5° and 21.7°), characteristic of a low degree of structural arrangement, the pure pectin film exhibits several sharp peaks, of different intensities, at 15.0° (corresponding to a d-spacing of 0.59 nm), 30.1° (d-spacing: 0.30 nm) and 45.9° (d-spacing: 0.20 nm). This is representative of a more organised structure. However, no characteristic crystal structure could be matched with these peaks.

Walkinshaw & Arnott (1981) performed X-ray diffraction on highly oriented fibres of high methoxyl pectinic acid. They deduced that pectinic acid has an hexagonal repeat unit (side: 0.84 nm). They believed that this structure is stabilised by hydrophobic binding from columns of methyl groups as well as by specific intermolecular hydrogen bonds.

ii. Morphology:

Scanning electron microscopy (SEM) was used to analyse the flat surfaces of the sodium alginate/pectin films (Some of them are shown in figure VI.1.2.b.). Hardly any features can be detected but only slight differences in contrast, especially with high alginate content. The very low degree of roughness certainly originates from the low viscosity of the solutions used.

The fracture surfaces (Figure VI.1.2.c.) appear, in general, as brittle type surfaces, especially with increasing pectin content. This implies that pectin is more brittle than the alginate. Indeed, mechanical tests performed on the same films showed that the fracture strain for sodium alginate was 10 % while that of pectin was only 3 %. At this magnification, the two polysaccharides appear to have formed a homogeneous blend.

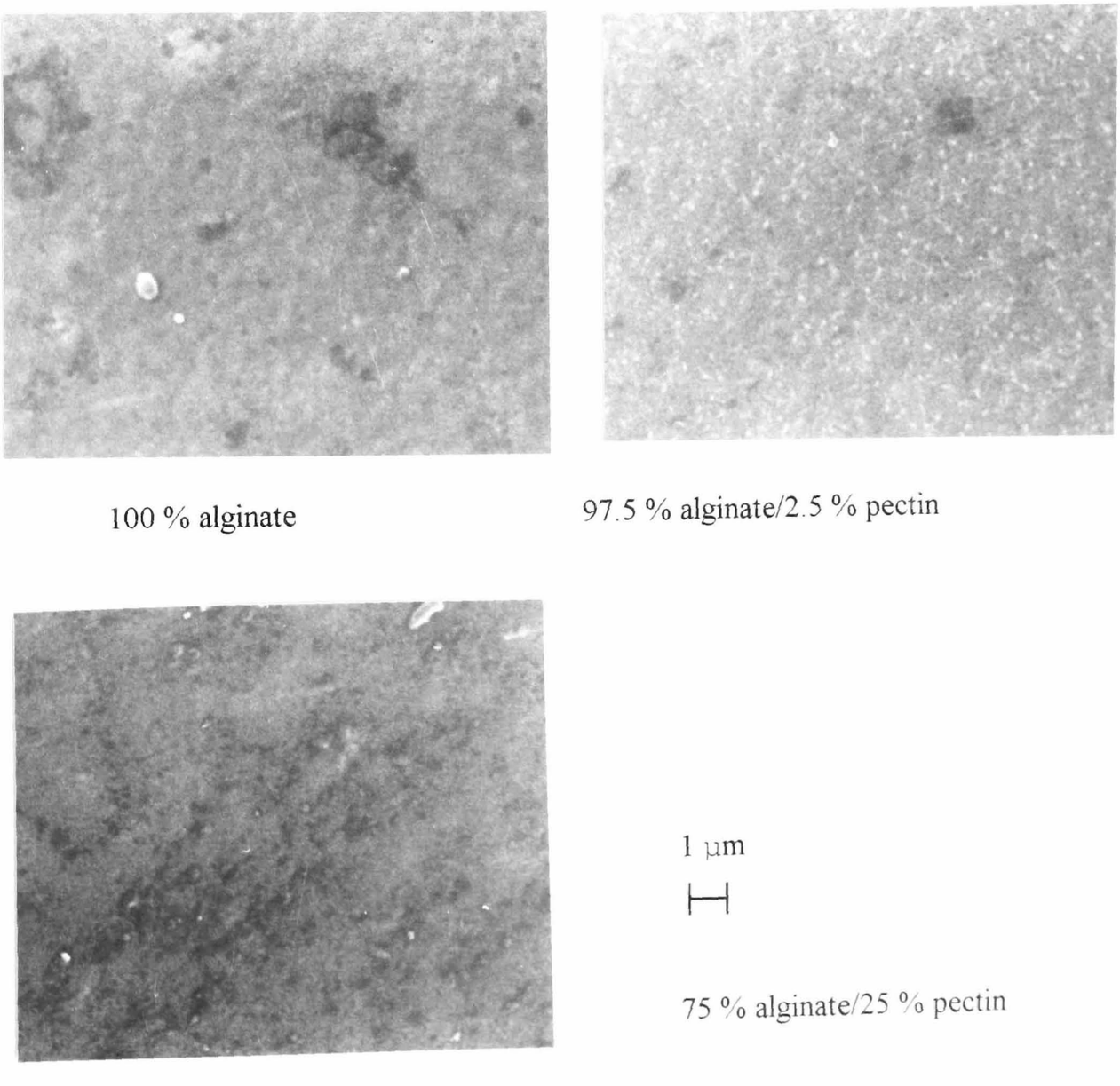

Figure VI.1.2.b. SEM pictures of the surfaces of sodium alginate/pectin films.

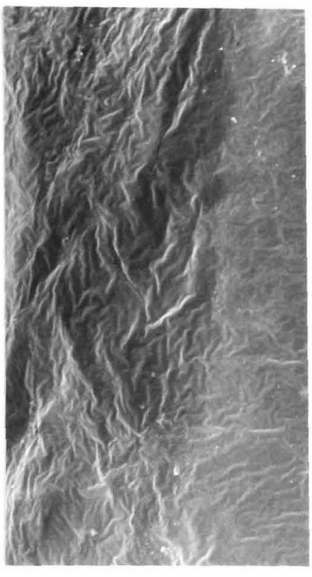

100 % alginate

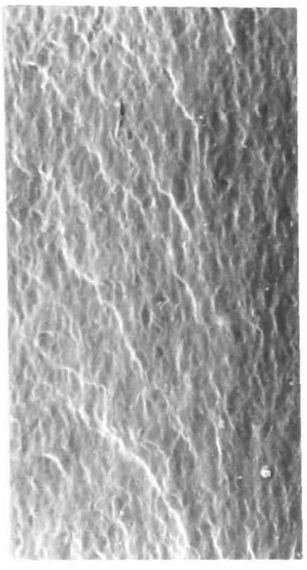

97.5 % alginate/2.5 % pectin

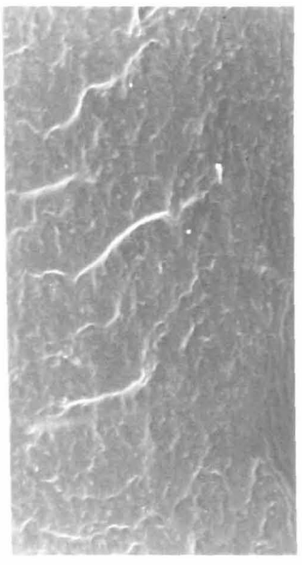

95 % alginate/5 % pectin

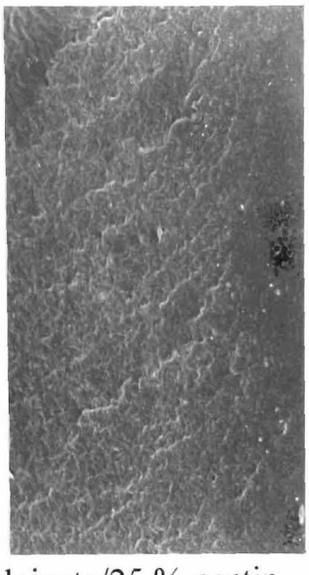

75 % alginate/25 % pectin

50 % alginate/50 % pectin

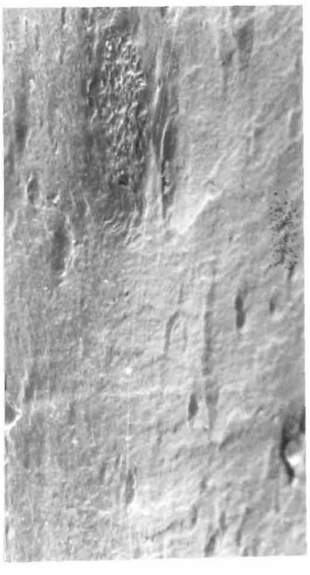

25 % alginate/75 % pectin

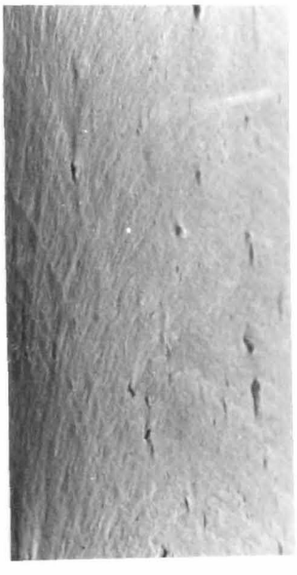

100 % pectin

10 μm

Figure VI.1.2.c. SEM pictures of fracture surfaces of sodium alginate/pectin films.

VI.1.3. Infrared analysis of the sodium alginate/pectin blends:

1 wt% solutions were used to prepare thin films (less than 10 μm), subsequently scanned by transmission infrared spectroscopy.

i. FTIR assignment of pectin:

A pectin FTIR spectrum is displayed in figure VI.1.3.a., from 4000 to 400 cm^{-1}. The fingerprint region follows (figure VI.1.3.b.).

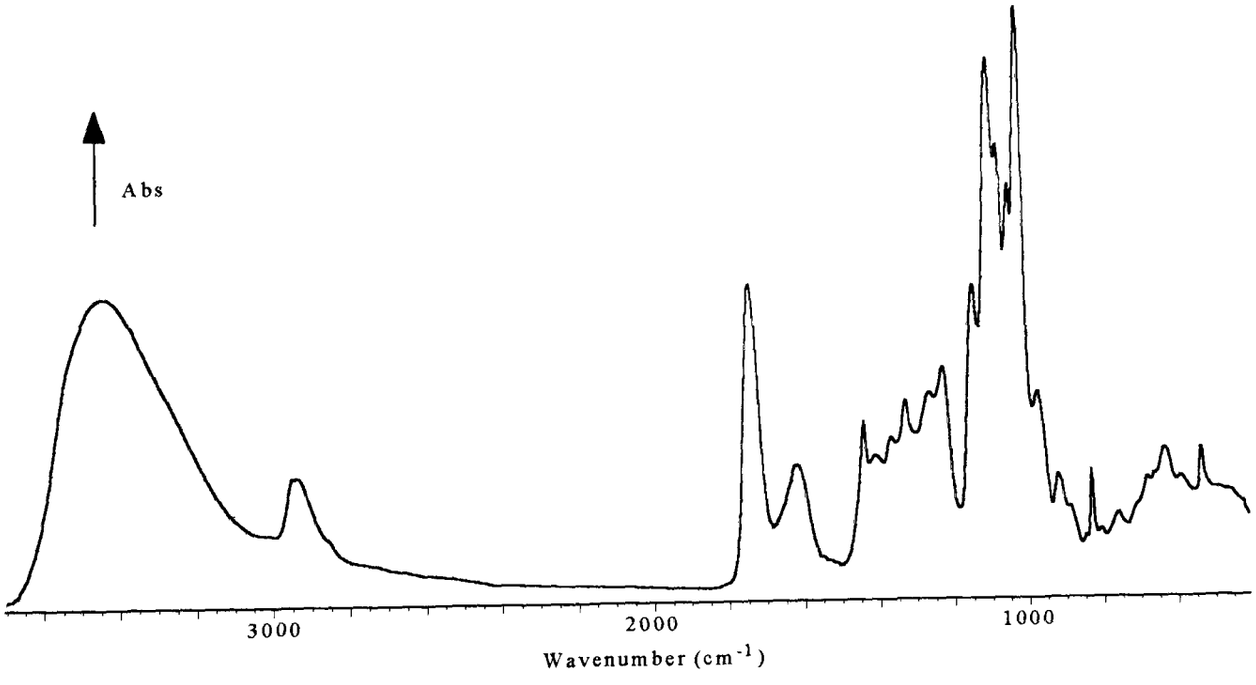

Figure VI.1.3.a. FTIR spectrum of pectin.

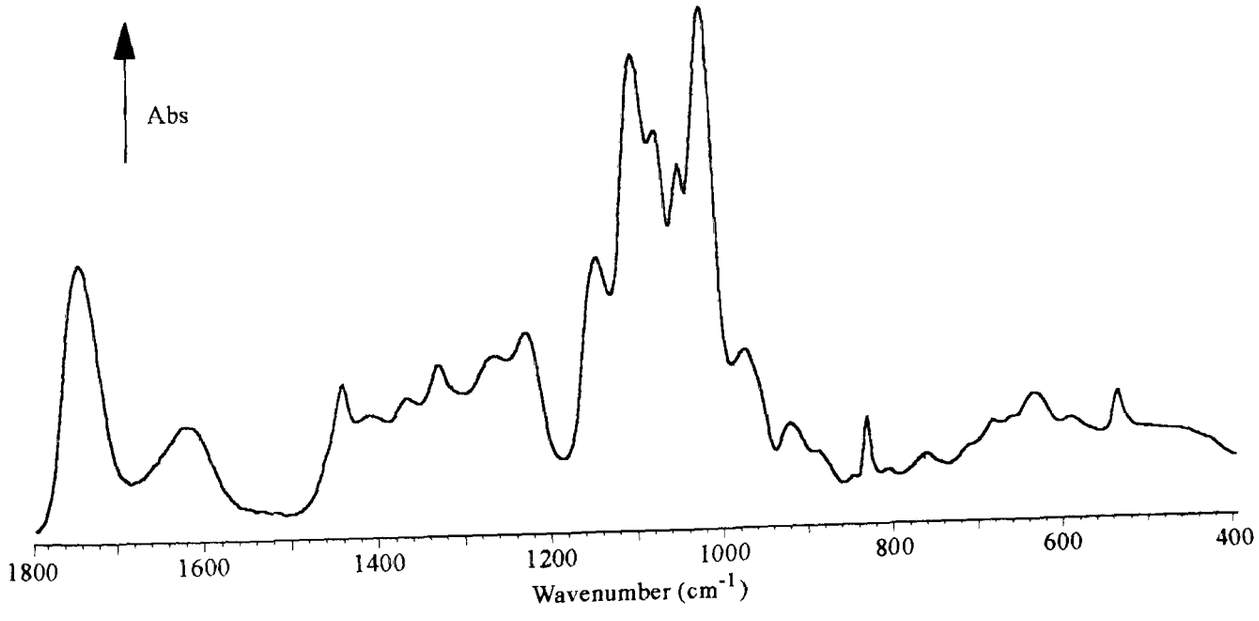

Figure VI.1.3.b. Fingerprint region of the pectin spectrum.

Amongst the three polysaccharides studied, pectin undeniably gives the most complex infrared spectrum. Furthermore, very little literature was found regarding the assignment of the IR bands. Alginate and pectin molecules are very similar. The comparison of D-galacturonic acid and L-guluronic acid units shows that they are mirror images with the exception of the configuration at C(3) (Cesàro *et al.*, 1988). Therefore an analogy between the alginate infrared spectrum and the pectin infrared spectrum would be expected, the differences arising mainly from the sodium ions (in the alginate) and the methyl ester groups (in the pectin).

Wavenumber (cm^{-1})	Intensity - Shape	Assignment
3440	strong - broad	O-H stretching
3270	strong - shoulder	O-H stretching
2950	medium - broad	C-H & $C-H_3$ stretching
2930	medium - broad	C-H & $C-H_3$ stretching
1744	strong - sharp	C=O stretching
1620	medium - broad	COO stretching
1440	medium - sharp	C-H & $C-H_3$ deformation
1410	medium - broad	C-O stretching & O-H def.
1365	medium - sharp	CH_3 deformation
1330	medium - sharp	C-H deformation
1265	medium - broad	COC stretching
1230	medium - sharp	?
1146	strong - sharp	C-O stretching
1103	very strong - sharp	C-O stretching
1075	very strong - sharp	C-O & C-C stretching
1050	strong - sharp	C-O & C-C stretching
1022	very strong - sharp	C-O & C-C stretching
973	medium - sharp	?
921	medium - broad	O-H deformation
833	medium - sharp	C-H deformation
633	medium - broad	?
535	medium - sharp	C-O deformation

Table VI.1.3. Band assignment of pectin spectrum.

The frequency of the O-H stretching peak for pectin (3440 cm^{-1}) is much higher than for alginate (3370 cm^{-1}) or for CMC (3380 cm^{-1}). It can be deduced that the O-H groups in pectin vibrate more freely, overall, compared with the other polysaccharides.

ii. Interaction between alginate and pectin:

In order to determine whether there is any interaction between alginate and pectin, polysaccharide blends were scanned by infrared spectroscopy. Figure VI.1.3.c. displays the spectrum of the 50 % sodium alginate/50 % pectin blend with the summation spectra of 100 % sodium alginate and 100 % pectin. A similar study has been carried out for the 25 % sodium alginate/75 % pectin blend (figure VI.1.3.d.). Prior to summation, the FTIR spectrum of pure sodium alginate and pure pectin were multiplied by a factor of 0.25 and 0.75 respectively. The spectra were corrected for the different film thicknesses.

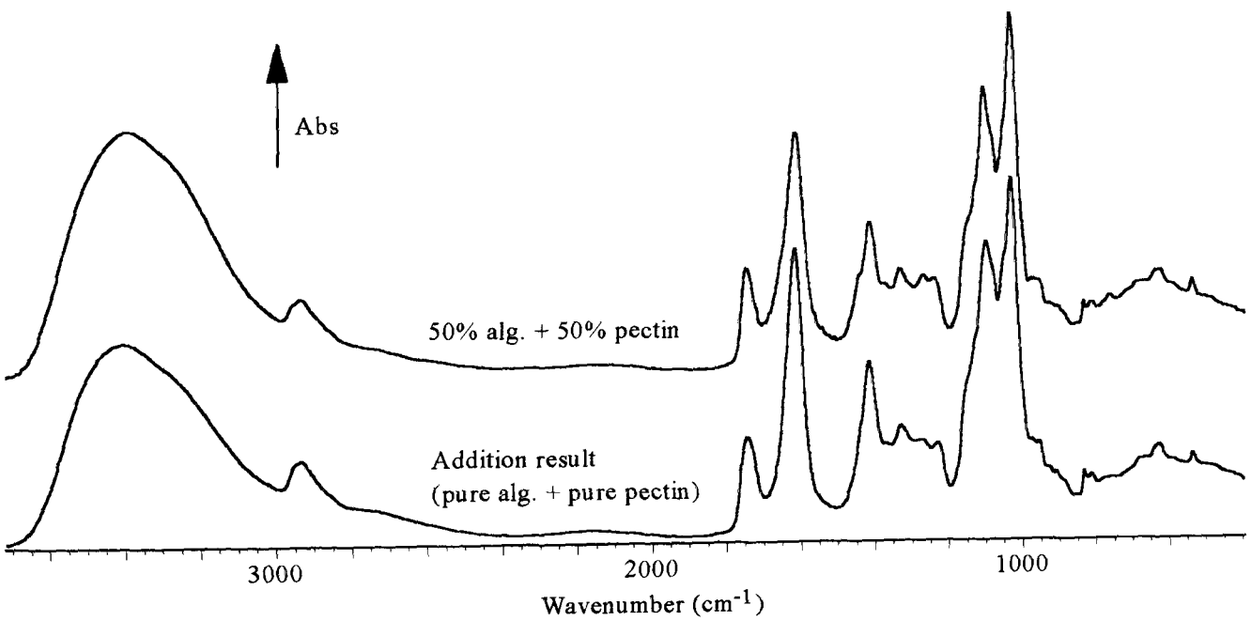

Figure VI.1.3.c. Addition FTIR spectrum of 50 % sodium alginate/50 % pectin.

The strong peak at 1028 cm^{-1} (C-C and C-O stretching in both polysaccharides) was used as the reference peak. Several differences can be detected between the two spectra, such as:

-the O-H peak increases in intensity and shifts to lower wavenumbers (from 3410 to 3390 cm^{-1}) from the addition spectrum to the "real" spectrum. This is certainly characteristic of a more specific type of hydrogen bonding, i.e. OH...OH (as opposed to COO^-...HO), taking place between the alginate and the pectin molecules;

-the decrease in intensity observed for the C-H and $C-H_3$ stretching vibrations (around 2940 cm^{-1}) implies that thse groups are restrained in their motion in the blend;
-the carboxyl peaks at *ca.* 1610 and 1413 cm^{-1} (mainly due to alginate) decrease in intensity and move towards lower frequencies. This is characteristic of hindrance in the movement of these groups in the blend; by contrast, the carboxyl peak at *ca.* 1740 cm^{-1} (from pectin) does not change greatly between the two spectra.

The 25 % alginate/75 % pectin blend was chosen because it was previously suggested that there was binding between the two polysaccharides (from the viscosity measurements), for this composition.

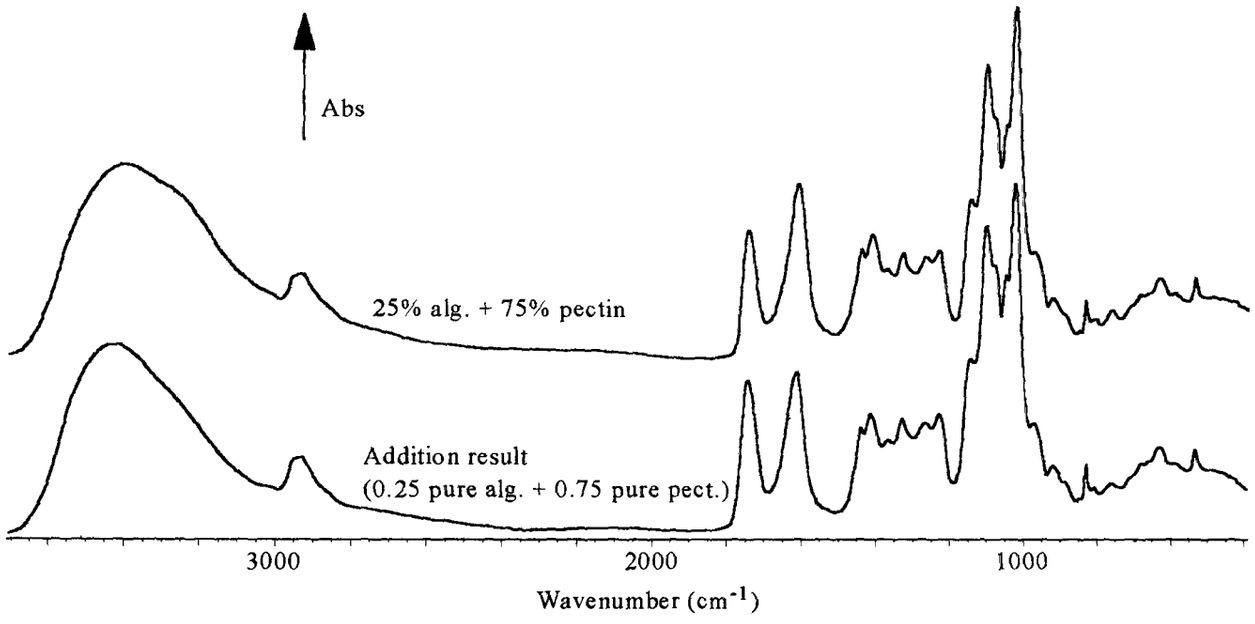

Figure VI.1.3.d. Addition FTIR spectrum of 25% sodium alginate/75% pectin.

The greater changes between the "real" and the "calculated" spectra are again observed for the hydroxyl and the carboxyl peaks. The increase of the shoulder (around 3300 cm^{-1}) in the "real" blend spectrum is indicative of intermolecular O-H...O-H bonding between the alginate and the pectin molecules (to the detriment of COO^-...HO bonding). The ratio of the peaks at *ca.* 1745 (COO^- in pectin) and 1620 cm^{-1} (COO^- in alginate) is also different. The increase in intensity of the second peak, together with a shift towards lower frequency, implies a greater $COO^-...Na^+$ bonding, again to the detriment of COO-...HO bonding. The carboxyl groups of the pectin are more hindered in their motion. This is the main difference compared with the 50/50 blend.

Thom *et al.* (1982) have suggested, from circular dichroism, that gelation involves intermolecular binding between methyl esterified polygalacturonic acid blocks (via the methyl groups) and polyguluronic acid blocks (via the hydrogen atoms attached to C(1) and C(2)). This was thought to be consistent with the almost exact mirror image between these blocks (as previously mentioned in section VI.1.3.). However, in our FTIR spectra, the OH...OH bonding seemed the most obvious way of linking.

VI.2. Conversion of sodium alginate/pectin into mixed sodium/calcium blends

Sodium alginate/pectin solutions were immersed for 30 minutes in a calcium chloride solution (0.8 wt%) to prepare the final samples (simulated wound dressing). After drying, sodium/calcium alginate/pectin films were thus obtained. These films were characterised, and the results of this follow. The solution containing 100 % pectin did not gel in contact with calcium ions (as expected for a high methoxyl pectin), and therefore no data are available at this composition. For most experiments, the average film thickness was 150 μm. For the infrared samples, a 1 wt% solution was used and films less than 10 μm were obtained.

VI.2.1. Water content:

Thermogravimetric analysis was performed on the different sodium/calcium blends in order to determine the water content, and to monitor the temperature where decomposition of the films starts. Table VI.2.1. summarises the results.

Sample	Temperature (K)	Water content (wt%)
100% alginate LF 10/60	471	12.9
75% alginate + 25% pectin	458	10.8
50% alginate + 50% pectin	461	11.2
25% alginate + 75% pectin	471	12.8

Table VI.2.1. Temperature of TGA inflection point for Na/Ca alginate/pectin blends.

Whilst the pure alginate and the 25 % alginate/75 % pectin films present similar values for both the decomposition temperature and the water content, the blends containing 25 and 50 % pectin contain less water and decompose earlier. Alginate is a hydrophilic polysaccharide while pectin is known to be hydrophobic (due to esterification, the content of neutral chains increases, thus lowering the water activity, Thom *et al.*, 1982). Therefore upon pectin addition, the amount of water retained is expected to decrease. However, with greater than 50 % of pectin, the opposite trend is observed. One explanation may be that incompatibility between the two polysaccharides is high. The low level of interaction between the chains would lead to greater space in the network, and thus to easier motion and penetration of the water molecules into the polymer blend.

VI.2.2. Crystallinity:

The X-ray diffraction spectra of the sodium/calcium alginate/pectin films appear very similar to those of the sodium salts (see figure VI.1.2.a.). This suggests that the introduction of calcium ions in the polysaccharide network does not intensify the degree of ordering. This is not surprising as the same conclusion was made for the pure alginate samples, and because the high methoxyl pectin is not known to bind to Ca^{2+} ions.

VI.2.3. Influence of the solution viscosity on the ion conversion:

The viscosity of various sodium alginate/pectin solutions was measured at 10 rpm. The ion contents were determined by atomic absorption spectroscopy on the final products (after immersion of the sodium alginate/pectin solutions for 30 minutes in $CaCl_2$ solution, as mentioned earlier). All the films had a thickness of 130 ± 15 μm.

Sample	Viscosity (mPa.s)	Na wt%	Ca wt%
2% (75% alginate + 25% pectin)	190	4.8	3.2
3% (75% alginate + 25% pectin)	510	5.5	2.3
4% (75% alginate + 25% pectin)	1150	5.3	2.9

Table VI.2.3. Influence of the viscosity on sodium and calcium content.

While the viscosity is multiplied by more than 5 from a 2 wt% to a 4 wt% alginate/pectin solution, there is only a factor of 1.1 difference between the ion percentages. However, a 3 wt% solution does lead to a marked difference in the ion contents, compared with the 2 wt% solution. Overall it appears that a change in viscosity (within the range studied) does not influence dramatically the ion content. Therefore all the films in this study were made from the same volume of solution, regardless of the viscosity, and the average thickness of the dried samples was kept close to 150 μm.

VI.2.4. Determination of the ion content:

The different sodium/calcium alginate/pectin films were analysed by atomic absorption spectroscopy to determine their sodium and calcium dry weight percentages. The standard error in measured ion content is ± 2-3 %. From these values, atomic percentages were derived (the detailed calculation is presented in appendix 3) as well as the charge equivalence (Na^+ at% + 2×Ca^{2+} at%). Table VI.2.4. gives the ion contents:

Sample	Na wt%	Ca wt%	Na at%	Ca at%	Charge eq.
100% alginate	6.5	3.2	2.8	0.8	4.4
97.5% alginate + 2.5% pectin	7.1	2.3	3.0	0.6	4.2
95% alginate + 5% pectin	7.1	2.3	3.0	0.6	4.2
75% alginate + 25% pectin	5.5	2.3	2.2	0.5	3.2
50% alginate + 50% pectin	4.5	2.1	1.8	0.5	2.8
25% alginate + 75% pectin	2.0	1.7	0.7	0.4	1.5

Table VI.2.4. Ion % of alginate/pectin blends after 30 minutes immersion in $CaCl_2$.

As the pectin percentage increases, there is a continuous drop in the charge equivalence, due to both sodium and calcium decay. The sodium decrease is understandable since pectin, as a starting material, contains only traces of this ion. The calcium drop reveals that gelation between Ca^{2+} ions and pectin molecules is not favoured. The first marked drop in the calcium percentage for a pectin content of 2.5 % indicates that small additions of pectin to alginate perturb notably the gelation process of alginate with the

divalent cations. Less divalent cations are allowed to penetrate into the polysaccharide network. However, with increasing pectin content (50 % and more), the levels of Na^+ and Ca^{2+} ions seem higher than expected. If alginate only is believed to gel in contact with the divalent cations, then the 50 % alginate/50 % pectin blend should contain 6.5/2 wt% sodium and 3.2/2 wt% calcium; the real values are higher. It is thus suspected that free ions are present in these blends, maybe due to a greater space between the molecules (due to possible incompatibility between alginate and pectin), or that some Ca^{2+} ions are bound to the pectin molecules.

VI.2.5. Morphology of the blend films:

i. Flat surfaces:

SEM performed on the surface of sodium/calcium alginate/pectin films (figure VI.2.5.a.) revealed, for 2.5 and 5 % pectin additions, 10 μm wide particles superimposed on the background. These are likely to be due to the $CaCl_2$ powder following the immersion in the $CaCl_2$ solution (although the samples were rinsed in water) as they do not appear on the sodium blends. They disappear for the samples containing a higher pectin content, certainly because these samples do not gel to the same extent as the low pectin content films (therefore they do not offer a strong affinity to the $CaCl_2$ solution). The surfaces appear rough with increasing pectin content, when compared with the sodium salts (figure VI.1.2.b). This may be due to a disruptive effect of the Ca^{2+} ions towards the pectin molecules.

ii. Fracture surfaces:

Overall, the fracture surfaces (figure VI.2.5.b.) are characteristic of a brittle-type failure. There are no evident signs of phase separation between the two polysaccharides at the levels of magnification studied.

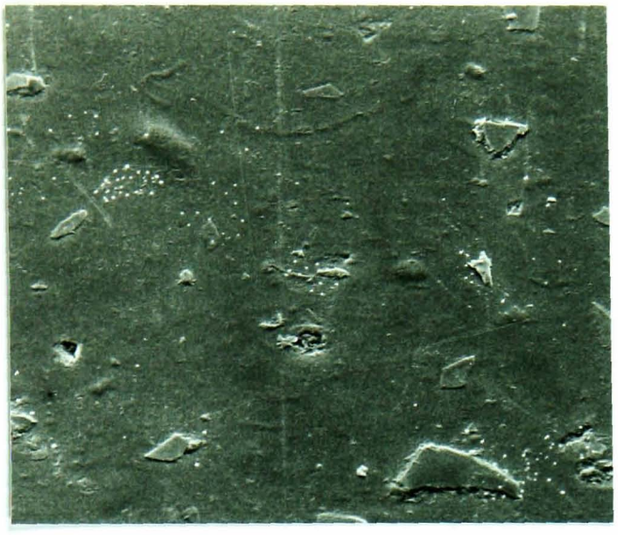

100 % alginate

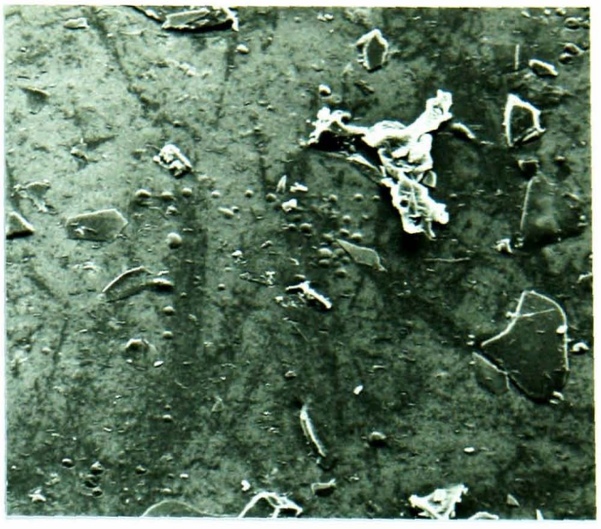

97.5 % alginate/2.5 % pectin

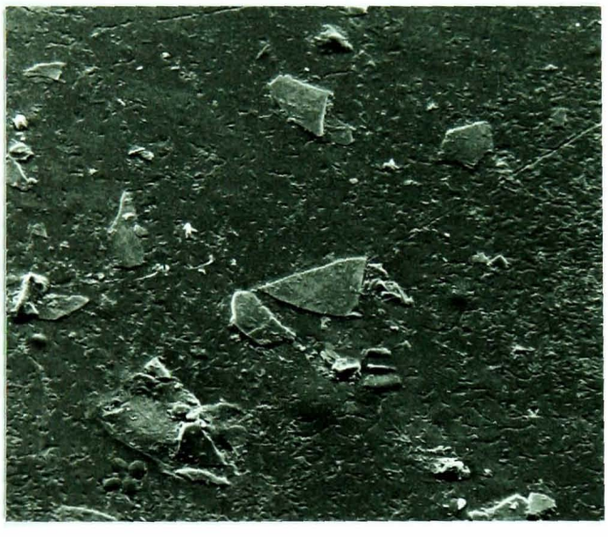

95 % alginate/5 % pectin

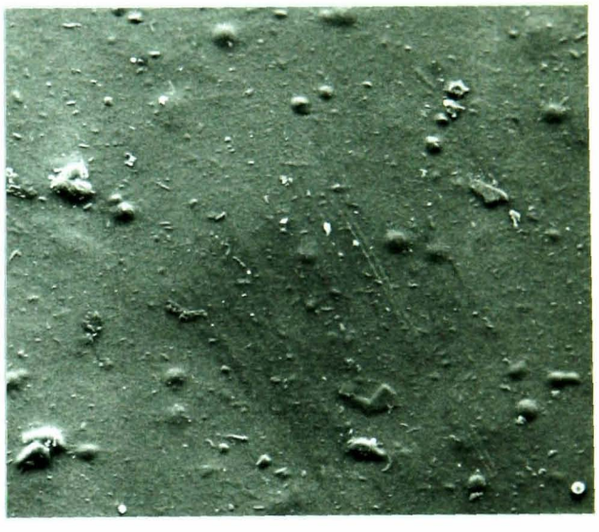

75 % alginate/25 % pectin

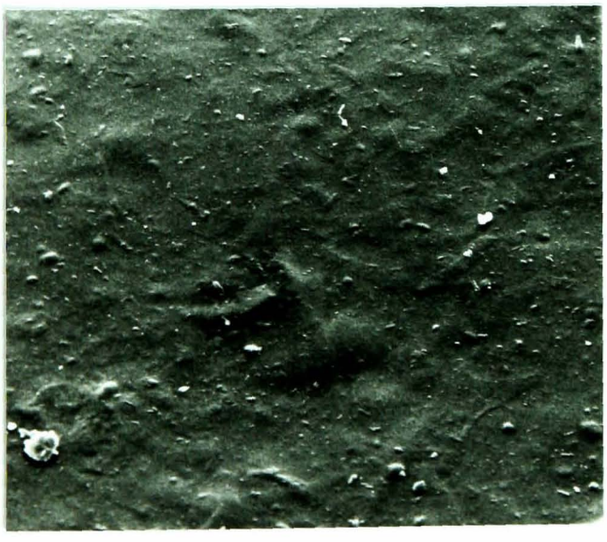

50 % alginate/50 % pectin

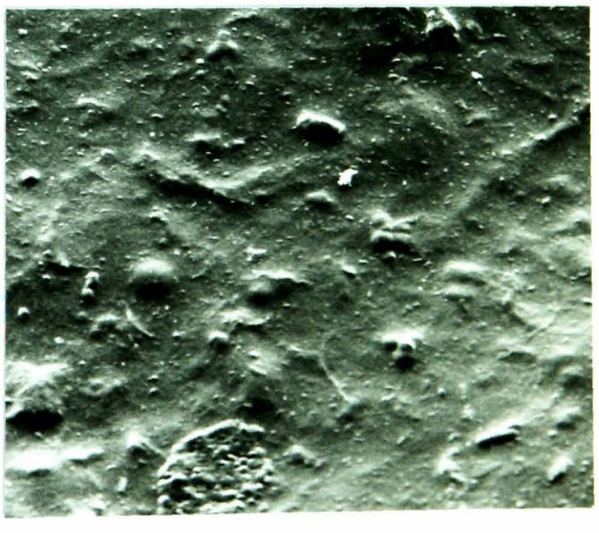

25 % alginate/75 % pectin

40 μm

Figure VI.2.5.a. SEM pictures of the surfaces of Na/Ca alginate/pectin blends.

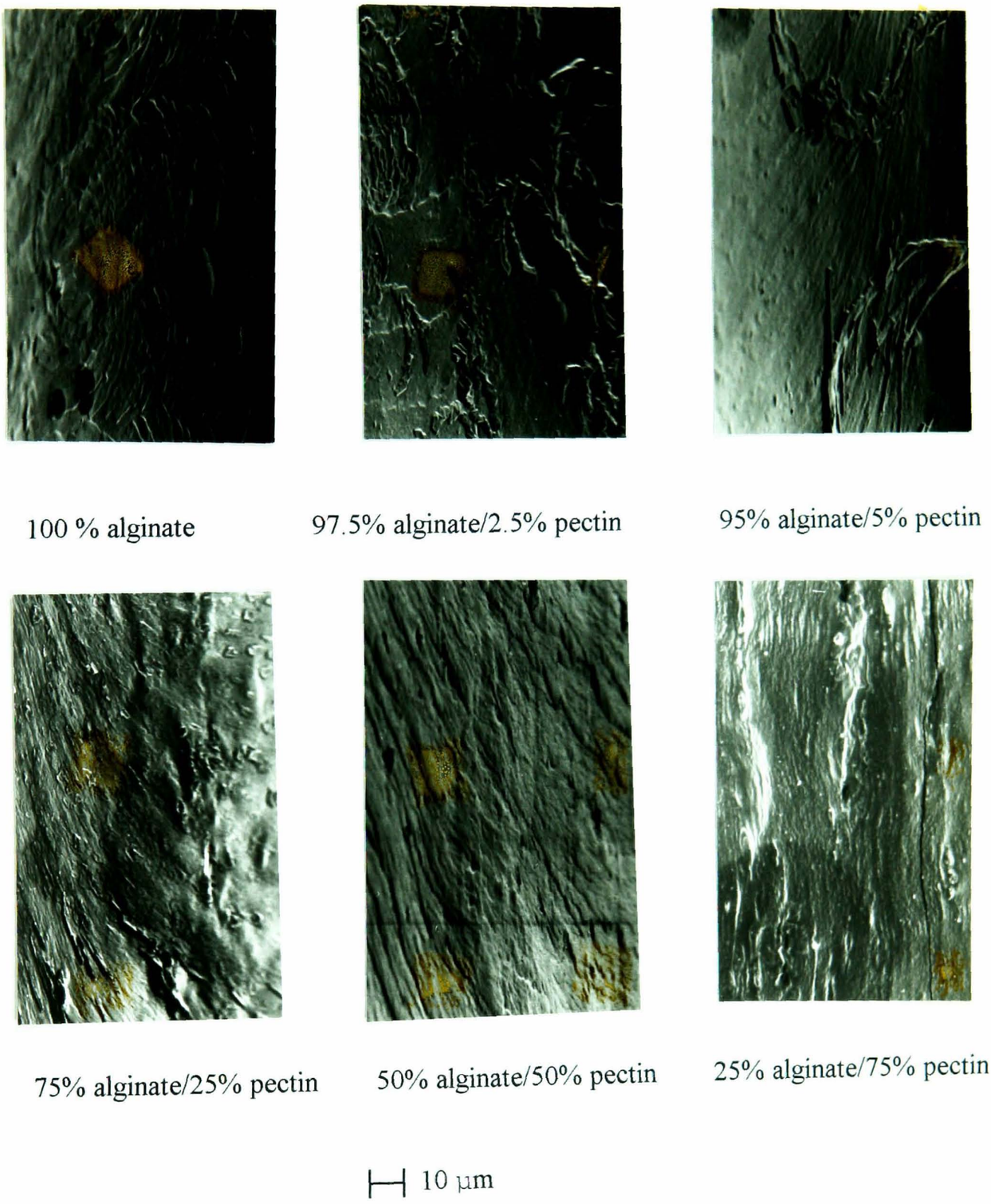

Figure VI.2.5.b. SEM pictures of fracture surfaces of Na/Ca alginate/pectin films.

VI.2.6. Mechanical tensile tests:

Tensile tests measurements were performed on the alginate/pectin films (after 30 minutes in $CaCl_2$ solution, and drying), at 0.05 mm.minute^{-1}. The results are presented in table VI.2.6.

Sample	Young's modulus (GPa)	Fracture stress (MPa)	Fracture strain (%)
100% alginate	3.0 ± 0.2	124 ± 18	10 ± 2
97.5% alginate + 2.5% pectin	3.0 ± 0.3	130 ± 6	11 ± 1
95% alginate + 5% pectin	3.4 ± 0.5	119 ± 13	9 ± 1
75% alginate + 25% pectin	3.2 ± 0.3	124 ± 9	10 ± 1
50% alginate + 50% pectin	3.2 ± 0.4	113 ± 8	7 ± 1
25% alginate + 75% pectin	2.8 ± 0.3	80 ± 9	4 ± 1

Table VI.2.6. Mechanical properties of dry films of Na/Ca alginate/pectin blends.

The pure polysaccharides, before immersion in the calcium chloride solution, have the following characteristics:

-sodium alginate: Young's modulus = 4.5 ± 0.3 GPa; fracture stress = 115 ± 2 MPa; fracture strain = 10 ± 1 %, and

-pectin: Young's modulus = 5.1 ± 1.4 GPa; fracture stress = 103 ± 15 MPa; fracture strain = 3 ±1 %. Therefore, pectin appears more brittle than sodium alginate.

From the sodium to the sodium/calcium alginate, there is a drop in the Young's modulus value. This is the opposite trend to what was observed with the 8 % alginate samples (chapter III); but the ion contents are different between the two sets of alginates (lower Na^+ and Ca^{2+} % with the 6 % sample) and, therefore, they cannot be compared directly.

The tensile tests performed on all samples showed little or no yield, characteristic of brittle materials. For the samples containing up to 50 % pectin, there is no great variation in the Young's modulus, the fracture stress and strain, considering the experimental error. An addition of 75 % of pectin leads to a decrease in all these parameters. Although this particular blend is supposed to present the highest degree of binding in the gel state

as a sodium salt, the introduction of calcium ions seems to reduce the molecular cohesion, thus weakening the mechanical performance. Alternatively, the poor mechanical properties could be attributed to poor distributive mixing. Overall, the addition of pectin does not come up to our expectations in the dry state; the blends weakness may be due to the surface roughness observed by SEM. These results reinforce the idea that calcium addition perturbs the alginate/pectin blends to the detriment of mechanical properties.

VI.2.7. FTIR analysis:

In order to study the changes associated with the introduction of calcium ions in alginate/pectin matrices, 1 wt% films were prepared and scanned by infrared spectroscopy. The same blends as in VI.1.3.ii. were studied (50 % alginate + 50 % pectin and 25% alginate + 75 % pectin blends), in both their sodium and their calcium forms (calcium film obtained after 300 minutes in $CaCl_2$). Figures VI.2.7.a. and VI.2.7.b. present their FTIR spectra.

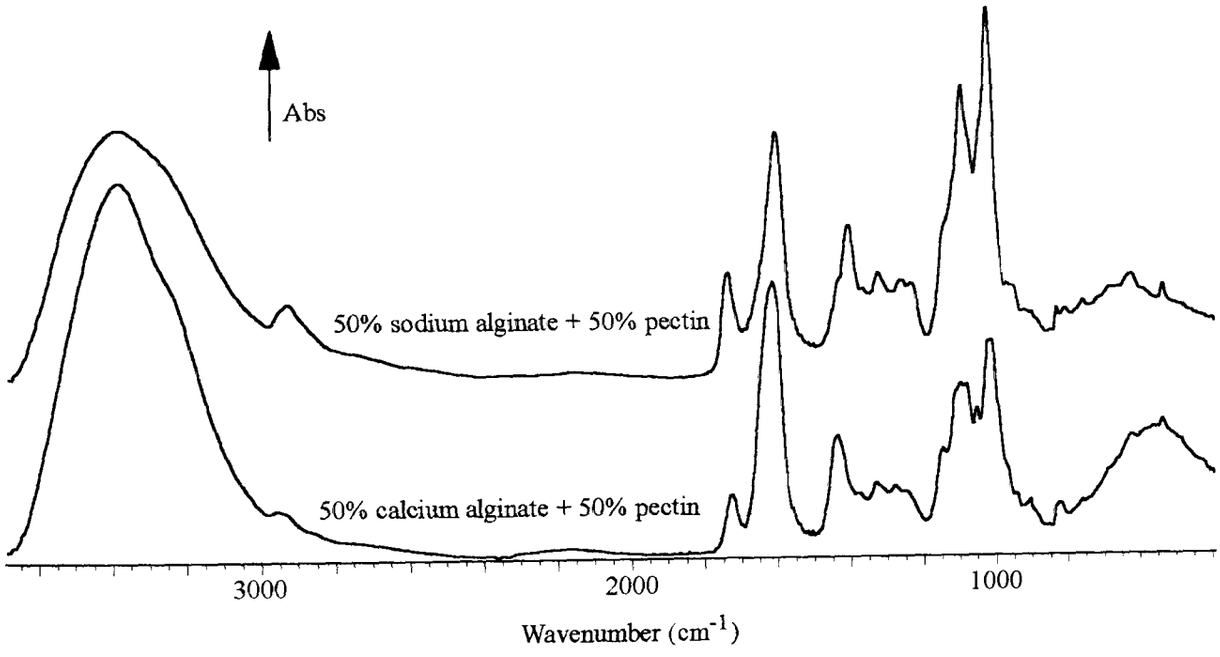

Figure VI.2.7.a. FTIR spectra of 50 % alginate + 50 % pectin blend as sodium and calcium salts.

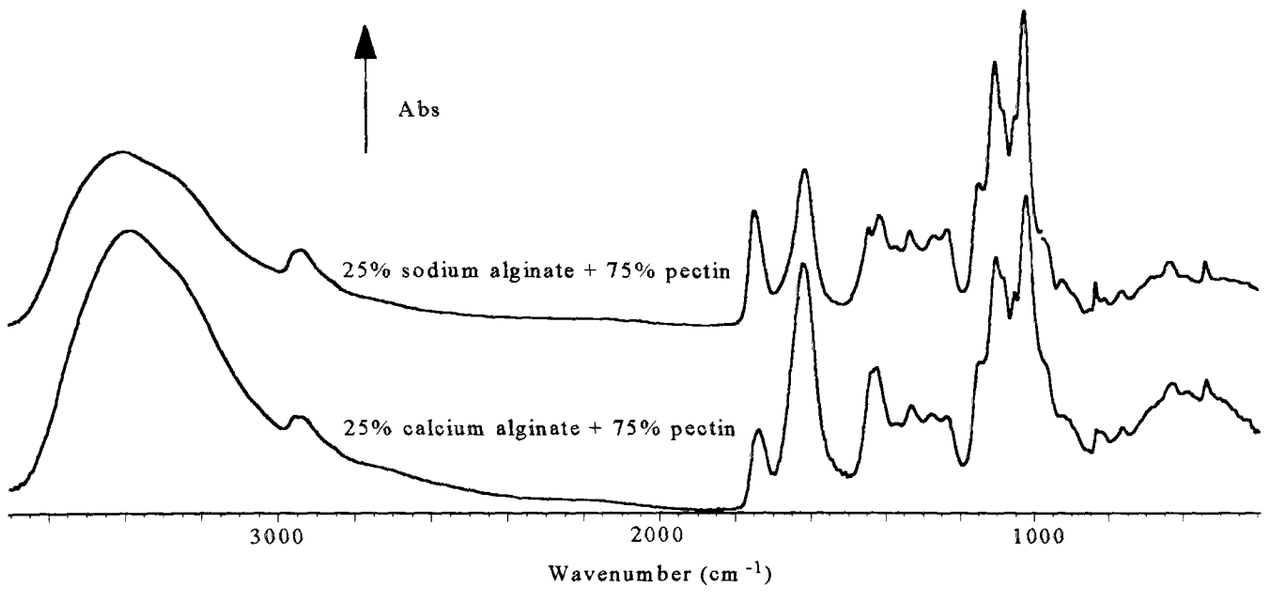

Figure VI.2.7.b. FTIR spectra of 25 % alginate + 75 % pectin blend as sodium and calcium salts.

In both blends, the introduction of Ca^{2+} ions led to great changes, and there was no obvious reference peak. Comparison studies have however been attempted. Some of the most noticeable differences between the sodium and calcium blends are presented below:

-the O-H peak (≈ 3400 cm^{-1}) has an increased intensity upon calcium addition, implying increased hydrogen bonding. Furthermore, there is a shift of 20 cm^{-1} towards lower wavenumbers for the 25/75 blend, involving predominantly OH...OH bonding. Only a 5 cm^{-1} shift is observed for the other blend;

-the peaks at *ca.* 2950 cm^{-1} (C-H & CH_3 vibration) have a reduced intensity upon calcium addition; these vibrations are therefore hindered by the presence of the Ca^{2+} ions;

-the pectin C=O stretching peak (close to 1740 cm^{-1}) has a decreased intensity and a lower frequency with calcium; it is also hindered in its motion, in both blends;

-in contrast, the alginate and pectin COO peak (≈ 1610 cm^{-1}) increases in intensity and shift slightly towards higher wavenumbers. One can suspect that these groups have more freedom of movement and therefore they are not so tightly bound to the calcium ions. Slight broadness may also suggest a new form of bonding for the carboxyl groups;

-the C-O stretching peak of pectin, at *ca.* 1230 cm^{-1}, reduces in intensity and is thus more vibrationally restricted in the presence of Ca^{2+} ions;

-the peak intensities at 1100 and 1020 cm^{-1}, characteristic of C-O and C-C groups in both polysaccharides, dramatically decrease in the 50/50 blend; these groups are highly

hindered upon Ca^{2+} addition. They may procure a centre of binding for the divalent cations. The 25/75 blend does not show such great differences between the two salts. Therefore, it is mainly the C-O and C-C groups of the alginates that are perturbed by the calcium.

It emerges that many groups of atoms in the pectin, and to a greater extent in the alginate, are perturbed and hindered in their motion by the introduction of calcium ions. While hydrogen bonds are present between the polysaccharide molecules, the calcium ions are thought to be bound partially to the polymers via oxygen atoms (from the COO and CO groups).

VI.3. Study of sodium/calcium alginate/pectin blends immersed in a simulated serum solution

Sodium/calcium alginate/pectin films have been previously prepared and characterised in the dry state. As potential wound dressings, they need to be tested for their performance in contact with a simulated wound exudate (Na/Ca solution). The tests include swelling and gel strength measurements. Calcium release experiments were not possible; the colour of the dye used (tetramethyl murexide) disappeared after minutes of immersion of the blend film. This disappearance is possibly due to the very acidic medium which develops as the pectin content in the sample increases.

VI.3.1. Volume ratio:

Each blend, prepared as a film, was immersed vertically in the simulated wound exudate, and the change in volume was recorded over one hour (figure VI.3.1.).

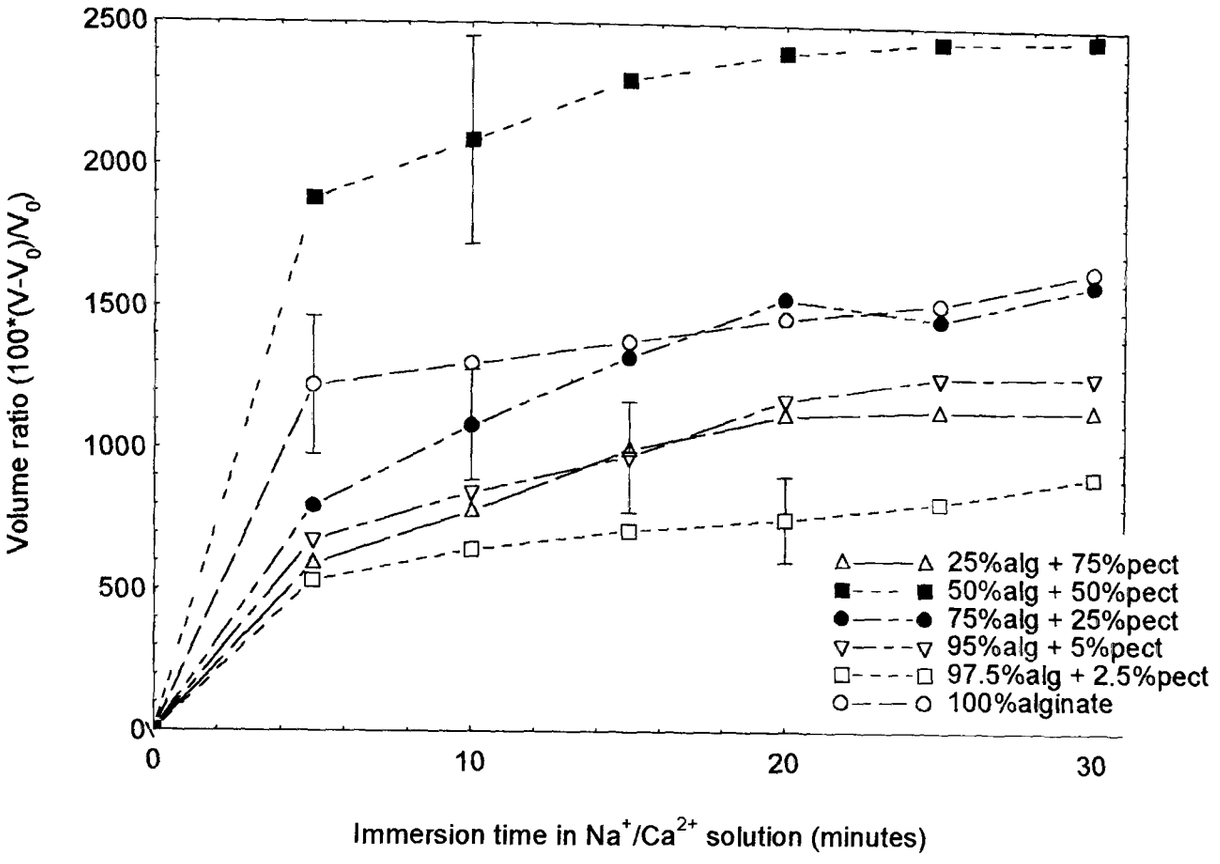

Figure VI.3.1. Volume ratio of alginate/pectin blends in Na/Ca solution.

There is a large spread in the experimental results, around ± 20 %. After 30 minutes of immersion in the Na/Ca solution, most samples have reached or are about to reach an equilibrium in volume. In the following table (VI.3.1.), the value of the volume ratio after this time is given as a function of pectin content:

Sample	Volume ratio (%)
100 % alginate	1640 ± 80
97.5 % alginate + 2.5 % pectin	910 ± 340
95% alginate + 5 % pectin	1270 ± 220
75 % alginate + 25 % pectin	1600 ± 160
50 % alginate + 50 % pectin	2460 ± 290
25 % alginate + 75 % pectin	1140 ± 770

Table VI.3.1. Volume ratio after 30 minutes immersion in Na/Ca solution, as a function of pectin content.

The initial drop in the volume change, following an addition of 2.5 % pectin, is clearly due to the hydrophobicity of pectin methoxylated units. With greater pectin amounts up to 50 %, the volume of the gel expands. This may be due to increased inhomogeneity in the blends, where empty cavities would be present, allowing for more water to penetrate. An alternative is that the hydrogen bonds between the pectin and the alginate molecules are disrupted and broken by the water molecules. However, for a pectin content equal to 75 %, the volume dramatically decreases again. Therefore, the hydrophobicity of pectin becomes dominant over the blend cohesion, in the gel state. For this last composition, a different behaviour was observed in the dry state, regarding the water contained in the dry films (VI.2.1.).

VI.3.2. Gel strength:

Gel strength tests were performed on the Na/Ca alginate/pectin films by holding them vertically, applying stress as a function of time, and by recording the strain. The average error in experimental results was ± 13 %. The plots are displayed in figures VI.3.2.a. and VI.3.2.b.

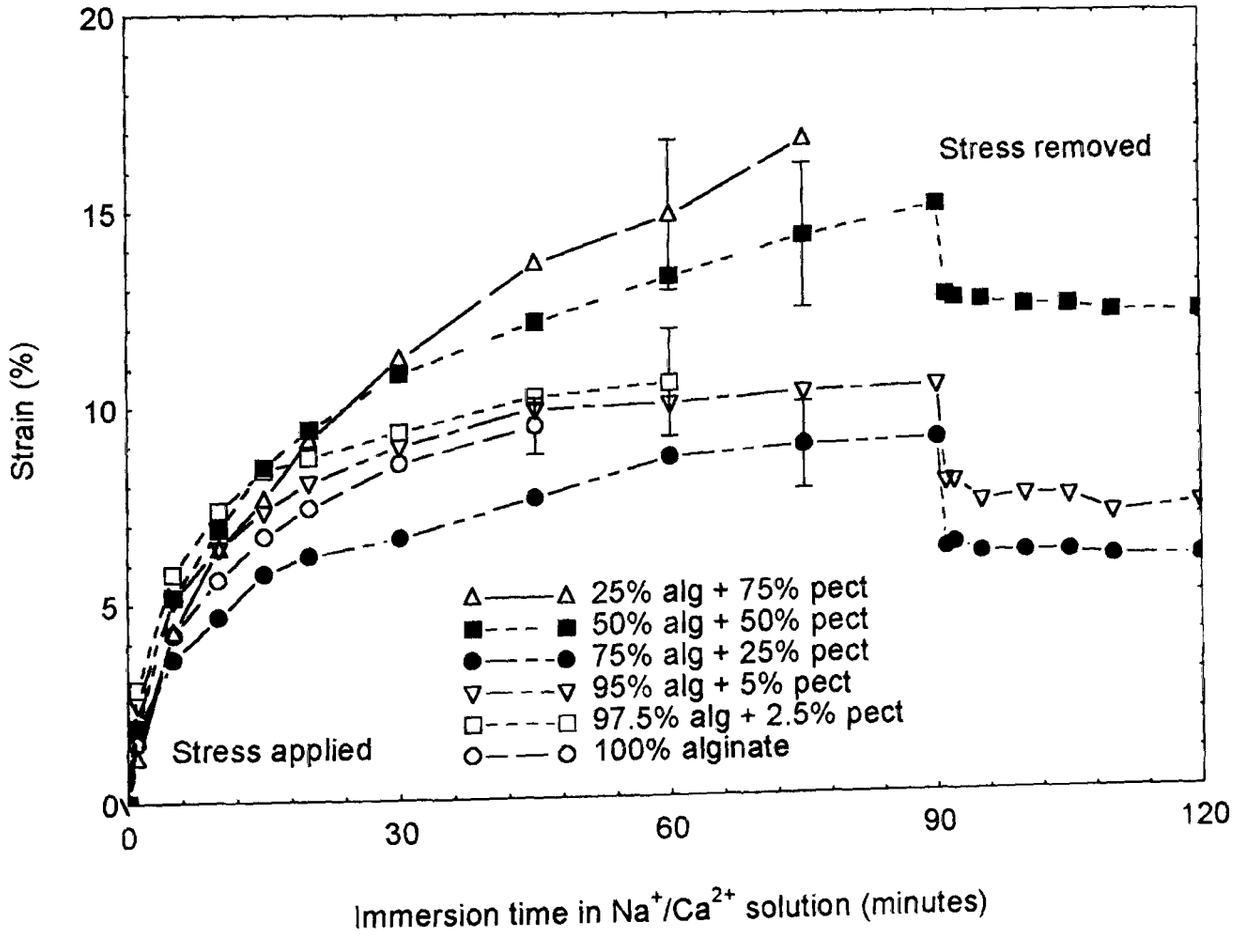

Figure VI.3.2.a. Gel strength of alginate/pectin blends.

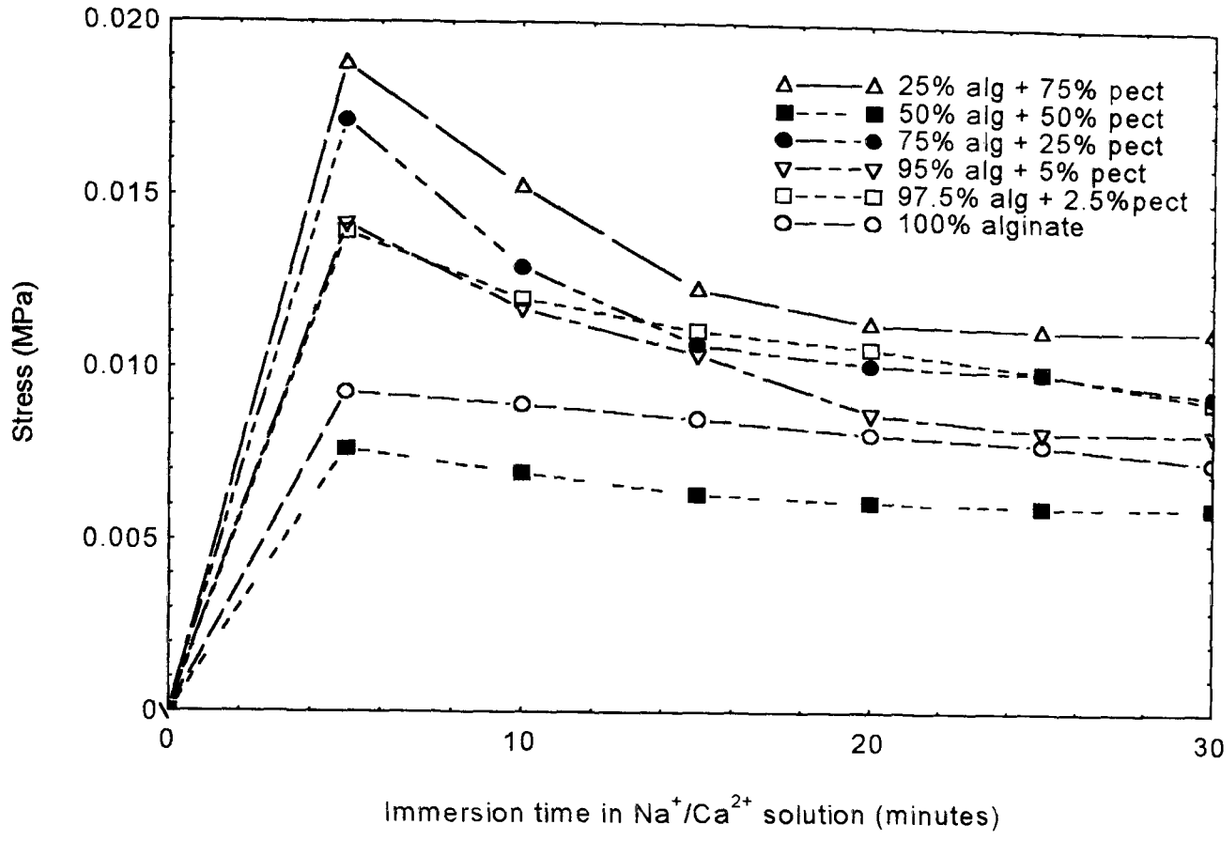

Figure VI.3.2.b. Stress applied to the alginate/pectin blends.

The average error in experimental results is ± 13 %. Three samples did break before the end of the test (100 % alginate, 97.5 % alginate + 2.5 % pectin and 25 % alginate + 75 % pectin). The strongest gels are found for 75 % alginate + 25 % pectin and 95 % alginate + 5 % pectin. According to Toft (1982), the strongest high-G alginate/H.M. pectin blends (without divalent cations) are obtained for the ratio 50/50. Obviously, a totally different behaviour is observed in the presence of Ca^{2+} ions. Likewise, it has been shown previously (VI.1.1) that sodium alginate/pectin could gel for the ratio 25/75 only and the lowest gel strength (i.e. higher strain) is found for this sample. However, Clare (1993) has stated that the presence of calcium adversely affects gelation between alginate and pectin. This observation seems indeed to be verified by our results.

Pectin was initially chosen because it was proposed that additions of this polymer could strengthen alginate gels. From this study, it appears that a content of 2.5 % pectin is not sufficient, while a 5 or 25 % addition is suitable. For these proportions, the pectin molecules are able to prove their strength while the proportion of weak interaction between alginate and pectin is not too high.

VI.4. Summary

The various properties studied in this section, and more particularly the gel ones, revealed that the presence of pectin did not have a mere additive effect on alginate. By contrast, the tests showed rather complex behaviour. This may be explained by some inhomogeneities brought about by sample preparation or in the sample composition. It is also bound to be due to the many factors influencing the gel properties, such as:

-the weak interaction suspected between the two polysaccharides;

-the calcium content in the blends. While overall its addition is beneficial for pure alginate samples, it was found to be rather detrimental to the properties of the alginate/pectin blends;

-the hydrophilic (alginate)/ hydrophobic (pectin) ratio.

CHAPTER VII: ALGINATE/CMC BLENDS

Alginates have been proved to be interesting candidates for wound dressing applications. However, it was brought to light, in chapter V, that improvement of the properties such as the calcium release and the gel strength of alginate dressings were made at the detriment of other properties such as the swelling capacity. It is believed that a small addition of carboxymethylcellulose into the alginate network might solve this problem. CMC has indeed been shown previously to exhibit good swelling ability (Keller, 1984b) with fairly good gel strength (Ichikawa *et al.*, 1994). It is the aim of this chapter to analyse alginate/CMC blends, and to find out whether their overall properties can be improved compared with the pure alginate samples. No work has been reported, in the literature so far, on these blends.

VII.1. Characteristics of the sodium alginate/CMC blends

From the GPC technique, the number average molecular weight of sodium alginate was approximately 2.1×10^5 (polydispersity = 2.0), and that of sodium CMC was 1.9×10^5 (polydispersity = 2.4).

Various amounts of sodium alginate LF 10/60 (high-G) and sodium CMC powders were mixed together in distilled deionised water, by mechanical stirring (using a rod occasionally). The total amount of powder was fixed at 6 wt% in all blends. The solutions so-prepared were analysed for their pH and viscosity. They were then placed into dishes to dry. Sodium alginate/CMC blend films were thus produced and further analysed.

VII.1.1. Characteristics of the sodium alginate/CMC blends as solutions:

i. pH measurements:

pH measurements of different sodium alginate/sodium CMC solutions gave the following results:

Sample	pH
100% alginate LF 10/60	6.4
95% alginate + 5% CMC	6.5
75% alginate + 25% CMC	6.5
50% alginate + 50% CMC	6.6
25% alginate + 75% CMC	6.8
100% CMC	6.9

Table VII.1.1.a. pH values of sodium alginate/sodium CMC solutions.

The resolution of the instrument was 0.01 pH. From Keller (1984b), extreme pH conditions should be avoided with CMC solutions as, in acidic media (below 3), the sodium CMC (soluble) reverts to the free acid form of CMC (insoluble). In basic media (above pH = 10), the CMC gum undergoes viscosity loss. All our data are well outside these two extreme ranges, and therefore the solutions should remain stable. These pH data points are plotted in figure VII.1.1.a., and compared to a straight line connecting the pH values of pure alginate and pure CMC solutions:

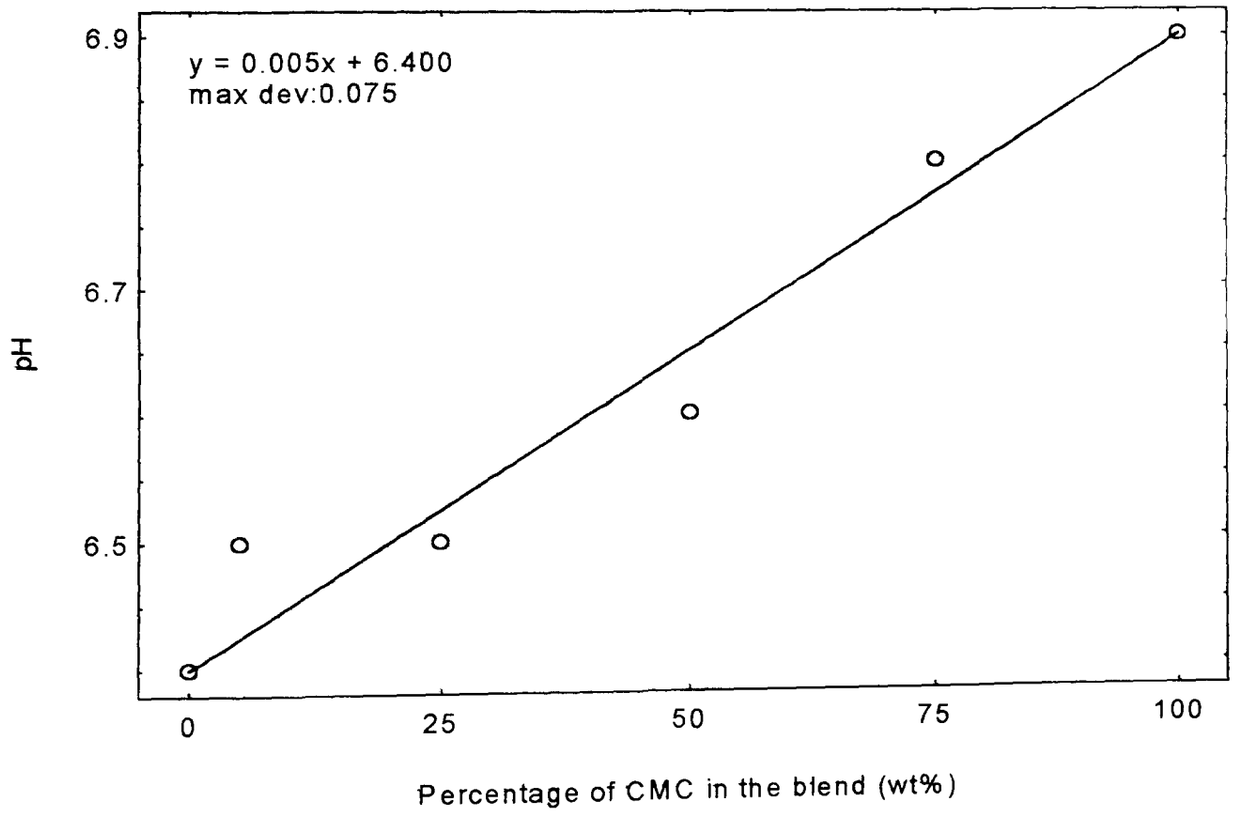

Figure VII.1.1.a. pH as a function of CMC content.

It seems that little interaction occurs between alginate and CMC molecules in the solution state, as the pH data points can be extrapolated with good precision from the straight line connecting the pH values for 100% alginate and 100% CMC. However, the gap between the pH of pure alginate and that of pure CMC is only 0.5, which is not very significant. Therefore, as far as acidity is concerned, all the blends are considered to lie in the same range (unlike the previous alginate/pectin blends studied).

ii. Viscosity:

The viscosity values of the blends in solution, at 5 rpm (a lower speed was used compared with the alginate/pectin blends due to the higher viscosity of the solutions. The corresponding shear rate was equal to 1.4 s^{-1}), were as follows:

Sample	Viscosity (mPa.s)
100% alginate LF 10/60	5,400
97.5% alginate + 2.5% CMC	4,400
95% alginate + 2.5% CMC	6,500
75% alginate + 25% CMC	12,000
50% alginate + 50% CMC	21,400
25% alginate + 75% CMC	44,300
100% CMC	64,500

Table VII.1.1.b. Viscosity values of sodium alginate/CMC solutions.

The precision of the viscosity values is of the order of ± 5 %. From pure alginate to pure CMC, the viscosity increases dramatically, the difference being one order of magnitude. The number average molecular weight of both polymers being comparable, the increase in viscosity may arise from a greater inflexibility of the CMC molecules (compared to the alginate molecules), certainly due to the presence of the bulky carboxymethyl groups. A brief study of the influence of the viscosity on the ion conversion of alginate/CMC blends will be presented in section VII.2.3.

The plot of the viscosity values as a function of the CMC content is depicted below:

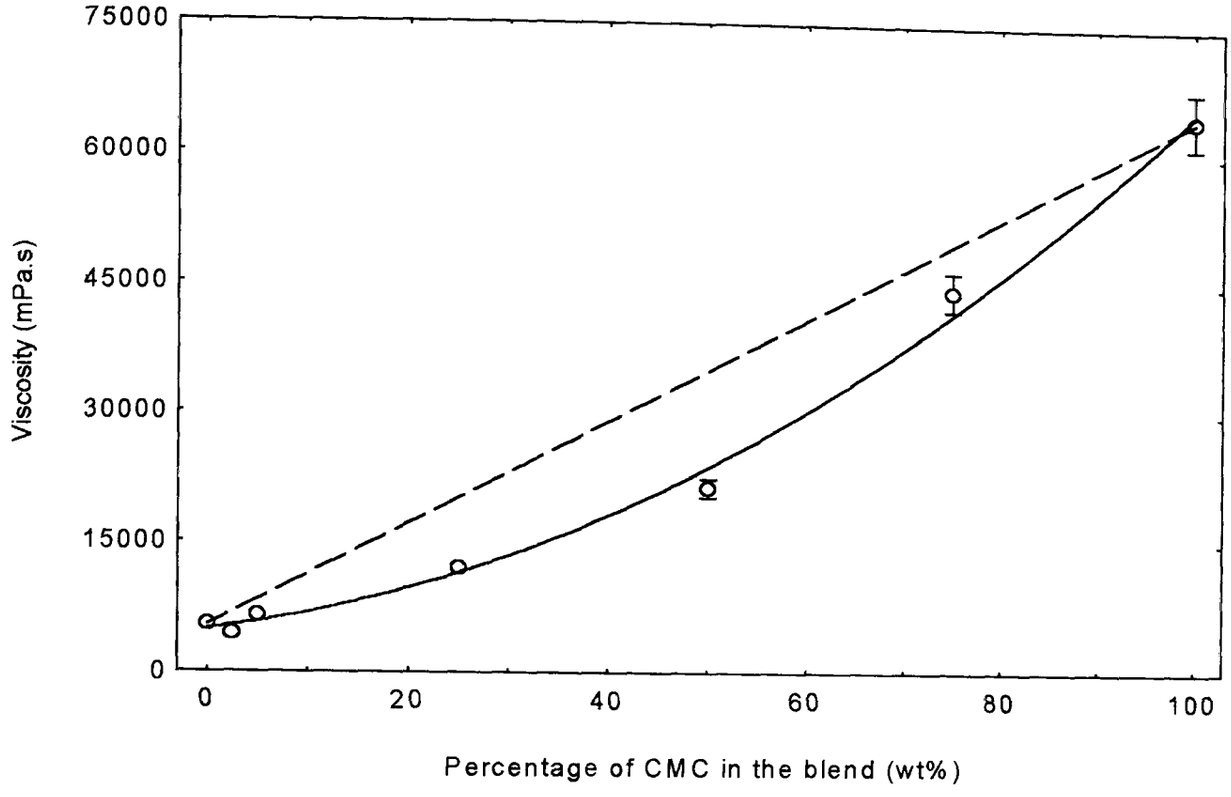

Figure VII.1.1.b. Viscosity as a function of CMC content.

The blends containing between 25 and 75 % of CMC deviate slightly from a straight line, but not to a great extent. Furthermore, the viscosities of these particular blends are found at lower values than the extrapolated line. Therefore the blend between alginate and CMC does not create additional molecular entanglements but gives slightly greater mobility of the chains in the solution.

VII.1.2. Characteristics of the sodium alginate/CMC blends as films:

i. Crystallinity:

The study of the degree of ordering of the alginate/CMC blends is important as this factor relates to the packing efficiency. An ordered structure will arise from strong hydrogen bonding (i.e. closer packing), whereas an amorphous structure will be more open (Tasker *et al.*, 1994). This aspect can then help to understand other properties such as mechanical deformation and water uptake.

Figure VII.1.2.a. shows the diffraction spectra of some sodium alginate/CMC blends:

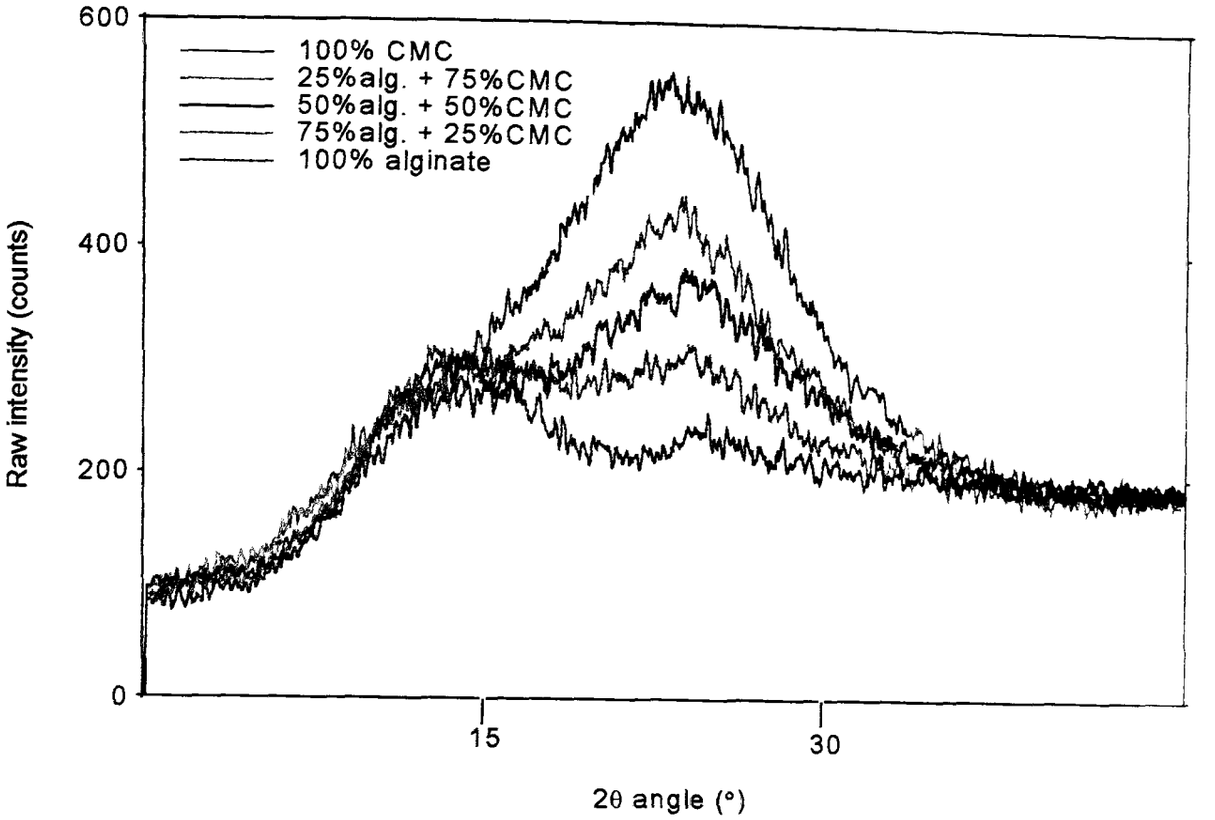

Figure VII.1.2.a. X-ray diffraction spectra of sodium alginate/sodium CMC blends.

All blends give patterns with broad peaks, typical of a disordered structure. The following table gives the positions of the centres of the main peaks for the sodium blends:

Sample	2Θ (degrees)
100% alginate LF 10/60	14 (21)
75% alginate + 25% CMC	14 / 21
50% alginate + 50% CMC	(14) 21
25% alginate + 75% CMC	(14) 21
100% CMC	(13) 21

Table VII.1.2. X-ray diffraction peaks of sodium alginate/sodium CMC blends.

The values in brackets represent smaller peaks. Tasker *et al.* (1994) performed X-ray diffraction on powdered cellulose (type I) and found peaks or shoulders with varying intensities at the following 2Θ angles: 23°(002), 21°(021), 17°(10 $\bar{1}$) and 15°(101).

However, the introduction of carboxymethyl groups to the cellulose is expected to lead to a different structure. In the present work, only broad peaks are observed for the pure CMC and, therefore, this carboxymethylcellulose offers a low degree of ordering.

ii. Morphology:

Some of the sodium blend flat surfaces are shown in figure VII.1.2.b. They present a high degree of roughness, presumably due to the high viscosity of the solutions used. All the circular encrustations are thought to be due to bubbles, brought about during the mixing process, and which have escaped the bulk very slowly. Thus, they have not been completely incorporated by the surface. Alternatively, this could be characteristic of a two phase morphology, with the circular particles characteristic of the CMC.

The images of the fractures of the sodium films are displayed in figure VII.1.2.c. They present relatively uneven surfaces. The 50% alginate/50% CMC blend exhibits the roughest surface, while the pure polysaccharides (100% alginate and 100% CMC) have a more regular surface. A fine, granular phase is observed in the background, for alginate-rich samples (100 down to 50 %). Some signs of ductility appear for the samples containing 25 and 50 % CMC. Finally, there are no apparently clear signs of phase separation between the two polysaccharides.

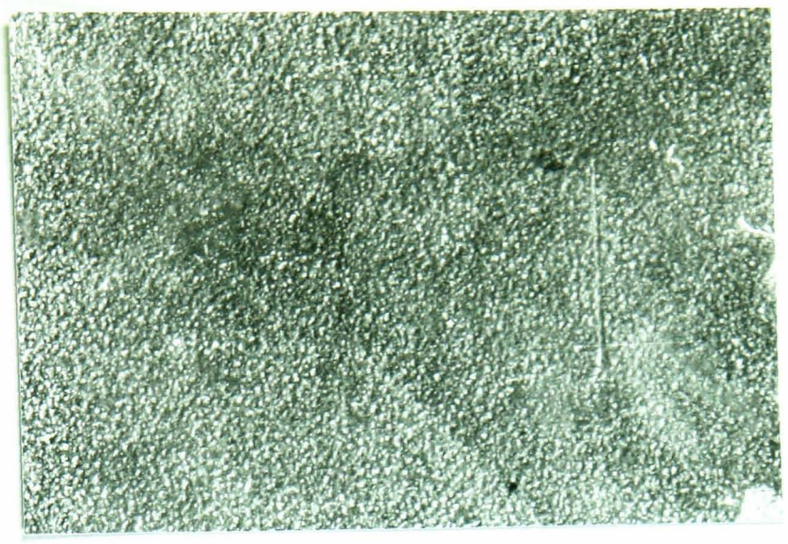

75 % sodium alginate/25 % sodium CMC

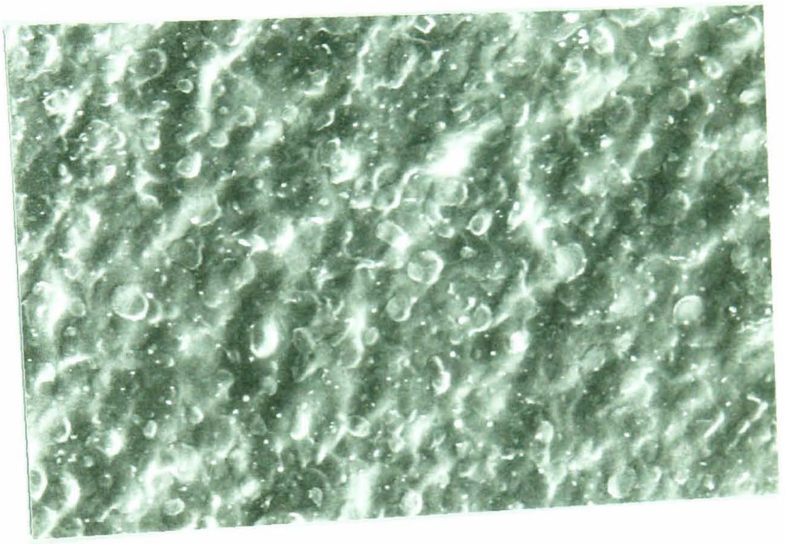

10 μm

50 % sodium alginate/50 % sodium CMC

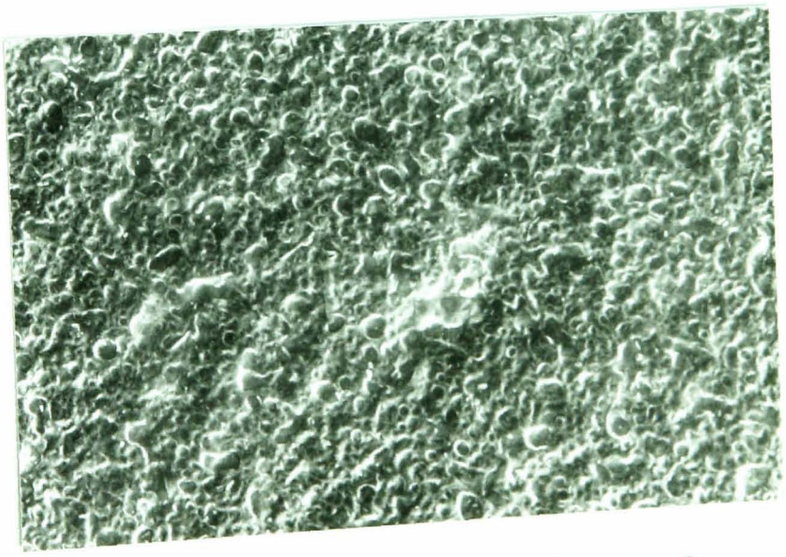

25 % sodium alginate/75 % sodium CMC

Figure VII.1.2.b. Flat surfaces of sodium alginate/CMC blends.

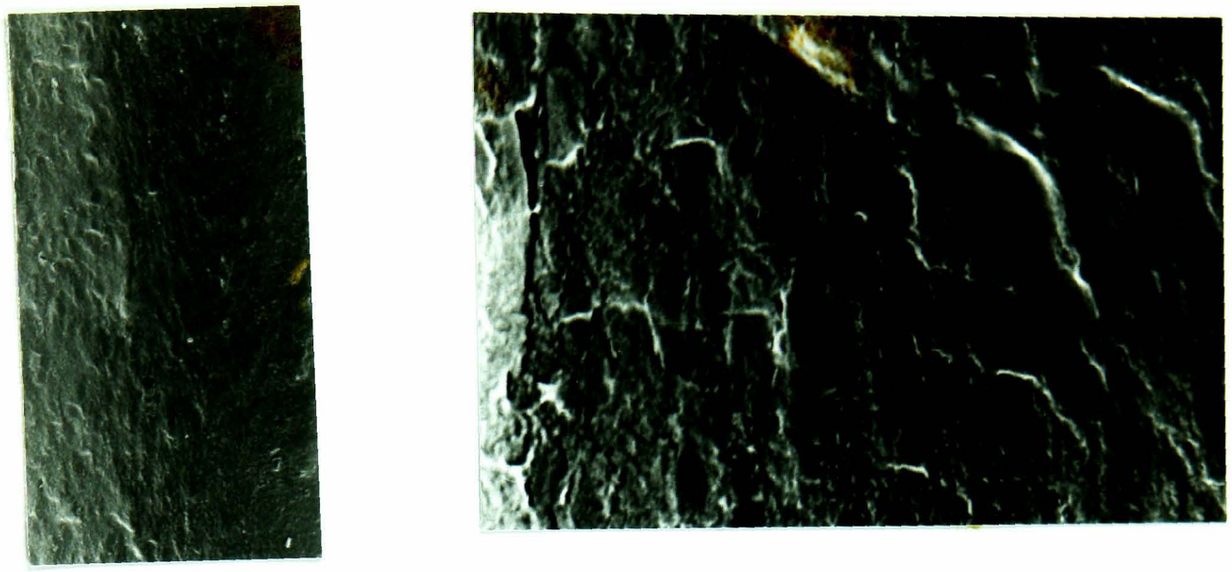

100 % sodium alginate LF 10/60

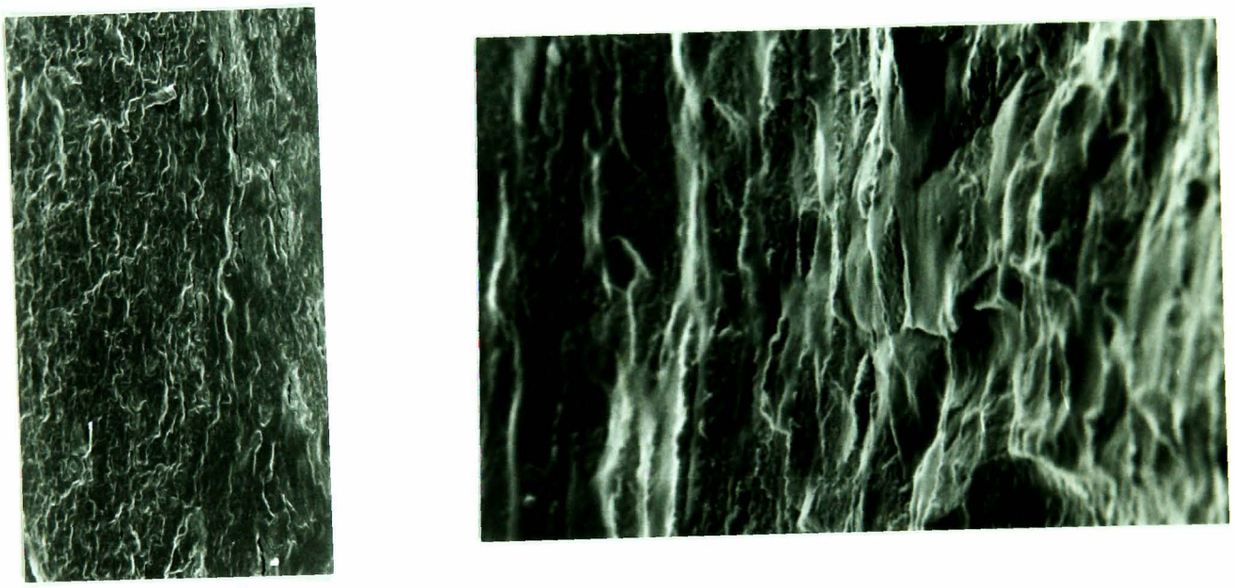

75 % sodium alginate/25 % sodium CMC

10 µm

10 µm

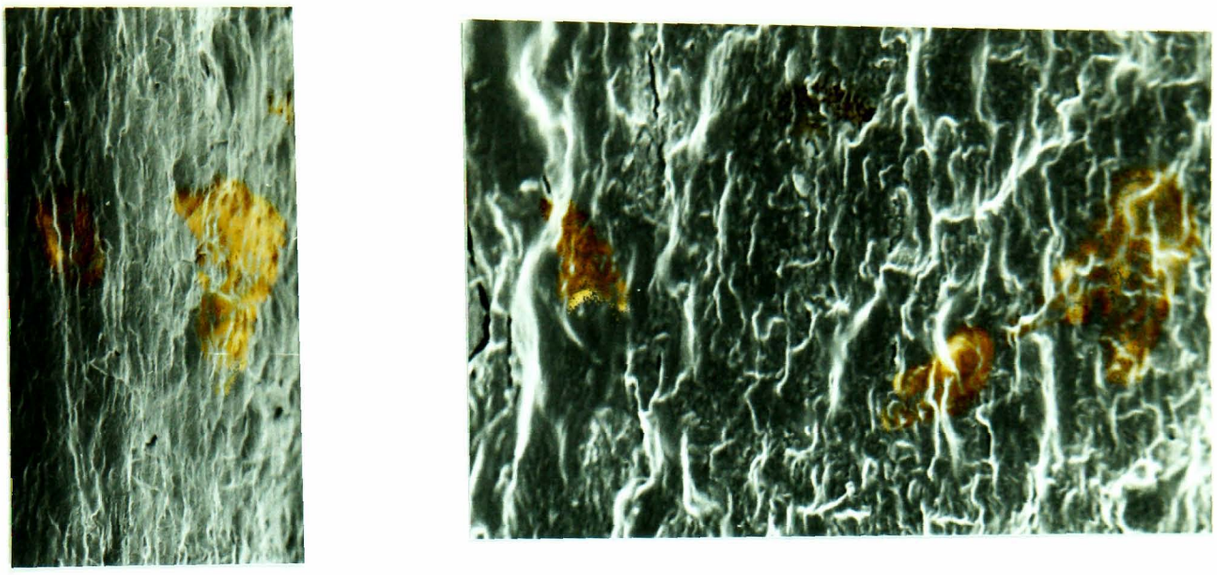

50 % sodium alginate/50 % sodium CMC

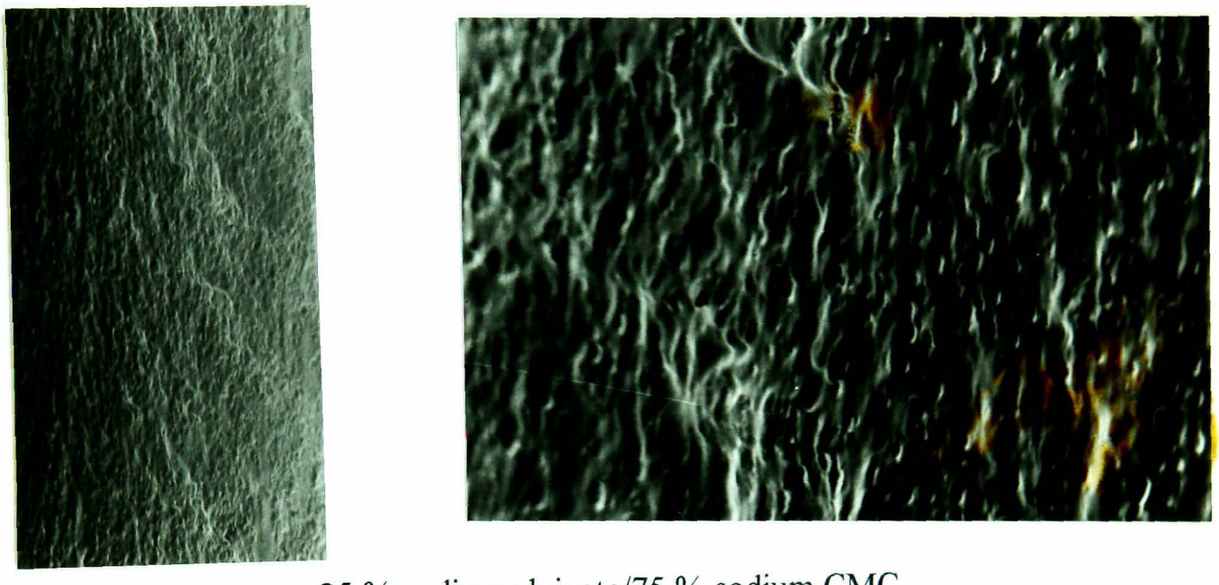

25 % sodium alginate/75 % sodium CMC

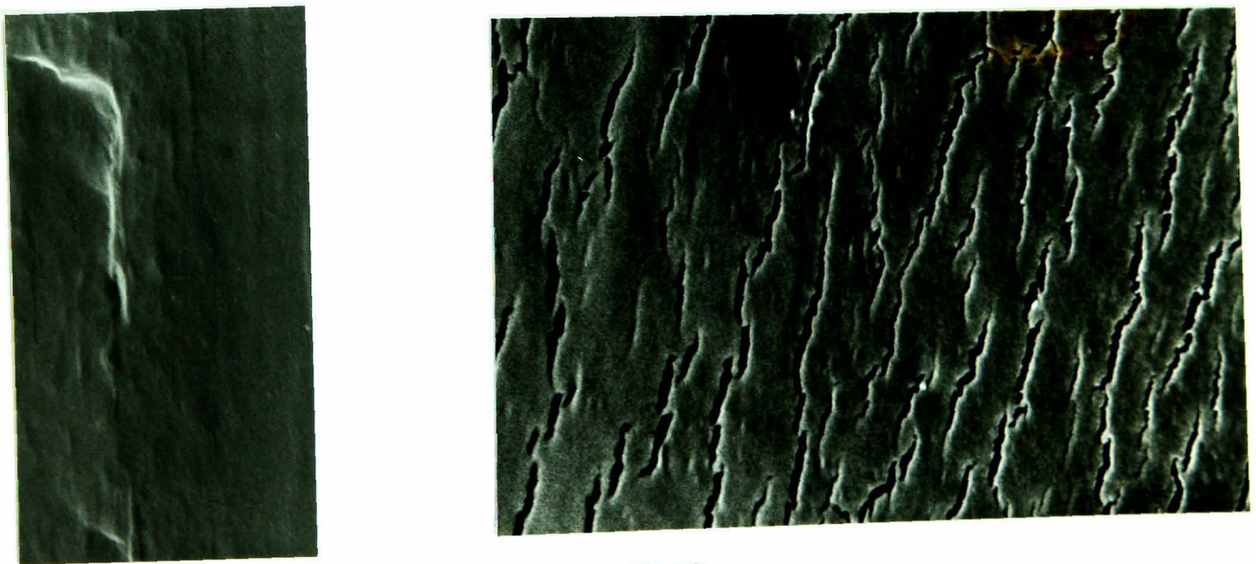

100 % sodium CMC

10 μm

10 μm

Figure VII.1.2.c. Fracture surfaces of sodium alginate/sodium CMC films.

VII.1.3. Infrared analysis of the sodium alginate/CMC blends:

Thin films were prepared from 1 wt% powder (sodium alginate + sodium CMC) and scanned by FTIR transmission spectroscopy. This analysis was performed in order to obtain information on the interaction, at a molecular level, between the polysaccharides.

i. FTIR assignment of CMC:

A typical sodium CMC FTIR spectrum is presented in figure VII.1.3.a. and the fingerprint region follows with figure VII.1.3.b.:

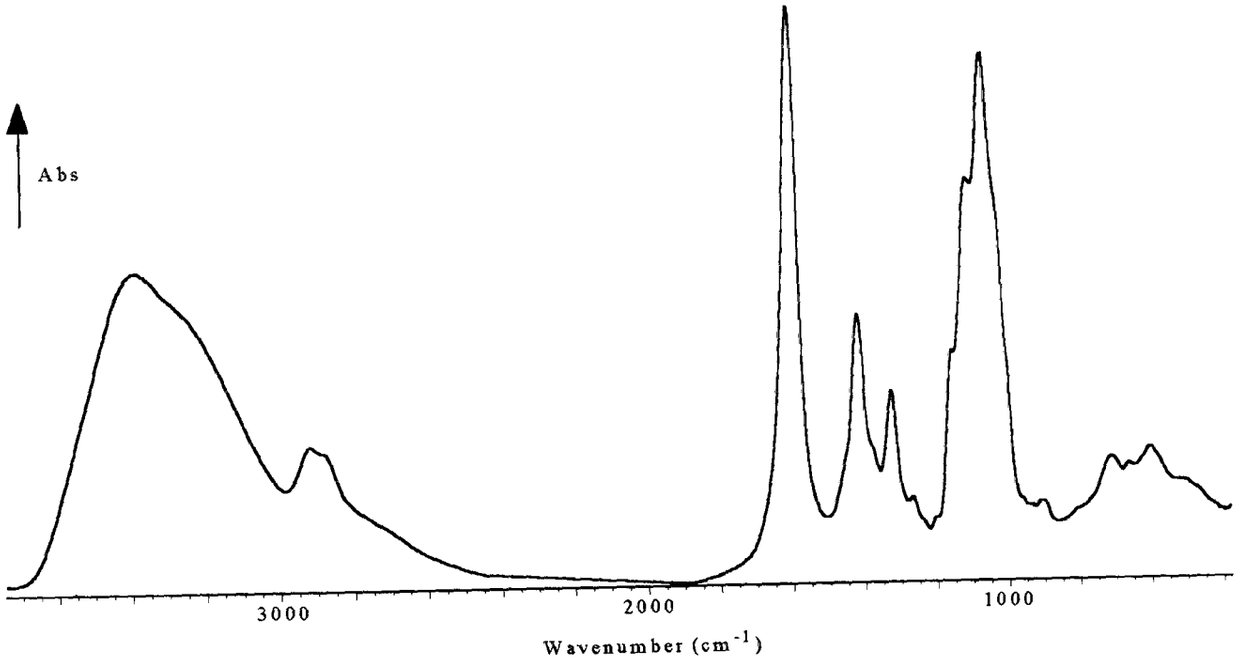

Figure VII.1.3.a. FTIR spectrum of sodium CMC.

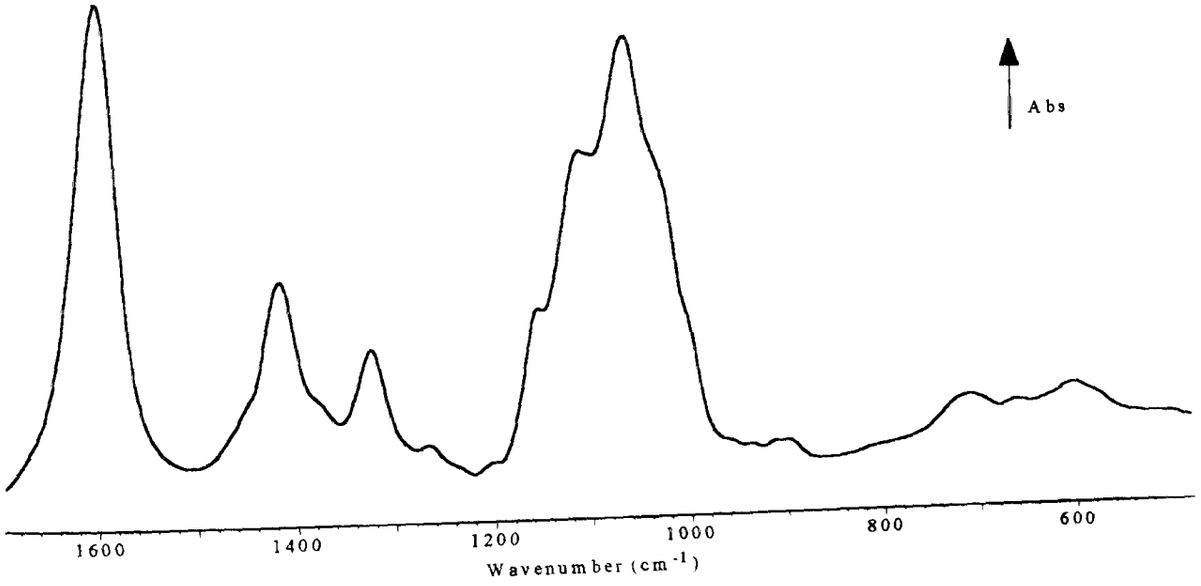

Figure VII.1.3.b. FTIR fingerprint region of sodium CMC.

Although not immediately obvious, there are observable differences between the spectrum of the alginate (figure IV.1.1.a) and that of the CMC, with the appearance of some small peaks, changes in band intensity and shifts in wavenumbers. Assignments of the FTIR spectrum for CMC are presented in table VII.1.3. This was assisted by previous assignments for cellulose materials (Brandrup & Immergut, 1975; Socrates, 1994; Tasker *et al.*, 1994).

Wavenumber (cm^{-1})	Intensity - Shape	Assignment
3380	strong - broad	O-H stretching
3250	strong - shoulder	O-H stretching
2920	medium - broad	C-H stretching
2880	medium - shoulder	C-H stretching
1600	very strong - sharp	COO^- stretching asym.
1450	weak - shoulder	CH_2 deformation
1417	medium - sharp	COO^- stretching sym.
1380	weak - shoulder	C-H in-plane deformation
1325	medium - sharp	O-H in-plane deformation
1265	weak - sharp	?
1205	weak - shoulder	O-H in-plane deformation
1155	medium - shoulder	?
1110	strong - sharp	CO (ether) & CC stretching
1065	very strong - sharp	O-H in-plane deformation
1025	strong - shoulder	CO stretching
1000	medium - shoulder	CO & CC stretching
900	weak - broad	C-H out-of-plane deformation
710	weak - broad	O-H out-of-plane deformation
605	weak - broad	?
500	weak - broad	C-O deformation

Table VII.1.3. Band assignment of CMC spectrum.

ii. Interaction between alginate and CMC:

To study the interaction between alginate and CMC, the spectrum of the 50% sodium alginate + 50% sodium CMC blend was compared with the summation of the spectra from pure alginate plus pure CMC (figure VII.1.3.c.):

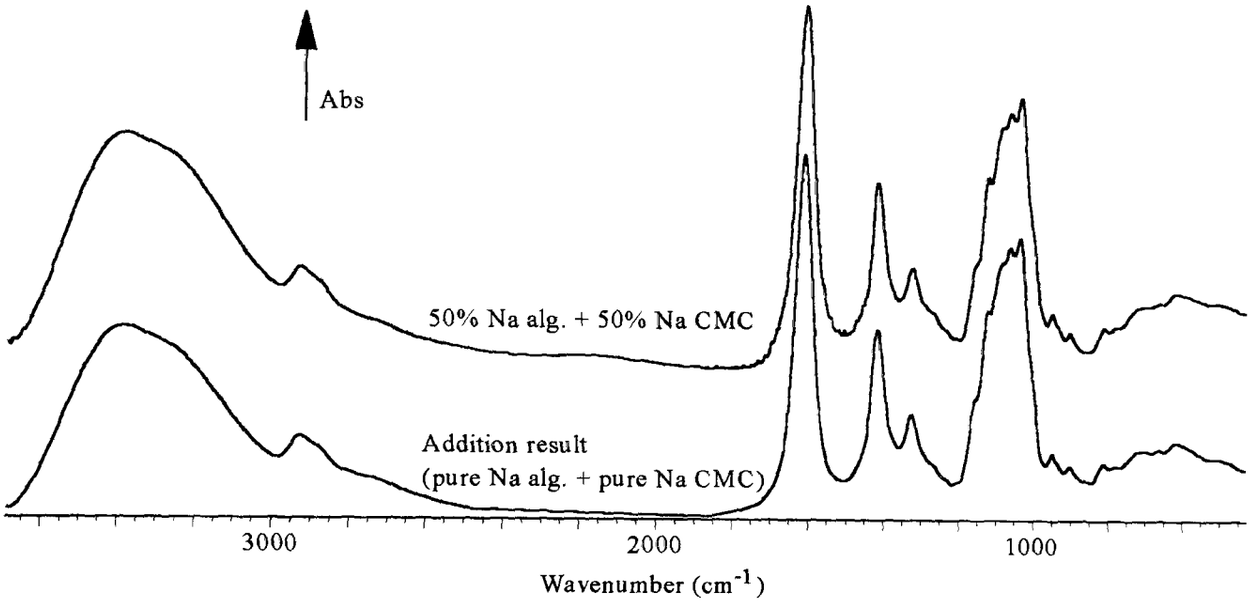

Figure VII.1.3.c. Addition FTIR spectrum of sodium alginate + sodium CMC.

Both infrared spectra are very similar and, therefore, addition of carboxymethylcellulose into an alginate sample does not produce significant changes in the molecular binding. Sodium alginate and CMC act as independent entities when prepared as a blend. From this comparison of spectra, there is no evidence of intermolecular binding between the two polysaccharides, otherwise shifts and changes in shape would be observed, specially for the main O-H stretching peak (3400 cm^{-1}), which is very sensitive to intermolecular binding. Ichikawa *et al.* (1994) performed a similar type of analysis on a different blend: poly(ε-Lysine)/CMC film. They did not note any substantial decrease in the bands from the CMC, upon blending with PEL. However, they noticed a band shift from 1639 cm^{-1} (characteristic of an amino group) to 1670 cm^{-1} for blends with 30 to 50% of PEL. This led them to the conclusion that strong ionic binding occurred between the two oppositely-charged compounds. No such shift can be observed between sodium alginate and sodium CMC in our study.

VII.2. Conversion of sodium alginate/CMC into mixed sodium/calcium blends

The next step in sample preparation consisted of immersing the sodium alginate/CMC solution into a $CaCl_2$ bath, in order to convert some Na^+ ions into Ca^{2+} ions. Mixed sodium/calcium salts were thus prepared, and dried prior to analysis. The average immersion time in the calcium chloride solution was 30 minutes for all the blends.

VII.2.1. Water content:

Thermogravimetric analysis performed on the 6 wt% sodium/calcium blends showed that the average water content was around 15 wt% (± 2 %) for all samples. No distinction could be made between free and bound water. The temperatures at the inflection point for the blends (immersed for 30 minutes in $CaCl_2$ solution) are reported below:

Samples	Temperature (K)
100% alginate LF 10/60	473
75% alginate + 25% CMC	478
50% alginate + 50% CMC	483
25% alginate + 75% CMC	498
100% CMC	518

Table VII.2.1. Temperature of TGA inflection point for alginate/CMC blends.

As the decomposition temperature clearly increases with the carboxymethylcellulose content, one can assume that water molecules are more tightly bound within the CMC molecules. The blends containing a higher percentage of CMC will thus be more resistant to exposure to higher temperatures.

VII.2.2. Crystallinity:

The diffraction patterns of the different blends immersed for 30 minutes in $CaCl_2$ solution were similar to the patterns obtained for the sodium blends (figure VII.1.2.a). Both Na/Ca CMC and Na/Ca alginate present X-ray diffraction patterns typical of fairly disordered samples. The 2θ angle values of the major broad peaks are also similar to

those found for the sodium alginate/CMC blends. Therefore the introduction of calcium ions into the mixed polysaccharide network does not seem to generate any additional ordering as measured by XRD.

VII.2.3. Influence of the solution viscosity on the ion conversion:

It was shown, in chapter III, that the viscosity of an alginate solution had little influence on the subsequent sodium/calcium exchange during sample preparation. By contrast, the film thickness (in the final product) was found to be proportional to the Na^+ content and to the Ca^{2+} contents. The following study is aimed at checking whether alginate/CMC blends exhibit a similar behaviour to that of the pure alginate.

Solutions with a similar alginate/CMC ratio (75/25) were prepared, with various percentages of powder in the water (4, 6 and 8 wt%), leading to different viscosities. The amount of solution required for each polysaccharide percentage was taken so as to lead afterwards to similar thickness between the three samples. This gave the same number of ion sites for Ca^{2+} (i.e. the same quantity of powder but different volumes of solution). The dishes containing the sodium alginate/CMC solutions were then immersed for 30 minutes in $CaCl_2$ for partial ion conversion. The films obtained after drying exhibited thicknesses around 90 μm. They were analysed by atomic absorption spectroscopy for their Na^+ and Ca^{2+} percentages:

Sample	Viscosity (mPa.s)	Na wt%	Ca wt%
4% (75% alginate + 25% CMC)	2,100	6.0	3.5
6% (75% alginate + 25% CMC)	12,000	6.1	3.7
8% (75% alginate + 25% CMC)	26,900	5.1	4.2

Table VII.2.3. Influence of the viscosity on sodium and calcium content.

While the viscosity varied by a factor greater than ten, sodium and calcium contents do not vary to the same extent, and again, it can be assumed that viscosity is not a dominant factor in the study of the ion conversion for this particular blend. The other alginate/CMC blends are expected to follow the same behaviour.

For the following experiments, all films were prepared using the same content of powder and the same volume of solution, but with varying viscosities (table VII.1.1.b). The film thickness in the dry state was also kept approximately constant (around 90 μm).

VII.2.4. Determination of the ion content:

All the sodium blends were immersed for a fixed time in calcium chloride solution, i.e. 30 minutes. The results obtained by AAS are presented in table VII.2.4, together with the atomic percentages (see annexe 3 for the calculations) and the charge equivalence (equal to Na^+ at% + 2×Ca^{2+} at%).

Sample	Na wt%	Ca wt%	Na at%	Ca at%	Charge eq.
100% alginate LF 10/60	4.9	4.3	2.1	1.1	4.3
97.5% alginate + 2.5% CMC	5.4	4.2	2.3	1.0	4.3
95% alginate + 5% CMC	5.4	3.8	2.3	0.9	4.1
75% alginate + 25% CMC	5.1	3.5	2.1	0.8	3.7
50% alginate + 50% CMC	5.0	3.5	2.0	0.8	3.6
25% alginate + 75% CMC	4.0	3.6	1.6	0.8	3.2
100% CMC	4.0	3.2	1.5	0.7	2.9

Table VII.2.4. Ion percentages of alginate/CMC blends.

The film thickness was 90 μm (± 5 %), and the standard error in ion content is ± 2-3 %. The starting materials have a sodium content of 11.4 wt% for sodium alginate and 7.8 wt% for sodium CMC. Under the experimental conditions, both alginate and CMC exchange their sodium for calcium ions in contact with the $CaCl_2$ solution. After 30 minutes of immersion, the sodium weight percentage drops by 57 wt % for the pure alginate and by 49 % for the pure CMC. The calcium wt% counts for 35 % of the initial sodium content of the alginate (11.4 wt%) and for 41 % of that of CMC (out of 7.8 wt%). There is an unexpected initial increase in the sodium content as CMC is introduced in alginate which is not explained so far.

Figure VII.2.4. represents the charge equivalence (y) as a function of the number of atoms per site (x), for the different blends (see appendix 3 for these values). The equation of the plain curve is $y = (4.3 \times 21.71) / x$, where 21.71 and 4.3 are the x and y values for the pure alginate sample.

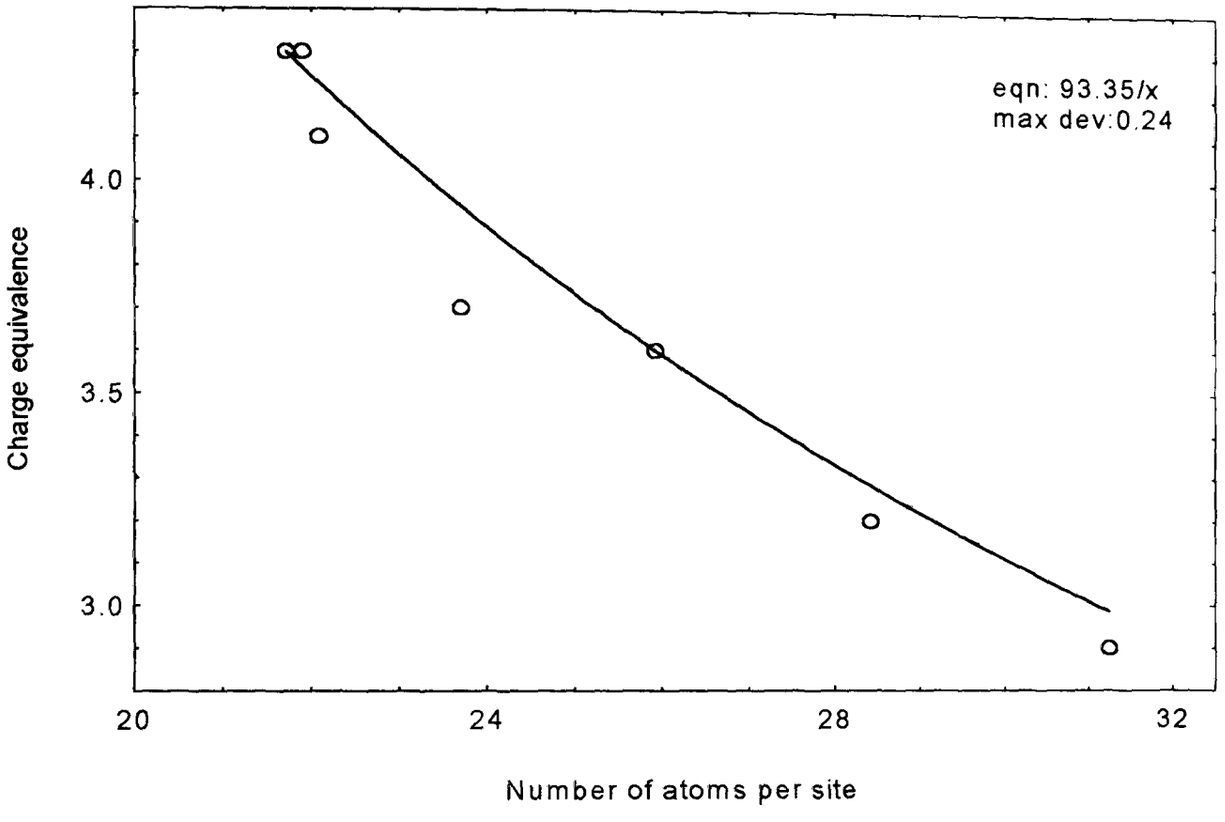

Figure VII.2.4. Charge equivalence as a function of the number of atoms per sites.

As the experimental points follow closely the theoretical curve (within ± 6 %), it follows that the calcium rate of filling in the CMC is similar to that of the alginate. Therefore the gelation process occurs independently of the various proportions of each polysaccharide present.

VII.2.5. Morphology of the blend films:

i-Flat surfaces:

SEM pictures of the surface of the films in the sodium/calcium blends are presented in figure VII.2.5.a. The surface roughness is not as pronounced for the mixed salts as for the sodium salts. This would suggest that one effect of gelation of alginate/CMC samples is to smooth the surface texture. Some impurities are found, attached to the surface. These defects are expected to affect such properties as wicking rate, but have little influence on swelling or gel strength as these are more properties of the bulk. Some features are apparent on the pure alginate film; surprisingly, these were not seen in the alginate/pectin study.

Prasad & Kalyanasundaran (1995) studied the surface morphology of different CMC salts by SEM. They observed a crystalline structure for Na-CMC, while Cu- and Fe-CMC both gave an amorphous and porous surface texture.

ii- Fracture surfaces:

For the blends immersed for 30 minutes in $CaCl_2$ solution, overall, the fracture surfaces have a more clean-cut appearance than the sodium samples, reflecting a more brittle type of behaviour (figure VII.2.5.b.). Therefore the calcium ions are expected to hold the polysaccharide chains closer together. There are no apparent signs of incompatibility in the various blends.

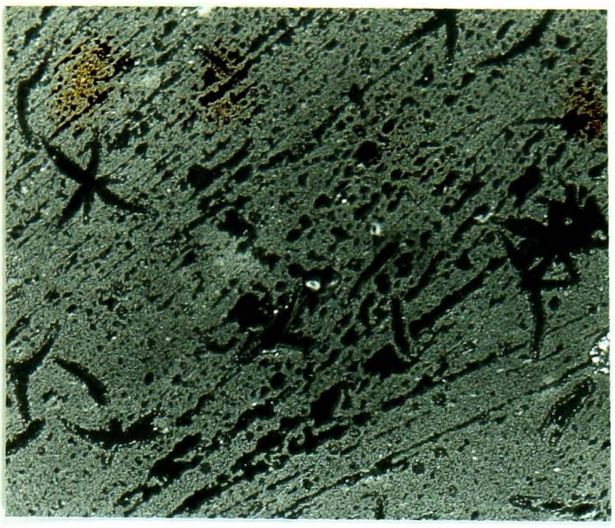

100% Na/Ca alginate

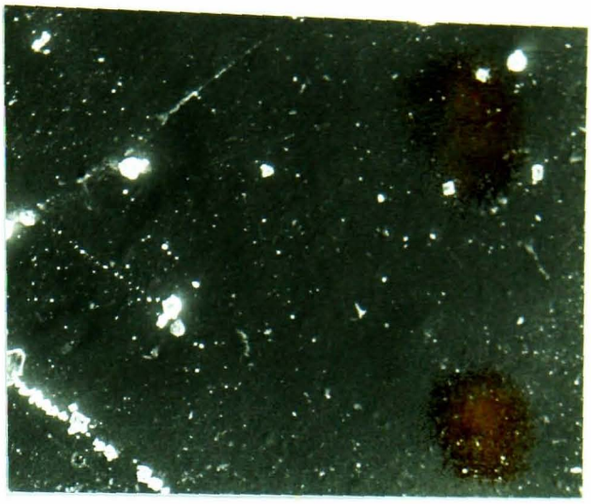

75% alginate + 25% CMC (Na/Ca)

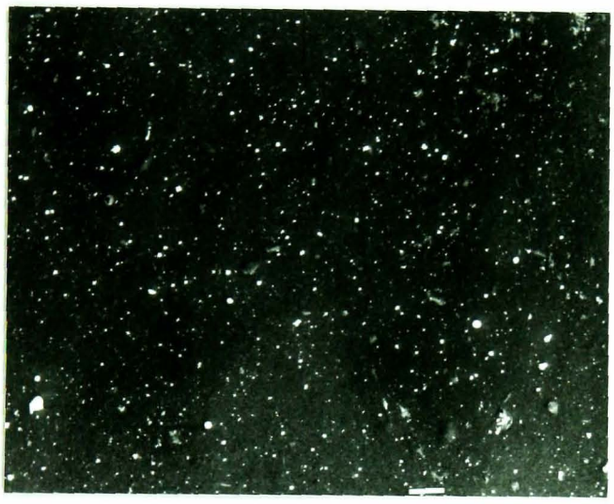

50% alginate + 50% CMC (Na/Ca)

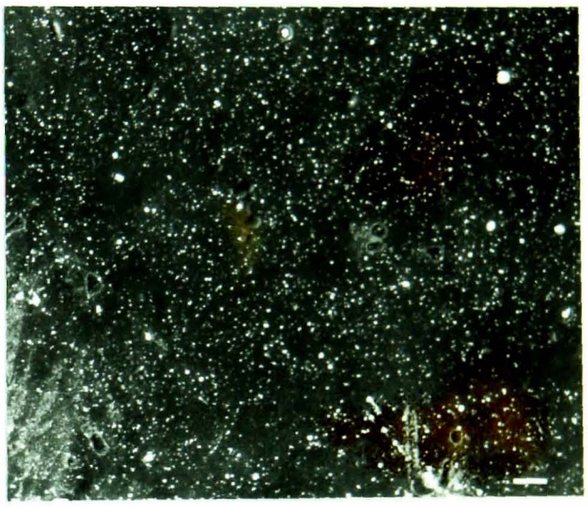

25% alginate + 75% CMC (Na/Ca)

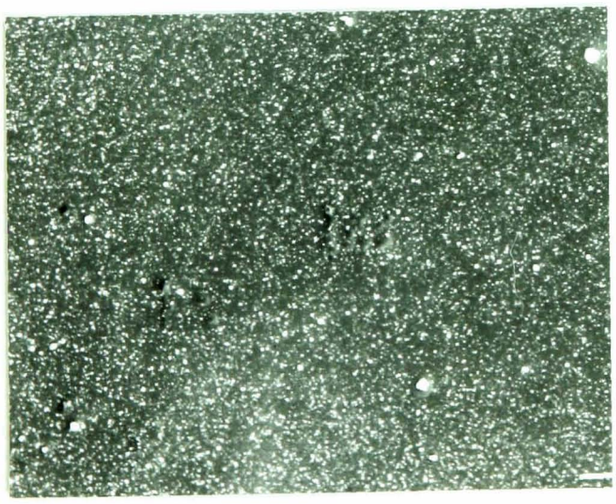

100% Na/Ca CMC

10 μm

Figure VII.2.5.a. SEM pictures of the surfaces of Na/Ca alginate/CMC blends.

100% Na/Ca alginate

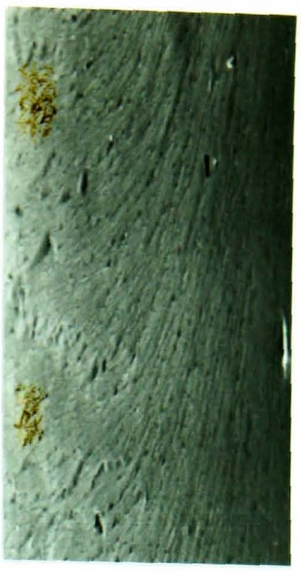

95% Na/Ca alginate + 5% Na/Ca CMC

75% Na/Ca alginate + 25% Na/Ca CMC

50% Na/Ca alginate + 50% Na/Ca CMC

25% Na/Ca alginate + 75% N/Ca CMC

100% Na/Ca CMC

10 μm

Figure VII.2.5.b. SEM pictures of fracture surfaces of Na/Ca alginate/CMC films.

VII.2.6. Mechanical tensile tests:

These experiments were performed on dry samples and the results averaged from five tests. The Young's modulus, fracture stress and fracture strain are presented in table VII.2.6:

Sample	Young's modulus (GPa)	Fracture stress (MPa)	Fracture strain (%)
Na/Ca (100% alginate)	3.0 ± 0.5	110 ± 10	9.4 ± 1.7
Na/Ca (97.5% alginate+2.5% CMC)	3.3 ± 0.3	123 ± 4	9.0 ± 0.7
Na/Ca (95% alginate+5% CMC)	2.5 ± 0.3	100 ± 9	10.4 ± 2.1
Na/Ca (75% alginate+25% CMC)	2.1 ± 0.3	99 ± 7	16.5 ± 1.4
Na/Ca (50% alginate+50% CMC)	2.3 ± 0.2	96 ± 6	16.0 ± 2.6
Na/Ca (25% alginate+75% CMC)	2.7 ± 0.2	102 ± 6	9.9 ± 2.1
Na/Ca (100% CMC)	3.6 ± 0.8	86 ± 9	5.3 ± 0.9

Table VII.2.6. Mechanical properties of dry films of alginate/CMC blends.

The sodium alginate samples (Modulus = 4.5 ± 0.2 GPa; Stress = 113 ± 9 MPa; Strain = 11.2 ± 1.6 %) have a higher Young's modulus than the sodium/calcium alginate films. Therefore, the introduction of calcium ions, although they have previously been found to create intermolecular bonding, may also create some defects in the alginate matrix (leading to poorer mechanical properties).

As for the CMC samples (for sodium CMC: Modulus = 3.3 ± 0.4 GPa; Fracture stress = 85 ± 9 MPa; Fracture strain = 6.9 ± 1.8 %), the mechanical properties of both the sodium and the mixed salt samples are similar. Therefore the calcium ions are possibly bound to the carboxymethylcellulose chains in a similar way to the sodium ions. Alternatively, the calcium ions may infiltrate the CMC matrix and fill voids, without creating strong intermolecular binding. The high viscosity solution used for the 100 % CMC samples leads to films having a rough surface; this may create defects which might account for the early fracture of these samples.

For the mixed salts, after 30 minutes immersion in $CaCl_2$, most blends (except the 97.5% alginate + 2.5% CMC samples) exhibit lower moduli than the pure materials. Further there is a more complex behaviour of the fracture stress. However, the general trend is a decrease in stress from the alginate to the carboxymethylcellulose. Regarding the fracture strain, most blends have higher values than the pure materials. The highest strain values are obtained for the 25 and 50 % CMC films (the same blends, in the sodium salt form, showed evidence of ductility under SEM).

In conclusion, it appears that the blends offer lower toughness and more flexibility than do the pure alginate or the pure CMC compound. Therefore, by blending alginate with CMC, the polymeric molecules acquire more freedom of movement (this would explain why the viscosity values were lower than expected; figure VII.1.1.b.) or greater free volume between them. From these results, it is also clear that these polysaccharides do not form homogeneous blends (specially the samples containing 25 and 50 % CMC).

VII.2.7. FTIR analysis:

The effect of the introduction of calcium ions into the alginate/carboxymethylcellulose network was analysed using FTIR spectroscopy. To begin with, the effect on the CMC alone is shown in figure VII.2.7.a. The spectra of the 50/50 blend then follow (figureVII.2.7.b) in both the sodium and the calcium salt form (obtained after 300 minutes immersion in $CaCl_2$ solution).

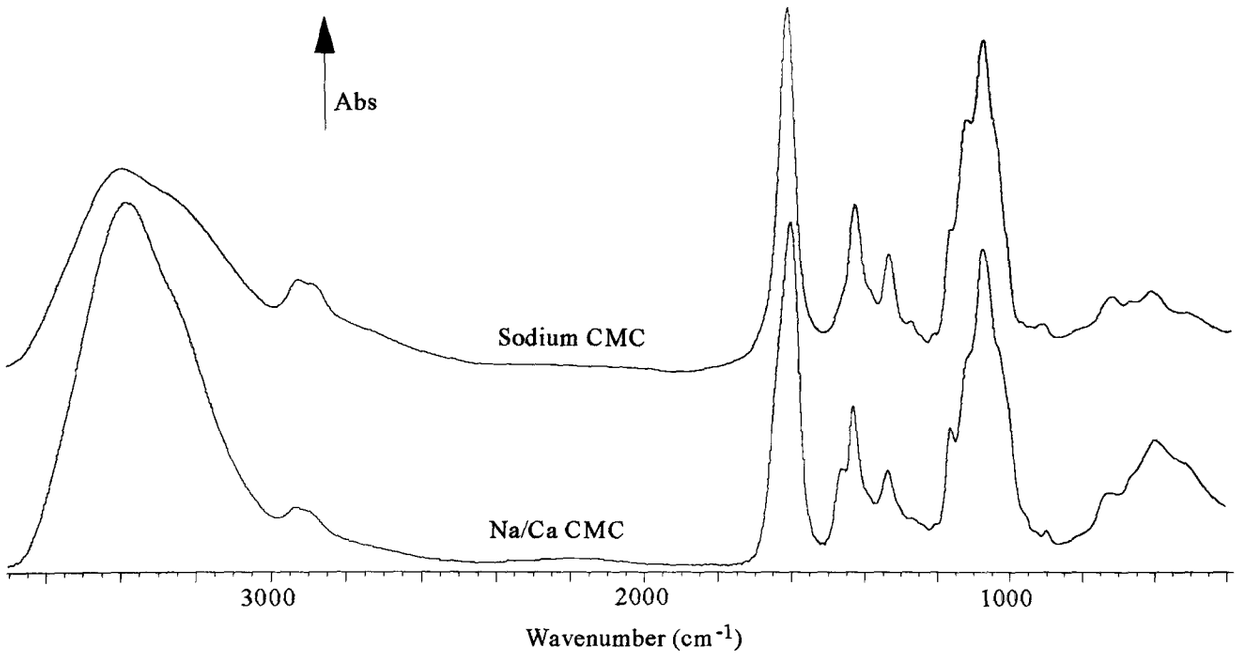

Figure VII.2.7.a. FTIR spectra of pure CMC, as sodium and as sodium/calcium salt.

Films scanned by infrared spectroscopy are typically prepared from 1 wt% solution. However, no gelation occurred for the CMC sample at that concentration, and a 3 wt% solution was used instead.

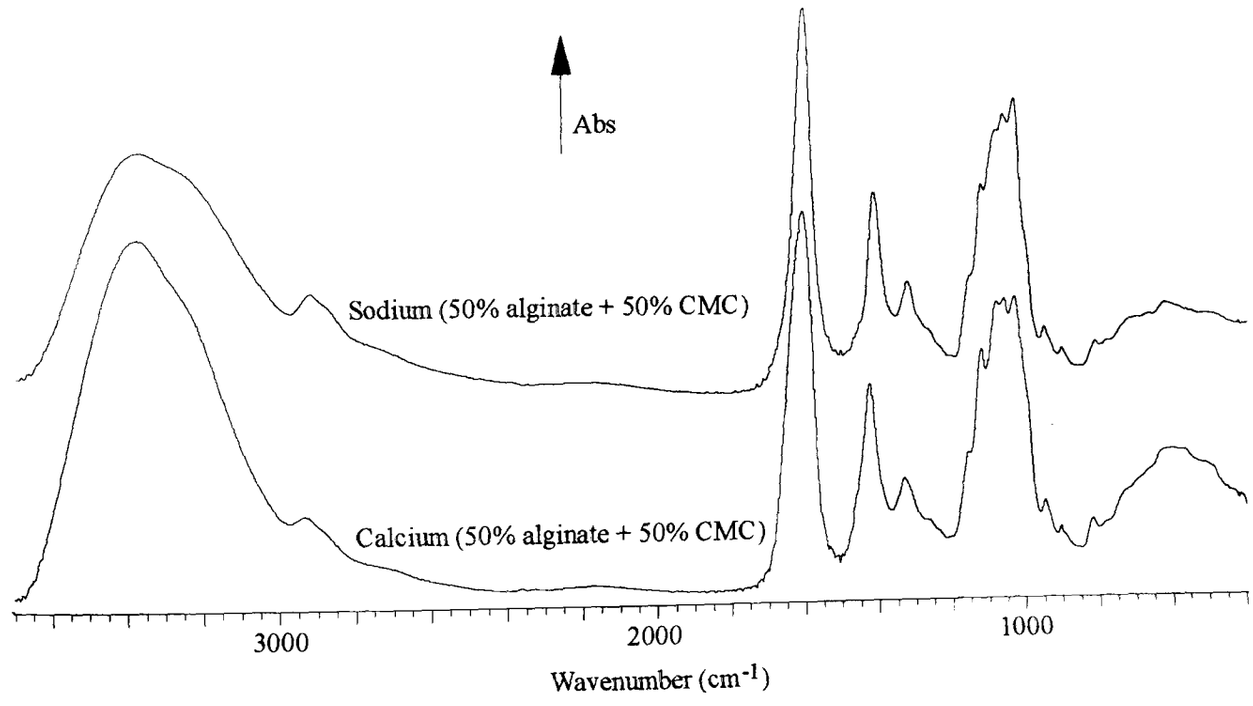

Figure VII.2.7.b. FTIR spectra of 50% alginate + 50% CMC, as sodium and as calcium salt.

Similar trends between the pure CMC and the 50/50 blend are observed. As in the case of the pure alginate samples (chapter IV), important changes between the two salts appear in the O-H (≈ 3380 cm^{-1}) and the COO^- (≈1600 and 1420 cm^{-1}) stretching bands. Other changes are noticeable for the set of peaks around 1000 cm^{-1}.

i. Hydroxyl vibrations:

The O-H stretching band (3380 cm^{-1}) is observed to narrow in shape and to increase in intensity upon calcium addition. This is characteristic of a more specific type of bonding. Similar changes were observed between the sodium and the calcium alginate films (chapter IV). However, there is no wavenumber shift between the two salts. This may be due to the bulky carboxymethyl groups (attached to the CMC) which hinder the O-H vibrations, thus lowering the frequency compared with calcium alginate. The OH in-plane deformation vibration appears at 1323 cm^{-1} for sodium and at 1331 cm^{-1} for calcium alginate/CMC. In the second case, the peak becomes asymmetric, indicative of different types of hydrogen bond. No change in frequency is obtained for the pure CMC samples.

Hosny *et al.* (1995) performed FTIR analysis on KBr disks prepared with different CMC samples (with varied DS), and containing copper and nickel ions. For a DS of 0.67 and 1.31, the O-H stretching vibration was found at 3434 cm^{-1} for nickel carboxymethylcellulose and at 3429 cm^{-1} for copper carboxymethylcellulose. These values are much higher than ours, for a DS = 0.8 and with calcium ions. There is either more water in the KBr disk samples, or the hydroxyl groups are freer to vibrate in CMC in the presence of copper or nickel ions. Hosny *et al.* (1995) also observed an increase in wavenumber compared with the starting CMC. They suggested that chelation through carboxymethyl groups was more kinetically favoured than through liberated hydroxyl groups. This statement was backed up by the observation that a higher percentage of chelating metal ions was obtained with increasing degree of substitution.

ii. C-H vibrations:

The frequency of the C-H stretching peak (around 2920 cm^{-1}) remains constant in the case of pure CMC. There is an increase in wavenumber of ≈ 10 cm^{-1} for the 50/50 blend; this difference was of 20 cm^{-1} between the sodium and calcium alginate samples.

iii. Carboxyl vibrations:

The COO^- stretching peaks (1600 and 1420 cm^{-1}) broaden and become asymmetric upon calcium addition. This implies that $COO^-...OH$ bonding exists, in addition to $COO^-...Ca^{2+}$; the COO groups are, thus, only partially bound to the Ca^{2+} ions. Hosny *et al.* (1995) observed, upon nickel ion addition to CMC, a shift to a higher frequency by more than 10 cm^{-1}, and increased broadness. They assumed that the carbonyls of the carboxymethyl groups were not involved in chelation. Regarding copper CMC, in addition to the shift of the carbonyl vibration bands, a new shoulder band appeared. It was thought to be due to the chelation of carboxyl groups with the copper ions through the oxygen of ether linkages of CMC. The absence of this band in the Ni-CMC was attributed to the presence of water molecules. This reduces the available space between the carboxymethylcellulose molecules. Thus, the vibrational movement of the C=O groups becomes restricted and consequently only one band is observed.

iv. Other vibrations:

Most of the peaks in the 1100-1000 cm^{-1} region (characteristic of C-O and C-C stretching vibrations) have slightly lower wavenumbers upon calcium addition. This is most likely to be due to these bonds being shared with the calcium ions. Some of the peaks have increased intensity while others weaken. Therefore some vibrations must be favoured while others are hindered in the presence of the Ca^{2+} ions.

It is apparent that alginate/CMC blends react in a comparable way to the pure alginate samples, when brought into contact with calcium. Similar types of binding are observed between them. However, because there are not as many changes for CMC as for alginate, calcium ions may be assumed not to be as tightly bound. This seems in contradiction with the mechanical properties.

VII.3. Study of sodium/calcium alginate/CMC blends immersed in a simulated serum solution:

Once sodium/calcium films of alginate/CMC have been prepared, they can be tested for their capacity to act as wound dressings. The tests include calcium ion release

measurements (this influences blood coagulation), swelling ability and gel strength. All these tests were performed by bringing the samples into contact with a simulated serum solution (also referred to as a Na/Ca solution).

VII.3.1. Ion exchange between the blends and the simulated serum solution:

The release of calcium ions as a function of immersion time in the simulated serum solution is given in figure VII.3.1.. The spread in the experimental results was ± 13 %.

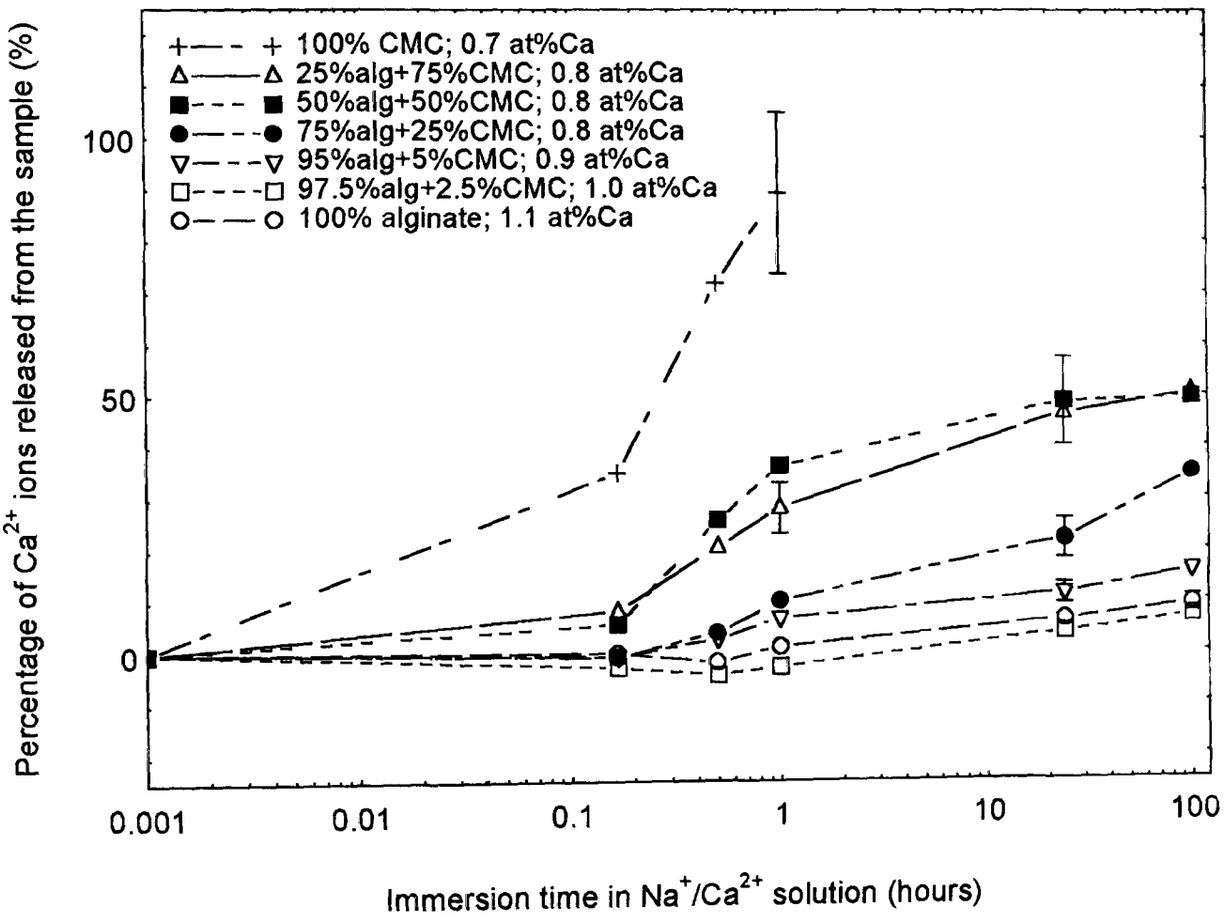

Figure VII.3.1. Release of calcium ions in a simulated solution, for alginate/CMC films.

Greater calcium ion release is observed with increasing CMC content. An addition of 25% CMC to the alginate improves noticeably the calcium release, by a factor of three. For the pure CMC sample, dissolution in the Na/Ca solution occurred after one hour exposure. This may explain why such a large calcium ion release is observed over a short period of time. For most of the other samples, it appears that, even after 100 hours immersion, no plateau value is reached. Therefore, the ion exchange process is expected

to continue (i.e. this is a very slow process). It should be pointed out that all samples have relatively similar Ca^{2+} contents initially; therefore the higher calcium releases observed with larger amounts of CMC are certainly due to the fact that the calcium ions are more tightly bound within the alginate than within the CMC network.

VII.3.2. Wicking rate experiments in the Na/Ca solution:

The samples were all prepared by immersion for 30 minutes in a 0.8 wt% calcium chloride solution. The maximum wicking rate values obtained in Na/Ca solution are presented below (table VII.3.2.):

Sample	Max. wicking rate ($mg.s^{-1}$)
100% alginate LF 10/60	89.3 ± 11.6
97.5% alginate + 2.5% CMC	97.9 ± 6.0
95% alginate + 5% CMC	92.4 ± 11.9
75% alginate + 25% CMC	94.3 ± 12.7
50% alginate + 50% CMC	99.7 ± 12.1
25% alginate + 75% CMC	77.8 ± 11.4
100% CMC	78.0 ± 12.0

Table VII.3.2. Wicking rate values of alginate/CMC blends.

Ten samples were tested on average. Both film weight and thickness were kept constant (30 ± 2 mg and 80 ± 8 μm respectively). The maximum wicking rate values tend to increase upon addition of CMC (even with small percentages) up to 50 %. Above this value, a drop occurs, maybe due to increasing impurity content on the surface (see section VII.2.5.). But overall, taking into account the experimental errors (around 25 %), there is no large change between the blends. Therefore the initial response of alginate/CMC blends when first brought into contact with a serum solution is fairly similar for all compositions. For longer exposures in Na/Ca solution, the following tests were performed.

VII.3.3. Volume ratio:

The results of swelling as a function of immersion time in the simulated serum solution are plotted in figure VII.3.3.a.

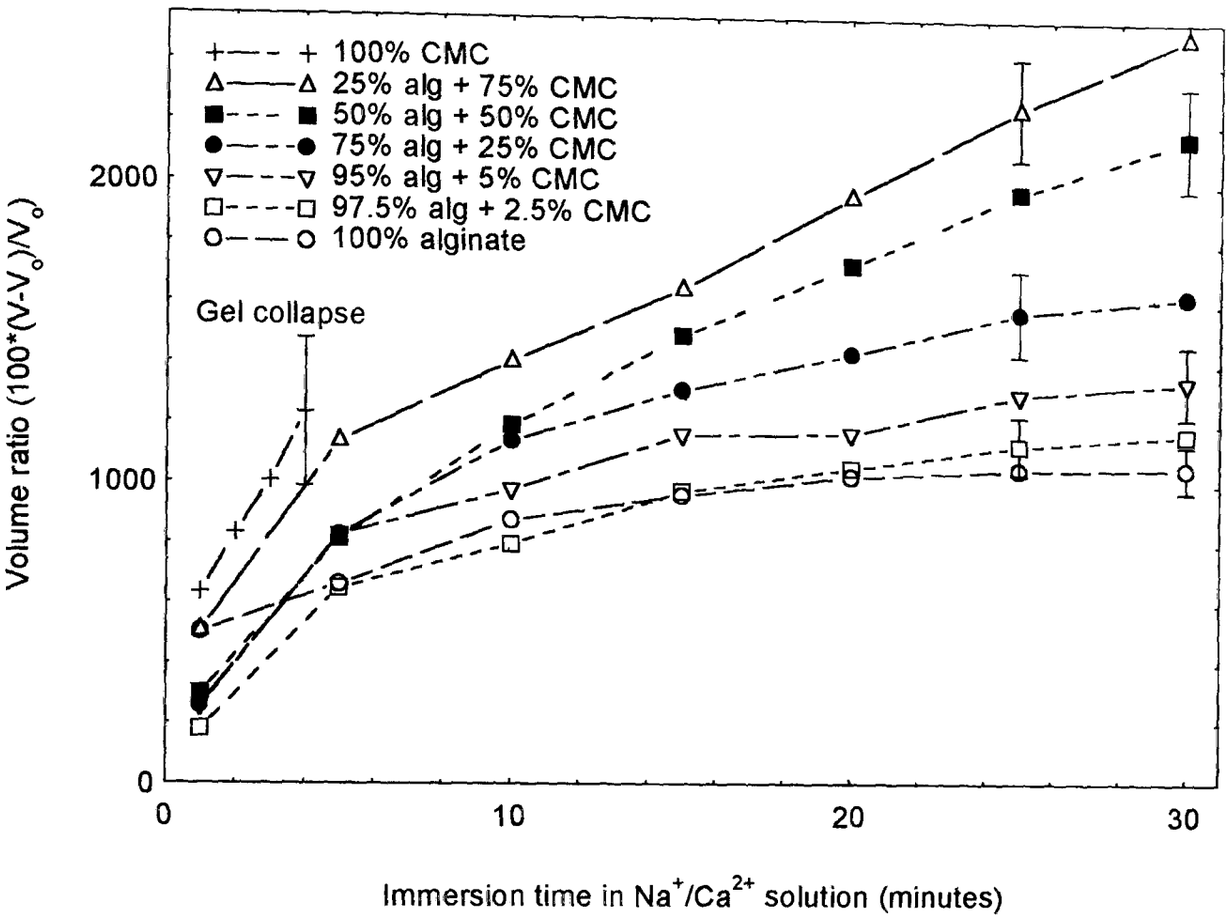

Figure VII.3.3.a. Volume change of Na/Ca alginate/CMC blends in Na/Ca solution.

There is a spread of around ± 10 % in the experimental results. A greater variation is encountered for the tests in the first 15 minutes; afterwards, the variation decreases. The 100 % CMC sample was broken after four minutes of immersion, due to disintegration in contact with the solution. For the blends containing between 0 and 25 % CMC, the corresponding curves reach a plateau after 30 minutes of immersion in the Na/Ca solution. By contrast, higher CMC content samples do not reach equilibrium after this time, and one would expect an increasingly higher volume change, even after one hour immersion.

Figure VII.3.3.b. shows the volume change of the different blends (except 100 % CMC) for a fixed immersion time (30 minutes). A time of 30 minutes was chosen because a

plateau value was reached at this point by many samples.

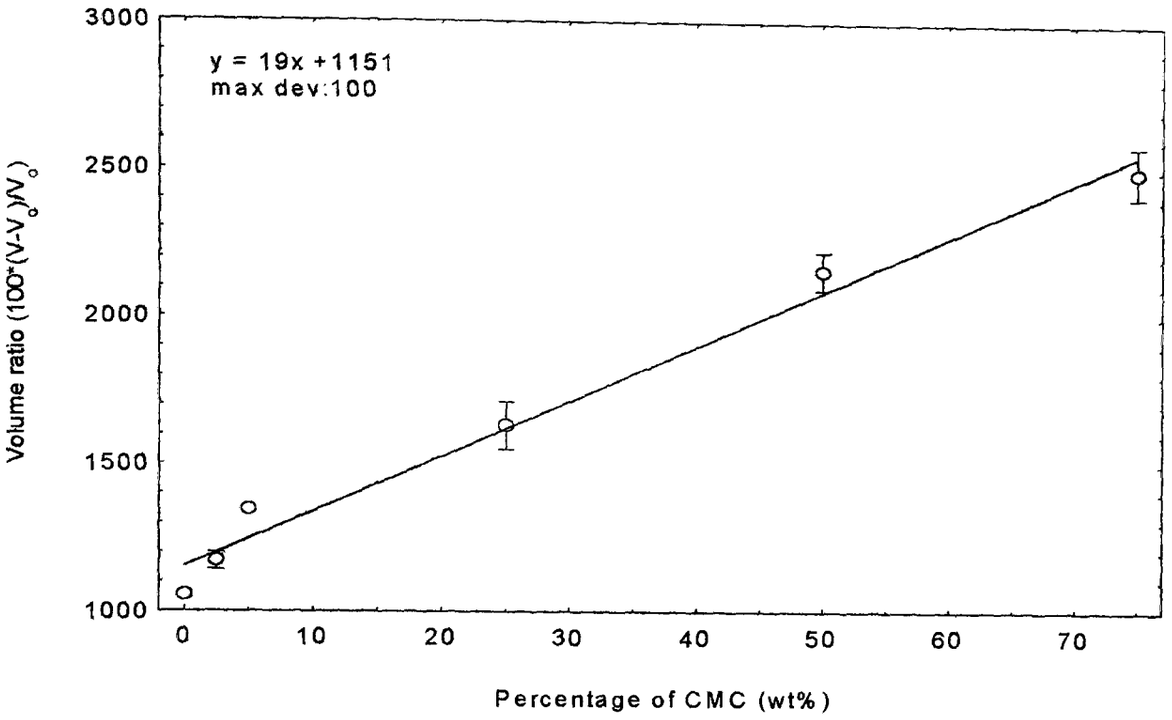

Figure VII.3.3.b. Volume ratio of alginate/CMC blends after 30 minutes immersion.

This graph shows a clear increase of the swelling with increasing CMC content. According to Tasker *et al.* (1994), CMC possesses great porosity, and this pore structure accommodates swelling. The increase in volume ratio follows an almost linear relationship. This type of behaviour would confirm the idea that alginate and CMC do not present any synergistic effect, when prepared as a blend. An addition of just 5 % of CMC gives rise to a 28 % improvement in the volume ratio. 75 % of CMC boosts the swelling to 137 %. Therefore, the addition of CMC to an alginate sample enhances the swelling behaviour. This is obviously of importance when considering wound dressing applications. However, gel strength might be a problem, as suggested by the early fracture of the 100 % CMC sample. This aspect will be studied in section VII.3.4.

Prasad & Kalyanasundaran (1995) have measured the swelling ratio (defined as the volume of swollen polymer over the volume of dry polymer) in water as a function of time for Cu-CMC and Fe-CMC. For the first sample, they observed a rapid increase in volume for the first 24 hours of immersion, then a low decrease until equilibrium, where the swelling was between 1.8 and 2.0, according to the degree of crosslinking (the

dynamic swelling ratios were inversely proportional to the crosslinking density). Fe-CMC reached an equilibrium within 20 hours, and the swelling ratio was then between 1.0 and 1.5. For our alginate/CMC films, the swelling ratio as defined by Prasad & Kalyanasundaran, is given in the following table, after 30 minutes immersion in the Na/Ca solution:

Sample	Swelling ratio (mm^3/mm^3)
100% alginate	12.2
97.5% alginate + 2.5% CMC	12.7
95% alginate + 5% CMC	14.4
75% alginate + 25% CMC	17.3
50% alginate + 50% CMC	22.6
25% alginate + 75% CMC	26.0

Table VII.3.3. Swelling ratio after 30 minutes immersion for the Na/Ca alginate/CMC blends.

These swelling values are much higher than those obtained for Cu-CMC and Fe-CMC. This may be due to a lower degree of crosslinking in our films, as they were immersed in the calcium chloride solution for 30 minutes, while Prasad & Kalyanasundaran immersed their samples for 12 hours at least in copper sulphate or ferric chloride. The degree of substitution of the CMC may be of importance as well. Keller (1984b) has indeed stated that higher DS types of CMC are more effective moisture binders. However, this parameter was not specified for the Cu- and Fe-CMC.

VII.3.4 Gel strength:

Gel strength measurements in a Na/Ca solution for the different alginate/CMC blends have been performed as a function of time, and are plotted in figure VII.3.4.a. It must be remembered that a constant weight (50 g in air, equivalent to 43 g in water) was used for these tests, but the stress applied varied with time and according to the sample, due to the increase of the cross-sectional area, with swelling (see figure VII.3.4.b.).

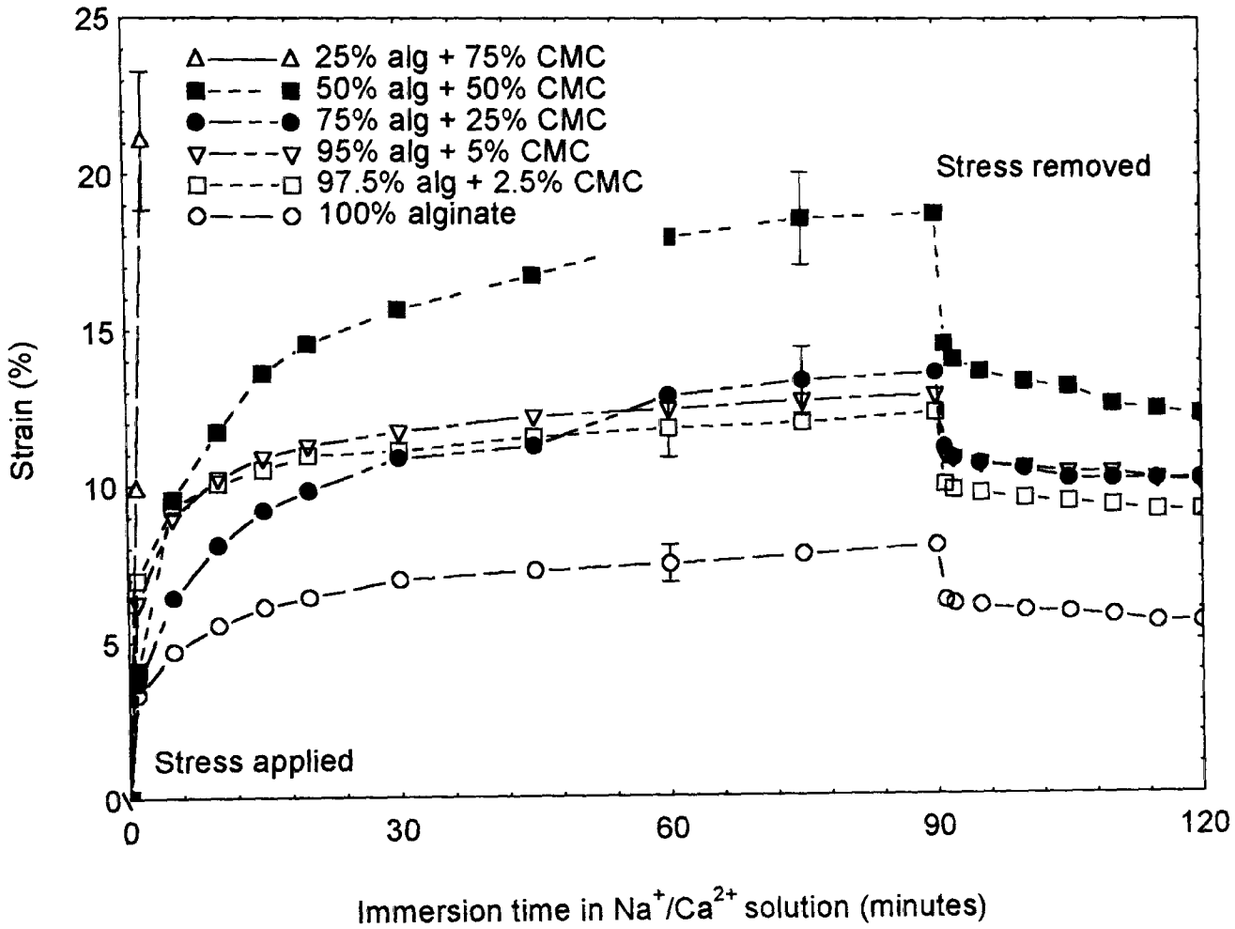

Figure VII.3.4.a. Gel strength of alginate/CMC blends.

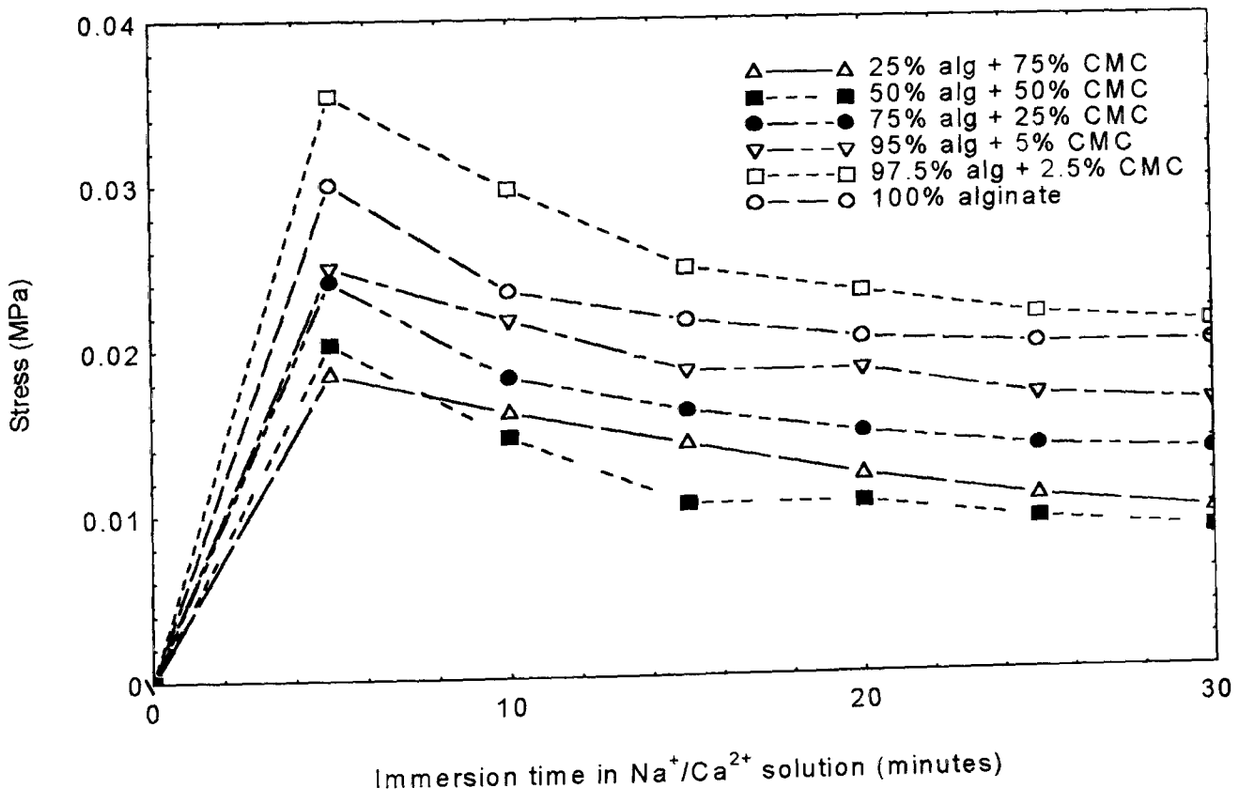

Figure VII.3.4.b. Stress applied to the alginate/CMC blends.

The experimental scatter in the strain values was ± 8 %. For a given time, as a general trend, the stress applied decreases from the pure alginate to the pure CMC sample. From the gel strength tests, it can be seen that an increase of the carboxymethylcellulose content is paralleled by an increase in the elongation. As the longest strains are observed for the lowest stress, it appears that the high-CMC gels are the weakest. Therefore in the gel state, the CMC molecules show greater flexibility than the alginate chains. An addition of 5 % CMC to alginate shows a clear effect on the elongation (showing that the gel strength decreases), but it still remains strong enough to prevent breakage. However, a high percentage of CMC is to be avoided: no measurements were possible on the pure CMC sample (it broke instantaneously), and the sample containing 75 % of carboxymethylcellulose broke after only a couple of minutes of loading. For all the other samples, a plateau is reached after 90 minutes.

Ichikawa *et al.* (1994) also performed strength tests on swollen complexes involving CMC. They found that a high compressive modulus was obtained for poly(ε-lysine)/ CMC blends when the CMC had a low average molecular weight ($\approx 5.10^4$), as well as a relatively low degree of substitution (0.8), and when a low proportion of poly(ε-lysine) was used.

VII.4. Summary

Ionic interactions between alginate and CMC have been shown to be weak under dry conditions (as seen from the FTIR study, and further proved with the mechanical testing). These two polysaccharides seem, therefore, to act as independent entities when prepared as blends. CMC addition has improved such properties as the calcium release and the swelling behaviour in a simulated wound exudate. This is of importance for wound dressings.

CHAPTER VIII. PROPOSED MECHANISMS FOR POLYSACCHARIDE SYSTEMS USED IN WOUND DRESSING APPLICATIONS

From the previous chapters, it emerged that alginates, as mixed sodium/calcium salts, could offer outstanding properties in terms of gelling, water uptake and gel strength. Furthermore, small additions of other polysaccharides (such as pectin or carboxymethylcellulose) can alter dramatically these properties, either positively or negatively. The aim of the present chapter is to summarise most of the experimental results performed on alginates and their blends, and to go beyond the interpretation of the individual results, i.e. to combine them in order to propose mechanisms for some of the properties studied.

VIII.1. Summary of the experimental results

VIII.1.1. Characterisation of the samples during and after their preparation:

During the sample preparation, a sodium alginate-based solution was immersed in a calcium chloride bath. There, sodium-calcium ion exchange took place, followed by rinsing and drying of the sample. Firstly, alginates of mixed salts were analysed. However, in order to improve some of their properties in the gel state, blends were also considered. The polymers in solution or in the dry state were tested for their viscosity, pH, water content and crystallinity. The main trends are presented below.

i. Viscosity and pH of the polysaccharide solutions:

Viscosity measurements performed on high-G and medium-G sodium alginate solutions gave values of 13,400 and 3,800 mPa.s respectively. This was indicative of a higher inflexibility of the G sequences in solution (in agreement with observations by Iso *et al.*, 1988). No change was observed between the pH values of the two types of alginates.

The sodium alginate/pectin blends displayed similar viscosity values (430-700 mPa.s), except for the 25/75 blend (3,400 mPa.s). Given that the number average molecular weight and the polydispersity of pectin are similar to that of alginate, the degree of entanglement of both polymers must be comparable (regardless of the 25/75 blend).

The pH values varied from 6.3 for the sodium alginate down to 2.9 for the pectin. For the 25/75 composition, the pH was lower than 4, and therefore gelation between the two polysaccharides was favoured (Toft, 1982). This explains the dramatic increase in viscosity.

The viscosity, and to a far lesser extent the pH, increased with increasing CMC content (from 5,400 to 64,500 mPa.s for the viscosity and from 6.4 to 6.9 for the pH). Furthermore, the viscosity values of the alginate/CMC blends were found to be lower than those expected for non-interaction between the two polysaccharides. It is also noteworthy that the CMC solution prepared from 6 wt% powder had the appearance of a paste rather than a liquid. When this mixture was placed into a calcium chloride solution bath, sodium/calcium ion exchange did occur (as shown by atomic absorption spectroscopy). However, no mixed salt of CMC could be prepared from a 1 % solution as gelation was not favoured in this condition. A 3 % powder content was found to be the minimum required, but the ion exchange which ensued cannot be considered as a gelation process of the type seen for the alginate (likewise for a 6 % solution).

ii. Water content and crystallinity of the sample films:

After the final stage of the sample preparation, TGA experiments were performed in order to determine the water content remaining in the films in the "dry state" (as the films absorbed water from the ambient humidity). It was found that the Na and the Na/Ca high-G and medium-G alginate films had an average water content of 15 wt%, giving two water molecules per block (M or G). Some of the sodium/calcium alginate/pectin samples (100/0 and 25/75 blends) had a water content of 13 wt% while others (75/25 and 50/50 blends) contained 11 wt% water. For the Na/Ca alginate/Na/Ca CMC films, the water content was on average 15 wt% for the whole range of blends. Furthermore, the water molecules seemed more tightly bound to the CMC molecules than to the alginate molecules (as seen from the temperature of inflection in the TGA curve).

Whilst the sodium alginate and the sodium CMC gave X-ray diffraction spectra characteristic of relatively disordered materials, the pectin was found to be crystalline. Furthermore, calcium addition to the various samples did not induce any measurable ordering of the molecules. However, there may be a shorter range order which is not

detectable with the technique we used.

iii. Ion content:

AAS results revealed an excess of calcium content (compared to the initial sodium content) for the alginate samples after long immersion times in a $CaCl_2$ solution. This was thought to be counterbalanced by Cl^- ions present as well in the samples (WDX/SEM experiments). Likewise, an excess of Ca^{2+} ions was detected in some of the sodium/calcium alginate/pectin blends (i.e. the Na^+ and Ca^{2+} wt% were higher than the percentages required to fill all the alginate sites). Again, Cl^- ions may play a role. It is also possible that some calcium ions may either exist as free ions or be partially bound to the pectin molecules. With reference to the mixed salts of alginate/CMC, both polysaccharides were found to attract the divalent cations, and the ion exchange rate was of the same order for the two polymers.

VIII.1.2. Spectroscopy studies:

This experimental part was based principally on FTIR analysis. The study of the sodium alginate samples suggested that the OH...OH binding was prevalent (between alginate-alginate molecules and between alginate-water molecules). Furthermore, the sodium ions were found to be mainly bound to the carboxyl groups. By contrast, in the calcium alginate, the hydroxyl groups seemed involved in both OH...OH and OH...$^-$OOC types of binding. There was only a partial Ca^{2+}...$^-$OOC binding. The calcium ions also appeared to be bound to the alginate groups via the C and O atoms. These observations led to the conclusion that the calcium ions are bound in a non-specific way to the alginate molecules (in contrast with the sodium ions) and preferentially to the G blocks.

Infrared experiments performed on the sodium alginate/pectin blends suggested that binding between the two polysaccharides occurs mainly via OH...OH bonding. Following calcium introduction, many groups of atoms, such as CH, CH_3 and CO, seemed perturbed. Lastly, the Ca^{2+} ions were thought to be partially bound to the COO^- and CO groups.

FTIR performed on the alginate/CMC blends in the sodium state did not show any evidence of intermolecular binding between the two polysaccharides. Calcium addition

induced new types of hydrogen binding, such as OH...⁻OOC, in a similar way to the alginates. However less changes were observed when compared with the pure alginate, suggesting that the calcium ions may not be bound to the same extent to the cellulose molecules.

VIII.1.3. Interaction between the polysaccharide samples and a simulated serum solution:

The polysaccharides, once prepared as sodium/calcium salts, were immersed in a simulated serum solution (Na/Ca solution, containing 142 millimoles of sodium ions and 2.5 millimoles of calcium ions). They were then studied for their calcium release, swelling and gel strength properties. These experiments were aimed at simulating the contact between a dressing and a wound.

i. Calcium release:

Calcium release experiments of sodium/calcium alginate films in a simulated serum solution showed that the divalent ions were released to a greater extent for a medium-G sample than for a high-G sample. A straightforward conclusion would imply that the calcium ions are more tightly bound to the G blocks than to the M blocks. However, both samples had a calcium content such that the G blocks were only partially filled (according to the "egg-box model", the G blocks are filled first, followed by the M blocks if the calcium content is high enough). This implies that the way the calcium ions are bound certainly needs consideration, with their surroundings (M or G blocks) being another important parameter to take into account. These observations favour a "hopping-trapping" type of mechanism to describe the calcium release process in alginate-based systems, as will be detailed in VIII.3.1. Upon CMC addition to the alginate, the calcium release was observed to increase. For several samples, no equilibrium plateau was reached, even after 100 hours immersion in a Na/Ca solution. As for the alginate/pectin blends, no experiments could be carried out due to their very acidic nature which caused disruption of the dye used to study Ca^{2+} release rates.

In all cases, the polymer films were not observed to revert to pure sodium salts after 100 hours immersion. An end point was reached in some cases (including most of the pure alginate samples), before a sodium sample could be obtained, and although the calcium

ion concentration in the sample was far greater than that of the simulated serum solution (between 700 and 2200 mmol.dm^{-3} Ca^{2+} in the alginate sample compared with 1.5-7.5 mmol.dm^{-3} Ca^{2+} in the solution). For these cases, a phenomenon prevented the calcium ions from moving as freely as possible from the sample to the solution.

ii. Swelling:

Wicking rate experiments performed on mixed salts of alginates and alginate/CMC blends revealed that water was absorbed within the first seconds of immersion.

The swelling ratio (at times greater than five minutes) was found to have an inverse relationship to the initial calcium content (i.e. degree of crosslinking) and to the G block content. In the blend studies, all films were prepared by immersion for 30 minutes in the calcium chloride solution. There was no straightforward trend observed in the swelling behaviour as the pectin content increases. However, the 50/50 blend displayed an improved swelling behaviour compared with the pure alginate, although H.M. pectin is considered to be hydrophobic. Therefore the water may have encountered only weak and easily disrupted cohesion between the molecules. For the alginate/CMC blends, a larger CMC addition was found to increase the swelling ability.

iii. Gel strength:

The wet strength was improved with greater G block and calcium contents in the alginate sample. For the alginate/pectin films, no obvious trend between the samples was observed. The strongest gels were the 75/25 and 95/5 blends while the weakest films were the 100/0, 97.5/2.5 and 25/75 blends. Finally, for the alginate/CMC blends, the general trend in the wet strength was a decrease of this property with increasing CMC content. This is expected to be due to the incompatibility between the polysaccharides, as well as an overall weaker calcium binding to the polymer molecules (as Ca^{2+} ions are supposed to be more tightly bound to the G blocks of the alginate than to the carboxymethyl groups of the CMC). The CMC molecules may also offer greater flexibility and therefore exhibit greater gel deformation.

From all the experimental data obtained, some mechanisms can be derived. By focusing on the polysaccharides at a molecular level, properties such as the binding behaviour can be determined. A model relating to the characteristics in the gel state is also proposed.

VIII.2. A model of the polysaccharides at the molecular level

VIII.2.1. Recall of the molecular structures of the different polysaccharides:

The structures of segments of sodium alginate, pectin and sodium carboxymethylcellulose (sodium CMC) are presented in figures VIII.2.1.a., b. and c. Many of the carbon and hydrogen atoms are omitted for clarity.

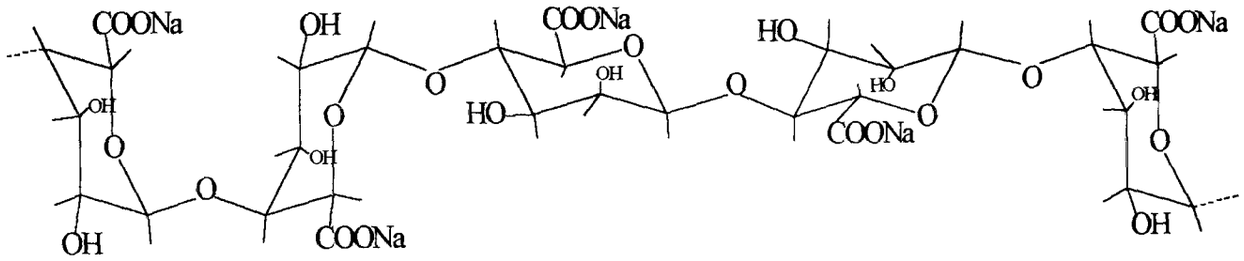

Figure VIII.2.1.a. Chemical structure of sodium alginate (sequence : GGMMG) (Smidsrød & Skjåk-Bræk, 1990).

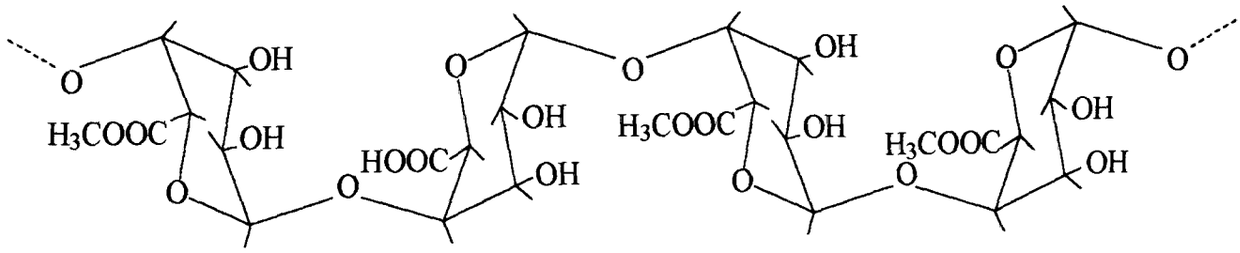

Figure VIII.2.1.b. Chemical structure of pectin (percentage of methoxylation = 75 %) (Keller, 1984a).

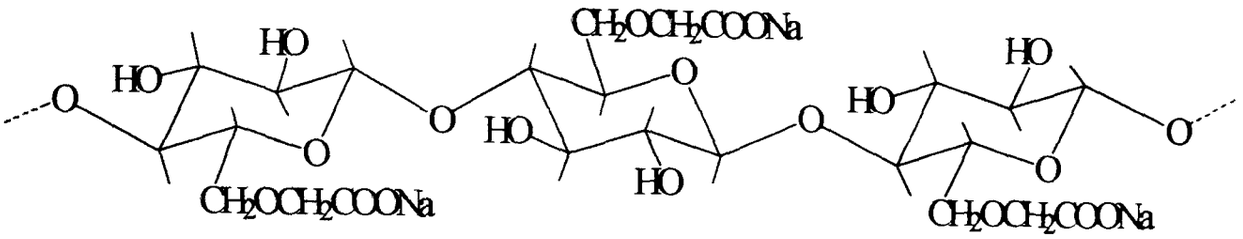

Figure VIII.2.1.c. Chemical structure of sodium carboxymethylcellulose (degree of substitution = 1) (Baar *et al.*, 1994).

All these polymers have six membered ring structures, linked together by glycosidic bonds.

VIII.2.2. Structure of calcium alginate:

The experimental results suggest that there exists some affinity between the Ca^{2+} ions and the G blocks in the alginate molecules (see infrared, gel strength and calcium release studies). This is most certainly due to their shape as buckled ribbons which leave interstices when they pack together (Rees, 1977). Various computer models have suggested that the G blocks form chains with two or three-fold screw symmetry, and that interaction of the Ca^{2+} ions occurred via oxygen atoms from the carboxylic groups, from the hydroxyl groups and possibly from the skeleton (Mackie *et al.*, 1983). This was referred to as the "egg-box" model (Gacesa, 1988; Grant *et al.*, 1973). FTIR spectroscopy gave evidence for most of the bonding states described above, with the calcium ions acting as crosslinking between chains (also suggested by the gel strength measurements). However, no evidence could be found of ordering in alginate films (from X-ray diffraction). The results obtained suggest non-specific binding between the divalent cation and the alginate molecules.

The influence of water on alginates in the "dry state" (as opposed to the gel state), has not been widely studied in the literature to date. Mackie *et al.* (1983) proposed that the Ca^{2+} ions were bound to H_2O. They also suggested that incidentally, the water molecules could provide extra crosslinking of neighbouring chains through hydrogen bonding with the oxygen atoms of the carboxylate groups. Binding to the calcium ions seems a reasonable statement as the calcium ions are initially in an aqueous medium, and the

water molecules may be a way to convey the divalent cations into the alginate network. However, water is also present in the sodium alginate films (as shown by TGA analysis). Therefore binding between the alginate and the water needs also to be considered. This is likely to occur partially through the O-H and COO^- groups of the alginate blocks as they are the blocks offering the greater charge.

In the light of our results, a simplified two-dimensional sketch of the calcium alginate molecules can be proposed. Chlorine ions have not been drawn as not enough knowledge was gained on their binding state.

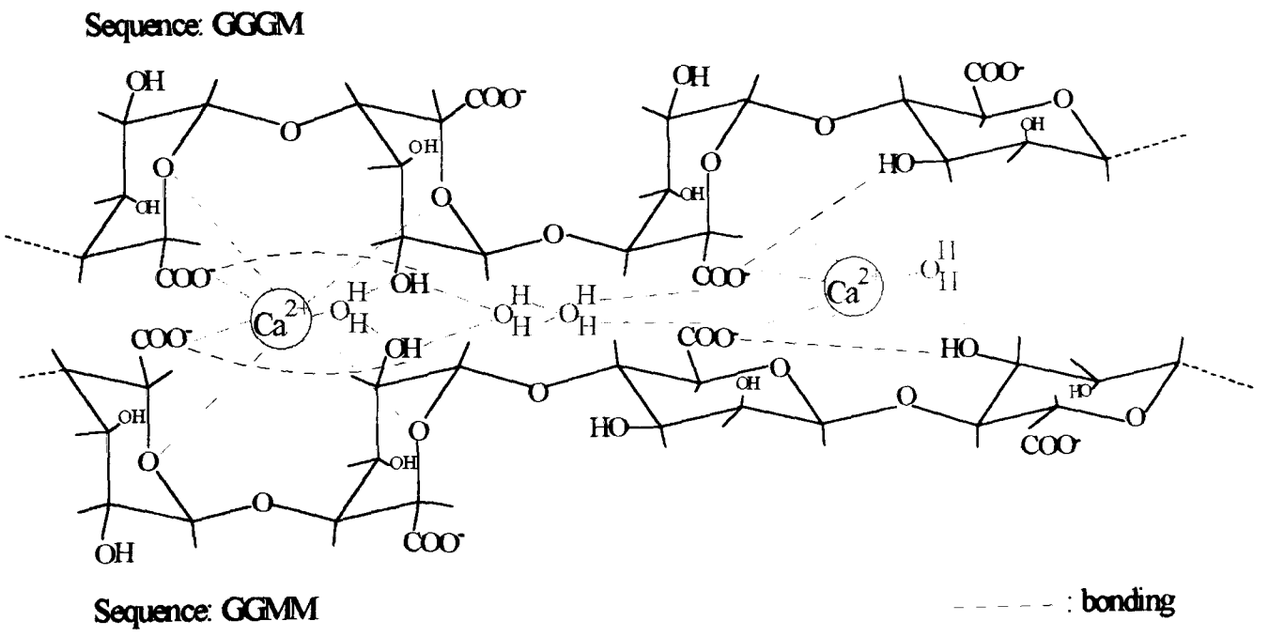

Figure VIII.2.2. Proposed representation of the main binding sites in calcium alginate.

Different types of binding are expected according to the location of the calcium ions in the alginate. The Ca^{2+} ion on the left in figure VIII.2.2. is contained within four G blocks, and its binding (primarily ionic) to the alginate is distributed all around the cation, and there is little opportunity to escape. The calcium ion on the right of the sketch is placed between one G and three M blocks. The bonds are concentrated on one side, and the opposite side offers space for the ion to escape. Therefore this situation leads to a weaker crosslinking of the calcium.

It must be pointed out that this representation is only two-dimensional, and more alginate molecules are expected to be located above and under the plane of interest. Therefore, the binding of calcium ions to the alginate molecules is distributed all around the cation, and the overall binding situation is rendered more complex.

VIII.2.3. Influence of pectin or CMC addition on alginate molecular structure:

For wound dressing applications, we are mainly interested in small additions of pectin or carboxymethylcellulose (CMC) to alginate (as it is mainly alginate which has been shown to offer good haemocompatibility). However, a wide range of both blends was studied, in order to provide a better understanding of the interaction between the polysaccharides.

i. Alginate/pectin blends:

Many authors (Clare, 1993; Morris & Chilvers, 1984; Toft, 1982) have looked into the modelling of high-G alginate/ H.M. pectin binding. According to Thom *et al.* (1982), intermolecular binding between these polysaccharides involves the methyl groups of pectin with the hydrogen atoms of alginate (mainly from the G groups). However, the influence of calcium additions has not been fully assessed, although it was found to be detrimental to the blend in terms of gelation (Clare, 1993; Thom *et al.*, 1982).

Infrared experiments and swelling experiments show that there exists some weak hydrogen bonding between the alginate and the pectin molecules. Upon calcium immersion, the divalent cations attach themselves preferentially onto the alginate molecules. Indeed, pectin is not found to chelate much calcium ions (AAS). This may be explained by the fact that the galacturonic acids do not offer many cavities like in the guluronic acids, due to the presence of the bulky methyl ester groups $COOCH_3$. However, it is believed that some degree of interaction does occur between the calcium ions and the pectin molecules (from the FTIR and AAS results) which might involve some of the alginate blocks. The addition of calcium ions seems to alter the mechanical properties (especially for the 25/75 sample where strong binding is expected in the sodium state, according to the viscosity measurements). It may be that the calcium ions break some of the intermolecular bonds between the alginate and the pectin. This

may also be due to the hydrophobicity of the high-methoxyl pectin (due to the methyl groups; Walkinshaw & Arnott, 1981). As the calcium ions are thought to be conveyed into the polymer network via the water molecules, the methoxylated groups may present a barrier to the divalent cations, again pulling the chains apart from one another.

A simplified representation of alginate/pectin molecules, which attempts to include most of our experimental results, is now proposed.

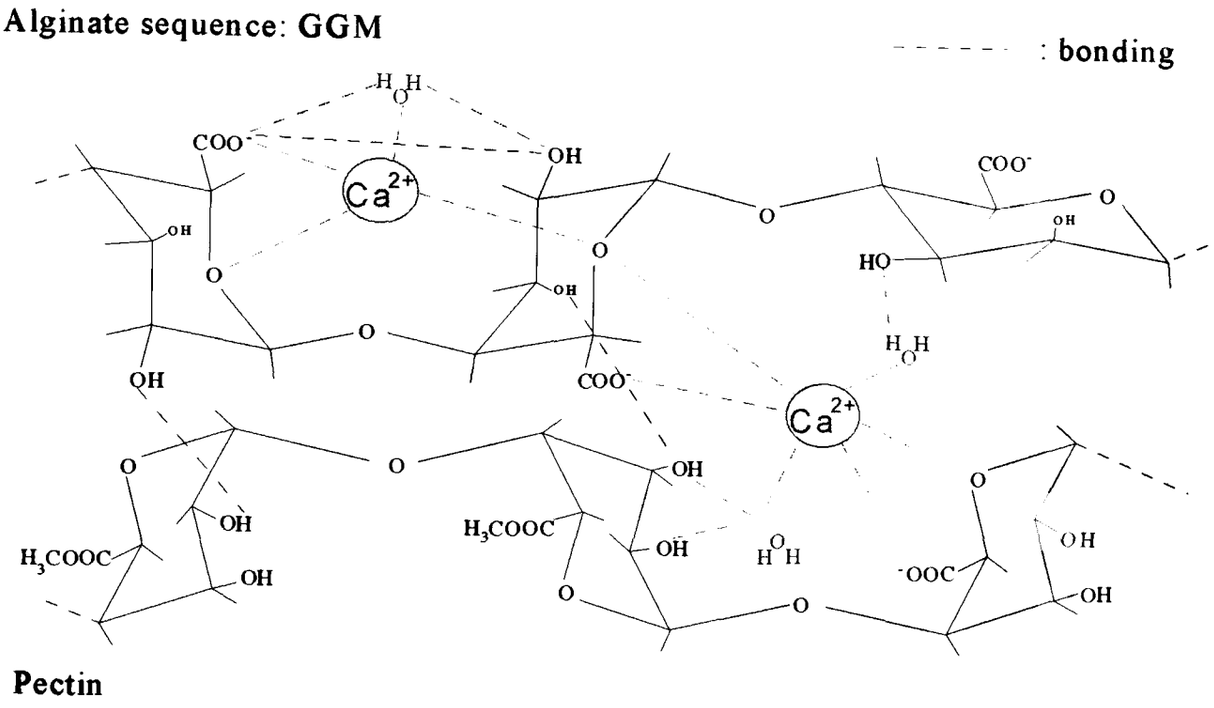

Figure VIII.2.3.a. Proposed representation of some of the binding sites in calcium alginate/pectin blends.

In alginate/pectin blends, various blocks are present, i.e. mannuronic acid, guluronic acid, methoxylated and non-methoxylated galacturonate residues. Therefore bonds with varied strength are expected to be found between the calcium ions and the polysaccharide chains. In figure VIII.2.3.a., the top Ca^{2+} ion is surrounded by two G blocks, leading to relatively strong binding (the divalent cation is expected to be bound to more polymer chains, not sketched here). Regarding the second calcium ion, it is bound rather weakly to the neighbouring alginate and pectin blocks, and has a greater degree of freedom.

ii. Alginate/CMC blends:

As for the alginate/CMC blends, no model has been proposed in the literature to date. In fact, hardly any work is found on these blends. As a sodium solution or in the dry state, little cohesion was found between the two polysaccharides (as observed from the pH, viscosity, FTIR and tensile test studies), and the possibility of greater chain freedom was observed. The polysaccharides seemed to act independently of each other. This may be due to the bulky carboxymethyl groups of the CMC preventing good packing and interaction between the two polymers. The TGA experiments showed that the water molecules are more tightly bound to the CMC than to the alginate molecules. Therefore the cellulose sample exhibits improved hydrophilic behaviour.

The interaction between calcium ions and the CMC molecules does not involve strong intermolecular binding (as seen from the calcium release and the FTIR results) as observed between calcium ions and the alginate. Ca^{2+} may be bound to the carboxymethyl groups of CMC, but hardly not to CO or CC groups, leading to a more fragile network. According to Hosny *et al.* (1995), the carboxymethyl group is the major site of bonding at high degree of substitution (DS > 0.7) whereas the OH and CH_2COO^- groups are the chelating centres for relatively low DS (≈ 0.5).

From these observations and suggestions, a model for the alginate/CMC blend can be derived.

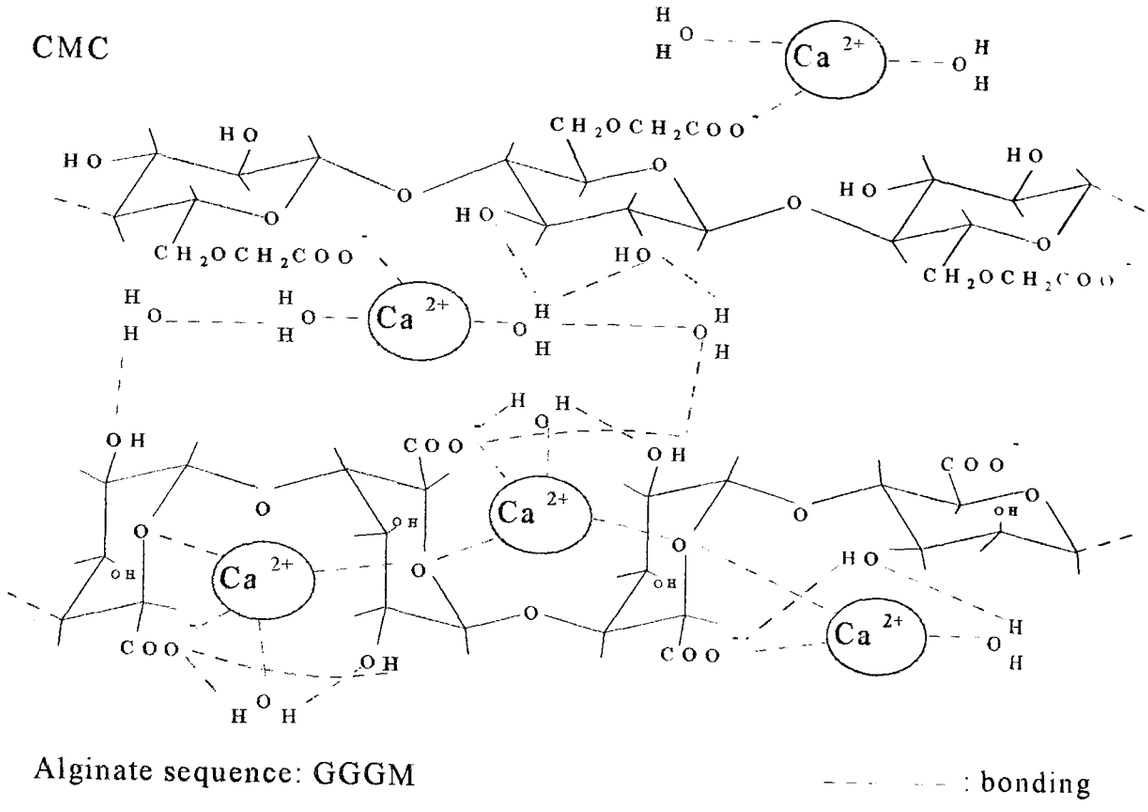

Figure VIII.2.3.b. Proposed representation of the main binding sites in calcium alginate/CMC blends.

In the alginate/CMC blends, the calcium ions do not act as crosslinks between the two polysaccharides. In contact with the CMC molecules, the divalent cations are bound essentially to the carboxymethyl groups (top Ca^{2+} ions in figure VIII.2.3.b.). By contrast, the alginate molecules offer more binding sites for the Ca^{2+} ions (via CO and COO^- groups), thus leading to stronger bond strength, especially with the G blocks (bottom left calcium ions in the above figure).

VIII.3. Proposed mechanisms for a polysaccharide system brought into contact with a simulated serum solution

Mechanisms of the gel properties enabling the interpretation of our experimental results are now proposed.

VIII.3.1. Calcium release:

When a sodium/calcium polysaccharide film (in the dry state) is immersed in a simulated

serum solution, water molecules penetrate into the polymer (leading to swelling). The water molecules are expected to be attracted to the OH groups (present in alginate, pectin and CMC) as well as to the COO^- groups (present in both alginate and CMC) due to their electronegativity. This certainly tends to destabilise the binding of the sodium ions, as well as the calcium ions, especially those bound to the M blocks (alginate) and to the carboxymethyl groups (CMC). High ion mobility is then expected (due to the anionic character of the carboxylic groups and to the water environment facilitating the diffusion). Once the divalent cations are free, they migrate until obstacles are found. These are primarily the free G blocks as they can chelate the Ca^{2+} ions. Therefore the higher the G content, the greater the opportunity to come across obstacles. The driving force drawing the divalent cations towards the simulated serum solution is thought to be the concentration gradient.

Let us now consider a calcium alginate film. With high levels of calcium, there will be a low percentage of unfilled G blocks. In contact with the wound serum solution, the M blocks will first be depleted in calcium ions, and there will be a high probability that the Ca^{2+} ions leave the polymer relatively easily and rapidly (as there would be only a small proportion of available G blocks as potential trapping sites). Indeed, a greater initial slope for the calcium release curve is observed with increasing Ca^{2+} wt% in the film. For a lower Ca^{2+} wt% in the sample, and in the case where the M blocks are unfilled and the G blocks only partially filled, the first step in the calcium release process is expected to differ. Although it will take more time and disruption, the calcium ions bound to the G blocks may be relocated. In a high-M sample, the Ca^{2+} ions will encounter essentially M-blocks along their way. They may be attracted to them, but because only a weak binding exists between the two, the probability for the divalent ions to escape promptly will be high. By contrast, in a high-G sample, the free calcium ions will be faced by newly available G blocks, with which strong binding will follow. The same type of migration may result, but at a much lower rate than in a high-M alginate.

The addition of CMC has the same effect as the M blocks, as both M and carboxymethyl groups imply weak binding with the calcium cations; therefore, increased swelling is observed with higher CMC content. Although no calcium release experiments could be performed, it is anticipated that the addition of pectin would increase the rate of calcium

release as it does not present any real obstacles for the divalent ions.

Different sequences of the "hopping-trapping" mechanism are displayed in figure VIII.3.1., for sequences of 10 blocks, in a high-G and a high-M alginate.

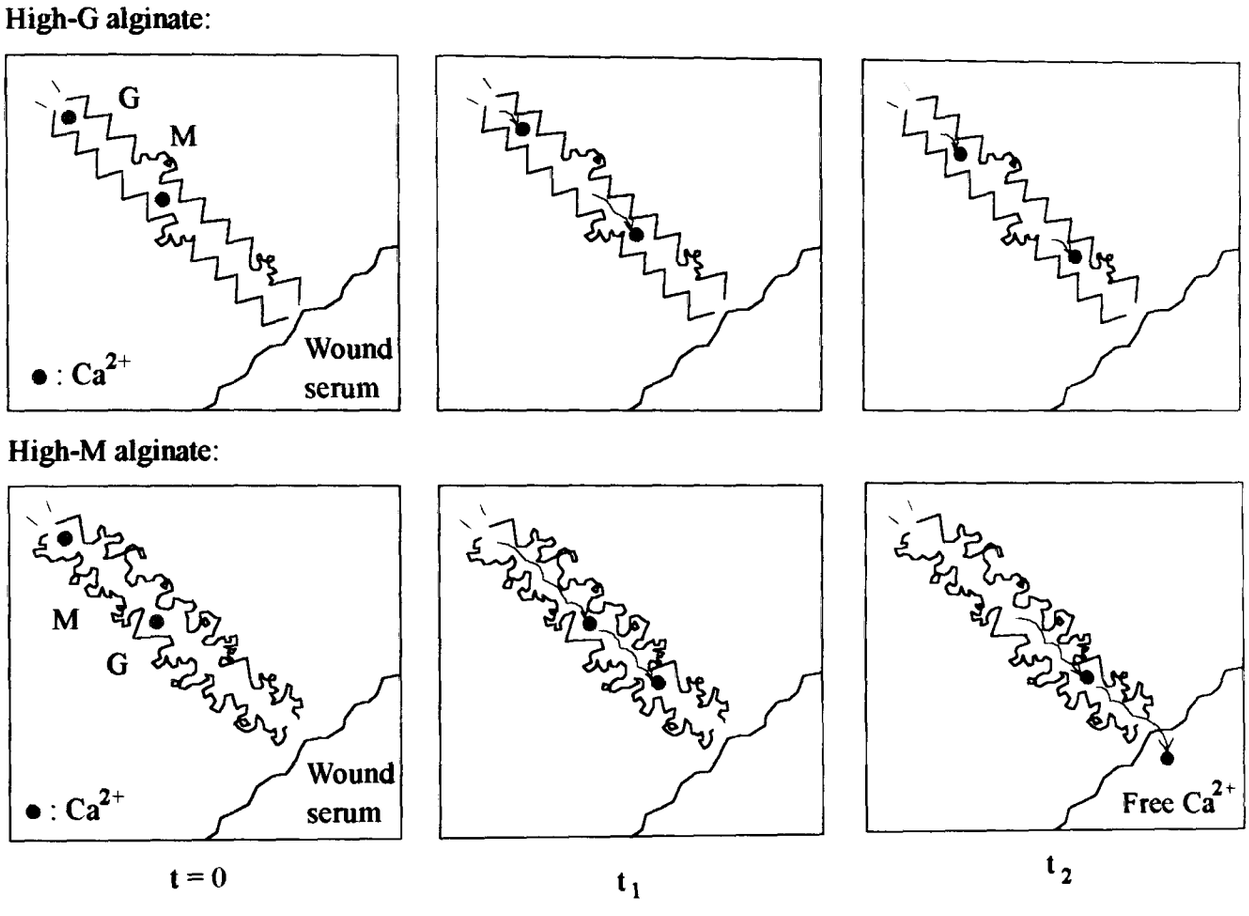

Figure VIII.3.1. Schematic representation of the "hopping-trapping" process.

When the alginate samples are brought into contact with the simulated serum solution, the calcium ions from the sample migrate towards the solution. In the case of the high-G alginate, the calcium ion, trapped between two polymer molecules, moves along fairly slowly as it encounters mainly G blocks with which strong binding ensues. When it comes in contact with an M block, the motion process is sped up until the Ca^{2+} ion is faced to all G blocks again. By contrast, the calcium ion in the high-M alginate is able to move along the polymer chains fairly easily due to weak binding, and it is able to reach the solution more quickly than in the previous case.

VIII.3.2. Swelling:

Water uptake occurs as soon as the polysaccharide films are immersed in the simulated serum solution (proved by the wicking rate experiments). Prasad & Kalyanasundaran (1995) suggested that the swelling behaviour of hydrogels was governed by the hydrophilicity, the nature and the extent of the crosslinking agent. The flexibility or rigidity of the chains are also of importance (Ichikawa *et al.*, 1994). According to our swelling experiments, the same parameters apply to our systems. From these observations, the water molecules are thought to enter the polysaccharide network mainly by two mechanisms:

-capillary; voids may exist between the molecules, particularly in the alginate/CMC blends where there is evidence of lack of interaction between the two polymers. Voids may also be present due to a low degree of chain entanglements (between the M blocks in alginate, for example). Water may then penetrate through these voids. In the case where there is a high calcium ion content in the sample, or when these calcium ions are known to be tightly bound (to the G blocks for example), this contribution to the swelling will decrease;
-ionic interaction with alginate and CMC molecules (OH and COO^- groups predominantly). Alginate and carboxymethylcellulose are commonly referred to as hydrophilic polymers, while pectin is more hydrophobic (due to the methoxyl groups).

In order for water to diffuse through the polymer network, the chains need to spread apart and to disentangle. First, the water molecules are expected to bind to the polymer molecules, via hydrogen bonding. As the sample is depleted in Ca^{2+} ions, the degree of crosslinking diminishes and, thus, water can enter into the film more freely. As more water is allowed in, the polymer molecules move further apart and the water will occur mainly in the free form. After a given time, an ionic equilibrium is reached, and no more Ca^{2+} release occurs. This, in turn, limits the extension of the molecules (as the remaining calcium ions in the sample still act as crosslinks), and brings the swelling to a stop.

From dynamic viscoelastic measurements, Yano (1993) has studied the behaviour of sorbed water in hydrophilic polymers, and the outcome was rather analogous to ours. He has divided the sorption phenomenon into three regions:

1- a few water molecules are absorbed onto hydrophilic groups and a monolayer of water molecules is formed. The molecular motion of water is strongly restricted by the hydrophilic groups;
2- multilayers of bound water are formed around hydrophilic polymers. In this region, water breaks intra- or intermolecular hydrogen bonds in the amorphous phase;
3- water molecules are absorbed in polymers as bulk water or free water.

CMC seems to have a greater water affinity than alginate, as observed from the TGA data. This may be explained as follows: the calcium ions have been shown to be weakly bound to the carboxymethylcellulose groups (due to the configuration of these groups which presumably does not allow for chelation). Therefore the carboxyl groups, as well as the calcium ions, offer more charges to bind to the water molecules, compared with the same constituents in the alginate structure. Secondly, alginate and CMC are similarly charged (due to their COO^- groups) and, therefore, repulsion between the two polysaccharides must occur (as suggested by the viscosity experiments). According to Ichikawa *et al.* (1995), polymer chains tend to extend in water as a result of repulsion between charges that are the same as those of the polymer. This, in turns, allows for more water to penetrate.

The complex behaviour observed for the alginate/pectin blends was thought to be due to various mechanisms, some of them conflicting. They include:
-the combination of hydrophilic/hydrophobic polymers;
-the calcium crosslinking, which lowers the water absorption in the alginate for the samples with low pectin content;
-the chain entanglement between the molecules (particularly high with the G blocks), which will also introduce more obstacles for the water molecules;
-the weak hydrogen intermolecular binding between alginate and pectin which may be easily disrupted by the water molecules;
-some degree of inhomogeneity between the two polymers, which may lead to greater chain mobility and, thus, to more water uptake.

VIII.3.3. Gel strength:

Gel strength is a complex property as it involves various parameters. When stress is applied, a deformation due to the stress itself is expected, but there are also contributions from the swelling and the calcium release phenomena. A proposed scenario for the gel strength property is as follows.

Upon immersion, water molecules penetrate into the polymer network (causing chains to move apart leading to swelling), and together with the applied stress, unwinding and extension of the polymer chains is expected to occur. This involves primarily the M blocks of the alginate as they are more flexible, and leads to an initially high strain of the sample. The high strain is typically characteristic of elastic deformation. However, in our case, the drifting apart of the chains due to the swelling is expected to be connected rather to viscous flow, and therefore is irreversible (as long as the sample remains in the same medium, i.e. liquid). As time elapses, a proportion of the calcium ions are released from the sample; the decrease in crosslinking which ensues enables chain reorganisation, and possibly some chain slippage. More water is then allowed in (a state close to equilibrium in swelling is reached after 30 minutes of immersion in the case of pure alginate). This promotes further chain slippage. However, deformation does not happen to the same extent as observed previously, as the degree of crosslinking in the polysaccharide system remains important. In the case where swelling does not reach an equilibrium, more and more water will be accommodated in the sample. As the degree of crosslinking further decreases, breakage may occur. At this point, the stress at chain entanglements caused by the sample weight together with the water molecules is too high to sustain and the sample breaks.

Following removal of the stress, high levels of strain generally remain. Contributions to permanent deformation arise from swelling (as mentioned earlier), from the Ca^{2+} ion release (the decrease of calcium crosslinking is indeed irreversible) and from chain slippage due to the applied stress.

CONCLUSIONS

This research project gives a greater insight into the molecular structure of some polysaccharide networks. This was achieved via FTIR, Raman and neutron spectroscopy, with the two last techniques barely or never used on alginate, pectin and CMC before. These molecular spectroscopy techniques suggested a specific type of binding between sodium ions and the alginate molecules. By contrast, various atomic groups were involved in the binding of calcium ions. Other salts were analysed, such as zinc and silver alginates. Introduction of Zn^{2+} ions in the alginate led to more complex bonding, compared with the addition of Ca^{2+} ions, whilst Ag^{+} addition reduced the water interaction to the polymer molecules. The water was believed to be bound to the polysaccharide groups via the hydroxyl as well as the carboxyl groups. Studies on blends gave evidence of weak binding between the alginate and pectin molecules. No evidence of interaction between the alginate and CMC molecules was obtained.

Measurements in the gel state were performed in order to assess the efficiency of the various polysaccharide systems, as sodium/calcium salts, for medical applications. For a material to be suitable as a wound dressing, special requirements must be fulfilled. The material must be primarily absorbent, to avoid discomfort for the patient; it must also be haemocompatible, to promote faster healing, and it must retain as much as possible its integrity, to facilitate its handling. For this purpose, volume change tests (i.e. absorbency), gel strength (to mimic the dressing gel handling) and calcium release experiments (to correlate with the haemocompatibility properties) were carried out on the samples in contact with a simulated serum solution.

It must be pointed out that alginates, as well as pectins and celluloses, are natural polysaccharides; hence they are intrinsically inhomogeneous in terms of molecular weight, sequence arrangement, etc... These inhomogeneities lead invariably to large variations in all experimental results, typically of the order of 20 %. However, differences observed between the various polysaccharide systems were generally large enough to be considered significant.

For the pure alginates, it was found that the gel properties were influenced by the M/G ratio and the initial calcium content of the films. The sample giving the best compromise in terms of calcium release, swelling and gel strength had the following characteristics: M/G = 25/75 and Ca^{2+} = 1.8 at%.

Regarding the polysaccharide blends, it is apparent that the main gel properties can be improved. The 75 % alginate/25 % pectin sample exhibited an enhanced gel strength, whilst retaining a similar swelling ratio when compared with a pure alginate film of similar thickness and $CaCl_2$ immersion time. Greater additions of H.M. pectin are to be avoided as they are detrimental to the calcium content (as the divalent cations do not bind significantly to the pectin molecules). This would possibly reduce the haemocompatibility of the alginate blends.

Alginate/CMC blends were also analysed. No work has been previously carried out on such blends. The addition of CMC improved both the calcium release and the swelling behaviour. By contrast, the gel strength was reduced. However, this parameter seems to be the least critical of the three. Taking into account the "basket of properties" required, the addition of up to 50 % CMC is beneficial for wound dressing applications. The optimum concentration was found to be 75 % alginate/25 % CMC. For this particular blend, the calcium release was improved by 3.5 times whilst the swelling ratio increased by 1.6 times, compared with the pure alginate. The gel strength decreased by 1.7 times that of pure alginate.

A new model was derived relating the structure of the alginate systems to the ability to release calcium ions in a simulated serum solution. This model is based on a "hopping-trapping" mechanism for the calcium migration, due to different affinity with the polysaccharide blocks.

SUGGESTIONS FOR FURTHER WORK

From the analysis of all our experimental results and keeping in mind the end-use of our materials, several directions for further work can be proposed. They have been divided into four main headings, as follows.

1- Complementary studies, using different techniques:

The use of new techniques would enable to clarify some aspects of the previous work as well as to deepen others. Some of the techniques could include:

-low angle X-ray diffraction in order to analyse more closely the possibility of crystallinity of alginate and CMC, before and after the introduction of calcium ions;
-differential scanning calorimetry, to get a better representation of the water contained in the samples; DSC would enable us to determine the proportion of "free" and bound water molecules as they exhibit different melting and crystallisation behaviours (Hatakeyama *et al.*, 1988; Marcus, 1995);
-environmental SEM, to visualise the sodium and calcium ion distribution in the gel samples at various time intervals as they liberate their calcium in a simulated serum solution. This would enable to test our Ca^{2+} ion release model by studying the migration pace of the calcium ions within the gel samples.
-transmission electron microscopy, to examine in closer detail eventual signs of phase separation in the polysaccharide blends;
-density measurements, to get information on the efficiency of packing between the polymer molecules, and in contact with various ions (i.e. Na^{+}, Ca^{2+}, Zn^{2+} and Ag^{+}).

2- Extension of the binary blend work to ternary blends:

This would clearly involve the alginate/pectin/CMC blends, with a view to improve all the gel properties. The work could be divided as follows:

-preliminary study on a selected range of pectins (with varying degree of methoxylation) and celluloses (with varying degree of substitution). This is necessary in order to select the more appropriate polysaccharides for the dressing applications. This work could be

concentrated on the 75 % alginate/25 % other polysaccharide blend as both additions of 25 % pectin and 25 % CMC to a high-G alginate were found to provide the best gel properties;

-preparation of ternary blends, varying the relative content of each polysaccharide. The resulting samples could be tested for their calcium release, swelling and gel strength behaviour, in a similar way to the binary blends. However, the number of blends to be prepared will be sensibly higher;

-in order to improve the efficiency of the experiments as well as their analysis, it would be judicious to use an experimental plan methodology. The difference between conventional analysis and this mathematical and statistical method is that all parameters are varied at once, in a controlled way. This enables one to get maximum information with the best possible quality while performing a minimum of experimental tests.

3- Progression from the film study to the fibre study:

Films were preferred in this project for ease of experimental procedures, and because the prime aim was to detect possible trends between the different formulations of polysaccharides. However, it is necessary to define precisely the characteristics of the samples used in the wound dressing production, i.e. as fibres. As the surface area of fibres is greater than that of films, most of the experimental results are expected to differ. For example, the gelation process in $CaCl_2$ solution will be accelerated (Thomas *et al.*, 1995), and the swelling ratio will tend to increase as well as the ability for calcium ion release in contact with serum. By contrast, the gel strength will become poorer. The orientation due to stretching during fibre production is also bound to alter some of the polymer properties. For the fibre study, a new experimental design will be required. An alternative is to derive mathematical calculations to transpose the results obtained for the samples in the film form to the fibre form.

4- Progression from the simulated serum solution to real wound exudate:

This last section involves an evolution from "in-vitro" to "in-vivo" studies. They must be performed on the final product to minimise the number of tests. It is therefore important to consider the way samples will be sterilised before their end-use. Sterilisation is

commonly achieved by ethylene oxide or by gamma irradiation. This process is of prime importance for wound dressing applications to ensure that no bacteria are brought into contact with the wound, thus avoiding any unnecessary infection. However, sterilisation is expected to bring some changes in the material properties, and these need to be fully assessed (Sébert *et al.*, 1994).

APPENDIX ONE: DETAILED CALCULATION OF THE ATOMIC PERCENTAGES FOR THE ALGINATE SAMPLES

Alginates are formed of mannuronic acid (M) and guluronic acid (G) blocks. These blocks are sketched in figure 1.

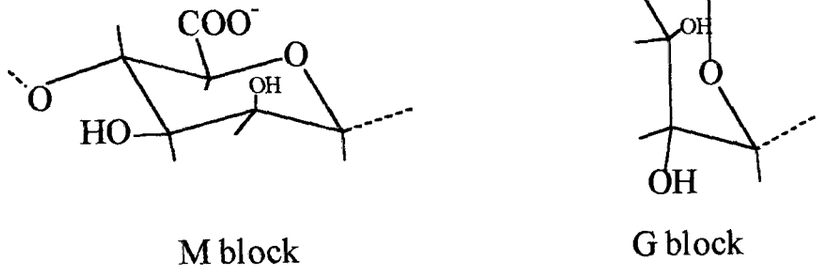

M block G block

Figure 1. M and G blocks.

For each M or G block, consider there is on average "x" atoms of sodium and "y" atoms of calcium. The molecular weight of sodium is 23 g/mol, and that of calcium is 40 g/mol. Theoretically, there are 6 carbon atoms, 6 oxygen atoms, 7 hydrogen atoms and 1 ion site per G or M block, giving a molecular weight of 175 g, excluding the mass of the ion(s). However, because alginate is a natural polymer, the M and G block are irregular, and the molecular weight is in practice closer to 200 (again excluding the mass of the ion). Let us call "Na" the experimental weight percentage of sodium and "Ca" the experimental weight percentage of calcium, on the dry basis.

For a particular alginate sample, after a given immersion time in $CaCl_2$ solution, Na and Ca are given by:

$Na = (100 \times 23x) / (23x + 40y + 200)$ and $Ca = (100 \times 40y) / (23x + 40y + 200)$

which re-arranged gives:

$x = 200Na / 23 (100 - Na - Ca)$ and $y = 5Ca / (100 - Na - Ca)$.

The atomic percentage of sodium and calcium are then given by:

Sodium at% $= 100x / (x + y + (19 \times 200 / 175))$ and

Calcium at% $= 100y / (x + y + (19 \times 200 / 175))$.

Table 1 gives the values of x, y, sodium and calcium at% for various initial weight percentages of 8% high-G alginate:

Immersion time in $CaCl_2$	Na wt%	Ca wt%	x	y	Na at%	Ca at%
0	11.4	0.06	1.12	0.003	4.90	0.01
30 s	10.2	0.57	0.994	0.032	4.37	0.14
3 min	9.3	1.5	0.907	0.084	3.99	0.37
30 min	6.7	4	0.652	0.224	2.89	0.99
100 min	5.1	7	0.505	0.398	2.23	1.76
300 min	1.8	10.1	0.178	0.573	0.79	2.55
3,000 min	0.1	11.4	0.01	0.644	0.04	2.88
30,000 min	0.1	11.5	0.01	0.65	0.04	2.91

Table 1. Percentages of sodium and calcium in 8% alginate LF 10/60 immersed for various times in $CaCl_2$ solution.

APPENDIX TWO: DETAILED CALCULATION FOR VISIBLE SPECTROSCOPY

During the visible spectroscopy experiments, an alginate film (10 × 10 mm) is immersed in 4 ml of a Na/Ca solution (with 142 mmol.l^{-1} of Na^+ and 2.5 mmol.l^{-1} of Ca^{2+} ions) containing an indicator (tetramethyl murexide to trace calcium; concentration: 0.02 g.l^{-1}). The purpose of this study was to determine the percentage of calcium which has migrated from the alginate sample into the simulated serum solution.

i. The alginate sample:

Let us call "Ca" the weight percentage of calcium in the alginate film, measured on a dry basis (by AAS), and "w" the dry sample weight, in mg (measured using a microbalance; it was between 15 and 25 mg). The molecular weight of calcium is 40.08. Initially, the alginate sample contains "x" mmol of calcium ions, equal to (Ca.w / 4008).

The standard error for x is: $dx / x = (dCa / Ca + dw / w)$.

dCa / Ca is estimated to be equal to 2 % (AAS specification). As for the weight, three samples were tested for each case, and their weight average shows a deviation of 12 % (due to dimensional differences). The error from the scale can be neglected.

It follows that $dx / x = 0.02 + 0.12 = 0.14$.

ii. The sodium/calcium solution:

The calcium content in the solution was recorded via visible spectroscopy. A standard curve was first obtained, in order to correlate directly the visible peak wavelength with the percentage of Ca^{2+} ions. As shown in Figure V.1.1.b., the experimental points can be extrapolated to a curve with the following equation:

$$\Delta C = (1 / (0.0103\lambda - 4.92)) - 4.35 \quad (1)$$

where ΔC is the difference in calcium concentration in the solution between the initial time (2.5 mmol.l^{-1}) and the time t;

λ is the wavelength, in nm. The resolution of the instrument used, $d\lambda$, was 0.8 nm, which leads to a standard error $d\lambda / \lambda$ of 0.2 % for the range of wavelength studied. The experimental error, averaged over three values, gave a similar value.

The standard error of ΔC can be derived as follows:

$$\Delta C = \frac{1}{0.0103\lambda - 4.92} - 4.35 = \frac{1 - 0.0448\lambda + 21.4}{0.0103\lambda - 4.92}$$

$$\ln \Delta C = \ln (22.4 - 0.0448\lambda) - \ln (0.0103\lambda - 4.92)$$

$$\frac{d\,\Delta C}{\Delta C} = \left| \frac{-0.0448\, d\lambda}{|22.4 - 0.0448\lambda|} \right| + \left| \frac{0.0103\, d\lambda}{|0.0103\lambda - 4.92|} \right| ,$$

$$\frac{d\,\Delta C}{\Delta C} = \frac{1}{|(\lambda / d\lambda) - (22.4 / 0.0448 d\lambda)|} + \frac{1}{|(\lambda / d\lambda) - (4.92 / 0.0103 d\lambda)|} ,$$

$$\frac{d\,\Delta C}{\Delta C} = \frac{1}{|500 - 625|} + \frac{1}{|500 - 597|} = 0.02.$$

From the standard curve, the actual number of Ca^{2+} in mmol in the solution for each immersion time can be calculated. But it is necessary to do some volume corrections as the sample swells when immersed in the Na/Ca solution; therefore the volume of the solution decreases with time. During each scan, the sample was removed and the volume "V" of simulated serum solution left (in ml) was measured; this thus takes into account the absorption of the alginate sample at time t. This was measured with an average error of 2 %.

V contains $y = (V.\Delta C) / 1000)$ mmol of Ca^{2+}.

The standard error on y is given by:

$(dy / y) = (dV / V) + (d\Delta C / \Delta C) = 0.02 + 0.02 = 0.04.$

iii. Percentage of calcium ions release:

From the calculations described above, it is now possible to determinate the percentage Ca^{2+} released by the alginate film in the simulated serum solution. Let us call "z" this quantity. It can be expressed as: $z = 100.\ y / x.$

It follows that the standard error on z is:

$dz = (dy / y) - (dx / x) = 0.04 + 0.14 = 0.18.$

APPENDIX THREE: DETAILED CALCULATION OF THE ATOMIC PERCENTAGES FOR THE BLENDS.

A. Alginate/pectin blends:

In the alginate samples, each M or G block weights in practice 200 and the average number of atoms is (19 × 200 / 175), i.e. ≈ 21.71 (excluding the ion, i.e. sodium or calcium ion). For each of these blocks, there is theoretically one ion site.

The citrus pectin we used contained no less than 6.7 wt% methoxyl groups, and no less than 74 wt% of galacturonic acid (on the dry basis), as given by the manufacturer. The remaining 26 wt% are sugars such as arabinose ($C_5H_{10}O_5$), rhamnose ($C_6H_{12}O_5$) and galactose ($C_6H_{12}O_6$). No further knowledge was given regarding these side groups. Methoxylated and non-methoxylated galacturonic acid units are sketched in figure 3.1.

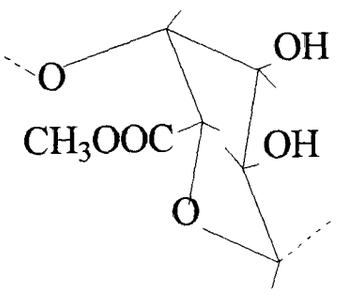

Methoxylated unit

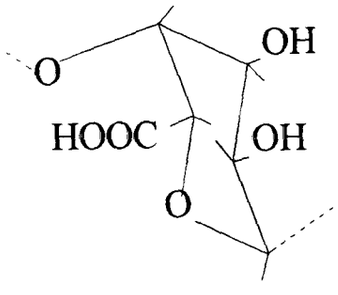

Non - methoxylated unit

Figure 3.1 Pectin blocks.

The characteristics of these units are:

-methoxylated unit: 190 g/ 23 atoms; the methoxyl group (CH_3O) weights 31 g;

-non-methoxylated unit: 176 g/ 20 atoms.

The degree of methoxylation DM (number of methoxyl units substituted per 100 monosaccharides of the molecule) can be approximated to:

0.067 * 100 / 74 = 31 DM / (190 DM + 176 (100 - DM)),

which leads to a DM value close to 55 %.

For this particular pectin, 100 g of the starting material contains approximately (74 * 0.55) g of methoxyl units, (74 * 0.45) g of non-methoxyl units and 26 g of sugar units (taken as being rhamnose for our calculations as it has an average weight and number of atoms). This leads to a number of atoms "N_p" equivalent to:

$N_p = (74 * 0.55 * 23 / 190) + (74 * 0.45 * 20 / 176) + (26 * 23 / 164) \approx 12.36.$

Atomic absorption spectroscopy did not reveal any sodium content in the starting pectin, and pectin did not gel in contact with a calcium chloride solution. For these two reasons, it was assumed that pectin did not contain any ion sites. Therefore in a blend of 100 g comprised of "a" wt% of sodium alginate and "p" wt% of pectin, there are "S_a" sites, all from the alginate. S_a is given by: $Sa = a / 223$.

Let M_{ap} be the mass of one virtual block in the blend containing one ion site (excluding the mass of sodium) and let N_{ap} be the number of atoms in this virtual block (again excluding Na^+). These parameters are given by:

$M_{ap} = ((200\ a / 223) + p) / S_a;$

$N_{ap} = 21.7 + (12.36\ p / 100\ S_a).$

Table 3.1. presents the values of S_a, M_{ap} and N_{ap} for the various sodium alginate/pectin blends.

Sample (wt %)	S_a	M_{ap} (g)	N_{ap}
100% alginate	0.45	200.00	21.71
97.5% alg. + 2.5% pect.	0.44	205.72	22.42
95% alg. + 5% pect.	0.43	211.74	23.16
75% alg. + 25% pect.	0.34	274.33	30.90
50% alg. + 50% pect.	0.22	423.00	49.27
25% alg. + 75% pect.	0.11	869.00	104.38

Table 3.1. Intermediate calculations.

The sodium alginate/pectin samples are then immersed for 30 minutes in a calcium chloride solution. Let us call "x" and "y" the number of sodium and calcium ions, respectively, in a virtual block of the blend. The sodium and the calcium weight percentages, Na and Ca, are given by:

$Na = (100 \times 23x) / (23x + 40y + M_{ap})$ and

$Ca = (100 \times 40y) / (23x + 40y + M_{ap})$

which re-arranged gives:

$x = (M_{ap} \times Na) / (2300 - 23Na - 23Ca)$ and $y = (M_{ap} \times Ca) / (4000 - 40Na - 40Ca)$.

The atomic percentages are then given by:

Sodium at% $= 100x / (x + y + N_{ap})$ and

Calcium at% $= 100y / (x + y + N_{ap})$.

Table 3.2. presents the sodium and calcium percentages of the various alginate/pectin blends (after immersion for 30 minutes in a $CaCl_2$ solution).

Sample (wt %)	Na wt%	Ca wt%	x	y	Na at%	Ca at%
100% alginate	6.50	3.20	0.63	0.18	2.78	0.79
97.5% alg. + 2.5% pect.	7.10	2.30	0.70	0.13	3.01	0.56
95% alg. + 5% pect.	7.10	2.30	0.72	0.13	3.00	0.56
75% alg. + 25% pect.	5.50	2.30	0.71	0.17	2.24	0.54
50% alg. + 50% pect.	4.50	2.10	0.89	0.24	1.76	0.47
25% alg. + 75% pect.	2.00	1.70	0.78	0.38	0.74	0.36

Table 3.2. Sodium and calcium percentages of alginate/pectin blends.

B. Alginate/CMC blends:

As recalled in A., there is one ion site for 200 g alginate (excluding the weight of the ion) and for ≈ 21.71 atoms (again excluding the ion).

For the CMC used in this study, the degree of substitution DS was 0.8. Therefore there are 80 % of groups A (219 g/ 26 atoms) and 20 % of groups B (162 g/ 21 atoms) (see figure 3.2.):

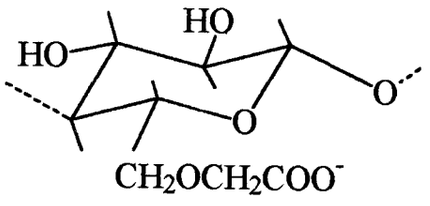

Group A

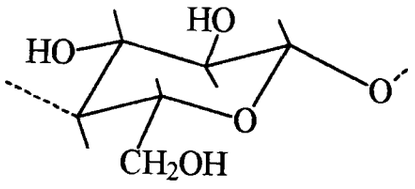

Group B

Figure 3.2. CMC groups.

Ion sites are available only within the A blocks (from the COO^- blocks). Therefore the mass of CMC (M_c) and the number of atoms (N_c) required to obtain one ion site are given by:

$M_c = ((0.8 \times 219) + (0.2 \times 162)) / 0.8 = 259.5$ g;

$N_c = ((0.8 \times 26) + (0.2 \times 21)) / 0.8 = 31.25$ atoms.

Let us call "S_a" and "S_c" the theoretical number of sites of alginate and CMC, respectively, in 100 g of sodium blend, initially. Let M_{ac} be the mass of one virtual block in the blend containing one ion site, and let N_{ac} be the number of atoms in this virtual block (excluding the ion). For a particular sodium blend containing a wt% alginate and c wt% of CMC, these parameters are given by:

$S_a = a / (200 + 23)$ & $S_c = c / (259.5 + 23)$;

$M_{ac} = ((200 \times S_a) / (S_a + S_c)) + ((259.5 \times S_c) / (S_a + S_c))$;

$N_{ac} = ((21.71 \times S_a) / (S_a + S_c)) + ((31.25 \times S_c) / ((S_a + S_c))$.

Table 3.3. presents the values of S_a, S_c, M_{ac} and N_{ac} for various sodium alginate/CMC blends:

Sample (wt %)	S_a	S_c	M_{ac} (g)	N_{ac}
100% alginate	0.45	/	200.00	21.71
97.5% alg.+2.5% CMC	0.44	0.01	201.18	21.90
95% alg.+5% CMC	0.43	0.02	202.37	22.09
75% alg.+25% CMC	0.34	0.09	212.39	23.70
50% alg.+50% CMC	0.22	0.18	226.25	25.92
25% alg.+75% CMC	0.11	0.27	241.83	28.42
100% CMC	/	0.35	259.50	31.25

Table 3.3. Intermediate calculations.

The sodium alginate/CMC samples are then immersed for 30 minutes in a calcium chloride solution. In a similar manner to the alginate/pectin blends, the sodium and calcium atomic percentages can be derived from "x" and "y" (number of sodium and calcium ions, respectively, in a virtual block of the blend). x and y can be expressed from the calcium weight percentages, Na and Ca, by:

$x = (M_{ac} \times Na) / (2300 - 23Na - 23Ca)$ and $y = (M_{ac} \times Ca) / (4000 - 40Na - 40Ca)$.

The atomic percentages are then given by:

Sodium at% $= 100x / (x + y + N_{ac})$ and Calcium at% $= 100y / (x + y + N_{ac})$.

Table 3.4. presents the weight and atomic percentages for the alginate/CMC blends:

Sample (wt %)	Na wt%	Ca wt%	x	y	Na at%	Ca at%
100% alginate	4.90	4.30	0.47	0.24	2.09	1.06
97.5% alg.+2.5% CMC	5.40	4.20	0.52	0.23	2.31	1.03
95% alg.+5% CMC	5.40	3.80	0.52	0.21	2.29	0.93
75% alg.+25% CMC	5.10	3.50	0.52	0.20	2.11	0.83
50% alg.+50% CMC	5.00	3.50	0.54	0.22	2.02	0.81
25% alg.+75% CMC	4.00	3.60	0.46	0.24	1.56	0.81
100% CMC	4.00	3.20	0.49	0.22	1.52	0.70

Table 3.4. Percentages of sodium and calcium for sodium/calcium alginate/CMC blends.

REFERENCES

-Abdel-Hadi A.K., Hosny W.M., Basta A.H., El-Saied H., *Polym.-Plast. Technol. Eng.* **33(6)** (1994) 781-791.

-Andresen I.-L. & Smidsrød O., *Carbohydrate Research* **58** (1977) 271-279.

-Argûelles-Monal W., Hechavarría O.L., Rodríguez L., Peniche C., *Polymer Bulletin* **31** (1993) 471-478.

-Aspinall G.O. (Ed.), *The polysaccharides,* Academic Press, **1** (1982) 172-184.

-Atkins E.D.T., Mackie W., Smolko E.E., *Nature* **225** (1970) 626-628.

-Atkins E.D.T., Nieduszynski I.A., Mackie W., Parker K.D., Smolko E.E., *Biopolymers* **12** (1973) 1879-1887.

-Baar A., Kulicke W.-M., Szablikowski K., Kieswetter R., *Macromol. Chem. Phys.* **195** (1994) 1483-1492.

-Barnett S.E. & Varley S.J., *Annals of the Royal College of Surgeons of England* **69** (1987) 153-155.

-Brandrup J. & Immergut E.M. (Eds.), *Polymer Handbook,* Wiley-Interscience Press, **2nd Ed.** (1975) V-98.

-Bryce T.A., McKinnon A.A., Morris E.R., Rees D.A., Thom D., *Faraday Discuss. Chem. Soc.* **57** (1974) 221-229.

-Callister W.D. Jr., *Materials Science and Engineering, An Introduction,* Wiley Press **3rd Ed.** (1994).

-Cesàro A., Delben F., Paoletti S., *J. Chem. Soc., Faraday Trans. I.* **84(8)** (1988) 2573-2584.

-Clare K., *Industrial Gums,* Academic Press, **3rd Ed.** (1993) 105-142.

-Coleman M.M. & Painter P.C., *Applied Spectroscopy Reviews* **20(3&4)** (1984) 255-346.

-Dawson C., Armstrong M.W.J., Fulford S.C.V., Faruqi R.M., Galland R.B., *J. R. Coll. Surg. Edinb.* **37** (1992) 177-179.

-Decleire M., van Huynh N., Motte J.C., De Cat W., *Appl. Microbiol. Biotechnol.* **22** (1985) 438-441.

-Draget K.I., Østgaard K., Smidsrød O., *Carbohydrate Polymers* **14** (1991) 159-178.

-Draget K.I., Simensen M.K., Onsøyen E., Smidsrød O., *Hydrobiologia* **260/261** (1993) 563-569.

-Dupuy B., Arien A., Perrot Minnot A., *Art. Cells, Blood Subs., and Immob. Biotech.*, **22(1)** (1994) 71-82.

-El-Nawawi S.A. & Heikal Y.A., *Carbohydrate Research* **27** (1995) 191-195.

-El-Saied H., Basta A.H., Abdel-Hadi A.K., Hosny W.M., *Polymer International* **35** (1994) 27-33.

-Filippov M.P., *Journal of Analytical Chemistry of the USSR* **39(1)** (1984) 73-75.

-Filippov M.P. & Kohn R. , *Chem. Svesti* **28(6)** (1974) 817-819.

-Filippov M.P. & Vaskan R.N., *Journal of Analytical Chemistry of the USSR* **42(9)** (1987) 1356-1359.

-Forshaw A., *Journal of Wound Care* **2(4)** (1993) 209-212.

-Fujihara M. & Nagumo T., *Carbohydrate Research* **224** (1992) 343-347.

-Fujii J.A.A., Slade D.T., Redenbaugh K., Walker K.A., *Tibtech* **5** (1987) 335-339.

-Gacesa P., *FEBS Letter* **212(2)** (1987) 199-202.

-Gacesa P., *Carbohydrate Polymers* **8** (1988) 161-182.

-Góral J. & Zichy V., *Spectrochimica Acta* **46A(2)** (1990) 253-275.

-Grant G.T., Morris E.R., Rees D.A., Smith P.J.C., Thom D., *FEBS Letters* **32(1)** (1973) 195-198.

-Grasdalen H., *Carbohydrate Research* **118** (1983) 255-260.

-Grasdalen H., Larsen B., Smidsrød O., *Carbohydrate Research* **56** (1977) C11-C15.

-Grasdalen H., Larsen B., Smidsrød O., *Carbohydrate Research* **68** (1979) 23-31.

-Grasdalen H., Larsen B., Smidsrød O., *Carbohydrate Research* **89** (1981) 179-191.

-Groves A.R. & Lawrence J.C., *Annals of the Royal College of Surgeons of England* **68** (1986) 27-28.

-Hatakeyama T., Nakamura K., Hatakeyama H., *Thermochimica Acta* **123** (1988) 153-161.

-Haug A., *Acta Chemica Scandinavica* **13(6)** (1959) 1250-1251.

-Haug A. & Larsen B., *Acta Chemica Scandinavica* **16** (1962) 1908-1918.

-Haug A. & Smidsrød O., *Acta Chemica Scandinavica* **19** (1965) 341-351.

-Haug A., Larsen B., Smidsrød O., *Acta Chemica Scandinavica* **17** (1963) 1466-1468.

-Haug A., Myklestad S., Larsen B., Smidsrød O., *Acta Chemica Scandinavica* **21** (1967a) 768-778.

-Haug A., Larsen B., Smidsrød O., *Acta Chemica Scandinavica* **21** (1967b) 691-704.

-Horncastle J., *Medical Device Technology* **6(1)** (1995) 30-36.

-Hosny W.M., Abdel Hadi A.K., El-Saied H., Basta A.H., *Polymer International* **37** (1995) 93-96.

-Ichikawa T., Mitsumura Y., Nakajima T., *Journal of Applied Polymer Science* **54** (1994) 105-112.

-Iso N., Mizuno H., Saito T., Enomoto M., Ohgoshi M., Ohzeki F., *Nippon Suisan Gakkaishi* **54(6)** (1988) 1023-1026.

-Jarvis P.M., Galvin D.A.J., Blair S.D., McCollum C.N, *Thrombosis and Haemostasis* **58** (1987) 80.

-Kawarada H., Hirai A., Odani H., Lida T., Nakajima A., *Polymer Bulletin* **24** (1990) 551-557.

-Keller J., *New York State Agricultural Experiment Station Special Report* **53** (1984a) 1-9.

-Keller J., *New York State Agricultural Experiment Station Special Report* **53** (1984b) 9-19.

-Kim C.-K. & Lee E.-J., *International Journal of Pharmaceutics* **79** (1992) 11-19.

-Kneafsey B., O'Shaughnessy M., Condon K.C., *Burns* **22(1)** (1996) 40-43.

-Kohn R., *Pure Appl. Chem.* **42** (1975) 371-397.

-Larsen B. & Grasdalen H., *Carbohydrate Research* **92** (1981) 163-167.

-Larsen B., Painter T., Haug A., Smidsrød O., *Acta Chemica Scandinavica* **23** (1969) 355-370.

-Larsen B., Hoøen K., Østgaard K., *Hydrobiologia* **260/261** (1993) 557-561.

-Liyanage J.A., Taylor D.M., Williams D.R., *Chemical Speciation and Bioavailability* **7(2)** (1995) 73-75.

-Mackie W., *Carbohydrate Research* **20** (1971) 413-415.

-Mackie W., Perez S., Rizzo R., Taravel F., Vignon M., *Int. J. Biol. Macromol.* **5** (1983) 329-341.

-Marcus Y., *Cell Biochemistry and Function* **13** (1995) 157-163.

-Martinsen A., Skjåk-Bræk G., Smidsrød O., *Biotechnology and Bioengineering* **33** (1989) 79-89.

-Matijević E. (Ed.), *Surface and colloid Science,* Wiley-Interscience Press, **2** (1969).

-Matsumoto T., Kawai M., Masuda T., *Biorheology* **30** (1993) 435-441.

-Matthew I.R., Browne R.M., Frame J.W., Millar B.G., *British Journal of Oral and Maxillofacial Surgery* **31** (1993) 165-169.

-Matthew I.R., Browne R.M., Frame J.W., Millar B.G., *Oral Surgery Oral Medicine Oral Pathology* **77(5)** (1994) 456-460.

-Mayer A.M.S., Krotz L., Bonfil R.D., Bustuobad O.D., Groisman J.F., de Lederkremer R.M., Stierle D.B., *Hydrobiologia* **151/152** (1987) 483-489.

-Michell A.J., *Carbohydrate Research* **197** (1990) 53-60.

-Moe S.T., Skjåk-Bræk G., Smidsrød O., *Food Hydrocolloids* **5(1/2)** (1991) 119-123.

-Moe S.T., Skjåk-Bræk G., Elgsaeter A., Smidsrød O., *Macromolecules* **26** (1993a) 3589-3597.

-Moe S.T., Elgsaeter A., Skjåk-Bræk G., Smidsrød O., *Carbohydrate Polymers* **20** (1993b) 263-268.

-Moe S.T., Skjåk-Bræk G., Smidsrød O., Ichijo H., *Journal of Applied Polymer Science* **51** (1994) 1771-1775.

-Morra M., Occhiello E., Garbassi F., *Advances in Colloid and Interface Science* **32** (1990) 79-116.

-Morris V.J. & Chilvers G.R., *J. Sci. Food Agric.* **35** (1984) 1370-1376.

-Morris E.R., Rees D.A., Thom D., Boyd J., *Carbohydrate Research* **66** (1978) 145-154.

-Morris E.R., Gidley M.J., Murray E.J., Powell D.A., Rees D.A., *Int. J. Biol. Macromol.* **2** (1980) 327-330.

-Ott C.M. & Day D.F., *Trends In Polymer Science* **3(12)** (1995) 402-406.

-Parker S.F., *Spectroscopy Europe* **6(6)** (1994) 14-20.

-Penman A. & Sanderson G.R., *Carbohydrate Research* **25** (1972) 273-282.

-Perry C.C., Li X., Waters D.N., *Spectrochimica Acta* **47A (9/10)** (1991) 1487-1494.

-Pistorius A.M.A., *Spectroscopy Europe* **7(4)** (1995) 8-15.

-Polk A., Amsden B., De Yao K., Goosen M.F.A., *Journal of Pharmaceutical Sciences* **83(2)** (1994) 178-185.

-Porter J.M., *British Journal of Plastic Surgery* **44** (1991) 333-337.

-Potter K., Herrod N.J., Carpenter T.A., Hall L.D., *Carbohydrate Research* **239** (1993a) 249-256.

-Potter K., Carpenter T.A., Hall L.D., *Carbohydrate Research* **246** (1993b) 43-49.

-Potter K., Balcom B.J., Carpenter T.A., Hall L.D., *Carbohydrate Research* **257** (1994) 117-126.

-Prasad M.P. & Kalyanasundaram M., *Carbohydrate Polymers* **26** (1995) 35-41.

-Ratner B.D., Johnston A.B., Lenk T.J., *Journal of Biomedical Materials Research: Applied Biomaterials* **21(A1)** (1987) 59-90.

-Rees D.A., *Biochem. J.* **126** (1972) 257-273.

-Rees D.A., *Polysaccharide Shapes,* Chapman and Hall Press (1977).

-Rodd E.H., *Rodd's Chemistry of Carbon Compounds: A Modern Comprehensive Treatise,* Elsevier Press, **2nd Ed.** (1965) 129-130.

-Rosdy M. & Clauss L.-C., *Journal of Biomedical Materials Research* **24** (1990) 363-377.

-Ryan T.J., *Dermatologic Clinics* **11(1)** (1993) 207-213.

-Sahin Y. & Saglam A., *Acta Obstet Gynecol Scand* **73** (1994) 70-73.

-Sartori C., Finch D.S., Ralph B., Gilding K., Parker S.F., *The ISIS Facility Annual Report* **1** (1996) 50-51.

-Sartori C., Finch D.S., Ralph B., Gilding K., *Polymer* **38(1)** (1997) 43-51.

-Scott C.D., *Enzyme Microb. Technol.* **9** (1987) 66-73.

-Sébert P., Bourny E., Rollet M., *International Journal of Pharmaceutics* **106** (1994) 103-108.

-Segeren A.J.M., Boskamp J.V., van den Tempel M., *Faraday Discuss. Chem. Soc.* (1974) 255-262.

-Sherwood T.K. & Pigford R.L. (Eds.), *Absorption and Extraction,* McGraw-Hill Press, (1952) 332-337.

-Skjåk-Bræk G., *Biochemical Society Transactions* **20(1)** (1992) 27-33.

-Skjåk-Bræk G., Grasdalen H., Larsen B., *Carbohydrate Research* **154** (1986a) 239-250.

-Skjåk-Bræk G., Smidsrød O., Larsen B., *Int. J. Biol. Macromol.* **8** (1986b) 330-336.

-Skjåk-Bræk G., Grasdalen H., Smidsrød O., *Carbohydrate Research* **10** (1989) 31-54.

-Smidsrød O., *Faraday Discuss. Chem. Soc.* **57** (1974) 263-274.

-Smidsrød O. & Haug A., *Acta Chemica Scandinavica* **19** (1965) 329-340.

-Smidsrød O. & Haug A., *Acta Chemica Scandinavica* **22** (1968) 1989-1997.

-Smidsrød O. & Skjåk-Bræk G., *Tibtech* **8** (1990) 71-78.

-Smidsrød O., Haug A., Lian B., *Acta Chemica Scandinavica* **26(1)** (1972a) 71-78.

-Smidsrød O., Haug A., Whittington S.G., *Acta Chemica Scandinavica* **26(6)** (1972b) 2563-2566.

-Smidsrød O., Glover R.M., Whittington S.G., *Carbohydrate Research* **27** (1973) 107-118.

-Socrates G., *Infrared Characteristics, Group Frequencies. Tables and Charts,* Wiley Press, **2nd Ed.** (1994).

-Speculand B., Down K., Hunter J., Smith I.M., *Journal of Dental Research* **69(4)** (1990) 1007.

-Stockton B., Evans L.V., Morris E.R., Rees D.A., *Int. J. Biol. Macromol.* **2** (1980a) 176-178.

-Stockton B., Evans L.V., Morris E.R., Powell D.A., Rees D.A., *Botanica Marina* **XXIII** (1980b) 563-567.

-Stokke B.T., Smidsrød O., Bruheim P., Skjåk-Bræk G., *Macromolecules* **24** (1991) 4637-4645.

-Stokke B.T., Smidsrød O., Zanetti F., Strand W., Skjåk-Bræk G., *Carbohydrate Polymers* **21** (1993) 39-46.

-Tagawa M., Yasukawa A., Gotoh K., Tagawa M., Ohmae N., Umeno M., *J. Adhesion Sci. Technol.* **6(6)** (1992) 763-776.

-Tasker S., Badyal J.P.S., Backson S.C.E., Richards R.W., *Polymer* **35(22)** (1994) 4717-4721.

-Thom D., Dea I.C.M., Morris E.R., Powell D.A., *Prog. Fd. Nutr. Sci.* **6** (1982) 97-108.

-Thomas S., *Journal of Wound Care* **1(1)** (1992) 29-32.

-Thomas S. & Loveless P., *The Pharmaceutical Journal* **June,27** (1992) 850-851.

-Thomas A., Gilson C.D., Ahmed T., *J. Chem. Tech. Biotechnol.* **64** (1995) 73-79.

-Toft K., *Prog. Fd. Nutr. Sci.* **6** (1982) 89-96.

-Tomkinson J., *Spectrochimica Acta* **48A(3)** (1992) 329-348.

-Varma S.K., Henderson H.P., Hankins C.L., *British Journal of Plastic Surgery* **44** (1991) 55-56.

-Walkinshaw M.D. & Arnott S., *J. Mol. Biol.* **153** (1981) 1075-1085.

-Wang Z.-Y., Zhang Q.-Z., Konno M., Saito S., *Chemical Physics Letters* **186(4,5)** (1991) 463-466.

-Wang Z.-Y., Zhang Q.-Z., Konno M., Saito S., *Biopolymers* **33** (1993) 703-711.

-Willard H.H., Merritt L.L. Jr., Dean J.A., Settle F.A, Jr., *Instrumental Methods of Analysis*, Wadsworth Press, **7nd Ed**. (1988).

-Wróblewski R., Wróblewski J., Roomans G.M., *Scanning Microscopy* **1(3)** (1987) 1225-1240.

-Yano S., *Polymer* **34(12)** (1993) 2528-2532.

-Yonezawa Y., Kijima M., Sato T., *Ber. Bunsenges. Phys. Chem.* **96(12)** (1992) 1828-1831.

-Zhbankov R.G., *Journal of Molecular Structure* **270** (1992) 523-539.

POSTCRIPT

"... and so there ain't nothing more to write about, and I am rotten glad of it, because if I'd 'a' knowed what a trouble it was to make a book I wouldn't 'a' tackled it, and ain't a-going to no more."

Mark Twain (Huckleberry Finn);
originally quoted by Dollish, Fateley & Bentley in "Characteristic Raman Frequencies of Organic Compounds" (1974).